พฤติกรรมของฟองก๊าซและการไหลวนภายในของของเหลวในถังสัมผัสอากาศยกประเภทที่มีการไหลวนแบบภายใน

นางสาว พรทิพย์ วงศ์สุโชโต

วิทยานิพนธ์นี้เป็นส่วนหนึ่งของการศึกษาตามหลักสูตรปริญญาวิศวกรรมศาสตรดุษฎีบัณฑิต
สาขาวิชาวิศวกรรมเคมี ภาควิชาวิศวกรรมเคมี
คณะวิศวกรรมศาสตร์ จุฬาลงกรณ์มหาวิทยาลัย
ปีการศึกษา 2545
ISBN 974-17-2463-2

BUBBLE CHARACTERISTICS AND LIQUID CIRCULATION IN INTERNAL LOOP AIRLIFT CONTACTORS

Miss Porntip Wongsuchoto

A Dissertation Submitted in Partial Fulfillment of the Requirements
for the Degree of Doctor of Engineering in Chemical Engineering
Department of Chemical Engineering
Faculty of Engineering
Chulalongkorn University
Academic year 2002

ISBN 974-17-2463-2

Thesis Title	BUBBLE CHARACTERISTICS AND LIQUID CIRCULATION IN INTERNAL LOOP AIRLIFT CONTACTORS
By	Miss Porntip Wongsuchoto
Field of study	Chemical Engineering
Thesis Advisor	Assistant Professor Prasert Pavasant, Ph.D.
Thesis Co-advisor	Associate Professor Tawatchai Charinpanitkul, D.Eng

---

Accepted by the Faculty of Engineering, Chulalongkorn University in Partial Fulfillment of the Requirements for the Doctor's Degree

…….. Dean of Faculty of Engineering
(Professor Somsak Panyakeow, D.Eng)

THESIS COMMITTEE

…….. Chairman
(Associate Professor Ura Pancharoen, D.Eng.Sc.)

…….……. Thesis Advisor
(Assistant Professor Prasert Pavasant, Ph.D.)

…….. Thesis Co-advisor
(Associate Professor Tawatchai Charinpanitkul, D.Eng)

…….. Member
(Professor Somsak Damronglerd, Dr.Ing (ChE))

…….. Member
(Assistant Professor Sunun Limtrakul, D.Sc. (ChE))

…….. Member
(Assistant Professor Seeroong Prichanont, Ph.D.)

พรทิพย์ วงศ์สุโชโต: พฤติกรรมของฟองก๊าซและการไหลวนภายในของของเหลวในถังสัมผัสอากาศยกประเภทที่มีการไหลวนแบบภายใน (BUBBLE CHARACTERISTICS AND LIQUID CIRCULATION IN INTERNAL LOOP AIRLIFT CONTACTORS) อาจารย์ที่ปรึกษาวิทยานิพนธ์: ผู้ช่วยศาสตราจารย์ ดร. ประเสริฐ ภวสันต์, อาจารย์ที่ปรึกษาวิทยานิพนธ์ร่วม: รองศาสตราจารย์ ดร. ธวัชชัย ชรินพาณิชกุล, 221 หน้า. ISBN 974-17-2463-2

งานวิจัยนี้มีจุดมุ่งหมายเพื่อพัฒนาความรู้พื้นฐานเกี่ยวกับพฤติกรรมของถังสัมผัสอากาศยกประเภทที่มีการไหลวนแบบภายในเพื่อเป็นประโยชน์ในการออกแบบใช้งานในระดับอุตสาหกรรมต่อไปในอนาคต โดยการศึกษาแบ่งออกเป็น 3 ส่วนหลัก คือ (ก) การศึกษาการกระจายตัวของฟองก๊าซภายในถังสัมผัส ฯ และผลกระทบของการกระจายตัวของฟองก๊าซต่ออัตราการถ่ายเทมวลระหว่างก๊าซและของเหลว (ข) การศึกษาปรากฏการณ์การไหลวนภายในของของเหลวภายในส่วนให้อากาศ (Riser) ของถังสัมผัส ฯ และ (ค) การพัฒนาแบบจำลองทางคณิตศาสตร์ที่ใช้ในการทำนายพฤติกรรมการถ่ายเทมวลสารของถังสัมผัส ฯ

การศึกษาการกระจายตัวของฟองก๊าซทำให้ทราบว่าฟองก๊าซภายในส่วนของการให้อากาศ (Riser) จะมีการกระจายตัวแบบปกติเมื่อความเร็วของก๊าซที่ให้กับระบบมีค่าต่ำกว่า 1 ซมต่อวินาที โดยมีค่าขนาดฟองก๊าซเฉลี่ยเท่ากับ 7-8 มิลลิเมตร และการกระจายตัวจะเปลี่ยนจากแบบปกติเป็นแบบ Multimodal เมื่อความเร็วของก๊าซอยู่ในช่วง 2-4 ซมต่อวินาที ซึ่งในช่วงนี้ ฟองก๊าซจะมี 2 กลุ่มหลัก คือกลุ่มที่มีขนาดเฉลี่ยค่อนข้างใหญ่ประมาณ 7-8 มิลลิเมตร และกลุ่มที่มีขนาดเฉลี่ยเล็กประมาณ 3-5 มิลลิเมตร และเมื่อความเร็วสูงขึ้น (จนกระทั่งถึงประมาณ 12 ซมต่อวินาที ซึ่งเป็นความเร็วสูงสุดที่ใช้ในงานวิจัยนี้) การกระจายตัวจะเป็นแบบ Lognormal โดยมีสัดส่วนของฟองก๊าซขนาดเล็กสูงขึ้น ซึ่งขนาดเฉลี่ยของฟองก๊าซในช่วงนี้มีค่าเท่ากับ 3-5 มิลลิเมตร การเพิ่มขนาดของส่วนการให้อากาศมีผลต่อขนาดของฟองอากาศเฉพาะในกรณีที่ความเร็วของอากาศที่ป้อนเข้าสู่ระบบมีค่าสูงกว่า 2.9 ซมต่อวินาที โดยงานวิจัยนี้พบว่าฟองก๊าซมีขนาดเล็กที่สุดเมื่อค่าอัตราส่วนระหว่างพื้นที่หน้าตัดของส่วนการไม่ให้อากาศและส่วนการให้อากาศมีค่าเท่ากับ 0.4 และเมื่อศึกษาถึงความสัมพันธ์ระหว่างขนาดของฟองก๊าซต่อพฤติกรรมการถ่ายเทมวลสารระหว่างวัฏภาคก๊าซและของเหลวพบว่า การเพิ่มความเร็วของก๊าซในช่วงของการทดลองในงานวิจัยนี้ไม่มีผลกระทบที่มีนัยสำคัญต่อค่าสัมประสิทธิ์การถ่ายเทมวล แต่การที่ฟองก๊าซมีขนาดเล็กลงมีส่วนทำให้พื้นที่ผิวการแลกเปลี่ยนมวลระหว่างวัฏภาคทั้งสองนี้มีค่ามากขึ้น และส่งผลให้มีค่าอัตราการถ่ายเทมวลสารระหว่างวัฏภาคมีค่าสูงขึ้น

การเปรียบเทียบความเร็วของของเหลวในส่วนการให้อากาศ (Riser) และส่วนไม่ให้อากาศ (Downcomer) ที่ได้จากการทดลองกับผลการคำนวณจากสมการอนุรักษ์มวลสารและพลังงานแสดงให้เห็นว่าการไหลของของเหลวภายในส่วนให้อากาศ (Riser) นั้นมีทั้งส่วนที่ไหลขึ้นและไหลลง โดยที่สัดส่วนของของเหลวที่ไหลขึ้นต่อของเหลวที่ไหลลงจะเพิ่มขึ้นเมื่อความเร็วก๊าซเพิ่มขึ้น ในขณะที่อัตราส่วนของพื้นที่ของส่วนให้อากาศ กับพื้นที่ของส่วนไม่ให้อากาศไม่มีผลต่อสัดส่วนของพื้นที่ที่ของเหลวไหลลงกับพื้นที่ที่ของเหลวไหลขึ้นในส่วนให้อากาศแต่มีผลกับสัดส่วนของของเหลวที่ไหลขึ้นต่อของเหลวที่ไหลลง ซึ่งสัดส่วนของของเหลวที่ไหลขึ้นต่อของเหลวที่ไหลลงนี้จะมีปริมาณมากขึ้นเมื่ออัตราส่วนระหว่างพื้นที่หน้าตัดของส่วนไม่ให้อากาศต่อพื้นที่หน้าตัดของส่วนให้อากาศเพิ่มขึ้น และสำหรับการพัฒนาแบบจำลองทางคณิตศาสตร์เพื่ออธิบายพฤติกรรมการถ่ายเทมวลสารนั้นได้ทำโดยการแบ่งถังสัมผัสออกเป็น 3 ส่วนที่มีพฤติกรรมการผสมผสานที่แตกต่างกัน คือ ส่วนของการให้อากาศ (Riser) และส่วนของการไม่ให้อากาศ (Downcomer) ให้มีพฤติกรรมแบบการไหลในท่อที่มีการกระจายตัวในแนวการไหล และส่วนการแยกก๊าซ (Gas-Liquid Separator) ให้มีการไหลแบบผสมผสานสมบูรณ์ ซึ่งแบบจำลองที่พัฒนาขึ้นมานี้สามารถทำนายพฤติกรรมการถ่ายเทมวลสารในระบบถังสัมผัสอากาศยกที่ใช้ในงานวิจัยนี้ได้ดี และยังสามารถใช้ในการอธิบายผลการทดลองที่ได้จากการรวบรวมเอกสารได้ในระดับที่น่าพอใจ

ภาควิชา……วิศวกรรมเคมี……..	ลายมือชื่อนิสิต…….
สาขาวิชา ……วิศวกรรมเคมี……..	ลายมือชื่ออาจารย์ที่ปรึกษา……..
ปีการศึกษา……2545…….	ลายมือชื่ออาจารย์ที่ปรึกษาร่วม……..……...

4170428721 : MAJOR CHEMICAL ENGINEERING
KEYWORD: AIRLIFT CONTACTOR/ HYDRODYNAMICS/ MASS TRANSFER/ BUBBLE SIZE DISTRIBUTION/ INTERNAL LIQUID CIRCULATION/ MATHEMATICAL MODEL

PORNTIP WONGSUCHOTO : BUBBLE CHARACTERISTICS AND LIQUID CIRCULATION IN INTERNAL LOOP AIRLIFT COTNACTORS. THESIS ADVISOR: ASSISTANT PROFESSOR PRASERT PAVASANT, Ph.D., THESIS CO-ADVISOR : ASSOCIATE PROFESSOR TAWATCHAI CHARINPANITKUL, D.ENG., 221 PP. ISBN 974-17-2463-2.

This work aimed at the development of the basic knowledge regarding the behavior of the internal loop airlift contactor (ALC). Three main aspects were investigated including: (i) the bubble size distribution in the contactor and its effect on gas-liquid mass transfer; (ii) the internal liquid flow within riser of the contactor; and (iii) the development of the mathematical model for the prediction of gas-liquid mass transfer behavior in the system.

The bubble size distribution in the riser of the ALC was found to follow a normal distribution when the supplied superficial gas velocity was lower than 1 $cm{\cdot}s^{-1}$. The average bubble size in the riser of the system at this condition was found to be about 7-8 mm. As the superficial gas velocity increased to approximately 2-4 $cm{\cdot}s^{-1}$, the size distribution changed from normal to multimodal types with two dominant bubble sizes at 3-5 and 7-8 mm. At a high range of superficial gas velocity (5 $cm{\cdot}s^{-1}$ up to the upper limit of this work at 12 $cm{\cdot}s^{-1}$), the bubble size followed a lognormal distribution with a small bubble at 3-5 mm dominating the system. The cross-sectional area ratio between downcomer and riser of the ALC was found to affect the bubble size only when the superficial gas velocity was greater than 2.9 $cm{\cdot}s^{-1}$ and the ratio of 0.4 was observed to give the lowest average bubble size. The analysis of the bubble size distribution revealed that the increase in the superficial gas velocity did not have significant effect on the gas-liquid mass transfer coefficient in the ALC, rather it caused the bubble to become smaller. This increased the mass transfer area between gas and liquid which increased the overall gas-liquid mass transfer rate.

The comparison between liquid velocity from experiment and from mass/energy balances indicated that there must exist an internal liquid circulation within the riser. The downflow liquid flowrate in the riser was found to increase with superficial gas velocity. The ratio between downcomer and riser cross sectional areas (A_d/A_r) was found not to influence the fraction of downflow and upflow areas but the extent of internal circulation was less pronounced in the system with a large A_d/A_r. The mathematical model for the ALC divided the system into three sections, each of which had different mixing performance. The first two sections were riser and downcomer for which the mixing were described by a plug flow with dispersion. The gas separation section at the top of the ALC, on the other hand, was described by a completely mixed model. Not only did the simulation results on the oxygen concentration profiles agreed well with the experimental results obtained from this work, it also could satisfactorily explain the results of the experiments reported in literature.

Department ….Chemical Engineering.. Student's signature…….
Field of study…Chemical Engineering… Advisor's signature…….
Academic year .2002……. Co-advisor's signature……...

Acknowledgements

This thesis is the result of five years of research whereby I have been accompanied and supported by many people. It is a pleasant aspect that I have now the opportunity to express my gratitude for all of them.

Firstly, I wish to express my deepest gratitude to my thesis advisor, Assistant Professor Dr. Prasert Pavasant. He is the first who provided me the opportunity to go on to Doctoral learning. During these years of my Doctoral learning he always kept an eye on the progress of my work and was available when I needed his advices. His mission for providing only high-quality work and not less has made a deep impression on me. The thoughts he has offered have enriched my thesis and he to me is not just an advisor, but is as close as a relative and a good friend. He could not even realize how much I have learned from him. I am really glad that I have come to get know him in my life. This thesis would not have been accomplished without his excellent supervision. Thank you for enormous time and energy dedicated to my success. Thank you doesn't seem sufficient but it is said with appreciation and respect. I would like to thank Associate Professor Dr. Tawatchai Charinpanitkul, my kindly co-advisor, for his invaluable advice regarding many interesting issues in bubble characteristics and for providing me useful comments and suggestions on my thesis and my first publication. His support and encouragement motivated me to continue my task.

I would also like to thank the other members of my Doctoral committee who monitored my work and took effort in reading and providing me with valuable comments: Associate Professor Dr. Ura Panchareon, chairman of the committee, Professor Dr. Somsak Damronglerd, Assistant Professor Dr. Seeroong Prichanont and Assistant Professor Sunan Limtrakul. I thank them all. This research has been supported and funded by Thailand research fund (TRF) and Engineering Faculty research fund. I thank them as well. I have learnt so much during the past five years and every bit of warm support from friends has always been appreciated. Many persons have contributed to this thesis. I would also like to gratefully acknowledge the support of some very special individuals. I am deeply indebted to Koi+ who helped me in finding necessary literatures tirelessly. Chean, your MATLAB source code prototype saved me many hours of labor, thank you. I would like to thank Pom for our many discussions and providing me advises and information that helped me in solving mathematical model in Chapter 6. Many enjoyable hours were spent with Thorn, my colleague, who has worked with me in the first and the second year of work. She helped me immensely by giving me encouragement and friendship. I could hardly have completed the thesis without my faithful friends, Oh, Lee and Pu. Thank you for being such wonderful and close friends who always are available when I need their help, and never stopped asking "When will it be finished?" Special thanks are given to Ko, a lovely technician in my department, and Kob for their part in assisting me in setting up and repairing my computer for several times. I would like to thank Nim for her wonderful blueberry pies. Many thanks for you all who gave me the feeling of being at home at work, Tar, Ku, Kib and Jung. Thank you for always being there for dinner. Special thanks to Tar and Ku for always being badminton and table tennis buddies. I thank Poom, Pom, Jung, Ku, Tar and Kib for having shared the time at night in our laboratory during the last two years of my Doctoral period. A special thanks goes to Ann, who showed to be a kind, mostly helpful and trustful friend. Thank you also goes to all other members of Biochemical Engineering Laboratory and Environmental Chemical Engineering and Safety Laboratory for their cooperation, assistance and support. The learning experience and memories with all of you will always be cherished.

Most of all, I would like to express my utmost gratitude to my parents and everyone in my family for their support in my decision to go on to Doctoral learning. Thank you for always believing in me and giving me emotional support. I thank them for their understanding and encouragement to finish this thesis. I feel a deep sense of gratitude for my parents who taught me the good things that really matter in life. Last, thank you for their love, inspiration and invaluable supports at all times.

Contents

List of Tables

List of Figures

List of Figures

Figure Page

List of Figures

Figure Page

List of Figures

Figure Page

List of abbreviations and notations

Abbreviations

ALC Airlift contactor

ALR Airlift reactor

BC Bubble column

Bo Bodenstein number $\left(\frac{D_L}{u_L D_o}\right)$

CSTR Continuous stirred tank reactor

Fr Froude number $\left(\frac{u_{sg}^2}{gD_o}\right)$

Ga Galileo number $\left(\frac{g\rho_L^2 D_o^3}{u_L^2}\right)$

Gr Grashof Number $\left(\frac{d_{Bs}^3 \rho_L \Delta\rho g}{\mu_L^2}\right)$

Mo Morton number $\left(\frac{g\mu_L^4}{\rho_L \sigma_L^2}\right)$

Pe Peclet number $\left(\frac{u_L D_o}{D_L}\right)$

PFR Plug flow reactor

Ra Rayleigh number $\left(\frac{d_{Bs}^3 \Delta\rho g}{\mu_L D_L}\right)$

Re Reynolds Number $\left(\frac{d_{Bs} v_s \rho_L}{\mu_L}\right)$

RHS Right hand side

Sc Schmidt number $\left(\frac{\mu_L}{\rho_L D_L}\right)$

Sh Sherwood Number $\left(\frac{k_L d_{Bs}}{D_L}\right)$

STR Stirred tank reactor

We Weber number $\left(\frac{\rho_L u_{b\infty}^2 d_{Bs}}{2\sigma_L} \right)$

Notations

A cross-sectional area [m^2]

a specific gas-liquid interfacial area of bubble per volume of reactor [$m^2 \cdot m^{-3}$]

A_b cross sectional area for flow under baffle or draft tube [m^2]

a_D specific gas-liquid interfacial area based on gas-liquid dispersion volume [$m^2 \cdot m^{-3}$]

A_{dc} apparent contacted cross-sectional area at downcomer entrance [m^2]

a_L specific gas-liquid interfacial area based on liquid volume [$m^2 \cdot m^{-3}$]

$A_{r,down}$ downflow area of riser when internal liquid circulation occurs [m^2]

$A_{r,up}$ upflow area of riser when internal liquid circulation occurs [m^2]

A_{rc} apparent contacted cross-sectional area at riser entrance [m^2]

C instantaneous oxygen concentration in the liquid [$kg \cdot m^{-3}$]

C^* saturation dissolved oxygen concentration in the liquid [$kg \cdot m^{-3}$]

C_0 initial oxygen concentration in the liquid [$kg \cdot m^{-3}$]

Crk^2/σ_L parameter of bubble coalescence proposed by Marrucci [-]

C_s Solid phase concentration [$kg \cdot m^{-3}$]

D column diameter [m]

d_B bubble diameter [m]

d_B equivalent size of the bubble [m]

d_{Bs} Sauter mean bubble diameter [m]

D_{dt} draft tube diameter [m]

De equivalent diameter [m]

D_G gas phase dispersion coefficient [$m^2 \cdot s^{-1}$]

D_i inner diameter of draft tube [m]

D_{io} outer diameter of draft tube [m]

D_L diffusivity of gas or solute in liquid [$m^2 \cdot s^{-1}$]

D_L liquid phase dispersion coefficient [$m^2 \cdot s^{-1}$]

D_o inner diameter of column [m]

d_o	orifice diameter [m]
D_{O2}	diffusivity of oxygen in liquid phase [$m^2 \cdot s^{-1}$]
DR	disengagement ratio
D_s	internal diameter of gas-liquid separator [m]
$\sum \ddot{E}$	rate of energy dissipation due to internal turbulence and friction between the gas-liquid interface [W]
$\sum \hat{E}$	rate of energy losses due to friction between the fluids and the reactor [W]
$\ddot{E}_b$	drift of gas with respect to the liquid in the bottom [W]
$\hat{E}_b$	energy loss due to the skin friction at the bottom [W]
$\ddot{E}_d$	energy losses associate with turbulence and internal friction in downcomer [W]
$\hat{E}_d$	energy loss due to the skin friction in the downcomer [W]
E_{in}	rate of energy input due to isothermal gas expansion [W]
$\ddot{E}_r$	energy losses associate with turbulence and internal friction in riser [W]
$\hat{E}_r$	energy loss due to the skin friction in the riser [W]
$\ddot{E}_t$	drift of gas with respect to the liquid in the top [W]
$\hat{E}_t$	energy loss due to the skin friction at the top [W]
e_v	friction factor
$\hat{E}_v$	friction loss that is the rate at which mechanical energy is irreversibly converted to thermal energy [W]
$f(d_B)$	relative frequency of bubble size, d_B (-)
f	friction factor [-]
F_f	filling factor [-]
$f_{r,down}$	friction factor in downflow region of riser [-]
$f_{r,up}$	friction factor in upflow region of riser [-]
G	mass flow rate of the gas [$kg \cdot s^{-1}$]
g	gravitational acceleration [$m \cdot s^{-1}$]
H	height [m]
H_D	dispersion height [m]
H_{DT}	dispersion height above draft tube [m]

H_{dt} draft tube height [m]

H_L unaerated liquid height [m]

H_{LT} unaerated liquid height above draft tube [m]

h_r height or riser [m]

H_r height of riser [m]

K Consistency index of fluid [$Pa \cdot s^n$]

K_b frictional loss coefficient for the bottom [-]

k_d acceleration coefficient at downcomer entrance [-]

K_f total friction coefficient [-]

k_L liquid phase mass transfer coefficient [$m \cdot s^{-1}$]

K_L liquid phase mass transfer coefficient [$m \cdot s^{-1}$]

K_La overall mass transfer coefficient [s^{-1}]

k_La overall volumetric oxygen transfer coefficient [s^{-1}]

k_La_D overall volumetric mass transfer coefficient based on dispersion volume [s^{-1}]

k_La_L overall volumetric mass transfer coefficient based on liquid volume [s^{-1}]

k_r acceleration coefficient at riser entrance [-]

K_t frictional loss coefficients for the top [-]

L length [m]

L_b bottom clearance [m]

L_c connection length between riser and downcomer of external loop airlift contactor [m]

L_d distance between measurement points in downcomer [m]

L_d downcomer length [m]

L_e equivalent length [m]

L_h height between horizontal connections [m]

L_r distance between measurement points in riser [m]

L_r length of riser [m]

$L_{r,down}$ length of downflow region in riser [m]

$L_{r,up}$ length of upflow region in riser [m]

L_t top clearance [m]

M Bubble separation group $\left(\frac{D_s}{4D_o} \right)$

M_w	molar mass of gas [$kg \cdot mol^{-1}$]
n	flow behavior index [-]
n_{O_2}	flux of oxygen transfer between phases [$mol \cdot m^{-2} \cdot s^{-1}$]
n	moles of a gas [mol]
n	orifice number
$\bar{O}_G$	dimensionless oxygen concentration in gas phase [-]
O_G	oxygen concentration in gas phase [$kg \cdot m^{-3}$]
$\bar{O}_L$	dimensionless oxygen concentration in liquid phase [-]
O_L	oxygen concentration in liquid phase [$kg \cdot m^{-3}$]
O_L^*	saturation concentration of transferring gas or solute in liquid [$kg \cdot m^{-3}$]
p	length of major axis of bubble [m]
P	pressure [Pa]
P_1	pressure at location 1 [Pa]
P_2	pressure at location 2 [Pa]
P_b	pressure at the bottom of the contactor [Pa]
P_{db}	static pressure in the annulus at the bottom of downcomer [Pa]
P_{ds}	static pressure in the annulus at the top of downcomer [Pa]
P_G	total power input in a pneumatic contactor [W]
P_G/V_L	specific power input per unit volume of liquid [$W \cdot m^{-3}$]
P_{GE}	potential energy during the isothermal expansion of the gas as it moves up the reactor [W]
P_h	pressure of gas at the column head [Pa]
P_{KE}	Kinetic energy transferred to the fluid by a jet of gas entering the reactor [W]
P_{rb}	static pressure in draft tube at the bottom of riser [Pa]
P_{rs}	static pressure in draft tube at the top of riser [Pa]
P_t	pressure at the top of the contactor [Pa]
q	length of minor axis of bubble [m]
Q_G	volumetric gas flowrate [$m^3 \cdot s^{-1}$]
$Q_{G,in}$	inlet volumetric gas flowrate [$m^3 \cdot s^{-1}$]
$Q_{G,out}$	outlet volumetric gas flowrate [$m^3 \cdot s^{-1}$]
Q_{Gm}	molar flow rate of the gas [$m^3 \cdot s^{-1}$]
$Q_{L,in}$	inlet volumetric liquid flowrate [$m^3 \cdot s^{-1}$]

$Q_{L,out}$ outlet volumetric liquid flowrate [$m^3 \cdot s^{-1}$]

$Q_{Lr,down}$ volumetric liquid flowrate in downflow region of riser [$m^3 \cdot s^{-1}$]

$Q_{Lr,up}$ volumetric liquid flowrate in upflow region of riser [$m^3 \cdot s^{-1}$]

R gas constant [$J \cdot mol^{-1} \cdot K^{-1}$]

R_h hydraulic radius [m]

$R_{hr,down}$ hydraulic radius of downflow region in riser [m]

$R_{hr,up}$ hydraulic radius of upflow region in riser [m]

S cross-sectional area [m^2]

T absolute temperature [K]

$\overline{t}$ dimensionless time [-]

t time [s]

t_c circulation times [s]

t_d average time of tracer traveling in downcomer along the distance L_d [s]

t_m mixing time [s]

t_r average time of tracer traveling in riser along the distance L_r [s]

u_∞ terminal rise velocity of bubbles [$m \cdot s^{-1}$]

u_{BT} terminal rise velocity of bubbles [$m \cdot s^{-1}$]

u_G superficial gas velocity[$m \cdot s^{-1}$]

u_{Go} superficial gas velocity at the sparger outlet [$m \cdot s^{-1}$]

u_{Gr} superficial gas velocity in riser [$m \cdot s^{-1}$]

u_L superficial liquid velocity [$m \cdot s^{-1}$]

u_{sg} superficial gas velocity [$m \cdot s^{-1}$]

v velocity [$m \cdot s^{-1}$]

V volume [m^3]

V_b gas volume at the bottom of the contactor [m^3]

V_D dispersion volume [m^3]

v_G linear gas velocity [$m \cdot s^{-1}$]

$v_{G,in}$ inlet gas velocity [$m \cdot s^{-1}$]

$v_{G,out}$ outlet gas velocity [$m \cdot s^{-1}$]

v_L linear liquid velocity [$m \cdot s^{-1}$]

V_L liquid volume [m^3]

$v_{Ld\alpha}$ linear velocities of the liquid phase at the contracted entrances of the downcomer [$m \cdot s^{-1}$]

$v_{Lr,down}$ linear liquid velocity of downflow region in riser [$m \cdot s^{-1}$]

$v_{Lr,up}$ linear liquid velocity of upflow region in riser [$m \cdot s^{-1}$]

$v_{Lr\alpha}$ linear velocities of the liquid phase at the contracted entrances of the riser [$m \cdot s^{-1}$]

v_s slip velocity [$m \cdot s^{-1}$]

V_t gas volume at the top of the contactor [m^3]

$\dot{w}$ mass flow rate [$kg \cdot s^{-1}$]

$\hat{W}$ rate at which the system performs mechanical work on its surroundings [W]

W rate of work done to promote liquid circulation [J]

$\hat{w}$ work done during isothermal expansion [J]

$\dot{w}_{Ld}$ liquid mass flow rate in downcomer [$kg \cdot s^{-1}$]

$\dot{w}_{Lr}$ liquid mass flow rate in riser [$kg \cdot s^{-1}$]

$\dot{w}_{Lr,down}$ liquid mass flowrate in downflow region of riser [$kg \cdot s^{-1}$]

$\dot{w}_{Lr,up}$ liquid mass flowrate in upflow region of riser [$kg \cdot s^{-1}$]

x axial distance from the sparger [m]

X, X_{dt} bottom clearance ratio $\left(\frac{L_b}{D_{dt}}\right)$

Y top clearance ratio $\left(\frac{L_t}{D_{dt}}\right)$

Z dimensionless length [-]

Z wetted perimeter

Z_d downcomer hydraulic head [m]

Z_r riser hydraulic head [m]

v_s slip velocity [$m \cdot s^{-1}$]

Greek letter

α constant in Table 2.1

$s.d.$ standard deviation [m]

σ surface tension [$N \cdot m^{-1}$]

ΔC concentration driving force between the two phases [$kg \cdot m^{-3}$]

Δh	distance between pressure measurement points [m]
ΔP	hydrostatic pressure difference between two measuring points [Pa]
Δz	difference of liquid height in a manometer [m]
$\Delta\rho$	difference between gas and liquid density [$kg \cdot m^{-3}$]
Φ	potential energy per unit mass
β	constant in Table 2.1
δ	sparger hole or nozzle diameter [m]
ε_G	gas holdup [-]
ε_{Go}	overall gas holdup [-]
$\varepsilon_{Gr,down}$	gas holdup in downflow region of riser [-]
$\varepsilon_{Gr,up}$	gas holdup in upflow region of riser [-]
ε_s	solid holdup [-]
η	efficiency of energy transfer [-]
μ	viscosity [$kg \cdot m^{-1} \cdot s^{-1}$]
μ_{app}	apparent viscosity [$kg \cdot m^{-1} \cdot s^{-1}$]
ρ	density [$kg \cdot m^{-3}$]
ρ_D	gas-liquid mixture density [$kg \cdot m^{-3}$]
σ	surface tension [$N \cdot m^{-1}$]
τ	dimensionless time [-]

Subscript

app	apparent
b	bottom of the contactor
D	dispersion
d	downcomer
dt	draft tube
G	gas
h	homogeneous phase
in	input
L	liquid
o	overall

out	output
r	riser
S	solid
t	top (or head space) of the contactor
T	total

Chapter 1

Introduction

1.1 Motivation

1.1.1 Why do we select airlift contactors?

Gas-liquid contactors are of common use in several fields such as biochemical fermentation, biological waste water treatment processes, production of beer, vinegar, citric acid, and biomass from yeast, lactic yeast production, production of biological metabolites, fuel ethanol production, chlorination of ethylene, gas absorption etc.[1-11]

At present, various designs of gas-liquid contacting devices are used in chemical and biochemical processes, among which the most common type found in commercial chemical processes is a stirred tank reactor (STR). However, several limitations (as summarized in Table 1.1) lead to relatively confined applications of the STR especially in biochemical fields, which are regularly operated at mild conditions (normal pressure and temperature, and low shear stress). Therefore pneumatic reactors such as bubble columns (BC) and airlift contactors (ALC) are proposed as alternative designs of gas-liquid contacting devices[3-4,12-16] because of its several advantages over the STRs.

The ALC is known as a gas-liquid contacting device modified from the BC. The main distinction between the ALC and the BC is that in the former the rate of liquid circulation depends on the gas flow rate, whereas in the latter the liquid flow is independent of gas flow. Consequently, large liquid throughput is hardly obtained in BCs, and this requires the BC to be equipped with an external liquid pump particularly in the case where high liquid circulation rate is needed. This simply implies extra operating cost for the BC. In ALCs, on the other hand, comparatively high liquid velocities may be achieved without the need for any external recirculation devices. For this reason, the ALC becomes an excellent alternative for a gas-liquid contacting apparatus.

In spite of several advantages over other types of gas-liquid contactors (as summarized in Table 1.1), the industrial application of ALCs is still limited because of several reasons as explained in the following section.

1.1.2 Important parameters characterizing airlift contactor performance

To design and operate ALCs with confidence, the knowledge of gas-liquid mass transfer is required to characterize the performance of the ALC. The main parameter used as an indicator for gas-liquid mass transfer rate is the gas-liquid mass transfer coefficient (K_La).

A large number of researchers[16,21-27] have investigated the mass transfer performance in the ALCs together with their hydrodynamic behavior. It was found that the knowledge of hydrodynamic behavior is critical for design purposes because of their strong influence on mass transfer. The characteristics generally used to describe hydrodynamic behavior in ALC consist of gas holdup, bubble average size and velocity, as well as liquid velocity or mixing time. In addition, each of these quantities may be influenced by several independent factors, such as superficial gas velocity, cross-sectional area ratio between downcomer and riser, gas sparger geometry, etc. Due to the rather complex interactions between these parameters, the design of ALC to fulfill specific purposes is still extremely difficult.

Although a large number of investigations[12,14-16,21-26,28-29] contributed to the knowledge of effect of various parameters on hydrodynamic and mass transfer characteristics in ALCs, available information frequently showed wide variations and conflicting claims. The contradiction is regularly attributed to the difference in the reactor geometries, experimental conditions and experimental techniques. Also the present knowledge suggests that this contradiction is brought about by some complicated phenomena taking place in ALC, such as the bubble size distribution, internal liquid circulation, etc.

Several researchers[30-41] reported that bubble properties played an important role in defining the hydrodynamic and mass transfer characteristics in gas-liquid contacting devices, such as stirred tanks and bubble columns. In ALC, most of available investigations assumed homogeneous flow in riser and downcomer in order to find the relationship between the bubble properties and the behavior of the system.[42-43] Nonetheless, some literature[30] showed that bubble size in the airlift

contactor was not constant along the column height especially at high gas flow rate. This is a result of the coalescence or breakup of bubbles. Therefore the estimation of the interfacial area from an average global bubble diameter and total gas volume is not usually satisfactorily accurate. Hence, information about bubble characteristics has to be considered in the attempt to understand the performance of airlift contactors. Although a large number of available research papers already have described the bubble size distribution and bubble behavior in some types of gas-liquid contactor, i.e. bubble column,[30-41] very few investigations on bubble characteristics in the airlift contactors have been published.[30,44-45] This unavailability of information regarding the bubble characteristics is due to the lack of precise measurement method for the in-situ evaluation of the bubble characteristics in the ALC.

There are only few reports on the internal liquid circulation in the ALCs.[28-29] The importance of this circulation on the ALC performance was stated[28-29,46] but none, thus far, has thoroughly looked into its mechanism. The disregard of these details leads to the misunderstanding in the ALC behavior and as long as the understanding of mass and momentum transport phenomena in ALC is not well established, the development of ALC in industrial application is still difficult.

This work focuses on the investigation of bubble characteristics, e.g., bubble size, bubble size distribution and of the internal liquid circulation in an internal loop airlift contactor. The ultimate goal of this work is to clarify the mechanism of mass and momentum transport and the performance of the internal loop airlift contactor over a wide range of geometrical and operational parameters for design purpose.

1.2 Objectives

1.2.1 To investigate bubble characteristics in internal loop airlift contactors.

1.2.2 To investigate internal liquid circulation in internal loop airlift contactors.

1.2.3 To establish empirical correlations to predict hydrodynamic behavior and mass transfer rate in internal loop airlift contactors.

1.2.4 To establish mathematical model to predict hydrodynamic behavior and mass transfer rate in internal loop airlift contactors.

1.3 Scope of the work

1.3.1 The investigations were restricted to bench-scale internal loop ALCs with dimensions as shown in Table 3.1.

1.3.2 The investigations were performed in an air-water system only.

1.3.3 The investigations of bubble characteristics were restricted to bubble size and bubble size distribution.

1.3.4 The investigations of mass transfer characteristics were restricted to oxygen transfer only, and in all investigations, the ALC systems were subject to the following assumptions:

- Gas composition is constant.
- The system is isothermal, and the effect of the dynamics of the dissolved oxygen electrode is negligible.
- For sparingly soluble gases such as oxygen, the liquid phase volumetric mass transfer coefficient (k_La) is nearly equal in value to that of the overall volumetric mass transfer coefficient (K_La).

1.3.5 In the investigations of hydrodynamic behavior, gas density was considered negligible compared to the density of the liquid.

1.4 References

1. Nakanoh, M., and Yoshida, J. 1980. Gas absorption by Newtonian and non-Newtonian liquids in a bubble column. Ind. Eng. Chem. Proc. Des. Dev. 19: 190.
2. Blenke, H. 1985. Biochemical loop reactors. In H. Brauer (ed.), Biotechnology, Vol. 2, Weinheim, 465-517.
3. Chisti, M.Y., and Young, M.M. 1987. Airlift reactors: characteristics, applications and design considerations. Chem. Eng. Commun. 60: 195-242.
4. Siegel, M.H., and Merchuk, J.C. 1988. Air-Lift reactors in chemical and biological technology. J. Chem. Tech. Biotech. 41: 105-120.
5. Pigache, S., Trystram, G., and Dhoms, P. 1992. Oxygen transfer modeling and simulations for an industrial continuous airlift fermentor. Biotech. Bioeng. 39: 923-931.

6. Russell, A.B., Thomas C.T., and Lilly M.D. 1994. The influence of vessel height and top-section size on the hydrodynamic characteristics of airlift fermentors. Biotech. Bioeng. 43: 69-76.
7. Dluhý, M., Šefčík, J., and Báleš, V. 1994. Mathematical modelling of airlift bioreactor for waste water treatment. Comp. Chem. Engng. 18: 725-729.
8. Khare, A.S. and Niranjan, K. 1995. Impeller-agitated aerobic reactor: The influence of tiny bubbles on gas hold-up and mass transfer in highly viscous liquids. Chem. Eng. Sci. 50(7): 1091-1105.
9. Tung, H.-L., Chiou, S.-Y., Tu, C.-C., and Wu, W.-T. 1997. An airlift reactor with double net draft tubes and its application in fermentation. Bioproc. Engng. 17: 1-5.
10. Vicente, A.A., Dluhy, M., and Teixeira, J.A. 1999. Increase of ethanol productivity in an airlift reactor with a modified draught tube. Can. J. Chem. J. 77: 497-502.
11. Orejas, J.A. 2001. Model evaluation for an industrial process of direct chlorination of ethylene in a bubble-column reactor with external recirculation loop. Chem. Eng. Sci. 56: 513-522.
12. Merchuk, J., and Siegel, M.H. 1988. Air-lift reactors in chemical and biological technology. J. Chem. Tech. Biotech. 41: 105-120.
13. Siegel, M.H., and Robinson, C.W. 1992. Applications of airlift gas-liquid-solid reactors in biotechnology. Chem. Eng. Sci. 47: 3215-3229.
14. Wu, W.-T., Wu, J.-Y., and Jong, J.-Z. 1992. Mass transfer in an airlift reactor with a net draft tube. Biotech. Prog. 8: 465-468.
15. Benyahia, F., Jones, L. Petit, S., and Plantaz D. 1996. Mass transfer studies in pneumatic reactors. Chem. Eng. Tech. 19: 425-431.
16. Tung, H.-L., Tu, C.-C., Chang, Y.-Y., and Wu, W.-T. 1998. Bubble characteristics and mass transfer in an airlift reactor with multiple net draft tubes. Bioproc. Eng. 18: 323-328.
17. Onken, U., and Weiland, P. 1980. Hydrodynamics and mass transfer in an airlift loop fermentor. Eur. J. Appl. Microbiol. Biotechnol. 10: 31-40.
18. Kang, Y., Min, B.T., Nah, J.B. and Kim, S.D. 1990. Mass transfer in continuous bubble columns with floating bubble breakers. AIChE J. 36(8): 1255-1258.

19. Yagna, P.K., and Ramanujam, T.K. 1995. Gas holdup and overall volumetric mass transfer coefficient in a modified reversed flow jet loop reactor. Can. J. Chem. Eng. 73: 190-195.
20. Verlaan, P., and Tramper, J. 1987. Hydrodynamics, axial dispersion and gas liquid oxygen transfer in an airlift loop bioreactor with three phase flow. Paper 14 International Conference on bioreactors and biotransformations Gleneagles, Scotland, UK: 9-12 Nov.
21. Bello, R. A., Robinson, C. W. and Moo-Young, M., 1985. Gas hold-up and overall volumetric oxygen transfer coefficient in airlift contactors. Biotech. Bioeng. 27: 369-381.
22. Chisti, M. Y., and Moo-Young, M. 1988. Hydrodynamics and oxygen transfer in pneumatic devices. Biotech. Bioeng. 31: 487 - 494.
23. Choi, K.H., and W.K. Lee. 1993. Circulation liquid velocity, gas holdup and volumetric oxygen transfer coefficient in external-loop airlift reactors. J. Chem. Tech. Biotech. 56: 51-58.
24. Koide K., Hiroyuki S., and Shinji I. 1983a. Gas holdup and volumetric liquid-phase mass transfer coefficient in bubble column with draught tube and with gas dispersion into annulus. J. Chem. Eng. Japan 16(5): 407-413.
25. Koide K., Katsumi K., Shinji I., Yutaka I., and Kazuyoshi H. 1983b. Gas holdup and volumetric liquid-phase mass transfer coefficient in bubble column with draught tube and with gas dispersion into tube. J. Chem. Eng. Japan 16(5): 413-419.
26. Merchuk, J.C., Ladwa N., Cameron A., Bulmer M., and Pickett A. 1994. Concentric-Tube Airlift Reactors: Effects of Geometrical Design on Performance. AIChE J. 40(7): 1105-1117.
27. Shimizu, K., Takada, S., Takahashi, T., and Kawase, Y. 2001. Phenomenological simulation model for gas holdups and volumetric mass transfer coefficients in external-loop airlift reactors. Chem. Eng. J. 84: 599-603.
28. Jones, A.G. 1985. Liquid circulation in a draft-tube bubble column. Chem. Eng. Sci. 40: 449-462.
29. Wachi, S., Jones, A.G., and Elson, T.P. 1991. Flow dynamics in a draft-tube bubble column using various liquids. Chem. Eng. Sci. 46(2), 657-663.

30. Colella, D., Vinci, D. Bagatin, R. Masi, M., and Bakr, E.A. 1999. A study on coalescence and breakage mechanisms in three different bubble columns. Chem. Eng. Sci. 54: 4767-4777.
31. Camarasa, E., Vial, C., Poncin, S., Wild G., Midoux N., and Bouillard J. 1999. Influence of coalescence behaviour of the liquid and of gas sparging on hydrodynamics and bubble characteristics in a bubble column. Chem. Eng. Proc. 38: 329-344.
32. Luewisutthichat, W., Tsutsumi A., and Yoshida, K. 1997. Bubble characteristics in multiphase flow systems: bubble sizes and size distributions. J. Chem. Eng. Japan 30: 461-466.
33. Yu, Y.H., and Kim, S.D. 1991. Bubble properties and local liquid velocity in the radial direction of cocurrent gas-liquid flow. Chem. Eng. Sci. 46: 313-320.
34. Lee, D.J., Luo, X., and Fan, L.-S. 1999. Gas disengagement technique in a slurry bubble column operated in the coalesced bubble regime. Chem. Eng. Sci. 54: 2227-2236.
35. Koide, K., Kato, S., Tanaka, Y., and Kubota, H. 1968. Bubble generated from porous plate. J. Chem. Eng. Japan 1: 51-56.
36. Kumar, A., Degaleesan, T.E., Laddha, G.S., and Hoelscher, H.E. 1976. Bubble swarm characteristics in bubble columns. Can. J. Chem. Eng. 54: 503-508.
37. Wilkinson, P.M., and Dierendonck, L.L.v. 1990. Pressure and gas density effects on bubble break-up and gas holdup in bubble columns. Chem. Eng. Sci. 45 (8): 2309-2315.
38. Sriram, K., and Mann, R. 1977. Dynamic gas disengagement: A new technique for assessing the behaviors of bubble columns. Chem. Eng. Sci. 32: 571-580.
39. Buchholz, H., Buchholz, R., Lücke, J., and Schügerl, K. 1978. Bubble swarm behaviour and gas absorption in non-Newtonian fluids in sparged columns. Chem. Eng. Sci. 33: 1061-1070.
40. Daly, J.G., Patel, S.A., and Bukur, D.B. 1992. Measurement of gas holdups and Sauter mean bubble diameters in bubble column reactors by dynamic gas disengagement method. Chem. Eng. Sci. 47: 3647-3654.
41. Chen, S., Timmons, M.B., Aneshansley, D.J., and Bisogni, J.J. 1992. Bubble size distribution in a bubble column applied to aquaculture systems. Aquacultural Eng. 11: 267-280.

42. Bailey, J.E., and Ollis, D.F. 1979. Biochemical Engineering Fundamentals. New York: McGrawHill.
43. van Krevelen, D.W., and Hoftijzer, P.J. 1950. Studies of gas bubble formation: Calculation of interfacial area in bubble contactor. Chem. Eng. Prog. 46: 29.
44. Miyahara, T., Hamaguchi M., Sukeda, Y., and Takahashi, T. 1986. Size of Bubbles and liquid circulation in a bubble column with a draught tube and sieve plate. Can. J. Chem. Eng. 64: 718-725.
45. Lo, C.-S., and Hwang, S.-J. 2003. Local hydrodynamic properties of gas phase in an internal-loop airlift reactor. Chem. Eng. J. 91: 3-22.
46. Calvo, E.G., and Leton, P. 1991. A fluid dynamic model for bubble columns and airlift reactors. Chem. Eng. Sci. 46(11): 2947-2951.

1.5 Table

Table 1.1 Comparison of gas-liquid contacting devices

Types of gas-liquid contacting devices	Advantages	Limitations
1. Stirred tank reactor (STR)	1) Well defined performance and scale-up characteristics[13] 2) High mass transfer 3) Easy control of the gas dispersion and medium mixing by stirrer speed 4) Efficient gas dispersion by stirrers 5) Suitable for highly viscous media	1) High power consumption per unit volume of liquid[17] 2) Difficulty in avoiding contamination due to sealing of shaft[17] 3) High shear stress and lack of uniformity in the fields of shear[13] 4) Low oxygen transfer efficiency of with respect to power input 5) Production of high degree of heat 6) Gas dispersion and mixing efficiency of stirrers are extremely low 7) Inappropriate for low performance process
2. Bubble column (BC)	1) Simplicity of their design and construction: no moving mechanical part needed for agitation[13,14,18] 2) Ease of maintenance[13,14] 3) Eliminating the danger of contamination through seals[13] 4) Low power consumption[13,18] 5) Low capital cost[15]	1) Low mass transfer efficiency 2) Lack of uniformity in the fields of shear[13]
3. Airlift contactor (ALC)	1) Simplicity of their design and construction: no moving mechanical part needed for agitation[3, 13-15,19] 2) Ease of maintenance[14] 3) Eliminating the danger of contamination	1) Low mass transfer efficiency

Types of gas-liquid contacting devices	Advantages	Limitations
	through seals[3,13,15] 4) Low power consumption per unit volume of liquid [3, 13, 15,19] 5) Low capital cost[15, 19] 6) Low and homogeneous shear stress region and uniform turbulence [12-13, 20] 7) Better defined flow pattern[3,19] 8) Controllable liquid circulation rate[20]	

Chapter 2

Backgrounds and Literature Reviews

2.1 Backgrounds: Airlift Contactor

An airlift contactor (ALC) is a class of gas-liquid contacting devices in which all mixing is produced by the movement of gas bubbles. This means that no mechanically agitated device is needed in the operation of the ALC. The configuration of the ALC enables a natural liquid circulation in the system, and this unique characteristic distinguishes the ALC from other types of pneumatic contactors such as bubble columns (BC). Figure 2.1 shows the configuration of an ALC showing an internal loop compared with a BC. Figure 2.1 (b) illustrates that the ALC consists of three different regions with distinct fluid flow patterns as described below:

1) Riser: The section into which gas is dispersed. This section contains higher gas content and consequently higher gas holdup so fluid density is rather low compared to that in other sections. For this reason, both gas and liquid flow upward co-currently.

2) Gas-liquid separator: The section from which gas disengages. This section locates at the top of riser and downcomer. Fluid enters this section through the riser and mixes rigorously with the fluid that stays here earlier. It leaves after spending some time in this section to the downcomer. Some of the gas bubbles separate from the fluid at the top of the contactor.

3) Downcomer: The section through which the fluid flows downwards. The fluid might be two phases (gas and liquid) or single phase (liquid only) depending on the hydrodynamic conditions in the system. The fluid in the downcomer recirculates to the riser again at the bottom of the contactor.

Although various designs of ALCs were used in the literature, the configurations of ALCs can be classified according to their physical appearance into two classes:

1) Internal loop ALC: This class can be represented simply by a simple bubble column split into a riser and a downcomer by an internal baffle. A baffle plate or a draft tube can be used as an internal baffle, creating a split cylinder (Fig. 2.2 (a)) or a concentric

tube configuration (Fig. 2.2 (b)), respectively. In the concentric tube ALC, the gas may be distributed either in the draft tube or in the annulus as shown in Figure 2.2 (b).

2) External loop ALC: In this category, the riser and the downcomer are two separated columns connected by horizontal sections near the top and the bottom. The fluid circulation takes place between these two separated columns. Usually less gas recirculates into the downcomer of this type of ALC when compared to the first type.[1] Figure 2.2 (c) shows this class of ALC.

Each category of ALCs can be equipped with either rectangular or circular cross-section column. In addition to conventional ALCs, additional parts such as static mixer, perforated plate can also be inserted into the column to modify ALC configuration for mass transfer improvement as shown in Figure 2.3.[2-9]

2.2 Fundamentals

2.2.1 Transport phenomena in ALCs

2.2.1.1 Flow structure

The circulation of fluid in the ALC is induced by two mechanisms:

(i) Momentum transfer due to gas expansion from the bottom to the top of the contactor,

(ii) Difference in mean densities between aerated and unaerated regions due to the difference of gas holdups in both regions.

When gas is dispersed into the liquid pool in the column, energy is transferred to the liquid and the liquid movement is induced. Furthermore, in the region into which gas is dispersed (riser), high gas content is accommodated and causes the fluid density to be lower than the density of fluid in the other section of the contactor (downcomer). Consequently, there exists a difference between the fluid density in the aerated and unaerated regions, and this difference also facilitates the liquid circulation pattern as shown in Figure 2.1 (b). This well-defined cyclic flow pattern of the fluid in the ALC results in a large liquid velocity compared to that in the bubble column where the liquid movement is in a random pattern.

2.2.1.2 Gas dispersion

There are two types of gas dispersion depending on the level of gas throughput into the ALC.

(i) Homogeneous gas dispersion

Generally, at a relatively low gas throughput, bubbles distributed uniformly along the column region as shown in Figure 2.4 (a). This is because, at this condition, gas bubbles rise almost straight ups the column with little interaction between them. This is the bubbly flow regime known also as unhindered and homogeneous bubbly flow. This type of gas dispersion is desirable, particularly in a situation where gas-liquid mass transfer is important as a relatively large specific gas-liquid interfacial area can be obtained.

(ii) Heterogeneous gas dispersion

Because most industrial gas-liquid contactors operate under conditions in which gas flow rate is too high to maintain the condition of bubbly flow, heterogeneous regime is developed where the number of bubble and bubble collision frequency in fluid can be observed. Due to the greater interaction between bubbles, bubbles tend to coalesce and breakup which results in a wide distribution of bubble size along the column as shown in Figure 2.4 (b-d). Usually this ends up with a smaller gas-liquid interfacial area, but with a highly turbulent condition caused by bubble movement, the mixing in the system can be quite attractive. However, if the gas throughput is too high, the system can enter a slug flow regime where extremely large bubbles appear (Fig. 2.4 (d)). This undesired situation results in a very low gas-liquid mass transfer due to a very small mass transfer area.

2.2.2 Power input requirement

In the ALC, the circulation of the liquid takes place due to the difference in the densities of the mixed phase in the aerated and unaerated regions so the mechanical agitated device is not needed in the ALC operation. Power input requirement in the ALC is much less than that in the stirred tank. Generally, the power input to any pneumatic contactors is derived from the two main sources:

(i) Potential energy during the isothermal expansion of the gas as it moves up the reactor (P_{GE})

(ii) Kinetic energy transferred to the fluid by a jet of gas entering the reactor (P_{KE})

The complete details for calculation of power due to each source are given below:

2.2.2.1 Potential energy during the isothermal expansion of the gas as it moves up the reactor

The work ($\hat{w}$) done during isothermal expansion of n moles of a gas from an initial volume, V_b, to a final volume, V_t, is given as:

$$\hat{w} = \int_{V_b}^{V_t} P dV \tag{2.1}$$

Assume ideal gas behavior,

$$P = \frac{nRT}{V} \tag{2.2}$$

Substitute Eq. (2.2) in Eq. (2.1) followed by integration at constant temperature yields:

$$\hat{w} = nRT \ln \frac{V_t}{V_b} \tag{2.3}$$

When both sides of Eq. (2.3) are divided by the time (t) over which the work is done, we get:

$$\frac{\hat{w}}{t} = \frac{nRT}{t} \ln \frac{V_t}{V_b} \tag{2.4}$$

$\hat{w}/t$ is the power input to the system due to the isothermal gas expansion (P_{GE}) and n/t is the molar flow rate of gas (Q_{Gm}). The gas volume at the bottom and at the top of the contactor (V_b and V_t in Eq. (2.4)), respectively) can be replaced by the corresponding pressures, P_b and P_t, so that

$$P_{GE} = Q_{Gm} RT \ln \frac{P_b}{P_t} \tag{2.5}$$

where subscripts b and t denote bottom and top (or the head-space) of the reactor. The substitution of

$$P_b = P_t + \rho_D g H_D \tag{2.6}$$

into Eq.(2.5) leads to

$$P_{GE} = Q_{Gm} RT \ln \left(\frac{P_t + \rho_D g H_D}{P_t} \right) \tag{2.7}$$

$$\rho_D = \rho_L \left(1 - \varepsilon_G\right) + \rho_G \varepsilon_G \tag{2.8}$$

$$\rho_D = \rho_L - \varepsilon_G \left(\rho_L - \rho_G \right) \tag{2.9}$$

because ρ_L □ ρ_G ,

$$\rho_D = \rho_L \left(1 - \varepsilon_G \right) \tag{2.10}$$

and

$$H_D = \frac{H_L}{\left(1 - \varepsilon_G \right)} \tag{2.11}$$

Substitute Eq. (2.10) and Eq. (2.11) into Eq. (2.7) obtains

$$P_{GE} = Q_{Gm} RT \ln \left(\frac{P_t + \rho_L g H_L}{P_t} \right) \tag{2.12}$$

Therefore, one can calculate the power input due to isothermal gas expansion from:

$$P_{GE} = Q_{Gm} RT \ln \left(1 + \frac{\rho_L g H_L}{P_t} \right) \tag{2.13}$$

2.2.2.2 Kinetic energy transferred to the fluid by the jet of gas entering the reactor

The kinetic energy (P_{KE}) can be calculated from:

$$P_{KE} = \frac{1}{2} G u_{Go}^2 \tag{2.14}$$

where G is the mass flow rate of the gas, and u_{Go} the superficial gas velocity at the sparger outlet. G can be replaced by the product between the molecular weight (M_w) and the molar flow rate of the gas (Q_{Gm}), and Eq.(2.14) becomes:

$$P_{KE} = \frac{1}{2} M_w Q_{Gm} u_{Go}^2 \tag{2.15}$$

In the non-ideal case where there are associated losses of energy, we can incorporate the inefficiency of the system in terms of the efficiency factor, η:

$$P_{KE} = \frac{1}{2} \eta M_w Q_m u_{Go}^2 \tag{2.16}$$

The total power input in a pneumatic contactor (P_G) is the summation of the power inputs from isothermal gas expansion (Eq.(2.13)) and kinetic energy (Eq.(2.16)):

$$P_G = Q_{Gm} RT \ln \left(1 + \frac{\rho_L g H_L}{P_t} \right) + \frac{1}{2} \eta M_w Q_{Gm} u_{Go}^2 \tag{2.17}$$

Usually, the kinetic energy term would be found negligible when compared to the isothermal gas expansion.

2.2.3 Gas-liquid mass transfer

The gas-liquid mass transfer is one of the most important design considerations in bioreactor design, especially in aerobic systems which require a maximum rate of oxygen transfer. Due to a low solubility of oxygen in water, the oxygen must be continually replenished to avoid the development of anoxic conditions. The rate of mass transfer from gas to liquid phase may be expressed in terms of an overall volumetric mass transfer coefficient, $K_L a_L$ or $K_L a_D$, based on unaerated liquid volume and gas-liquid dispersion volume, respectively. This volumetric oxygen transfer coefficient is also an important indicator for comparing the oxygen transfer capabilities of various aerobic bioreactors. The volumetric oxygen transfer coefficient is defined by the following equation:

$$K_L a = \frac{n_{O_2}}{\Delta C} \tag{2.18}$$

where n_{O_2} is the flux of oxygen transfer between phases, ΔC the concentration driving force between the two phases.

Generally the determination of a mass transfer coefficient (k_L) in a system with a single bubble is much different from that in a system with a swarm of bubbles. The following subsections will give detail on how to estimate the overall mass transfer coefficient from these two cases:

2.2.3.1 Single bubble systems

The determination of the mass transfer coefficient in a single bubble system can be done theoretically, although it is more common to find empirical correlations that relate bubble characteristics to physical properties of the contacting system. The reported correlations for the estimation of the mass transfer coefficient in a single bubble system are summarized in Table 2.1.

2.2.3.2 Systems with a swarm of bubbles

In industrial aerated reactors, air bubbles usually form swarms. The oxygen transfer coefficient correlations for air bubble swarms are different from single bubble correlations since hydrodynamics of the liquid around the bubbles are different. In

addition, bubbles generally interact in some ways making the study of their behavior far more complicated than for a single bubble system.

The mass transfer coefficient in the bubble-swarm systems can also be estimated from the correlations between various dimensionless parameters. For example, Bailey and Ollis (1977)[10] and Calderbank, (1967)[11] provided this kind of correlation as summarized in Table 2.1.

The gas-liquid interfacial area based on liquid volume or gas-liquid dispersion volume (a_L or a_D, respectively) need to be determined to evaluate overall mass transfer coefficient (K_La). The value of a_L and a_D can be evaluated from Eq. (2.19) and Eq. (2.20), respectively.

$$a_L = \frac{6\varepsilon_G}{d_B(1-\varepsilon_G)} \tag{2.19}$$

$$a_D = \frac{6\varepsilon_G}{d_B} \tag{2.20}$$

However, instead of determining K_L and a separately, the mass transfer behavior in these systems were usually presented in terms of the overall mass transfer coefficient (K_La) which was often determined using empirical correlations reported in literature. These correlations are summarized in Table 2.2 for both bubble column and airlift gas-liquid contacting systems.

To facilitate the determination of the overall gas liquid mass transfer coefficient in this work, preliminary experiments were carried out where the resulting relationship between K_La and superficial gas velocity are displayed in Figures 2.5 and 2.6 for draft tube sparged and annulus sparged mode, respectively. This suggests the use of following empirical equations in estimating K_La.

For draft tube sparged ALC:

$$K_La = 0.44u_{sg}^{0.91}\left(\frac{A_d}{A_r}\right)^{-0.48} \tag{2.21}$$

For annulus sparged ALC:

$$K_La = 0.34u_{sg}^{0.8}\left(\frac{A_d}{A_r}\right)^{-0.19} \tag{2.22}$$

2.2.4 Hydrodynamic behavior

Hydrodynamic behavior is essential for the understanding of the phenomena taking place in ALC. Due to their strong influence on mass transfer performance, they have received considerable attentions from most investigators. Hydrodynamic parameters of interest in design are the overall gas holdup, the gas holdups in the riser and in the downcomer, the magnitude of the induced liquid circulation and the liquid-phase dispersion coefficients in various regions of the contactor. Some of the hydrodynamic parameters including the results from preliminary experiments from this work are presented below.

2.2.4.1 Gas holdup

Gas holdup is the volume fraction of gas phase in the gas-liquid dispersion. Gas holdup is important for determining residence time of the gas in liquid. It directly affects the gas-liquid interfacial area available for mass transfer. A large number of correlations for gas holdup prediction (for both bubble column and airlift gas-liquid contacting systems) have been proposed in literature and they are summarized in Table 2.3. Figures 2.7-2.9 displays the relationship between gas holdups and superficial gas velocity obtained from the draft tube sparged ALC and Figures 2.10-2.12 displays the relationship between gas holdups and superficial gas velocity obtained from the annulus sparged ALC employed in this work. The results suggest the use of following empirical equations in estimating gas holdups.

For draft tube sparged ALC:

$$\varepsilon_{Go} = 1.66 u_{sg}^{1.01} \left(\frac{A_d}{A_r} \right)^{-1.17} \tag{2.23}$$

$$\varepsilon_{Gr} = 3.06 u_{sg}^{1.14} \left(\frac{A_d}{A_r} \right)^{-0.42} \tag{2.24}$$

$$\varepsilon_{Gd} = 0.99 u_{sg}^{0.97} \left(\frac{A_d}{A_r} \right)^{-1.31} \tag{2.25}$$

For annulus sparged ALC:

$$\varepsilon_{Go} = 1.1 u_{sg}^{0.92} \left(\frac{A_d}{A_r} \right)^{-0.29} \tag{2.26}$$

$$\varepsilon_{Gr} = 1.56 u_{sg}^{1.01} \left(\frac{A_d}{A_r} \right)^{-0.3} \quad (2.27)$$

$$\varepsilon_{Gd} = 0.865 \varepsilon_{Gr} - 0.0038 \quad (2.28)$$

2.2.4.2 Liquid circulation

Liquid circulation in the ALC originates from the difference in bulk densities or static heads between the aerated and unaerated sections. The fluid circulation is a major design characteristic of the ALC because it determines the residence time of the liquid in various zones and controls the reactor performance. Accordingly, it is one of the key parameters in design and scale-up. It affects the mixing characteristics of both gas and liquid phases, volumetric mass and heat transfer coefficients, suspension of solid particles, etc., which determines the chemical reaction rate and therefore the performance of the ALC. There are a few theoretical background in determining liquid velocities in the pneumatic contactors. They are summarizes below:

A. Liquid circulation model of Jones, 1985[12]

Principles:

(1) This model is based on the rule of energy conservation.

(2) The work required to promote liquid circulation is equal to isothermal work done by the bubbles of gas expanding through the liquid contents of a vessel.

Model assumptions:

(1) Steady-state conditions

(2) Isothermal conditions

(3) Ideal gas behavior

(4) Negligible gas holdup in the downcomer ($\varepsilon_{Gd} = 0$)

(5) Negligible kinetic energy

Model validation:

The energy balance over an airlift reactor loop is given by the following equation:

$$\begin{bmatrix} \text{Rate of energy input due to} \\ \text{isothermal gas expansion} \end{bmatrix} = \begin{bmatrix} \text{Rate of work done to} \\ \text{promote liquid circulation} \end{bmatrix}$$

or $$E_{in} = W \quad (2.29)$$

The energy input due to isothermal expansion of ideal gas (supplied at pressure of P_h and a volumetric gas flowarte of Q_{Gr}) is approximately given by:

$$E_{in} = P_h Q_{Gr} \ln\left(1 + \frac{\rho_L g H_D}{P_h}\right) \tag{2.30}$$

where P_h is the pressure of gas at the column head, Q_{Gr} the volumetric gas flow rate in riser, ρ_L liquid density, and H_D dispersion height.

However, Jones (1985)[12] stated that, in airlift reactors, not all of the energy in the compressed gas is transferred to generate liquid motion as some is "lost" due to the turbulent energy dissipation caused by the relative velocity between gas and liquid. Nicklin (1963)[13] showed that the efficiency of this energy transfer process is simply related to the relative flow rates of liquid and gas and this can be given by an expression of the form:

$$\eta = \frac{v_{Lr}}{v_{Lr} + v_s} \tag{2.31}$$

where η is efficiency of energy transfer, v_{Lr} the liquid velocity in the riser and v_s the slip velocity. Since it was known that the slip velocity is the difference between the absolute gas and liquid velocities:

$$v_s = v_{Gr} - v_{Lr} \tag{2.32}$$

therefore

$$\eta = \frac{v_{Lr}}{v_{Lr} + v_s} = \frac{v_{Lr}}{v_{Gr}} \tag{2.33}$$

The gas velocity can be computed from:

$$v_{Gr} = \frac{u_{Gr}}{\varepsilon_{Gr}} = \frac{Q_{Gr}}{A_r \varepsilon_{Gr}} \tag{2.34}$$

Substitute Eq.(2.34) into Eq.(2.33) gives

$$\eta = \frac{v_{Lr} A_r \varepsilon_{Gr}}{Q_{Gr}} \tag{2.35}$$

Hence,

$$E_{in} = \frac{v_{Lr} A_r \varepsilon_{Gr}}{Q_{Gr}} \left[P_h Q_{Gr} \ln\left(1 + \frac{\rho_L g H_D}{P_h}\right) \right] \tag{2.36}$$

For the draft-tube bubble column the rate of work done to promote liquid circulation (W) in the absence of bubble recirculation into the downcomer ($\varepsilon_{Gd} = 0$) is given by:

$$W = wgZ \tag{2.37}$$

where w is mass flow rate, and Z is total hydraulic head, and since

$$Z = \frac{(v_{Lr}^2 + v_{Ld}^2)}{2g} \tag{2.38}$$

W can be calculated from the information on the liquid velocity and riser gas holdup:

$$W = v_{Lr} A_r (1-\varepsilon_{Gr}) \rho_L \frac{(v_{Lr}^2 + v_{Ld}^2)}{2} \tag{2.39}$$

This work is equal to the energy from the isothermal gas expansion (Eq. (2.36)).

$$v_{Lr} A_r \left(1-\varepsilon_{Gr}\right) \rho_L \frac{\left(v_{Lr}^2 + v_{Ld}^2\right)}{2} = \frac{v_{Lr} A_r \varepsilon_{Gr}}{Q_{Gr}} \left[P_h Q_{Gr} \ln\left(1 + \frac{\rho_L g H_D}{P_h}\right)\right] \tag{2.40}$$

$$\left(1-\varepsilon_{Gr}\right) \rho_L \frac{\left(v_{Lr}^2 + v_{Ld}^2\right)}{2} = \frac{\varepsilon_{Gr}}{Q_{Gr}} \left[P_h Q_{Gr} \ln\left(1 + \frac{\rho_L g H_D}{P_h}\right)\right] \tag{2.41}$$

Continuity equation of liquid is written as:

$$v_{Ld} A_d \left(1-\varepsilon_{Gd}\right) = v_{Lr} A_r \left(1-\varepsilon_{Gr}\right) \tag{2.42}$$

Eq.(2.42) can be written in explicit term of v_{Lr} as:

$$v_{Lr} = v_{Ld} \left(\frac{A_d}{A_r}\right)\left(\frac{1}{1-\varepsilon_{Gr}}\right) \tag{2.43}$$

Substitute Eq. (2.43) into Eq. (2.41) yields

$$\varepsilon_{Gr} \left[P_h \ln\left(1 + \frac{\rho_L g H_D}{P_h}\right)\right] = \frac{\left(1-\varepsilon_{Gr}\right)\rho_L}{2} \left\{ \left[v_{Ld} \left(\frac{A_d}{A_r}\right)\left(\frac{1}{1-\varepsilon_{Gr}}\right)\right]^2 + v_{Ld}^2 \right\} \tag{2.44}$$

$$v_{Ld} = \left[\frac{\frac{2}{\rho_L}\left(\frac{\varepsilon_{Gr}}{1-\varepsilon_{Gr}}\right) P_h \ln\left(1 + \frac{\rho_L g H_D}{P_h}\right)}{1 + \left(\frac{A_d}{A_r}\right)^2 \left(\frac{1}{1-\varepsilon_{Gr}}\right)^2} \right]^{0.5} \tag{2.45}$$

However, when bubbles are entrained down the downcomer ($\varepsilon_{Gd} \neq 0$) the gas is compressed in a manner analogous to the expansion up the riser. Thus some work is effectively recovered by the gas resulting in a reduction in the portion of energy which is transferred to promote liquid circulation. Eq. (2.30) can be rewritten as:

$$E_{in} = \eta \left[P_1 Q_{Gr} \ln\left(1 + \frac{\rho_L g H_D}{P_h}\right) - P_h Q_{Gd} \ln\left(1 + \frac{\rho_L g H_D}{P_h}\right)\right] \tag{2.46}$$

Finally, the downcomer liquid velocity can be obtained from

$$v_{Ld} = \left\{ \frac{\frac{2P_h}{\rho_L} \ln\left[\frac{P_h + \rho_L g H_L}{P_h}\right]\left[\frac{\varepsilon_{Gr}}{(1-\varepsilon_{Gr})} - \frac{\varepsilon_{Gd}}{(1-\varepsilon_{Gd})}\right]}{1 + \left[\frac{A_d(1-\varepsilon_{Gd})}{A_r(1-\varepsilon_{Gr})}\right]^2} \right\}^{0.5} \quad (2.47)$$

B. Liquid circulaion model of Chisti et al., 1988[14]

Principles:

(1) This model is based on the rule of energy conservation.

(2) The energy balance approach considers that the driving force for circulation in the reactor is produced by the change in energy as gas bubbles rise and expand up the riser. This energy is dissipated by friction losses in the fluids itself and losses against the reactor wall.

Model assumptions:

(1) Steady-state conditions

(2) Isothermal conditions

(3) Ideal gas behavior

(4) Negligible drift of gas with respect to the liquid in both the top and bottom sections $\left(\ddot{E}_t = \ddot{E}_b = 0\right)$

(5) Negligible mass transfer between the gas and the liquid

(6) Negligible energy loss due to the skin friction in the riser and the downcomer when compared with the other dissipation terms. $\left(\hat{E}_r = \hat{E}_d = 0\right)$

(7) Negligible pressure drop due to acceleration

Model validation:

This model was shown to be applicable to all types of ALCs.

The energy balance over an airlift reactor is given by the following equation:

$$\begin{bmatrix}\text{Rate of energy input}\\ \text{due to isothermal}\\ \text{gas expansion}\end{bmatrix} = \begin{bmatrix}\text{Rate of energy dissipation due to}\\ \text{internal turbulence and friction}\\ \text{between the gas - liquid interface}\end{bmatrix} + \begin{bmatrix}\text{Rate of energy losses}\\ \text{due to friction between}\\ \text{the fluids and the reactor}\end{bmatrix}$$

or

$$E_{in} = \sum \ddot{E} + \sum \hat{E} \tag{2.48}$$

$$\sum \ddot{E} = \ddot{E}_r + \ddot{E}_d + \ddot{E}_t + \ddot{E}_b \tag{2.49}$$

$$\sum \hat{E} = \hat{E}_r + \hat{E}_d + \hat{E}_t + \hat{E}_b \tag{2.50}$$

Follow Assumption (4), $\ddot{E}_t$ and $\ddot{E}_b = 0$, hence

$$\sum \ddot{E} = \ddot{E}_r + \ddot{E}_d \tag{2.51}$$

The energy associated with turbulence and internal friction, $\ddot{E}_r$ and $\ddot{E}_d$ were obtained by an energy balance on the riser and on the downcomer.

The energy balance on the riser is given by:

$$\left[\text{Energy input}\right] = \begin{bmatrix}\text{Energy dissipation}\\ \text{in riser}\end{bmatrix} + \left[\text{Pressure energy loss }\right] - \left[\text{Potential energy gain}\right]$$

$$E_{in} = \ddot{E}_r - \rho_L g H_D \left(1-\varepsilon_{Gr}\right) u_{Lr} A_r + \rho_L g H_D u_{Lr} A_r \tag{2.52}$$

Hence,

$$\ddot{E}_r = E_{in} - \rho_L g H_D \varepsilon_{Gr} u_{Lr} A_r \tag{2.53}$$

The energy balance on the downcomer is given by:

$$\begin{bmatrix}\text{Energy dissipation}\\ \text{in downcomer}\end{bmatrix} + \left[\text{pressure energy gain}\right] = \left[\text{potential energy loss}\right]$$

$$0 = \ddot{E}_d + \rho_L g H_D \left(1-\varepsilon_{Gd}\right) u_{Ld} A_d - \rho_L g H_D u_{Ld} A_d \tag{2.54}$$

or,

$$\ddot{E}_d = \rho_L g H_D \varepsilon_{Gd} u_{Ld} A_d \tag{2.55}$$

$$\sum \ddot{E} = E_{in} - \rho_L g H_D \left(\varepsilon_{Gr} u_{Lr} A_r - \varepsilon_{Gd} u_{Ld} A_d\right) \tag{2.56}$$

Follow Assumption (6), $\hat{E}_r$ and $\hat{E}_d = 0$

$$\sum \hat{E} = \hat{E}_t + \hat{E}_b \tag{2.57}$$

The energy losses in the top and the bottom sections of an airlift reactor can be calculated in exactly the same manner as for pipe flow. Thus,

$$\hat{E}_b + \hat{E}_t = \frac{1}{2}\rho_L \left[v_{Lr}^3 k_t A_r \left(1-\varepsilon_{Gr}\right) + v_{Ld}^3 k_b A_d \left(1-\varepsilon_{Gd}\right)\right] \tag{2.58}$$

where K_t and K_b are the friction loss coefficients for the top and the bottom connecting sections, respectively. v_{Lr} and v_{Ld} in Eq. (2.58) are the true linear liquid velocities or the

interstitial velocities in the riser and the downcomer, respectively and are related to the corresponding superficial velocities in the following fashion:

$$v_{Lr} = \frac{u_{Lr}}{\left(1-\varepsilon_{Gr}\right)} \tag{2.59}$$

and

$$v_{Ld} = \frac{u_{Ld}}{\left(1-\varepsilon_{Gd}\right)} \tag{2.60}$$

Furthermore, the continuity equation for the liquid flow between the riser and the downcomer can be written as:

$$v_{Lr} A_r \left(1-\varepsilon_{Gr}\right) = v_{Ld} A_d \left(1-\varepsilon_{Gd}\right) \tag{2.61}$$

Substitute Eqs. (2.59) and (2.60) in Eq. (2.58) results in:

$$\sum \hat{E} = \hat{E}_b + \hat{E}_t = \frac{1}{2}\rho_L u_{Lr}^3 A_r \left[\frac{k_t}{\left(1-\varepsilon_{Gr}\right)^2} + k_b \left(\frac{A_r}{A_d}\right)^2 \frac{1}{\left(1-\varepsilon_{Gd}\right)^2} \right] \tag{2.62}$$

Finally, the substitution of Eqs. (2.56) and (2.62) in Eq. (2.48) yields the following expression

$$\begin{aligned} E_{in} = E_{in} &- \rho_L g H_D \varepsilon_{Gr} u_{Lr} A_r + \rho_L g H_D \varepsilon_{Gd} u_{Ld} A_d \\ &+ \frac{1}{2}\rho_L u_{Lr}^3 A_r \left[\frac{k_t}{\left(1-\varepsilon_{Gr}\right)^2} + k_b \left(\frac{A_r}{A_d}\right)^2 \frac{1}{\left(1-\varepsilon_{Gd}\right)^2} \right] \end{aligned} \tag{2.63}$$

Eq. (2.63) can be rearranged to give an equation for predicting the superficial liquid velocity.

$$u_{Lr} = \left[\frac{\dfrac{2gH_D\left(\varepsilon_{Gr}-\varepsilon_{Gd}\right)}{k_t}}{\left(1-\varepsilon_{Gr}\right)^2 + k_b \left(\dfrac{A_r}{A_d}\right)^2 \left(\dfrac{1}{1-\varepsilon_{Gd}}\right)^2} \right]^{0.5} \tag{2.64}$$

C. Liquid circulation model of Calvo, 1989[15]

Principles:

(1) This model is based on the rule of energy conservation.

(2) The energy balance approach considers that the driving force for circulation in the reactor is produced by the change in energy as gas bubbles rise and expand up the riser. This energy is dissipated by the internal friction losses in the fluids and the friction losses against the reactor wall.

Model assumptions:

(1) Steady state operation

(2) Isothermal system

(3) Ideal gas behavior

(4) Negligible drift of gas with respect to the liquid in both the top and bottom sections $\left(\ddot{E}_t = \ddot{E}_b = 0\right)$

(5) Negligible internal recirculation

(6) Negligible mass transfer between the gas and the liquid

(7) Negligible gas holdup in the downcomer ($\varepsilon_{Gd} = 0$)

(8) The average density of the gas-liquid equal to the liquid density

(9) The pressure drop due to acceleration negligible

(10) Constant slip velocity in the riser

(11) Gas holdup in the riser considered to be the mean gas holdup

Model validation:

The energy balance over an airlift reactor is given by the following equation:

$$\begin{bmatrix}\text{Rate of energy input}\\ \text{due to isothermal}\\ \text{gas expansion}\end{bmatrix} = \begin{bmatrix}\text{Rate of energy dissipation due to}\\ \text{internal turbulence and friction}\\ \text{between the gas - liquid interface}\end{bmatrix} + \begin{bmatrix}\text{Rate of energy losses}\\ \text{due to friction between}\\ \text{the fluids and the reactor}\end{bmatrix}$$

or

$$E_{in} = \sum \ddot{E} + \sum \hat{E} \tag{2.65}$$

$$\sum \ddot{E} = \ddot{E}_r + \ddot{E}_d + \ddot{E}_t + \ddot{E}_b \tag{2.66}$$

$$\sum \hat{E} = \hat{E}_r + \hat{E}_d + \hat{E}_t + \hat{E}_b \tag{2.67}$$

According to Assumptions (2) and (3), the energy input due to the isothermal expansion of an ideal gas (supplied at a pressure of P_h and a superficial gas velocity of u_{sg}) is given by:

$$E_{in} = P_h Q_{Gr} \ln\left(1 + \frac{\rho_L g H_L}{P_h}\right) \tag{2.68}$$

We know that $Q_{Gr} = u_{sg} A_r$, hence

$$E_{in} = u_{sg} A_r P_h \ln\left(1 + \frac{\rho_L g H_L}{P_h}\right) \tag{2.69}$$

Assumption (4) implies that $\ddot{E}_t = \ddot{E}_b = 0$, therefore

$$\sum \ddot{E} = \ddot{E}_r + \ddot{E}_d \tag{2.70}$$

$$\sum \hat{E} = \hat{E}_r + \hat{E}_d + \hat{E}_t + \hat{E}_b \tag{2.71}$$

Assumption (7) leads to $\ddot{E}_d \approx 0$, and

$$\sum \ddot{E} = \ddot{E}_r = \int_{P_1}^{P_2} v_s \varepsilon_{Gr} A_r dP = v_s A_r \varepsilon_{Gr} \left(P_2 - P_1\right) = v_s A_r \varepsilon_{Gr} \rho_L g H_L \tag{2.72}$$

$$v_s = \frac{u_{sg}}{\varepsilon_{Gr}} - v_{Lr} = \frac{u_{sg}}{\varepsilon_{Gr}} - \frac{u_{Lr}}{\left(1-\varepsilon_{Gr}\right)} \tag{2.73}$$

$$\sum \hat{E} = K_f \dot{w}_{Ld} \frac{v_{Ld}^2}{2} = K_f \rho_L A_d \frac{u_{Ld}^3}{2} = \frac{1}{2} K_f \rho_L A_d \left[\left(1-\varepsilon_{Gr}\right)\left(\frac{A_d}{A_r}\right)\left(\frac{u_{sg}}{\varepsilon_{Gr}} - v_s\right)\right]^3 \tag{2.74}$$

$$0 = u_{sg} P_h \ln\left(1 + \frac{\rho_L g h}{P_h}\right) - v_s \varepsilon_{Gr} \rho_L g h - \frac{1}{2} K_f \rho_L \left(\frac{A_r}{A_d}\right)^2 \left[\left(1-\varepsilon_{Gr}\right)\left(\frac{u_{sg}}{\varepsilon_{Gr}} - v_s\right)\right]^3 \tag{2.75}$$

The corresponding superficial liquid velocity in the riser is obtained from the definition of the slip velocity in Eq. (2.76)

$$u_{Lr} = \left(1-\varepsilon_{Gr}\right)\left(\frac{u_{sg}}{\varepsilon_{Gr}} - v_s\right) \tag{2.76}$$

D. Liquid circulation model of Gavrilescu and Tudose, 1998[16]

Principles:

(1) This model is based on the rule of energy conservation.

(2) There are changes of the cross-sectional areas for liquid circulation at both ends of the draft tube. The changes in linear velocity should be accompanied by changes in static pressure so as to maintain the energy balance. The flowing liquid turns 180 degree at the entrance to the draft tube and annulus. As a result, the pressure and velocity fields will be subject to entrance effect which reduces the effective flow area, and produces local liquid acceleration. These accelerations are the result of an apparent diminishing of flow cross-sectional area as shown in Figure 2.13.

(3) The model takes into account the energy losses along the total circulation loop, especially in the bottom and top sections. Such losses are caused by apparent contraction of the flow cross sectional area, and quantified by the acceleration coefficients that are estimated using measurements of static pressure profiles.

Model assumptions:

(1) The contribution of the backflow velocity field induced in the liquid phase by the relative motion of the bubbles is totally ignored at the bottom and top sections.
(2) The energy losses associated with the relative motion between the gas and liquid phases including the bubble-wake effect are not taken into account at the bottom and top sections.
(3) The radial velocity distribution of the gas-liquid flow near the elbow and separator regions are uniform: the volume change of gas phase associated with static pressure variation follows the isothermal expansion/contraction of an ideal gas.

Model validation:

This model is shown to be applicable to concentric tube internal loop airlift contactors.

$$\Delta\frac{1}{2}\rho v^2 + \Delta\rho gZ + \Delta P + \hat{W} + \hat{E}_v = 0 \tag{2.77}$$

The Bernoulli's equation is applied at each end of the draft tube. The linear velocities of the liquid phase at the contracted entrances of the riser and downcomer are related to the effective linear velocities, $v_{Lr\alpha}$ and $v_{Ld\alpha}$, respectively. The energy balance equations can be summarized as follows (Consult the referred paper for detailed derivation):

$$\frac{1}{2}\rho_L v_{Ld}^2 + P_{db} = \frac{1}{2}\rho_L v_{Lr\alpha}^2 + P_{rb} \tag{2.78}$$

$$\frac{1}{2}\rho_L v_{Lr}^2 + P_{rs} = \frac{1}{2}\rho_L v_{Ld\alpha}^2 + P_{ds} \tag{2.79}$$

$$P_{db} - P_{ds} = \rho_L g\left(1-\varepsilon_{Gr}\right)H_D \tag{2.80}$$

$$P_{rb} - P_{rs} = \rho_L g\left(1-\varepsilon_{Gd}\right)H_D \tag{2.81}$$

$$\left(1-\varepsilon_{Gd}\right)A_d v_{Ld} = \left(1-\varepsilon_{Gr}\right)A_{rc} v_{Lr\alpha} \tag{2.82}$$

$$\left(1-\varepsilon_{Gr}\right)A_r v_{Lr} = \left(1-\varepsilon_{Gd}\right)A_{dc} v_{Ld\alpha} \tag{2.83}$$

$$2gH_D(\varepsilon_{Gr}-\varepsilon_{Gd}) = v_{Lr}^2\left[\frac{(1-\varepsilon_{Gr})^2}{(1-\varepsilon_{Gd})^2}\frac{A_r^2}{A_{dc}^2}-1\right] + v_{Ld}^2\left[\frac{(1-\varepsilon_{Gd})^2}{(1-\varepsilon_{Gr})^2}\frac{A_d^2}{A_{rc}^2}-1\right] \tag{2.84}$$

$$u_{Lr} = v_{Lr}\left(1-\varepsilon_{Gr}\right) \tag{2.85}$$

$$u_{Ld} = v_{Ld}\left(1-\varepsilon_{Gd}\right) \tag{2.86}$$

The continuity equation for the liquid flow between the riser and the downcomer can be written as:

$$A_r\left(1-\varepsilon_{Gr}\right)v_{Lr} = A_d\left(1-\varepsilon_{Gd}\right)v_{Ld} \tag{2.87}$$

Hence,

$$2gH_D\left(\varepsilon_{Gr}-\varepsilon_{Gd}\right) = u_{Lr}^2 A_r^2\left[\frac{1}{\left(1-\varepsilon_{Gr}\right)^2 A_{rc}^2}-\frac{1}{\left(1-\varepsilon_{Gd}\right)^2 A_d^2}+\frac{1}{\left(1-\varepsilon_{Gd}\right)^2 A_{dc}^2}-\frac{1}{\left(1-\varepsilon_{Gr}\right)^2 A_r^2}\right] \quad (2.88)$$

Let k_r and k_d be the contraction coefficient in the riser and downcomer respectively.

$$k_r = \frac{A_{rc}}{A_r} \quad (2.89)$$

$$k_d = \frac{A_{dc}}{A_d} \quad (2.90)$$

$$2gH_D(\varepsilon_{Gr}-\varepsilon_{Gd}) = u_{Lr}^2 A_r^2\left[\left(\frac{1}{k_r^2}-1\right)\frac{1}{(1-\varepsilon_{Gr})^2 A_r^2}+\left(\frac{1}{k_d^2}-1\right)\frac{1}{(1-\varepsilon_{Gd})^2}\frac{A_r^2}{A_d^2}\right] \quad (2.91)$$

One can then estimate the superficial liquid velocity from:

$$u_{Lr} = \left[\frac{2gH_D(\varepsilon_{Gr}-\varepsilon_{Gd})}{A_r^2\left[\left(\frac{1}{k_r^2}-1\right)\frac{1}{(1-\varepsilon_{Gr})^2 A_r^2}+\left(\frac{1}{k_d^2}-1\right)\frac{1}{(1-\varepsilon_{Gd})^2}\frac{A_r^2}{A_d^2}\right]}\right]^{0.5} \quad (2.92)$$

Reported empirical correlations for the prediction of liquid velocity in ALC are shown in Table 2.4.

Again, preliminary experiments were performed in this work to find the relationship between liquid velocities and the gas throughput for the employed ALC. Figures 2.14 - 2.15 illustrate these results in draft tube sparged ALC and Figures 2.16 - 2.17 illustrate these results in annulus sparged ALC where the following empirical correlation for predicting downcomer and riser liquid velocities can be formulated:
For draft tube sparged ALC:

$$v_{Ld} = 1.04u_{sg}^{0.26}\left(\frac{A_d}{A_r}\right)^{-0.77} \quad (2.93)$$

$$v_{Lr} = 0.27+1.37u_{sg}^{0.53}\left(\frac{A_d}{A_r}\right)^{0.17} \quad (2.94)$$

For annulus sparged ALC:

$$v_{Ld} = 0.21+2.5u_{sg}^{1.31}\left(\frac{A_d}{A_r}\right)^{-0.2} \quad (2.95)$$

$$v_{Lr} = 0.24 + 0.43u_{sg}^{0.26}\left(\frac{A_d}{A_r}\right)^{0.85} \quad (2.96)$$

2.3 Literature reviews: hydrodynamic and mass transfer

ALCs have attracted attention of many chemical industries and researchers due to their several attractive advantages as specified in Table 1.1. During the last two decades, a wide range of experimental investigations on hydrodynamics and mass transfer characteristics in the ALC has been conducted, and a large number of related papers have appeared (see Tables 2.2-2.4). For design and operating purposes, most of these papers focused on effects of various parameters, both geometrical and operational, on ALC performance. These parameters included superficial gas velocity, cross-sectional area ratio between downcomer and riser, column diameter, unaerated liquid height, sparger design, draft tube height, bottom clearance (the distance between the bottom end of draft tube and the base of outer column), etc. These results showed that geometrical and operational parameters had strong influences on ALC performance. However, among these papers, several showed contradictory results. For example, with regards to the effect of downcomer to riser cross-sectional area ratio (A_d/A_r) on gas holdup, Jones (1985),[12] and Hwang and Cheng (1997)[17] found that riser gas holdup increased with increasing A_d/A_r. Hwang and Cheng (1997)[17] explained that riser gas holdup increased due to the increasing gas velocity in the riser when A_d/A_r increased. On the contrary, Weiland (1984)[18] and Bello et al. (1985)[19] reported a reverse trend, i.e. Bello et al (1985)[19] explained that when A_d/A_r increased circulating liquid velocity increased and resulted in a shorter residence time of bubbles in the riser, thus riser gas holdup decreased. There were also disagreements on the effect of sparger design. For instance, Merchuk and Stein (1981),[20] Koide et al. (1983),[21] Mcmanamey et al. (1984)[22] and Bovonsombat et al. (1987)[23] stated that a multiple orifice sparger gave higher riser gas holdup and liquid velocity than a single orifice sparger. This might be due to the fact that the multiple orifice sparger generated smaller bubbles than the single nozzle or the single orifice sparger. On the other hand, Merchuk (1986),[24] Kembloski et al. (1993),[25] and Gavrilescu and Tudose (1998)[16] reported that sparger designs had no effect on riser gas holdup but they did not give further detail on this matter. The role of liquid level or liquid volume in the ALC was also found to be rather uncertain. Siegel and Merchuk (1991)[26] cited, at the same time, that riser gas holdup was reduced due to a

shorter residence time of gas caused by an increase in liquid velocity. Bentifraouine et al. (1997)[27] also found the same results in their work. They explained that the increase in liquid volume caused a decrease in gas recirculation in the downcomer because the fluid spent a longer time in the gas-liquid separator, which resulted in more bubbles removal at the top surface. Consequently the driving force acting on liquid circulation velocity (hydrostatic pressure difference between riser and downcomer) was enhanced. In contrast, Snape et al. (1995)[28] reported that the liquid volume had no influence on liquid circulation velocity as the additional volume of liquid would be in the gas separator section which had negligible interaction with the rest of the contactor. Thus the gas holdups in the riser and downcomer remained constant, and so did the circulation velocity. It is possible that these contradictions appeared because most researchers often interpreted their experimental data based only on the accessible information such as gas holdup and liquid velocity. The essential detailed knowledge, which are necessary for defining gas-liquid flow behaviors such as bubble behaviors and fluid movement were not considered in these works. Furthermore, the neglected or disregarded phenomena such as internal liquid circulation (liquid circulation within riser or downcomer itself) might be mis-leading to the researchers. This led to the contradictions as mentioned earlier. The significance of bubble characteristics and internal liquid circulation are investigated in the following chapter in this thesis.

2.4 References

1. Couvert, A., Roustan M., and Chatellier P. 1999. Two-phase hydrodynamic study of a rectangular air-lift loop reactor with an internal baffle. Chem. Eng. Sci. 54: 5245-5252.
2. Tung, H.-L., Chiou, S.-Y., Tu, C.-C., Wu, W.-T. 1997. An airlift reactor with double net draft tubes and its application in fermentation. Bioproc. Eng. 17: 1-5.
3. Margaritis, A., and Sheppard, J.D. 1981. Mixing time and oxygen transfer characteristics of a double draft tube airlift fermenter. Biotech. Bioeng. 23: 2117- 2135.
4. Bando, Y., Nishimura, M., Sota, H., Suzudi, S., and Kawase, N. 1992. Flow characteristics of countercurrent bubble column with perforated draft tube. Chem. Eng. Sci. 47: 3371-3378.

5. Zhao, M., Niranjan, D., and Davidson, J. F. 1994. Mass transfer to viscous liquids in bubble columns and airlift reactors: Influence of baffles. Chem. Eng. Sci. 49 (14): 2359-2369.
6. Vorapongsathorn, T., Wongsuchoto, P., and Pavasant, P. 2001. Performance of airlift contactors with baffles. Chem. Eng. J. 84: 551-556.
7. Krichnavaruk, S., and Pavasant, P. 2002. Role of perforated plates in the airlift contactor. J. Chem. Eng. Japan 35(6): 533-539.
8. Krichnavaruk, S., and Pavasant, P. 2002. Analysis of gas-liquid mass transfer in an airlift contactor with perforated plates. Chem. Eng. J. 89: 203-211.
9. Chisti M.Y. 1989. Airlift Bioreactors. Elsevier Applied Science. London and New York.
10. Bailey, J.E. and Ollis, D.F. 1977. Biochemical Engineering Fundamentals. McGraw-Hill, New York.
11. Calderbank, P.H. 1967. Mass transfer in fermentation equipment. In biochemical and Biological Engineering Science, ed. N. Blakebrough, Vol. 1, pp. 102-180. Academic, New York
12. Jones, A.G. 1985. Liquid circulation in a draft-tube bubble column. Chem. Eng. Sci. 40(3): 449-462.
13. Nicklin D. J. 1963. Trans. Inst. Chem. Eng. 46:29.
14. Chisti, M.Y., Halard, M., and Young, M.M. 1988. Liquid circulation in airlift reactors. Chem. Eng. Sci. 43: 451-457.
15. Garcia-Calvo, E. 1989. A fluid dynamic model for airlift reactors. Chem. Eng. Sci. 44: 321-323.
16. Gavrilescu, M., Tudose, R.Z. 1998. Modelling of liquid circulation velocity in concentric-tube airlift reactors. Chem. Eng. J. 69: 85-91.
17. Hwang, S.-J. and Cheng Y.,-L. 1997. Gas holdup and liquid velocity in three-phase internal-loop airlift reactors. Chem. Eng. Sci. 52(21/22): 3949-3960.
18. Weiland, P. 1984. Influence of draught tube diameter on operation behavior of airlift loop reactors. Ger. Chem. Eng. 7: 374-385.
19. Bello, R. A., Robinson, C. W., and Young, M.M. 1985a. Prediction of the volumetric mass transfer coefficients in pneumatic contactors. Chem. Eng. Sci. 40(1): 53-58.
20. Merchuk, J. C., and Stein, Y. 1981. Local hold-up and liquid velocity in air-lift reactors. AIChE J. 27(3): 377-388.

21. Koide K., Kurematsu, K., Iwamoto, S., Iwata, Y., and Horibe, K. 1983a. Gas holdup and volumetric liquid-phase mass transfer coefficient in bubble column with draught tube and with gas dispersion into tube. J. Chem. Eng. Japan 16(5): 413-419.
22. McManamey, W.J., Wase C.A.J., Raymahasay S., and Thayanithy K. 1984. The Influence of Gas Inlet Design on Gas Hold-up Values for Water and Various Solutions in a Loop-type Air-lift Fermenter. J. Chem. Tech Biotech. 34B: 151-164.
23. Bovonsombat, S., Wilhelm A.-M. and Riba J.-P. 1987. Influence of Gas Distributor Design on the Oxygen Transfer Characteristics of an Airlift Fermenter. J. Chem. Tech. Biotech. 40: 167-176.
24. Merchuk, J. C. 1986, Gas hold-up and Liquid velocity in a two-dimensional airlift reactor. Chem. Eng. Sci. 41(1): 11-16.
25. Kemblowski, Z., Przywarski, J., and Diab, A. 1993. An average gas hold-up and liquid circulation velocity in airlift reactors with external loop. Chem. Eng. Sci. 48 (23): 4023-4035.
26. Siegel, M., and Merchuk, J. C. 1991. Hydrodynamics in rectangular air-lift reactors: scale-up and the influence of gas-liquid separator design. Can. J. Chem. Eng. 69: 465-473.
27. Bentifraouine C., Xuereb C. and Riba J.P. 1997. An Experimental Study of the hydrodynamic Characteristics of External loop Airlift Contactors. J. Chem. Biotech. 69: 345 -349.
28. Snape, J.B., Zahradník, J. Fialová, M. and Thomas, N.H. 1995. Liquid-phase properties and sparger design effects in an external-loop airlift reactor. Chem. Eng. Sci. 50(20): 3175-3186.
29. Ranz, W.E., and Marshall, W.-R. 1952. Evaporation from drops. Chem. Eng. Prog. 48: 141.
30. Calderbank, P. H., and Young, M.M. 1961. The continuous phase heat and mass reactors. Chem. Eng. Sci. 43: 451-457.
31. Calderbank, P.H. 1967. Mass transfer in fermentation equipment. In *Biochemical and Biological Engineering Science*. Ed. N. Blakebrough, vol. 1, pp. 102-180. Acacemic, New York.
32. Skelland, A.H.P. 1974. Diffusional Mass Transfer. Wiley, New York.
33. Kargi, F. and Young, 1976. M.M. Transport phenomena in bioprocesses.

34. Nakanoh, M., and Yoshida J. 1980. Gas absorption by Newtonian and Non-Newtonian liquids in a bubble column. Ind. Eng. Chem. Proc. Des. Dev. 19: 190.

35. Shah, Y. T., Kelkar, B.G., Godbole, S. P., and Deckwer, W. D. 1982. Design parameter estimations for bubble column reactors. AIChE J. 28: 353-379.

36. Koide K., Sato, H., and Iwamoto, S.. 1983b. Gas holdup and volumetric liquid-phase mass transfer coefficient in bubble column with draught tube and with gas dispersion into annulus. J. Chem. Eng. Japan 16(5): 407-413.

37. Popovic, M., and Robinson, C. W. 1984. Estimation of some important design parameters for non-Newtonian liquids in pneumatically agitated fermenters. In Proceedings of the 34th Canadian Chemical Engineering Congress, 30th September-3rd October, Quebec City, 258-263.

38. Bello, R. A., Robinson, C. W., and Young, M.M. 1984. Liquid circulation and mixing characteristics of airlift contactors. Can. J. Chem. Eng. 62: 573-577.

39. Bello, R. A., Robinson, C. W., and Young, M.M. 1985b. Gas holdup and overall volumetric oxygen transfer coefficient in airlift contactors. Biotech. Bioeng. 27: 369-381.

40. Koide, K., Horibe, K., Kawabata, H., and Ito, S. 1985. Gas holdup and volumetric liquid-phase mass transfer coefficient in solid-suspended bubble column with draught tube. J. Chem. Eng. Japan 18: 248-254.

41. Kawase, Y., and Young, M.M. 1986. Influence of non-Newtonian flow behavior on mass transfer in bubble columns with and without draft tubes. Chem. Eng. Commun. 40: 67-83.

42. Merchuk, J.C., and Siegel, M.H. 1988. Air-Lift reactors in chemical and biological technology. J. Chem. Tech. Biotech. 41: 105-120.

43. Chisti, M.Y., and Young, M.M. 1988. Gas holdup in pneumatic reactors. Chem. Eng. J. 38: 149-152.

44. Popovic, M.K., and Robinson, C.W. 1989. Mass transfer studies of external-loop airlifts and a bubble column. AIChE J. 35(3): 393-405.

45. Choi, K.H., and Lee, W. K. 1993. Circulation liquid velocity, gas holdup and volumetric oxygen transfer coefficient in external-loop airlift reactors. Chem. Tech. Biotechnol. 56: 51-58.

46. Merchuk, J. C., Ladwa, N., Cameron, A., Bulmer, M., and Pickett, A. 1994. Concentric-tube airlift reactors: Effects of geometrical design on performance, AIChE J. 40: 1105 - 1117.

47. Shamlou, P. A., Pollard, D.J., and Iaon, A.P. 1995. Volumetric mass transfer coefficient in concentric tube airlift bioreactors. Chem. Eng. Sci. 50: 1579 – 1590.

48. Li, G.-Q., Yang, S.-Z., Cai, Z.-L., and Chem, J.-Y. 1995. Mass transfer and gas-liquid circulation in an airlift bioreactor with viscous non-Newtonian fluids. Chem. Eng. J. 56: B101-B107.

49. Merchuk, J.C., Ladwa, N., Cameron, A., Bulmer, M., Berzin, J. and Pickett, A.M. 1996. Liquid flow and mixing in concentric tube air-lift reactors. J. Chem. Tech. Biotech. 66: 174-182.

50. Contreras, A., Garcia, F., Molina, E., and Merchuk, J.C. 1999. Influence of sparger on energy dissipation, shear rate, and mass transfer to sea water in a concentric-tube airlift bioreactor. Enzyme Microbiol Tech. 25: 820-830.

51. Chakravarty, M., Begum, S., Singh, H.D., Baruah, J.N., and Iyengar, N.A. 1973. Gas holdup distribution in gas-lift column. Biotechnology and Bioengineering Symposium. No.4: 363.

52. Chakravarty, M., Singh, H. D. B., and Lyengar, M.S. 1974. Indian Chem. Eng. 16: 17-22.

53. Hills, J. H. 1976. The operation of a bubble column in high throughputs 1. Gas hold-up measurement. Chem. Eng. J. 12: 89-99.

54. Weiland, P., and Onken, U. 1981. Fluid dynamics and mass transfer in an airlift fermenter with external-loop. Ger. Chem. Eng. 4: 40-42.

55. Akita and Kaweasaki. 1983. Proceeding 48th Meet. Of Chem. Engrs. Engrs. Jpn. Kyoto (1983) 122-126.

56. Kimura and Kubota 1984 J. Chem. Eng. Japan 17: 611-618.

57. Godbole, S. P., Schumpe, A., Shah, Y. T., and Carr, N. L. 1984. Hydrodynamics and mass transfer in non-Newtonian solutions in a bubble column. AIChE J. 30: 213-220.

58. Vatai, G. and Tekic, M. N., 1986, Effect of pseudoplasticity on hydrodynamic characteristics of airlift loop contactor, Paper presented at the 2nd Conference of European Rheologists EURO-RHEO'86, Prague.

59. Chisti, M.Y., Fujimoto, D., and Young, M.M. 1986. Paper 117a presented at AIChE Annual Meeting, Meeting, Miami Beach, November 2-7.
60. Siegel, M. H., Merchuk, J.C., and Schugerl, D. 1986. Airlift reactor analysis: Interrelationships between riser, downcomer and gas liquid separator. AIChE J. 32(10): 1585-1596.
61. Miyahara, T., Hamaguchi, M., Sukeda, Y., and Takahashi, T. 1986. Size of Bubbles and liquid circulation in a bubble column with a draught tube and sieve plate Can. J. Chem. Eng. 64: 718-725.
62. Chisti, M.Y., and Young, M.M. 1987. Airlift reactors: Characteristics, applications and design considerations. Chem. Eng. Commun. 60: 195-242.
63. Kawase, Y., and Young, M.M. 1987. Chem. Eng. Res. Des. 65: 121-126.
64. Chisti, M. Y., and Young, M.M. 1988a. Prediction of liquid circulation velocity in airlift reactors with biological media. J. Chem. Tech. Biotech. 42: 211-219.
65. Chisti, M. Y., and Young, M.M. 1988b. Hydrodynamics and oxygen transfer in pneumatic devices. Biotech. Bioeng. 31: 487 - 494.
66. Koide K., Kimura, M., Nitta, H., and Kawabata, H. 1988. Liquid circulation in bubble column with draught tube. J. Chem.Eng.Japan. 21: 393-399.
67. Popovic, M., and Robinson, C.W. 1988. External-circulation loop airlift bioreactors: study of the liquid circulating velocity in highly viscous non-Newtonian liquids. Biotech. Bioeng. 32: 301-312.
68. Philip, J., Proctor, J. M., Niranjan, K., and Davidson, J. F. 1990. Gas hold-up and liquid circulation in internal loop reactors containing highly viscous Newtonian and non-Newtonian liquids. Chem. Eng. Sci. 45: 651-664.
69. Pošarac, D., Petrović, D., Dudukovic, A., and Skala, D. 1991. J. Serb. Chem. Soc. 56: 227-240.
70. Cai, J., Niewstad, T. J., and Kop, J.H. 1992. Fluidization and sedimentation of carrier material in a pilot-scale airlift internal-loop reactor. Water Sci. Technnol. 26: 2481-2484.
71. Ghirardini, M., Donati, G., and Rivetti, F. 1992. Gas lift reactors: hydrodynamics, mass transfer, and scale up. Chem. Eng. Sci. 47: 2209-2214.
72. Chisti, M.Y. and Young, M.M. 1993. Improve the performance of airlift reactors. Chem. Eng. Prog. 38-45.

73. Ganzeveld, K.J., Chisti, Y., and Young, M.M. 1995. Hydrodynamic behavior of animal cell microcarrier suspensions in split-cylinder airlift bioreactors. Bioproc. Eng. 12: 239-247.

74. Gavrilescu, M., Tudose, R.Z. 1996. Effects of downcomer-to-riser cross sectional area ratio on operation behavior of external-loop airlift bioreactors. Bioproc. Eng. 15: 77-85.

75. Choi, K.H., Chisti, M.Y., and Young, M.M. 1996. Comparative evaluation of hydrodynamic and gas-liquid mass transfer characteristics in bubble column and airlift slurry reactors. Chem. Eng. J. 62: 223-229.

76. Korpijarvi J., Oinas, P., Reunanen, J. 1999. Hydrodynamics and mass transfer in an airlift reactor. Chem. Eng. Sci. 54: 2255-2262.

77. Levich, V.G. 1962 Physicochemical Hydrodynamics, p.434. Prentice-Hall, Englewood Cliffs, NJ.

78. Marucci, G. 1969. A theory of Coalescence. Chem. Eng. Sci. 23: 976.

79. Bello, R. A. 1981. A characterization study of airlift contactors for applications to fermentations, Ph.D. thesis, University of Waterloo, Waterloo, Canada.

80. Koide K., Iwamoto, S., Takasaka, Y., Matsuura, S., Takahashi, E., and Kimura, M. 1984. Liquid circulation, gas holdup and pressure drop in bubble column with draught tube. J. Chem. Eng. Japan 17(6): 611-618.

81. Popovic, M. K., and Robinson, C. W. 1987b. The specific interfacial area in external-circulation-loop airlifts and a bubble column--II. Carboxymethyl cellulose/ sulphite solution. Chem. Eng. Sci. 42: 2825-2832.

82. Assa, A., and Bar, R. 1991. Biomass Axial Distribution in Airlift Bioreactor with Yeast and Plant Cells. Biotech. Bioeng. 38: 1325-1330.

83. Russell, A.B., Thomas, C.R., and Lilly, M.D. 1994. The influence of vessel height and top-section size on the hydrodynamic characteristics of airlift fermenters, Biotech. Bioeng. 43: 69-76.

84. Choi, K. H. 1996. Circulation liquid velocity in external-loop airlift reactors. Korean J. Chem. Eng. 13(4): 379-383.

85. Bando, Y., Hayakawa, H., and Nishimura, M. 1998. Effects of equipment dimensions on liquid mixing time of bubble column with draft tube. J. Chem. Eng. Japan 31(5): 765-770.

2.5 Tables and figures

Table 2.1 Correlations for mass transfer coefficient (k_L)

Literatures	Correlation	Condition	System
Ranz and Marshall (1952)[29]	$Sh = 2+0.6Re^{1/2}Sc^{1/3}$	Laminar flow field	For single bubbles with large Re (Re>>1)
	$Sh = 0.39Ra^{1/3} = 0.39Gr^{1/3}Sc^{1/3}$		For single bubbles with small Re (Re <<1)
Calderbank and Young (1961)[30]	$k_L = \alpha Gr^{1/3}Sc^{\beta}$ where	Natural convection	For large bubbles
	$\alpha = 0.42$ and $\beta = -1/2$		Aqueous glycol soutions-CO_2
			Water-CO_2
			Water-O_2
			Brine-O_2
			Polyacrylamide solution-CO_2
			$1000 \le \rho_L \le 1178$ kgm^{-3}
			$0.0006 \le \mu_L \le 0.0897$ Pa s
			$1000 \le \Delta\rho \le 1178$ kgm^{-3}
			$d_B > 2.5$ mm
	$\alpha = 0.31$ and $\beta = -2/3$		For small bubbles
			Aqueous glycol solutions-CO_2
			Brine-O_2
			Wax-H_2
			Aqueous ethanol solution-C_6H_6
			$698 \le \rho_L \le 1160$ kgm^{-3}
			$0.00084 \le \mu_L \le 0.001$ Pa s
			$174 \le \Delta\rho \le 1160$ kgm^{-3}
			$d_B < 2.5$ mm
Bailey and Ollis (1977)[10] and Calderbank (1967)[31]	$Sh = 0.42Gr^{1/3}Sc^{1/2}$	Natural convection	For large size bubble swarms ($d_B > 2.5$ mm)
	$Sh = 2+0.31Ra^{1/3}2 = 2+0.31Gr^{1/3}Sc^{1/3}$	Natural convection	For small size bubble swarms ($d_B < 2.5$ mm)

Literatures	Correlation	Condition	System
Skelland (1974)[32]	$k_L = \sqrt{\frac{D_L}{4\pi d_B}}$	Penetration theory	
Kargi and Young (1976)[33]	$Sh = 0.664Sc^{1/3} Re^{1/2}$	Laminar flow boundary layer theory	$Re < 2{,}000$
	$Sh = 0.036Sc^{1/3} Re^{0.8}$	Turbulent flow mass transfer theory	$Re > 10{,}000$

Table 2.2 Summary of experimental volumetric mass transfer coefficient correlations of airlift reactor

No.	Authors	Equations	Parameters
1.	Calderbank and Young (1961)[29]	For small bubbles ($d_B < 0.5$mm) $k_L a_D = 1.86\mathrm{Gr}^{1/3}\mathrm{Sc}^{2/3}\frac{\varepsilon_G}{d_B}$ For large bubbles ($d_B > 2.5$mm) $k_L a_D = 2.52\mathrm{Gr}^{1/3}\mathrm{Sc}^{-1/2}\frac{\varepsilon_G}{d_B}$	
2.	Nakanoh and Yoshida (1980)[34]	$k_L a = 0.799 u_G(1-\varepsilon_{Go})$	Medium: Low viscosity solution
3.	Margaritis and Sheppard (1981)[3]	For sparger with 1.27 mm i.d. orifices: $k_L a = 0.904\left(\frac{P_G}{V_L}\right)^{0.74}$	Medium: Water Device: Bubble column
		$k_L a = 0.31\left(\frac{P_G}{V_L}\right)^{0.92}$	Device: Internal loop airlift reactor (double concentric tube) Parameter range: $A_d/A_r = 0.94$
		$k_L a = 0.2\left(\frac{P_G}{V_L}\right)$	Device: Internal loop airlift reactor (annulus sparged) Parameter range: $A_d/A_r = 0.35$
		$k_L a = 0.318\left(\frac{P_G}{V_L}\right)^{0.92}$	Device: Internal loop airlift reactor (draft tube sparged) Parameter range: $A_d/A_r = 0.25$
		For sparger with 3.81 mm i.d. orifices: $k_L a = 3.06\times10^{3}\left(\frac{P_G}{V_L}\right)^{2}$	Device: Bubble column
		$k_L a = 2.46\times10^{3}\left(\frac{P_G}{V_L}\right)^{1.6}$	Device: Internal loop airlift reactor (double concentric tube) Parameter range:

No.	Authors	Equations	Parameters
		$k_L a = 3.91\times10^3 \left(\frac{P_G}{V_L}\right)^{1.5}$	$A_d/A_r = 0.94$ Device: Internal loop airlift reactor (annulus sparged) Parameter range: $A_d/A_r = 0.35$
		$k_L a = 3.06\times10^3 \left(\frac{P_G}{V_L}\right)^{2}$	Device: Internal loop airlift reactor (draft tube sparged) Parameter range: $A_d/A_r = 0.25$
4.	Shah et al. (1982)[35]	$k_L a = 0.467 u_{sg}^{0.82}$	Device: Bubble column Medium: Water
5.	Koide et al. (1983a)[21]	$\frac{k_L a_D D_o^2}{D_L} = 0.477\left(\frac{\mu_L}{\rho_L D_L}\right)^{0.5}\left(\frac{gD_o^2\rho_L}{\sigma_L}\right)^{0.873}\left(\frac{gD_o^3\rho_L^2}{\mu_L^2}\right)^{0.257}\left(\frac{D_i}{D_o}\right)^{-0.542}\varepsilon_{Go}^{1.36}$	Device: Internal loop airlift contactor (draft tube sparged) Media: Demineralized water, aqueous solutions of glycerol, glycol, barium chloride and sodium sulfate and sodium sulfite Sparger: Single nozzle sparger, perforated plate and porous glass plate Parameter ranges: $0.013 \le u_{sg} \le 0.17$ m· s^{-1} $1.93\times10^{-4} \le (u_G\mu_L/\sigma_L) \le 2.85\times10^{-2}$ $1.31\times10^{6} \le \left(\rho_L\sigma_L^3/g\mu_L^4\right) \le 6.04\times10^{10}$ $0.471 \le (D_i/D_o) \le 0.743$ $0 \le (Crk^2/\sigma_L) \le 67.3$
6.	Koide et al. (1983b)[36]	$\frac{k_L a_D \sigma_L}{D_L g \rho_L} = 2.25\left(\frac{\mu_L}{\rho_L D_L}\right)^{0.5}\left(\frac{\rho_L\sigma_L^3}{g\mu_L^4}\right)^{0.136}\left(\frac{\delta}{D_o}\right)^{-0.0905}\varepsilon_{Go}^{1.26}$	Device: Internal loop airlift contactor (annulus sparged) Media: Demineralized water, aqueous solutions of glycerol, glycol, barium chloride and sodium sulfate Sparger: Multi-nozzles sparger Parameter ranges: $0.0098 \le u_{sg} \le 0.156$ m· s^{-1} $3.71\times10^2 \le (u_G\sigma_L/D_L) \le 6\times10^4$

No.	Authors	Equations	Parameters
			$1.18\times10^{6} \le \left(\rho_L\sigma_L^3/g\mu_L^4\right) \le 5.93\times10^{10}$ $0.471 \le (D_i/D_o) \le 0.743$ $7.14\times10^{-3} \le (\delta/D_o) \le 2.86\times10^{-2}$ $0.0302 \le \varepsilon_G \le 0.305$
7.	Popovic and Robinson (1984)[37]	$k_L a_D = 1.911\times10^{-4} u_{sg}^{0.525}\left(1+\frac{A_d}{A_r}\right)^{-0.853}\mu_{app}^{-0.83}$	Device: External-loop airlift reactor Medium: Non-Newtonian CMC solution Parameter ranges: A_d/A_r = 0, 0.11, 0.25, 0.44 $0.015 \le \mu_{app} \le 0.5$ Pa· s
8.	Bello et al. (1985a)[19]	$k_L a_D = 0.47\varepsilon_{Gr}^{1.2}$ or in terms of A_d/A_r and u_{sg}: $k_L a_D = 0.76\left(1+\frac{A_d}{A_r}\right)^{-2} u_{sg}^{0.8}$ or in terms of $(P_G/V_D)_T$: $k_L a_D = 5.5\times10^{-4}\left(1+\frac{A_d}{A_r}\right)^{-1.2}\left(\frac{P_G}{V_D}\right)_T^{0.8}$	Devices: External and Internal loop airlift contactors Media: Water and 0.15 kmol· m^{-3} NaCl solution Parameter ranges: For external loop airlift contctor $0.11 \le A_d/A_r \le 0.69$ D_r = 0.152 m, H_d = 1.8 m $0.05 \le D_d \le 0.102$ m, $0.0137 \le u_{sg} \le 0.086$ m· s^{-1} For internal loop airlift contactor Sparger: Perforated stainless plate with 52 holes of 1.02 mm $0.13 \le A_d/A_r \le 0.56$
9.	Bello et al. (1985b)[39]	$\frac{(k_L a_D)_r H_D}{u_{Lr}} = 2.28\left(\frac{u_{sg}}{u_{Lr}}\right)^{0.9}\left(1+\frac{A_d}{A_r}\right)^{-1}$	Devices: External and Internal loop airlift contactors Media: Water and 0.15 kmol· m^{-3} NaCl solution Parameter ranges: For external loop airlift contctor $0.11 \le A_d/A_r \le 0.69$ D_r = 0.152 m, H_d = 1.8 m $0.05 \le D_d \le 0.102$ m, $0.0137 \le u_{sg} \le 0.086$ m· s^{-1} For internal loop airlift contactor Sparger: Peorated stainless plate with 52 holes of 1.02 mm $0.13 \le A_d/A_r \le 0.56$

No.	Authors	Equations	Parameters
10.	Koide et al. (1985)[40]	$\mathrm{Sh} = 2.66\mathrm{Sc}^{0.5}\mathrm{Bo}^{0.715}\mathrm{Ga}^{0.25}\left(\frac{D_i}{D_o}\right)^{-0.429}\varepsilon_{Go}^{1.34}$	Device: Internal loop airlift contactor
11.	Kawase and Young (1986)[41]	$\frac{k_L a_L D_o^2}{D_L} = 6.8n^{-6.72}\left(\frac{D_o u_{sg}\rho_L}{\mu_L}\right)^{0.38n+0.52}\left(\frac{\mu_L}{D_L\rho_L}\right)^{0.38n-0.14}$	Devices: Internal loop airlift reactors and bubble columns Media: Water and pseudoplastic fluids Parameter ranges: $0.008 \le u_g \le 0.285$ m· s^{-1} $0.14 \le D_o \le 0.35$ m $0.28 \le n \le 1$ $0.001 \le K(\mathrm{Pa\ s^n}) \le 1.22$
12.	Siegel and Merchuk (1988)[42]	$k_L a = 913\left(\frac{P_G}{V_D}\right)^{1.04} u_L^{-0.15}$	Device: External loop airlift contactor
13.	Chisti et al. (1988)[43]	$k_L a = 0.349 - 0.102C_s\left(1+\frac{A_d}{A_r}\right)^{-1} u_{Gr}^{0.837}$	Device: External loop airlift contactor
14.	Popovic and Robinson (1989)[44]	$k_L a = 0.5\times10^{-2} u_{Gr}^{0.52}\left(1+\frac{A_d}{A_r}\right)^{-0.85} D_L^{0.5}\rho_L^{1.03}\sigma_L^{-0.25}\mu_{app}^{-0.89}$ $k_L a = 1.911\times10^{-4} u_{Gr}^{0.52}\left(1+\frac{A_d}{A_r}\right)\mu_{app}^{-0.85}$ $k_L a = 0.24 u_{Gr}^{0.837}\left(1+\frac{A_d}{A_r}\right)^{-1}$	Device: External loop airlift contactor
15.	Choi and Lee (1993)[45]	$k_L a_L = 0.176 u_{sg}^{0.761}\left(\frac{A_d}{A_r}\right)^{-0.056}\left(\frac{L_c}{L_h}\right)^{-0.168}$	Devices: External loop airlift reactors Medium: Water Parameter ranges: $D_r = 0.158$ m $0.049 \le D_d \le 0.108$ m $0.11 \le A_d/A_r \le 0.53$ $0.091 \le L_c/L_h \le 0.455$ $0.1 \le L_c \le 0.5$ m

No.	Authors	Equations	Parameters
			u_{sg}<0.2 m· s^{-1}
16.	Zhao et al. (1994)[5]	When $H_L \geq 0.8$ m. $\frac{k_L a D_o}{u_{sg}} = 9.33\times10^{-5}\left(\frac{D_o u_{sg}\rho_L}{\mu_L}\right)^{0.56}\left(\frac{u_{sg}\mu_L}{\sigma_L}\right)^{0.09}\left(\frac{u_{sg}}{\sqrt{gD_o}}\right)^{-0.86}$ When $H_L < 0.8$ m. $\frac{k_L a D_o}{u_{sg}} = 2.95\times10^{-3}\left(\frac{D_o u_{sg}\rho_L}{\mu_L}\right)^{0.89}\left(\frac{u_{sg}^2 D_o \rho_L}{\sigma_L}\right)^{-0.13}\left(\frac{u_{sg}}{\sqrt{gD_o}}\right)^{-0.31}\left(\frac{H_L}{D_o}\right)^{-0.5}$	Devices: Internal loop airlift reactor and bubble column Media: Newtonian and non-Newtonian liquids Parameter ranges: $0.007\leq u_G \leq 0.6$ m· s^{-1} $0.001\leq \mu_L \leq 1.26$ Pa· s $0.03\leq \sigma_L \leq 0.07$ N· m^{-1}
17.	Merchuk et al. (1994)[46]	$\mathrm{Sh} = 17.3\times10^{3}\,\mathrm{Fr}^{0.9}\mathrm{M}^{-3.4}\mathrm{Ga}^{0.13}X_{dt}^{-0.07}Y^{-0.18}$	Device: Internal loop airlift reactors Media: Water and carboxymethyl cellulose solutions Parameter ranges: $0.001<\mu_{app}<0.025$ Pa· s $6\times10^{-4}<\mathrm{Fr}<350\times10^{-4}$ $3\times10^{7}<\mathrm{Ga}<6\times10^{11}$ $0.04<X_{dt}<0.4$ $0.22<M<0.34$
18.	Shamlou et al. (1995)[47]	$k_L a = 12\left(\frac{D_L}{\pi}\right)^{1/2}\left[\frac{u_{b\infty}+C_0\left(u_{sg}+u_{Lr}\right)}{d_B^3}\right]^{1/2}\frac{\varepsilon_G}{\left(1-\varepsilon_G\right)^{3/2}}$	Device: Internal loop airlift bioreactor Medium: Fermentation broth of *Saccharovisiae cerevisiae*
19.	Li et al. (1995)[48]	$k_L a_L = 0.0343 u_{Gr}^{0.524}\mu_{app}^{-0.255}$ $\gamma = 5000 u_{Gr}$ for $u_{Gr} \geq 0.04$ms^{-1} $\gamma = 5000 u_{Gr}^{0.5}$ for $u_{Gr} \leq 0.04$ms^{-1}	Devices: Internal loop airlift contactors Parameter ranges: $0.02>\mu_{app}>0.85$ Pa s
20.	Merchuk et al. (1996)[49]	$\mathrm{Sh} = 3\times10^{4}\,\mathrm{Fr}^{0.97}\mathrm{M}^{-5.4}\mathrm{Ga}^{0.045}\left(1+\frac{A_d}{A_r}\right)^{-1}$	Device: Internal loop airlift reactor Medium: Deionized water

No.	Authors	Equations	Parameters
21.	Contreras et al. (1999)[50]	P.S. $\mathrm{Fr} = \frac{u_{sg}}{\sqrt{gD_o}}$ $K_L a_L = 0.1633 \varepsilon_G^{1.0187} u_{Lr}^{-0.6187}$	Device: Internal loop airlift reactor (draft tube sparged) Medium: Sea water Parameter ranges: A_d/A_r=1 u_{Gr}<0.21 m· s^{-1} V_L = 12 L.

Table 2.3 Summary of experimental gas holdup correlations of airlift reactor

No.	Authors	Equations	Parameters
1.	Chakravarty et al. (1973)[51] and Chakravarty et al. (1974)[52]	$\varepsilon_{Gd} = 0.00123\frac{(74.2-\sigma_L)}{(79.3-\sigma_L)}\mu_L^{0.45}\left(\frac{A_r}{A_d}\right)^{1.08} u_{sg}^{0.88}$ and $\varepsilon_{Gr} = 0.0001\left[\left(\mu_L-\mu_w\right)^{2.75}+161\left(\frac{73.3-\sigma_L}{74.1-\sigma_L}\right)\right]u_{sg}^{0.88}$	Devices: Internal loop airlift reactors (draft tube sparged) Media: Water, sodium sulfate, glycerol and iso-butyl alcohol solutions Parameter ranges: $0.015 \le u_{sg} \le 0.2$ m· s^{-1} $D_o = 0.1$ m $D_i = 0.074, 0.059, 0.045$ m $0.83 \le A_d/A_r \le 3.94$
2.	Hills (1976)[53]	$\varepsilon_{Gr} = \frac{u_{sg}}{0.24-1.35\left(u_{sg}+u_{Lr}\right)^{0.93}}$	Medium: Water Parameter ranges: $u_{Lr} > 0.3$ m· s^{-1}
3.	Merchuk and Stein (1981)[20]	$\varepsilon_{Gr} = \frac{2u_{Lr}^2}{gD_r}\left[\left(1+\frac{u_{sg}}{u_{Lr}}\right)f_r + f_d\left(1+\frac{L_e}{L}\right)\left(\frac{A_r}{A_d}\right)^{0.25}\right]$ $f_r = 0.046\,\mathrm{Re}^{-0.2}$ $f_d = 0.0791\,\mathrm{Re}^{-0.25}$	Device: Rectangular column 0.14×0.14 m Medium: Water Sparger: Single-orifice and multi-nozzle spargers Parameter ranges: $H = 4.05$ m.
4.	Weiland and Onken (1981)[54]	$\frac{u_G}{\varepsilon_G}-\frac{u_L}{\left(1-\varepsilon_G\right)} = u_{b\infty}\left(1-\varepsilon_G\right)^{1.39}$	Device: External loop airlift reactor Media: Air-water system, NaCl solution (0.1 and 1 M), Propanol solution ($0.05 \le \sigma_L \le 0.06$ N· m^{-1}), Saccharose solution ($0.004 \le \mu_L \le 0.016$ Pa· s) Sparger: Sintered Plate Sparger Parameter ranges: $D_d = 0.05$ m, $D_r = 0.1$ m, $H_d = H_r = 10$ m

No.	Authors	Equations	Parameters
5.	Koide et al. (1983a)[21]	$\frac{\varepsilon_{Go}}{(1-\varepsilon_{Go})^4}=\frac{0.124\left(\frac{u_{sg}\mu_L}{\sigma_L}\right)^{0.966}\left(\frac{\rho_L\sigma_L^3}{g\mu_L^4}\right)^{0.294}\left(\frac{D_i}{D_o}\right)^{0.114}}{\left\{1-0.276\left[1-\exp\left(-0.00386\frac{Crk^2}{\sigma_L}\right)\right]\right\}}$	Device: Internal loop airlift reactor (annulus sparged) Parameter ranges: $1.93\times10^{-4}\le(u_G\sigma_L/D_L)\le 2.85\times10^{-2}$ $1.31\times10^{6}\le\left(\rho_L\sigma_L^3/g\mu_L^4\right)\le 6.04\times10^{10}$ $0.471\le(D_i/D_o)\le 0.743$ $0\le(Crk^2/\sigma_L)\le 67.3$
6.	Koide et al. (1983b)[36]	$\frac{\varepsilon_{Go}}{(1-\varepsilon_{Go})^4}=\frac{0.16\left(\frac{u_{sg}\mu_L}{\sigma_L}\right)^{0.964}\left(\frac{\rho_L\sigma_L^3}{g\mu_L^4}\right)^{0.283}\left(\frac{D_i}{D_o}\right)^{-0.222}\left(\frac{\delta}{D_o}\right)^{-0.0237\exp(-0.00185Crk^3/\sigma_L)}}{\left\{1-1.61\left[1-\exp\left(-0.00565\frac{Crk^2}{\sigma_L}\right)\right]\right\}}$	Device: Internal loop airlift reactor (draft tube sparged) Parameter ranges: $1.21\times10^{-4}\le(u_{sg}\mu_L/\sigma_L)\le 1.57\times10^{-2}$ $1.18\times10^{6}\le\left(\rho_L\sigma_L^3/g\mu_L^4\right)\le 5.93\times10^{10}$ $0.471\le(D_i/D_o)\le 0.743$ $0\le(Crk^2/\sigma_L)\le 93$ $7.14\times10^{-3}\le(\delta/D_o)\le 2.86\times10^{-2}$
7.	Akita and Kaweasaki (1983)[55]	$\varepsilon_{Gr}=0.364u_{sg}$	Device: Internal loop airlift reactor
8.	Popovic and Robinson (1984)[37]	$\varepsilon_{Gr}=0.02u_{sg}^{0.6504}\left(1+\frac{A_d}{A_r}\right)^{-1.0516}\mu_{app}^{-0.1059}$	Device: External loop airlift reactor Medium: Non Newtonian CMC solution Parameter ranges: $A_d/A_r=0,\ 0.11,\ 0.25,\ 0.44$ $0.015\le\mu_{app}\le 0.5$ Pa· s
9.	Bello et al. (1984)[38]	$\varepsilon_{Gr}=0.16\left(\frac{u_{sg}}{u_{Lr}}\right)^{0.57}\left(1+\frac{A_d}{A_r}\right)$ For external loop airlift reactor: $\varepsilon_{Gd}=0.46\varepsilon_{Gr}-0.024$ For internal loop airlift reactor: $\varepsilon_{Gd}=0.89\varepsilon_{Gr}$	Media: Water and 0.15 kmol· m^{-3} NaCl solution Device: External loop airlift reactor Parameter ranges: $0.11\le A_d/A_r\le 0.69$ $D_r=0.152$ m, $H_D=1.8$ m $0.05\le D_d\le 0.102$ m,

No.	Authors	Equations	Parameters
			$0.0137 \leq u_{sg} \leq 0.086$ m· s^{-1} Device: Internal loop airlift reactor Sparger: Perforated stainless plate with 52 holes of 1.02 mm Parameter ranges: $0.13 \leq A_d/A_r \leq 0.56$
10.	Kimura and Kubota (1984)[56]	$\varepsilon_{Gr} = 0.441 u_{sg}^{0.841} \mu_{app}^{-0.135}$ $\varepsilon_{Gd} = 0.297 u_{sg}^{0.935} \mu_{app}^{-0.107}$	
11.	Godbole et al. (1984)[57]	$\varepsilon_G = 0.07 u_{sg}^{-0.5} \mu_L^{-0.04} \sigma_L^{0.75}$	Device: Bubble Column 0.305 m in diameter Medium: CMC solution Parameter ranges: Churn turbulent flow regime
12.	Bello et al. (1985a)[19]	$\varepsilon_{Gr} = 1.27\left(1+\frac{A_d}{A_r}\right)^{-1.7} u_{sg}^{0.67}$ $\varepsilon_{Gd} = 0.79\varepsilon_{Gr}$-0.0057	As same as that specified in the work of Bello et al.[9]
13.	Bello et al. (1985b)[19]	$\varepsilon_{Gr} = 0.0034\left(\frac{P_G}{V_D}\right)_T^{2/3}\left(1+\frac{A_d}{A_r}\right)^{-1}$	
14.	Merchuk (1986)[24]	$\varepsilon_G = 0.047 u_G^{0.59}$	Device: External loop air lift reactor or bubble column Medium: Water Air, He, CO_2 or Freeon 114 used as gas phase
15.	Kawase and Young (1986)[41]	$\varepsilon_{Go} = 0.24n - 0.6\left(\frac{u_{sg}}{\sqrt{gD_o}}\right)^{0.84-0.14n}\left(\frac{gD_o^3\rho_L^2}{\mu_L^2}\right)^{0.07}$	Device: Internal loop airlift reactors and bubble columns Media: Water and pseudoplastic fluids Parameter ranges: $0.008 \leq u_{sg} \leq 0.285$ m· s^{-1} $0.14 \leq D_o \leq 0.35$ m. $0.28 \leq n \leq 1$

No.	Authors	Equations	Parameters
			$0.001 \le K(\text{Pa}\cdot\text{s}^n) \le 1.22$
16.	Vatai and Tekic (1986)[58]	$\varepsilon_{Gr} = 0.128\left(\frac{u_{sg}}{u_{Lr}}\right)\text{Re}^{0.062}\ \text{We}^{0.164}$	Media: Water, CMC solutions Parameter ranges: n=0.866 $0.304 \le K \le 0.745$ Pa· s^n
17.	Chisti et al.(1986)[59]	$\varepsilon_{Gd} = 0.46\varepsilon_{Gr} - 0.024$	Device: External loop airlift reactor Media: same fluids as in the work of Chisti et al. (1986)[22] Sparger: Perforated plate with 52 holes of 0.001m. Parameter ranges: $0.026 \le u_{sg} \le 0.21$ m· s^{-1} D_r=0.152 m, H=1.75 m, A_d/A_r=0.25, 0.44
18.	Siegel et al. (1986)[60]	$\varepsilon_{Gr} = 0.017u_{sg}^{0.71}\left(\frac{De_r}{De_d}\right)^{0.32}$ $\varepsilon_{Gd} = 0.031u_{sg}^{-0.68}$	Device: Split rectangular Medium: Water Parameter ranges: Riser 0.09×0.25 m Downcomer 0.01×0.25 m H=4 m, V_L=0.3 m^3
19.	Miyahara et al. (1986)[61]	$\varepsilon_{Gr} = \frac{0.4\text{Fr}}{1+0.4\text{Fr}\left(1+\frac{u_{Lr}}{u_{sg}}\right)}$ $\varepsilon_{Gd} = 4.51\times10^6\, Mo^{0.115}\left(\frac{A_r}{A_d}\right)^{4.2}\varepsilon_{Gr}^{4.2}$ when $\varepsilon_{Gr} < 0.0133\left(\frac{A_d}{A_r}\right)^{-1.32}$	Device: Internal loop airlift reactor (draft tube sparged) Media: Water, ethanol/water, glycerine/water, millet jelly/water Parameter ranges: $952 \le \rho_L \le 1168$ kg· m^{-3} $1 \le \mu_L \le 4.9$ mPa· s $34.1 \le \sigma_L \le 72$ mN· m D_o = 0.148 m Maximum H_D = 1.2 m

No.	Authors	Equations	Parameters
			$0.0005 \le d_o \le 0.0015$ m $0.128 \le A_d/A_r \le 0.808$
		$\varepsilon_{Gd} = 0.05 Mo^{-0.22} \left[\left(\frac{A_r}{A_d} \right)^{0.6} \varepsilon_{Gr} \right]^{0.32 Mo^{-0.0273}}$	
		when	
		$\varepsilon_{Gr} > 0.0133 \left(\frac{A_d}{A_r} \right)^{-1.32}$	
		P.S. $\mathrm{Fr} = \frac{u_{sg}^2}{g D_o}$, $\mathrm{Mo} = \frac{g \mu_L^4}{\rho_L \sigma_L^3}$	
20.	Chisti and Young (1987)[62]	$\varepsilon_{Gr} = 0.65 \left(1 + \frac{A_d}{A_r} \right)^{-0.258} u_{sg}^{0.603}$	Device: External loop airlift reactor Medium: Water
21.	Kawase and Young (1987)[63]	$\varepsilon_{Gr} = 1.07 \mathrm{Fr}^{0.333}$	Device: External loop airlift reactor
		P.S. $\mathrm{Fr} = \frac{u_{sg}^2}{g D_r}$	
22.	Chisti et al. (1988)[43]	$\varepsilon_{Gr} = 0.65 u_{sg}^{(0.603 - 0.078 C_0)} \left(1 - \frac{A_d}{A_r} \right)^{-0.258}$	
		$\varepsilon_{Gd} = 0.46 \varepsilon_{Gr} - 0.0244$	
23.	Chisti and Young (1988a)[64]	Churn-turbulent regime: $\varepsilon_G = 1.16 \exp - (0.273 C_s + 0.782) \mathrm{Fr}^{0.362}$ Bubble flow regime: For 0.15 M NaCl solution $\varepsilon_G = 1.481 u_G^{0.826}$ For SF suspensions $\varepsilon_G = u_G^{(0.293 C_s - 0.38)} \exp(0.426 C_s - 0.549)$ where u_G = Superficial gas velocity based either on the bubble column cross-	Device: Rectangular bubble column Media: Water, 0.15 M NaCl solutions and Solka Floc suspensions

No.	Authors	Equations	Parameters
		section or on the riser cross section in the airlift (m/s) d_c = equivalent diameter of bubble column and airlift riser (d_c= 4×flow area/wetted perimeter) m	
24.	Chisti and Young (1988b)[65]	$\varepsilon_G = 2.47u_G^{0.97}$ for $u_G < 0.05$m/s $\varepsilon_G = 0.49u_G^{0.46}$ for $u_G > 0.05$m/s	Device: Airlift reactor and bubble column Medium: Water
25.	Koide et al. (1988)[66]	$\varepsilon_{Gr} = \dfrac{\mathrm{Fr}}{0.415 + 4.27\left(\dfrac{u_{sg}+u_{Lr}}{\sqrt{gD_r}}\right)\left(\dfrac{g\rho_L D^2}{\sigma_L}\right)^{-0.188} + 1.13\mathrm{Fr}^{1.22}\mathrm{Mo}^{0.0386}\left(\dfrac{\Delta\rho}{\rho}\right)^{0.0386}}$	Device: Internal loop airlift reactor
26.	Popovic and Robinson (1988)[67]	$\varepsilon_{Gr} = 0.456u_{sg}^{0.65}\left(1+\dfrac{A_d}{A_r}\right)^{-1.06}\mu_{app}^{-0.103}$	Media: CMC solutions, 51.8% sucrose Parameter ranges: $0.03 \le u_{sg} \le 0.26$ m· s^{-1} $0.11 \le A_d/A_r \le 0.44$ $0.02 \le \mu_{app} \le 0.5$ Pa· s $1003 \le \rho_L \le 1240$ kg· m^{-3} $0.059 \le \sigma_L \le 0.079$ N· m^{-1}
27.	Chisti (1989)[9]	$\varepsilon_{Gd} = 0.46\varepsilon_{Gr} - 0.024$	Devices: External loop airlift reactors Medium: Aqueous salt solutions (0.15 kmol m^{-3} NaCl in water) with and without paper pulp fiber solids (1%-3% (w/v))
28.	Philip et al.(1990)[68]	$\varepsilon_{Gr} = \dfrac{u_{sg}}{C_1(u_{sg}+u_{Lr}) + C_2\sqrt{gD_r}}$ $C_1 = \dfrac{3n+1}{n+1}$ C_2 = 0.24-0.33 for Newtonian liquid and = 0.35 for non-Newtonian liquid	Device: Internal loop airlift reactor Media: Mineral oils, sugar syrub, CMC, xanthan

No.	Authors	Equations	Parameters
29.	Siegel and Merchuk (1991)[26]	$\varepsilon_{Go} = 0.46\left(\frac{P}{V_L}\right)^{0.99} DR^{0.6}$	Device: Rectangular split vessel airlift reactors
30.	Pasarac and Petrovic (1991)[69]	$\varepsilon_{Gr} = \frac{0.6\rho_G^{0.062}\rho_L^{0.069}\mu_G^{0.107}}{\mu_L^{0.053}\sigma_L^{0.158}} \frac{u_{sg}^{0.936}}{\left(u_{sg}+u_{Lr}\right)^{0.474}}$	Device: External loop airlift reactor
31.	Cai et al. (1992)[70]	$\varepsilon_{Gr} = 2.47u_{sg}^{0.97}$	Device: Internal loop airlift reactor
32.	Ghirardini et al. (1992)[71]	$\varepsilon_G = 0.55u_{Gr}^{0.78}F_f^{0.2}D_r^{0.42}$ $F_f = \frac{V_{Lt}}{V_L}$	Device: External loop airlift reactor
33.	Kemblowski et al. (1993)[25]	$\varepsilon_{Gr} = 0.203\frac{\mathrm{Fr}^{0.31}}{\mathrm{Mo}^{0.012}}\left(\frac{u_{sg}A_r}{u_{Lr}A_d}\right)^{0.74}$ $\mathrm{Mo} = \frac{g\left(\rho_L-\rho_g\right)}{\rho_L^2\sigma_L}K^4\left(\frac{8u_{Lr}}{D_r}\right)^{4(n-1)}\left(\frac{3n+1}{4n}\right)^{4n}$ $\mathrm{Fr} = \frac{\left(u_{Lr}+u_{Gr}\right)^2}{gD_r}$	Device: External loop airlift reactors Media: Water, water with surfactant, glycol solutions, sugar syrub, CMC solution Parameter ranges: $0.001 \le u_{sg} \le 0.5$ m· s^{-1} $0.07 \le u_{Lr} \le 1.3$ m· s^{-1} $1 \le u_{Lr}/u_{sg} \le 153$ $0.0005 \le \mathrm{Fr} \le 14.1$ $2.47\times10^{-11} \le \mathrm{Mo} \le 0.39$ $0.11 \le A_d/A_r \le 1$ $10.2 \le H/D_r \le 228$ $40 \le \mathrm{Re_{Lr}} \le 130{,}000$
34.	Choi and Lee (1993)[45]	$\varepsilon_{Gr} = 0.288u_{sg}^{0.504}\left(\frac{A_d}{A_r}\right)^{-0.098}\left(\frac{L_c}{L_h}\right)^{-0.094}$ $\varepsilon_{Gd} = 0.049\left(\frac{u_g}{u_{Lr}}\right)^{1.138}\left(\frac{A_d}{A_r}\right)^{0.885}\left(\frac{L_c}{L_h}\right)^{-0.462}$	Device: External loop airlift reactor Medium: Water Parameter ranges: $D_r = 0.158$ m. $0.049 < D_d < 0.108$ m $0.11 < A_d/A_r < 0.53$ $0.091 < L_c/L_h < 0.455$

No.	Authors	Equations	Parameters
			$0.1 < L_c < 0.5$ m u_{sg}<0.2 m· s^{-1}
35.	Chisti and Young (1993)[72]	$\varepsilon_{Gr} = \frac{u_{sg}}{0.24 + 1.35(u_{sg} + u_{Lr})^{0.93}}$	
36.	Merchuk et al.(1994)[46]	$\varepsilon_{Go} = 0.29\mathrm{Fr}^{1.05} M^{-2.5} X_{dt}^{0.1} Y^{-0.07}$ $\varepsilon_{Gr} = 1.5\mathrm{Fr}^{0.87} M^{-0.4} X_{dt}^{-0.19} Y^{-0.2}$ $\varepsilon_{Gd} = 4.76\mathrm{Fr}^{1.3} M^{-3.8} X_{dt}^{0.65} \mathrm{Ga}^{-0.09}$	Device: Internal loop airlift reactors (draft tube sparged) Media: Water and carboxymethyl cellulose solutions Parameter ranges: $0.001 < \mu_{app} < 0.025$ Pa· s $6\times10^{-4} < \mathrm{Fr} < 350\times10^{-4}$ $3\times10^{7} < \mathrm{Ga} < 6\times10^{11}$ $0.04 < X_{dt} < 0.4$ $0.22 < M < 0.348$ For 30 L nominal volume A_d/A_r=0.94 $0.0017 < u_{sg} < 0.044$ m· s^{-1} For 300 L nominal volume A_d/A_r=0.86 $0.001 < u_{sg} < 0.026$ m· s^{-1}
37.	Ganzeveld et al. (1995)[73]	$\varepsilon_{Gd} = 0.63\varepsilon_{Gr} - 0.0008$	Devices: Split cylinder internal loop airlift reactors Parameter ranges: For suspensions of animal cell culture microcarrier support particles (0-10 kg· m^{-3})
38.	Merchuk et al. (1996)[49]	$\varepsilon_{Gr} = 0.137\mathrm{Fr}^{0.87} M^{-1.57} X_{dt}^{-0.19} \left(1 + \frac{A_d}{A_r}\right)$ $\varepsilon_{Gd} = 29\mathrm{Fr}^{1.34} M^{-3} X_{dr}^{0.68} \mathrm{Ga}^{-0.09} \left(1 + \frac{A_d}{A_r}\right)^{-1}$	Device: Internal loop airlift reactor (draft tube sparged)

No.	Authors	Equations	Parameters
		$\varepsilon_{Go} = 0.017\mathrm{Fr}^{1.05} M^{-4} X_{dt}^{0.09}\left(1+\frac{A_d}{A_r}\right)$	
		$\mathrm{Sh} = 3\times10^{4}\,\mathrm{Fr}^{0.97} M^{-5.4}\mathrm{Ga}^{0.045}\left(1+\frac{A_d}{A_r}\right)^{-1}$	
39.	Gavrilescu and Tudose (1996)[74]	$\varepsilon_{Gr} = 0.9 H_L^{-0.38}\left(1+\frac{A_d}{A_r}\right)^{-0.626} u_{sg}^{0.54}$	Device: External loop airlift reactor Medium: Water
40.	Choi et al. (1996)[84]	$\varepsilon_{Gd} = 0.988\varepsilon_{Gr} - 0.016$	
41.	Tung et al (1997)[2]	$\varepsilon_G - 0.029 u_G^{1.26}$ for $u_G < 0.05$ m· s^{-1} $\varepsilon_G = 0.143 u_G^{0.27}$ for $u_G > 0.05$ m· s^{-1}	Media: Fermentation broths of *Saccharomyces cerevisiae* Device: Airlift reactor with double net draft tubes or bubble column
42.	Hwang and Cheng (1997)[17]	$\varepsilon_{Gd} = 0.00174 Q_G^{0.735}\left(\frac{A_d}{A_r}\right)^{-0.378} \mu_h^{-0.388} H_D^{0.125}\left(1+\varepsilon_s\right)^{-2.06}$	Device: Internal loop airlift reactors (draft tube sparged) Media: Water and various concentrations of CMC aqueous solutions with poly-styrene particles Parameter ranges: A_d/A_r = 0.69, 1.33 and 3.22
43.	Bentifraouine et al.(1997)[27]	$\varepsilon_{Gr} = 2u_{sg}^{0.88}(1-0.97u_{Lr}^{0.49})$	Device: External loop airlift reactor Medium: Water Parameter ranges: D_r = 0.194 m, D_d = 0.093 m $1 \le H_D \le 1.6$ m. A_d/A_r = 0.23
44.	Gavrilescu and Tudose (1998)[16]	$\varepsilon_{Gr} = 0.32\left(1+\frac{A_d}{A_r}\right)^{0.744} u_{sg}^{0.36+0.078C_s}\mu_{app}^{-0.29}$	Media: Fermentation broths of *P. chrysogenum, S. griseus, S. erythreus, B. lidheniformis* and *C. acremonium* Device: Lab scale external loop airlift

No.	Authors	Equations	Parameters
		$\varepsilon_{Gr} = 4386\left(\frac{u_{sg}}{u_{Lr}}\right)^{0.82}\left(\frac{A_d}{A_r}\right)^{0.21}\left(\frac{H_D}{D_D}\right)^{-1}\mathrm{Fr}^{0.164}\mathrm{Mo}^{-0.051}$ where Fr = Froude Number = $\frac{(u_{Lr}+u_{sg})^2}{gD_r}$ Mo = Morton Number = $\frac{g(\rho_L-\rho_G)k^4}{\sigma_L^3\rho_L^2}\left(\frac{8u_{Lr}}{D_r}\right)^{4(n-1)}\left(\frac{3n+1}{4n}\right)^{4n}$	reactor Parameter ranges: $1.189\times10^{-3} \le V_L \le 1.880\times10^{-3}$ m^3 $1.16 \le H_{Lr} \le 1.56$ m $H_{Ld} = 1.10$ m $0.111 \le A_d/A_r \le 1$ $0.16 \le u_{sg} \le 0.178$ m· s^{-1} Device: Pilot scale external loop airlift reactor Parameter ranges: $0.157 \le V_L \le 0.17$ m^3 $4.3 \le H_{Lr} \le 4.7$ m $4 \le H_{Ld} \le 4.4$ m $0.04 \le A_d/A_r \le 0.1225$ $0.01 \le u_{sg} \le 0.12$ m· s^{-1}
45.	Couvert et al. (1999)[1]	$\varepsilon_{Gr} = 1.37u_{sg}^{0.92}$ for $u_{sg} < 0.005$ ms^{-1} $\varepsilon_{Gd} = 0$ for $u_{sg} > 0.005$ ms^{-1} $\varepsilon_{Gd} = 1.4u_{sg}$	Device: Rectangular internal loop airlift loop reactor Medium: Water Parameter ranges: $0.0045 \le u_{sg} \le 0.057$ m· s^{-1} $A_d/A_r = 1$ Reactor dimension = 0.5×0.5×3 m $2.5 \le H_L \le 2.8$ $0.625 \le V_L \le 0.7$ m^3
46.	Korpijarvi et al. (1999)[76]	$\varepsilon_{Gd} = 0.84\varepsilon_{Gr}$ $\varepsilon_{Gr} = 0.67u_{sg}^{0.57}$ for $A_d/A_r = 0.59$ $\varepsilon_{Gr} = 0.85u_{sg}^{0.66}$ for $A_d/A_r = 1.22$ $\varepsilon_{Gr} = 0.77u_{sg}^{0.66}$ for $A_d/A_r = 2.7$ $\varepsilon_{Gr} = 0.65u_{sg}^{0.78}$ for $A_d/A_r = 7.14$	Device: Internal loop airlift reactor Parameter ranges: $0 \le u_{sg} \le 0.14$ m· s^{-1} $0.59 \le A_d/A_r \le 7.14$

Table 2.4 Summary of experimental liquid circulation velocity correlations of airlift reactor

No.	Authors	Equations	Parameters
1.	Levich (1962)[77]	$u_{Ld} = 2\left(\frac{gd_B}{1.8}\right)^{0.5}$	
2.	Marucci (1969)[78]	$\frac{v_{Lr}}{u_{sg}} = \frac{\left(1-\varepsilon_{Gr}\right)^2}{\left(1-\varepsilon_{Gr}^{5/3}\right)}$	Medium: Coalescence free-system
3.	Bello (1981)[79]	$v_{Lr} = \left(\frac{2gH_D u_{sg}}{\varepsilon_{Gr}}\right)^{1/3}$	Device: Airlift contactor Medium: Water
4.	Popovic and Robinson (1984)[37]	$u_{Lr} = \alpha u_{sg}^{0.322}\left(\frac{A_d}{A_r}\right)^{0.794}\mu_{app}^{-0.395}$ where For bubble flow regime: $\alpha = 0.052$ For slug flow regime: $\alpha = 0.0204$	Devices: External loop airlift reactors Media: non-Newtonian CMC solutions Parameter ranges: $0.015 < \mu_{app} < 0.5$ Pa· s
5.	Bello et al. (1984)[38]	For external loop airlift reactor: $u_{Lr} = 1.55u_{Gr}^{0.33}\left(\frac{A_d}{A_r}\right)^{0.74}$ For internal loop airlift reactor: $u_{Lr} = 0.66u_{sg}^{0.33}\left(\frac{A_d}{A_r}\right)^{0.78}$	Devices: External and Internal loop airlift contactors Media: Water and 0.15 kmol· m^{-3} NaCl solution Parameter ranges: For external loop airlift contctor $0.11 \le A_d/A_r \le 0.69$ $D_r = 0.152$ m, $H_D = 1.8$ m $0.05 \le D_d \le 0.102$ m, $0.0137 \le u_{sg} \le 0.086$ m· s^{-1} For internal loop airlift contactor

No.	Authors	Equations	Parameters
			Sparger: Perforated stainless plate with 52 holes of 1.02 mm $0.13 \le A_d/A_r \le 0.56$
6.	Merchuk (1986)[24]	$v_L = 9.9u_{sg}^{0.4}$	Devices: External loop airlift reactors or bubble column Sparger: Straight copper tube with orifices with diameters =0.0003, 0.0005 and 0.001 m and a porous plate Medium: Water, Solutions of Na_2So_4 7.9% by weight and glycerine 23.7 % be weight Parameter ranges: $0.002 \le u_{sg} \le 0.5$ ms^{-1}
7.	Vatai and Tekic (1986)[58]	$u_{Lr} = 2.858\left(\frac{A_r}{A_d}\right)^{0.416} u_{sg}^{0.482}\mu_{app}^{0.0105}$ $u_{Lr} = 2.858u_{Gr}^{0.482}\left(\frac{A_d}{A_r}\right)^{0.97} 416\mu_{app}^{-0.0105}$	Media: Water and CMC solutions Parameter ranges: $n = 0.866$ $0.304 \le K \le 0.745$ Pa· s^n
8.	Siegel et al. (1986)[60]	$u_{Lr} = 33.868u_{sg}^{0.4}\left(\frac{De_r}{De_d}\right)^{-0.41}$	Devices: Split rectangular airlift reactors Medium: Water Parameter ranges: Riser: 0.09×0.25 m Downcomer: 0.01×0.25 m $H = 4$ m, $V_L = 0.3$ m^3
9.	Popovic and Robinson (1987)[81]	$u_{Lr} = 0.23u_{sg}^{0.32}\left(\frac{A_d}{A_r}\right)^{0.97}\mu_{app}^{-0.39}$	Devices: External loop airlift reactors Media: CMC solutions Parameter ranges: $0.015 \le \mu_{app} \le 0.5$ Pa· s

No.	Authors	Equations	Parameters
			$0.11 \le A_d/A_r \le 0.44$ D_r=0.15 m, H_D=1.88 m
10.	Chisti et al. (1988)[14]	$$u_{Lr} = \left[\frac{2gH_D\left(\varepsilon_{Gr} - \varepsilon_{Gd}\right)}{\frac{K_t}{\left(1-\varepsilon_{Gr}\right)^2} + \frac{K_b}{\left(1-\varepsilon_{Gd}\right)^2}\left(\frac{A_r}{A_d}\right)^2} \right]^{0.5}$$ For an external loop airlift device: $$u_{Lr} = \left[\frac{2gH_D\left(\varepsilon_{Gr} - \varepsilon_{Gd}\right)}{K_b\left(\frac{1}{\left(1-\varepsilon_{Gr}\right)^2} + \frac{1}{\left(1-\varepsilon_{Gd}\right)^2}\left(\frac{A_r}{A_d}\right)^2\right)} \right]^{0.5}$$ where $$K_b = 11.402\left(\frac{A_d}{A_b}\right)^{0.789}$$ For split cylinder or concentric tube internal loop airlift devices: $$u_{Lr} = \left[\frac{2gH_D\left(\varepsilon_{Gr} - \varepsilon_{Gd}\right)}{\frac{K_b}{\left(1-\varepsilon_{Gd}\right)^2}\left(\frac{A_r}{A_d}\right)^2} \right]^{0.5}$$	Devices: External and internal loop airlift reactors Medium: Water Parameter ranges: H= 3.21 m D_r = 0.142 m $0.11 \le A_d/A_r \le 1$ V_L= 1.46 m^3
11.	Assa and Bar (1991)[82]	$$u_{Lr} = 0.96u_{sg}^{0.39}$$	Devices: Internal loop airlift reactor (draft tube sparged) Medium: Water Parameter ranges: A_d/A_r = 1

No.	Authors	Equations	Parameters
12.	Siegel and Merchuk (1991)[26]	$v_{Ld} = 45\left(\frac{P_G}{V_L}\right)^{0.33} DR^{-0.85}$	Devices: Rectangular split-vessel airlift reactors Medium: Water
13.	Choi and Lee (1993)[45]	$v_{Lr} = 0.607 u_{sg}^{0.263}\left(\frac{A_d}{A_r}\right)^{0.593}\left(\frac{L_c}{L_h}\right)^{0.169}$ $\frac{t_m}{t_c} = 4.608\left(\frac{u_{sg}}{u_{Lr}}\right)^{0.082}\left(\frac{A_d}{A_r}\right)^{0.316}\left(\frac{L_c}{L_h}\right)^{0.107}$ $u_{Lr} = \left[\frac{2gH_D(\varepsilon_{Gr}-\varepsilon_{Gd})}{11.402\left(\frac{A_d}{A_b}\right)^{0.789}\left(\frac{A_r}{A_d}\right)^{2}\frac{1}{(1-\varepsilon_{gGd})^2}}\right]^{0.5}$ where $K_b = 12.705\left(1+\frac{A_d}{A_r}\right)^{2.05}\left(1+\frac{L_c}{L_h}\right)^{-1.119}$	Devices: External loop airlift reactors Medium: Water Parameter ranges: $D_r = 0.158$ m $0.049 \le D_d \le 0.108$ m $0.11 \le A_d/A_r \le 0.53$ $0.091 \le L_c/L_h \le 0.455$ $0.1 \le L_c \le 0.5$ m $u_{sg} < 0.2$ m· s^{-1}
14.	Russell et al. (1994)[83]	$v_{Lr} = 0.9 u_{sg}^{a} H_{dt}^{b}$ where a = 0.44±0.03 and b = 0.47±0.07	Devices: Internal loop airlift fermentor (draft tube sparged) Medium: Non-Newtonian fermentation broth containing the *yeast Saccharomyces cerevisiae* Sparger: Perforated plate sparger Parameter ranges: $0.025 \le u_{sg} \le 0.2$ m· s^{-1} $A_d/A_r = 1.26$ $1.17 \le H_{dt} \le 3.22$ m 120×0.001m. diameter orifices

No.	Authors	Equations	Parameters
15.	Choi et al. (1996)[75]	For draft tube sparged: $t_m = 13.714 u_{sg}^{-0.277}$ For annulus sparged: $t_m = 11.243 u_{sg}^{-0.36}$	Devices: Internal loop airlift reactors
16.	Choi (1996)[84]	$v_{Lr} = 0.795 u_{sg}^{0.233} \left(\frac{A_d}{A_r}\right)^{0.33} \left(\frac{L_c}{L_h}\right)^{0.137}$	Devices: External loop airlift reactors
17.	Bando et al. (1998)[85]	$t_m = c u_{sg}^{0.5} D_o^{1.4} \left(\frac{H_D}{D_o}\right)^{1.2} \left(\frac{D_i}{D_o}\right)^{-1.4} \left(1 - \frac{D_i}{D_o}\right)^{-1.1}$ For draft tube sparged c=2.2 For annulus spaged c=2.6	Devices: Internal loop airlift reactors Parameter ranges: $0.114 \le D_o \le 0.5$ m $5 \le H_D/D_o \le 40$ $0.4 \le D_i/D_o \le 0.8$ $L_b/D_i = 0.5$, $L_t/D_o = 2$

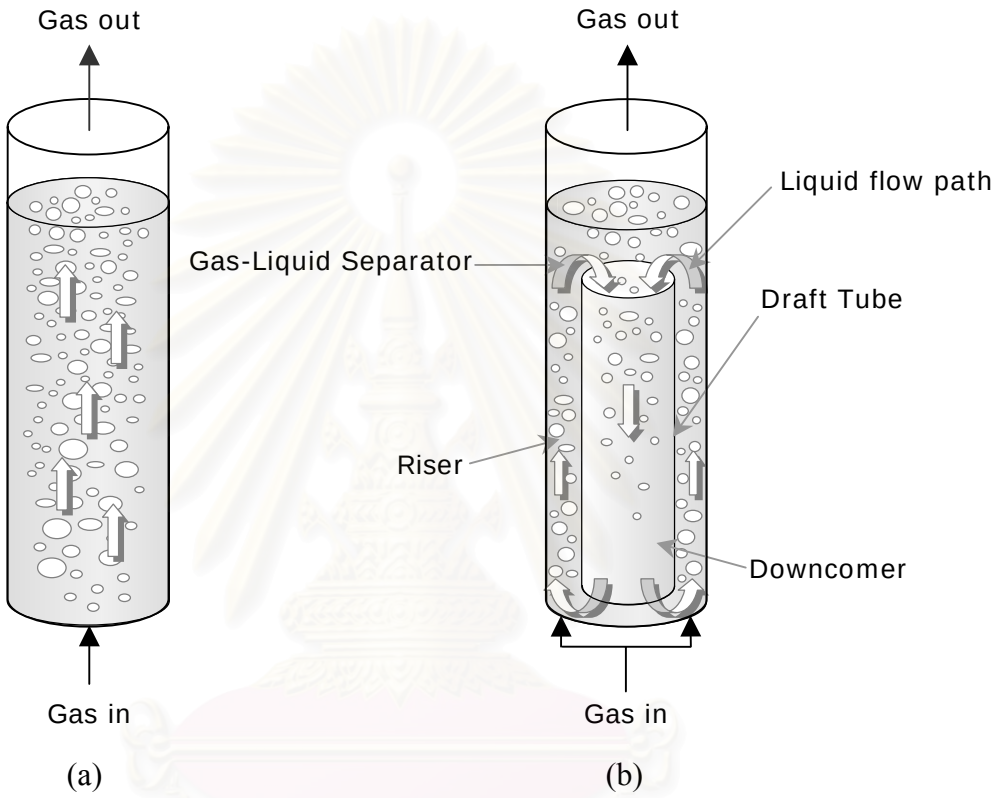

Figure 2.1 Configurations of pneumatic contactor: (a) a bubble column and (b) an airlift contactor

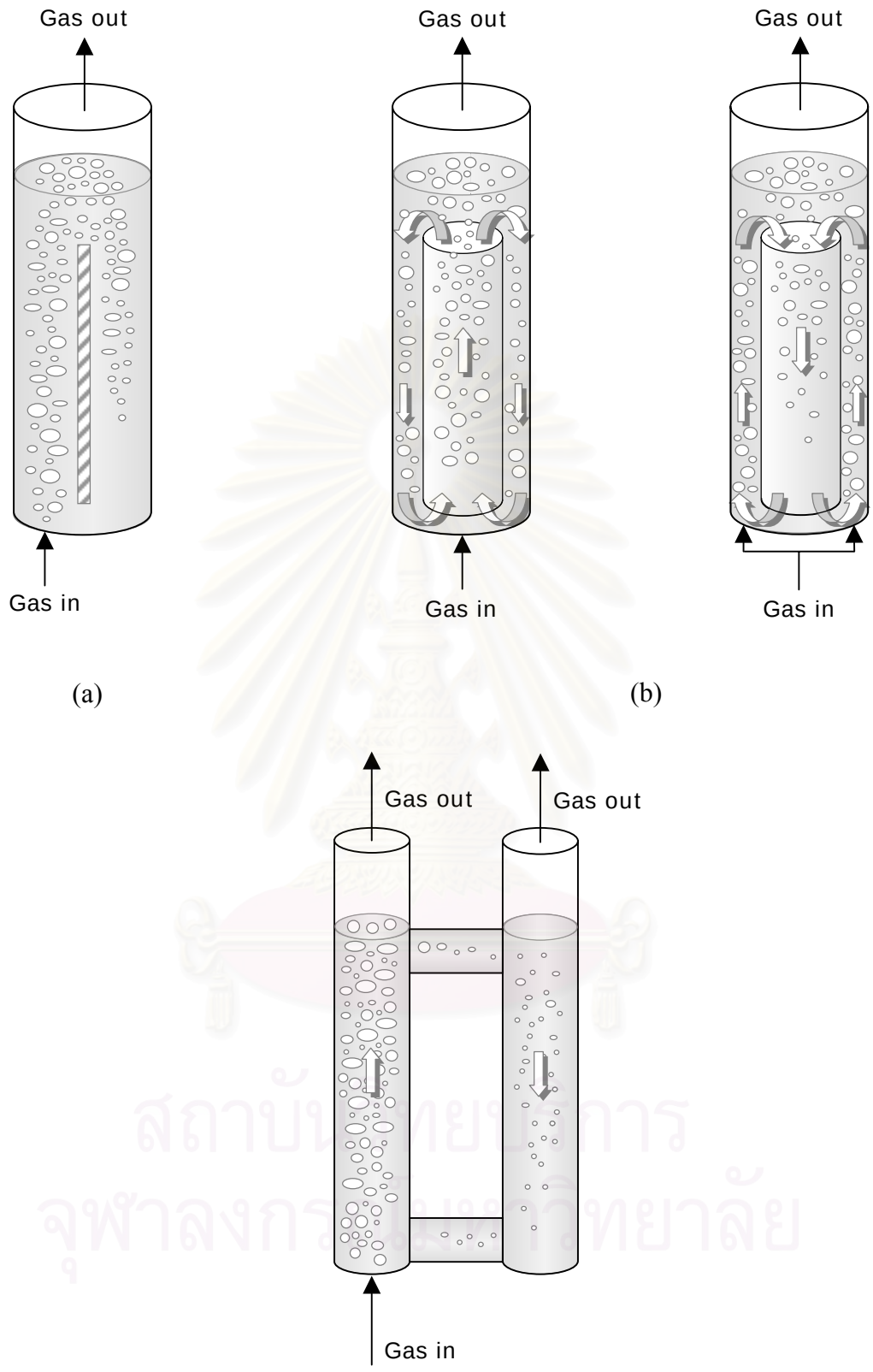

Figure 2.2 Two configurations of ALCs: (a) split cylinder internal loop ALC, (b) concentric tube ALC (c) external loop ALC

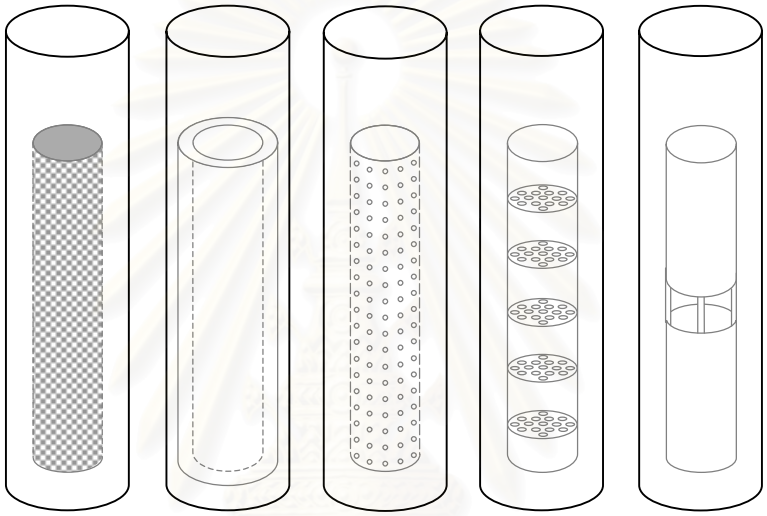

Figure 2.3 Various configurations of modified ALCs: (a) net draft tube[2], (b) multiple draft tube[3], (c) perforated draft tube[4], (d) baffle draft tube[5-8], (e) vertically-split draft tube[9].

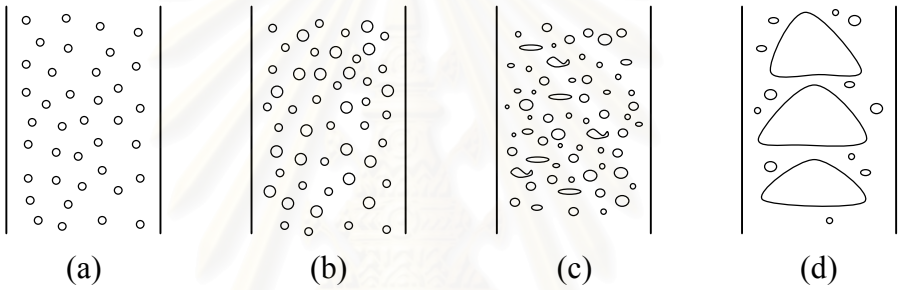

Figure 2.4 Gas-liquid dispersion classification: (a) Homogeneous gas-liquid dispersion, (b-d) Heterogeneous gas-liquid dispersion

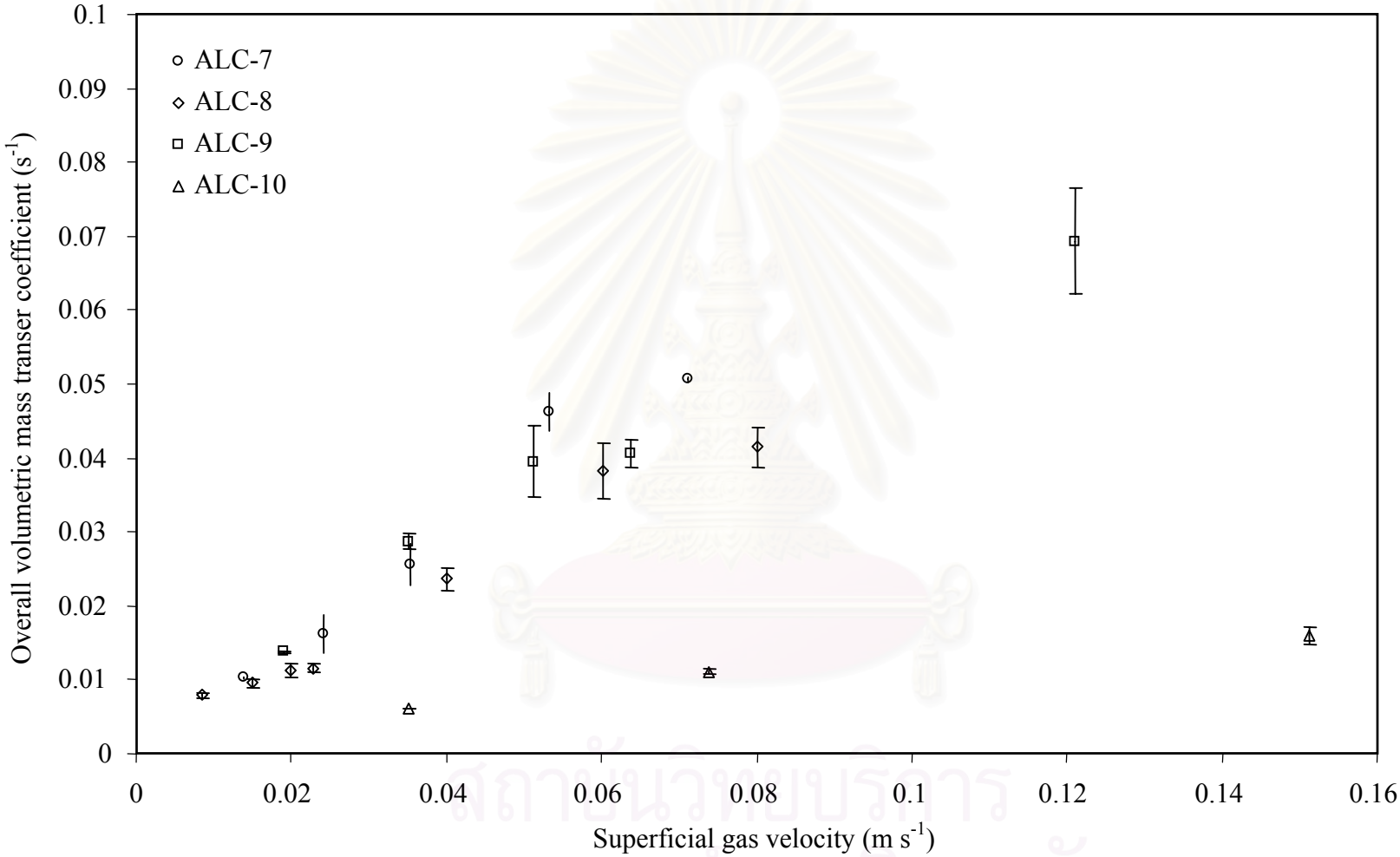

Figure 2.5 Relationship between overall gas-liquid mass transfer coefficient and superficial gas velocity obtained from the draft tube sparged ALC employed in this work

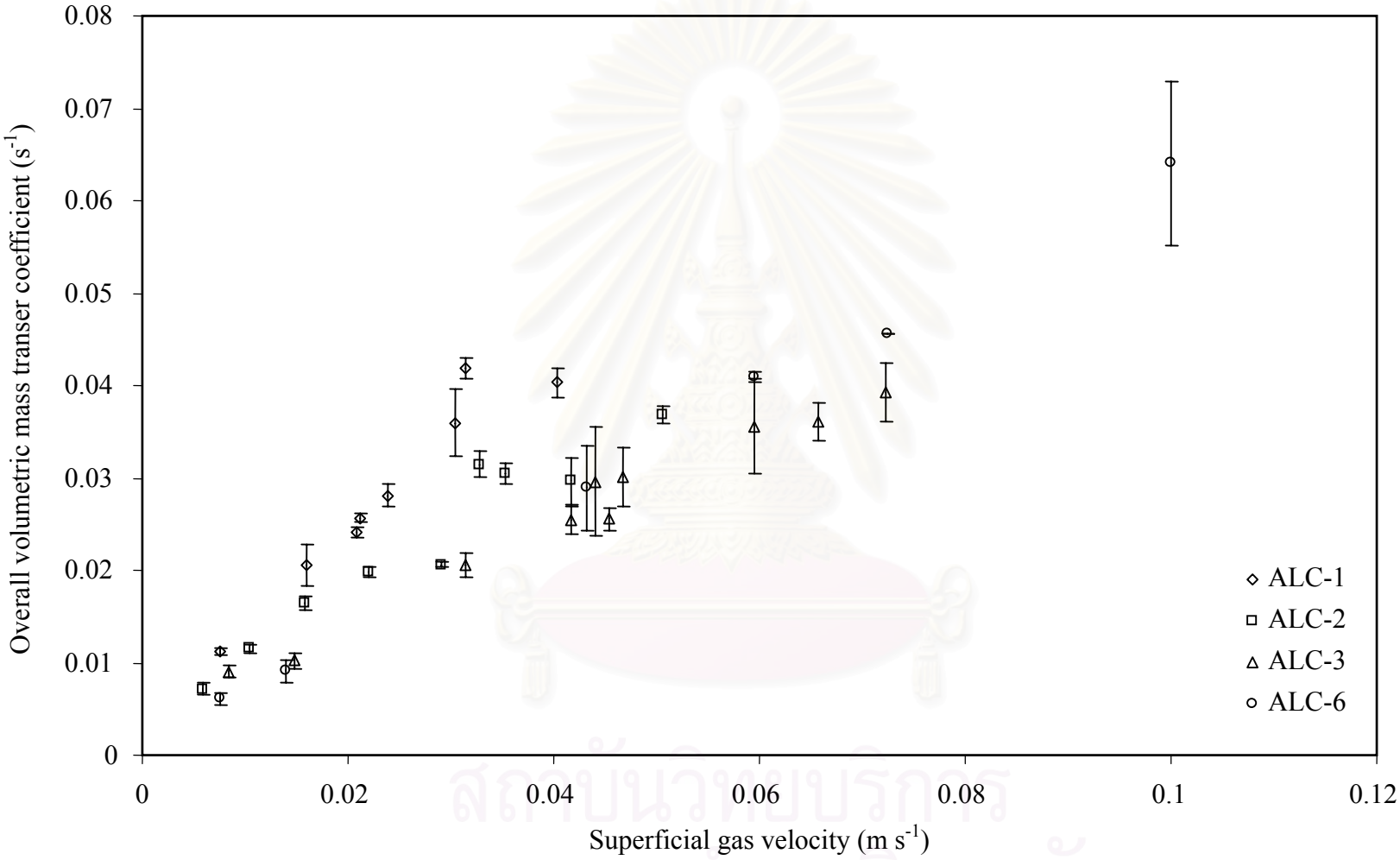

Figure 2.6 Relationship between overall gas-liquid mass transfer coefficient and superficial gas velocity obtained from the annulus sparged ALC employed in this work

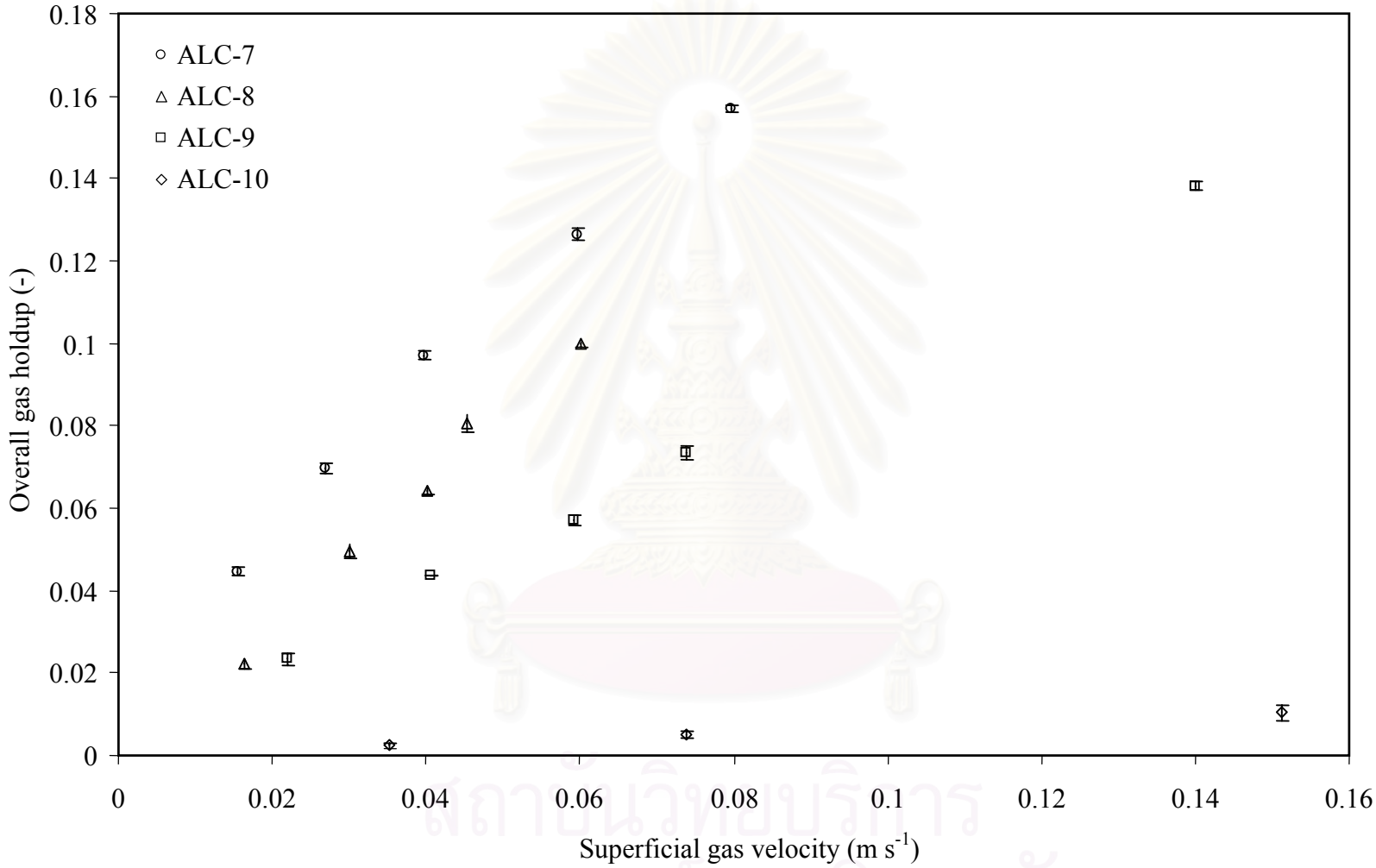

Figure 2.7 Relationship between overall gas holdup and superficial gas velocity obtained from the draft tube sparged ALC employed in this work

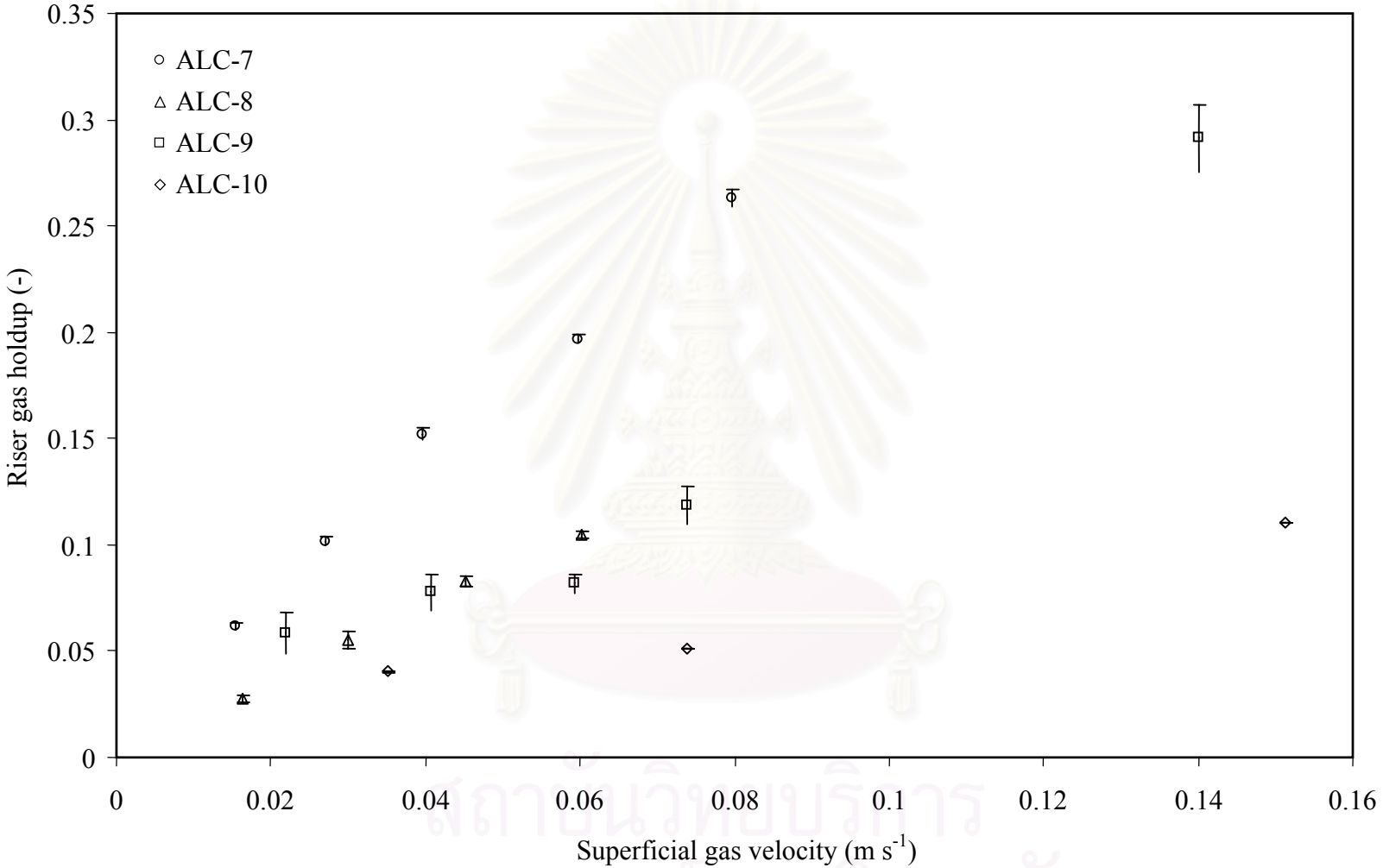

Figure 2.8 Relationship between riser gas holdup and superficial gas velocity obtained from the draft tube sparged ALC employed in this work

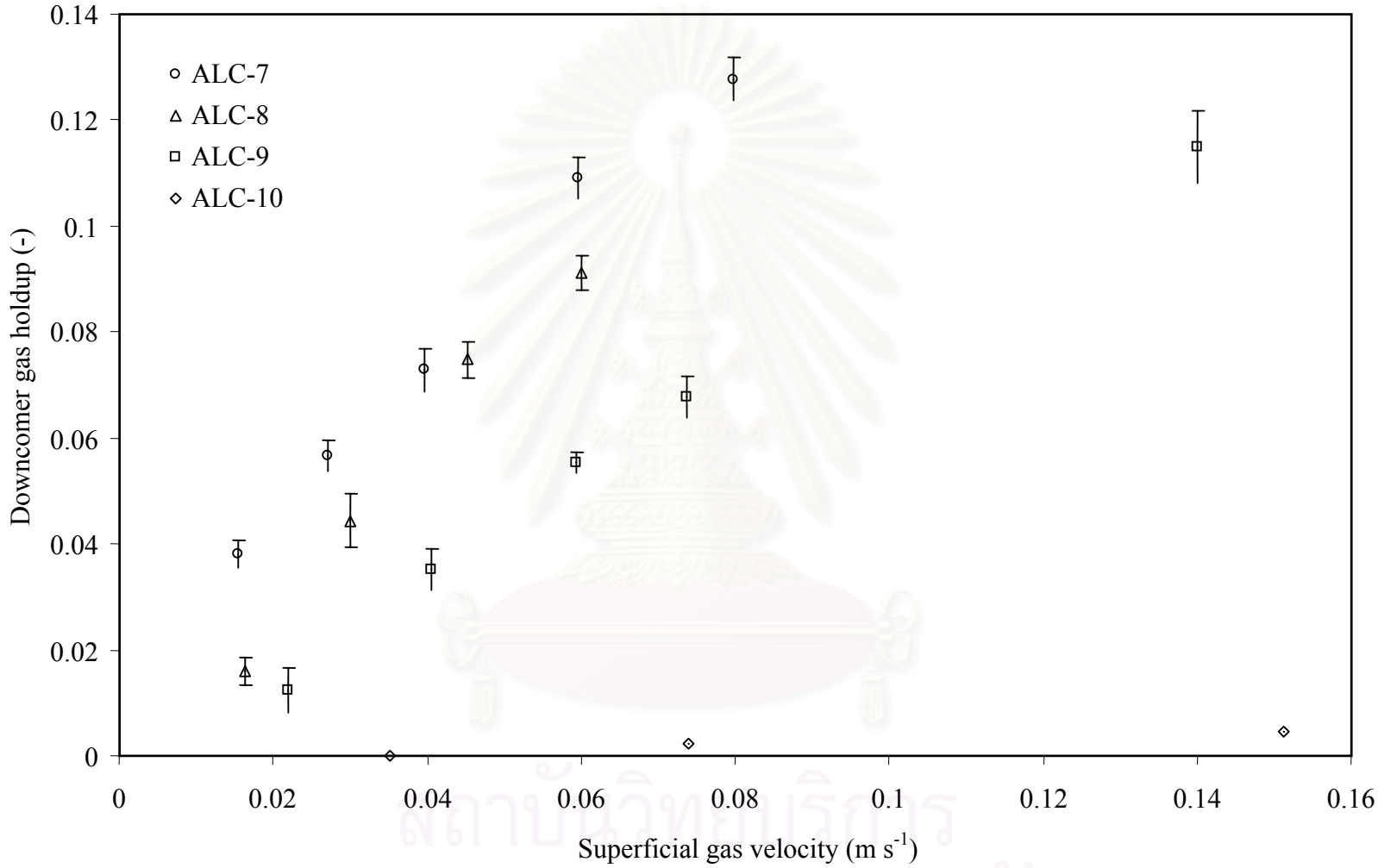

Figure 2.9 Relationship between downcomer gas holdup and superficial gas velocity obtained from the draft tube sparged ALC employed in this work

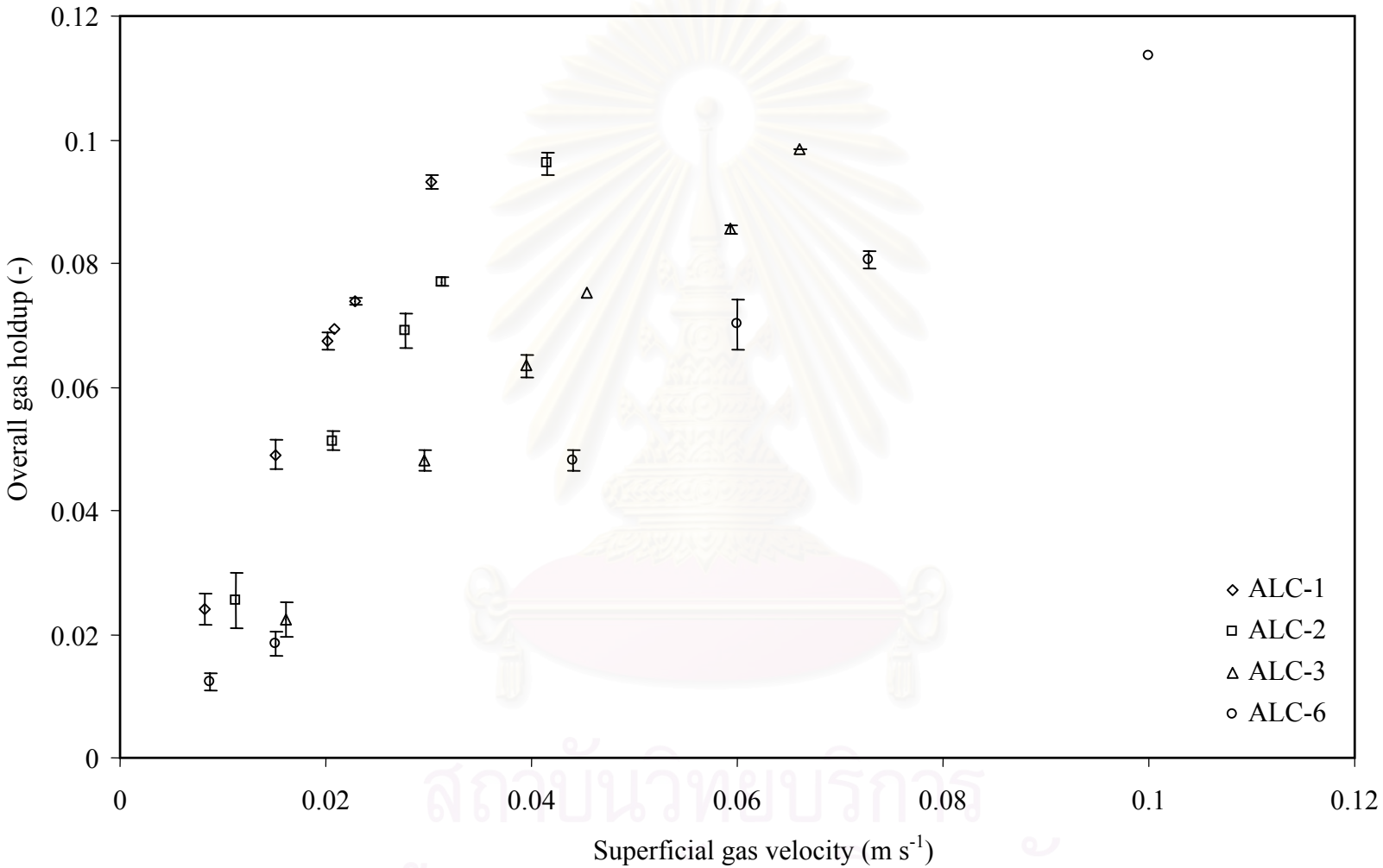

Figure 2.10 Relationship between overall gas holdup and superficial gas velocity obtained from the annulus sparged ALC employed in this work

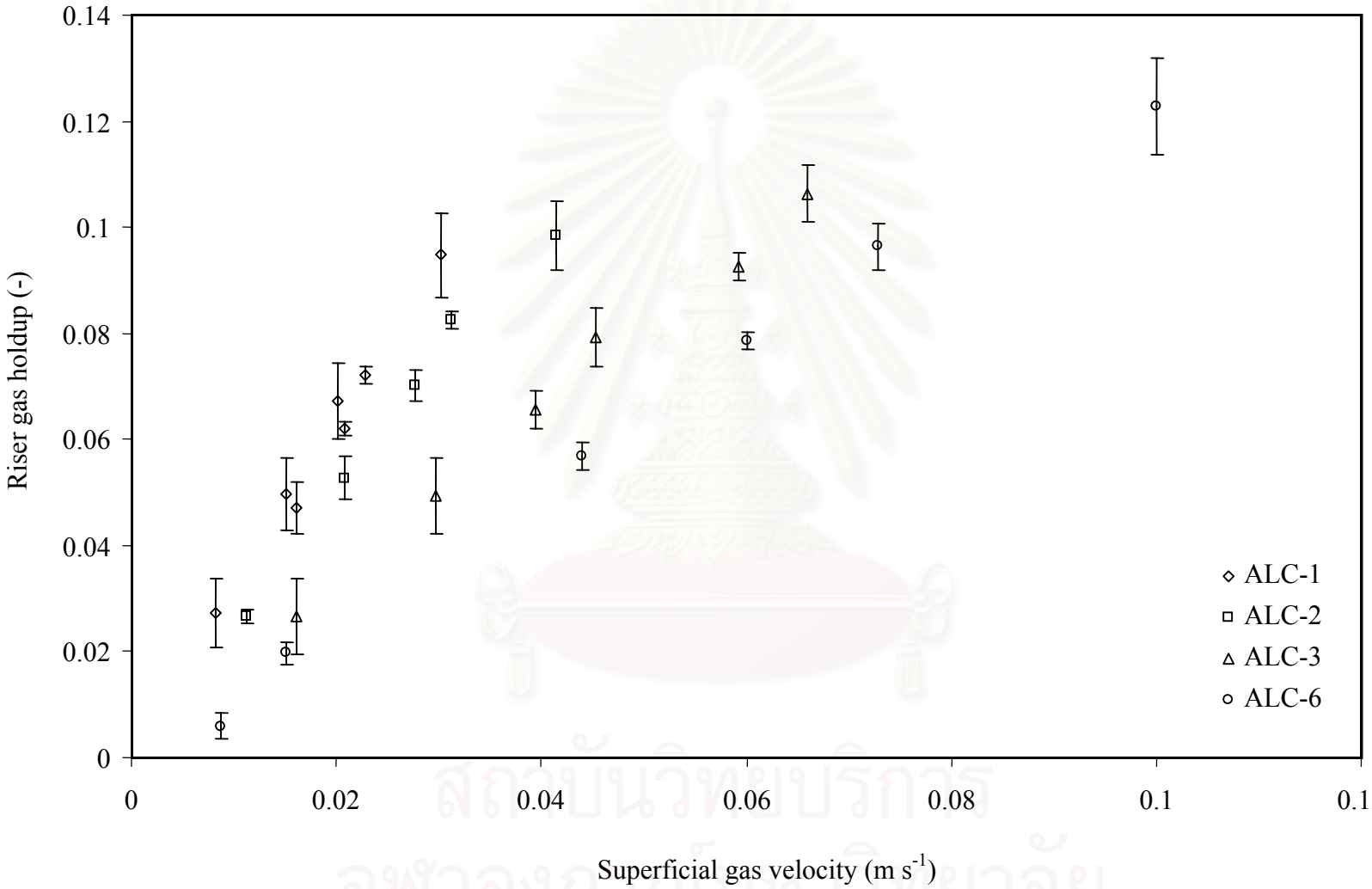

Figure 2.11 Relationship between riser gas holdup and superficial gas velocity obtained from the annulus sparged ALC employed in this work

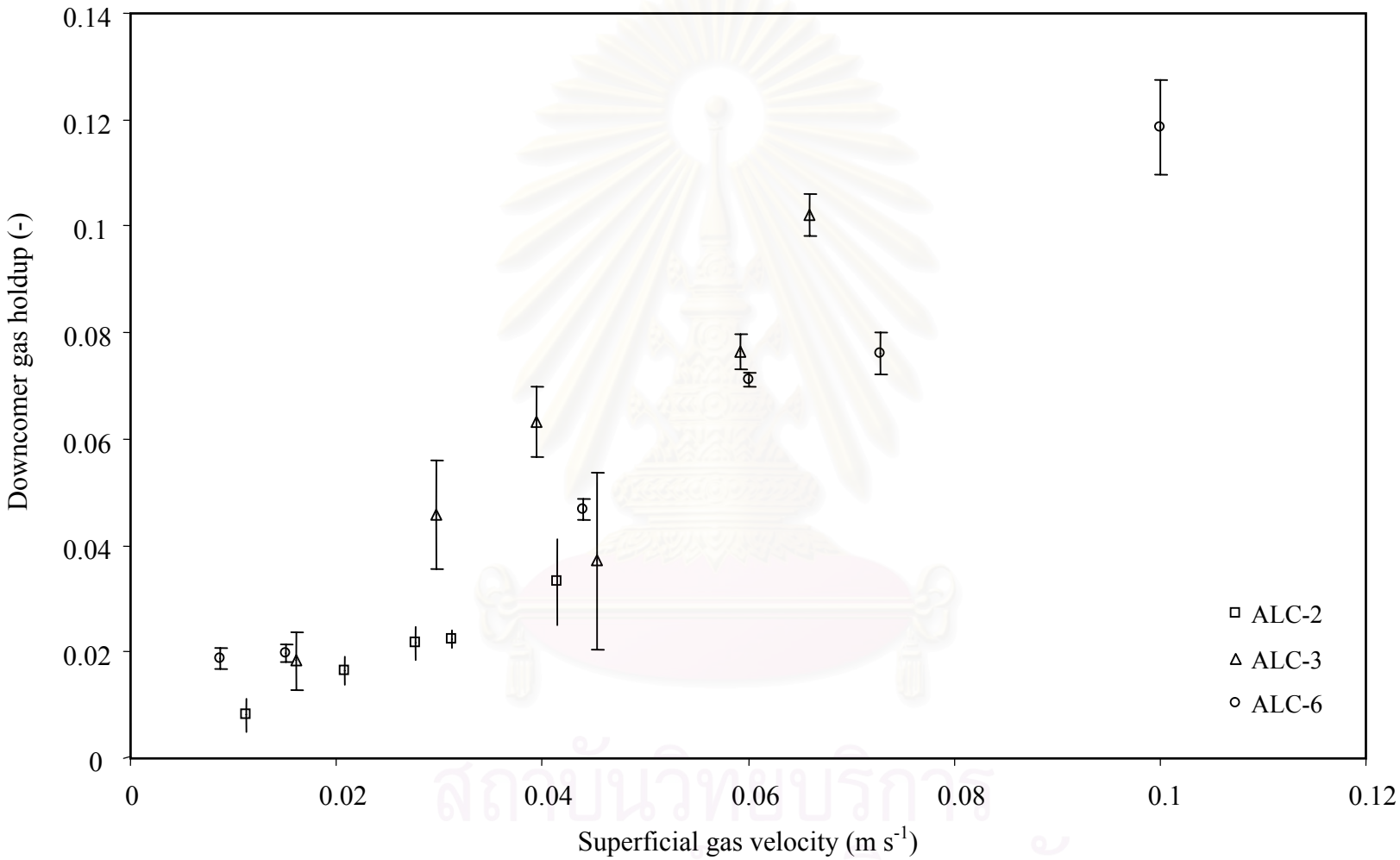

Figure 2.12 Relationship between downcomer gas holdup and superficial gas velocity obtained from the annulus sparged ALC employed in this work

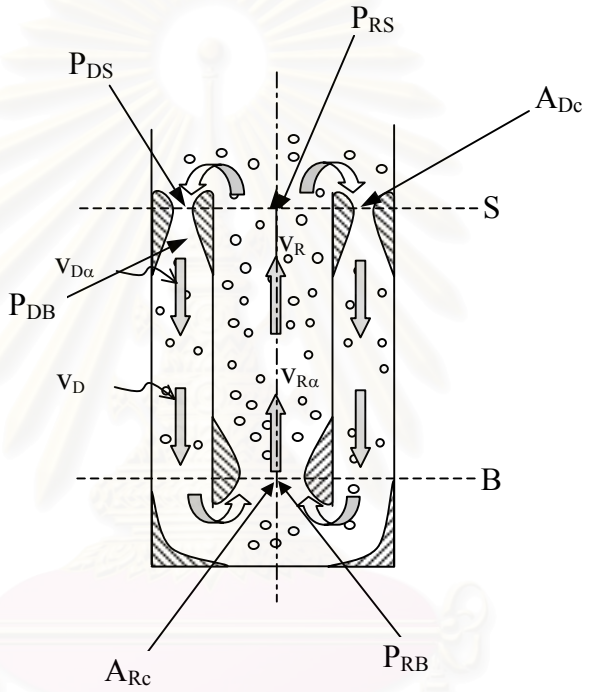

Figure 2.13 Liquid flow with flow contractions at the entrances of riser and downcomer based on Bernoulli's equation

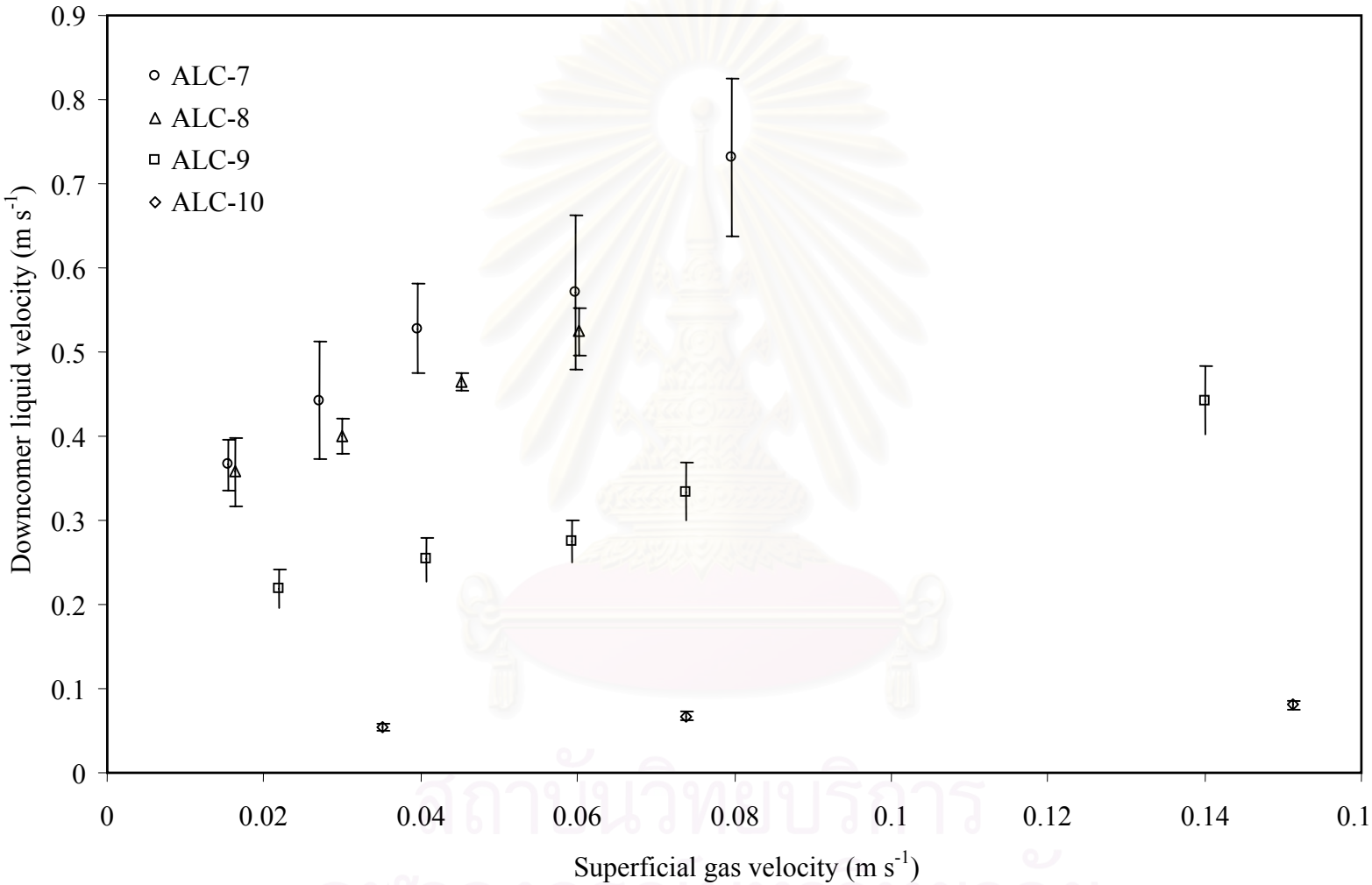

Figure 2.14 Relationship between downcomer liquid velocity and superficial gas velocity obtained from the draft tube sparged ALC employed in this work

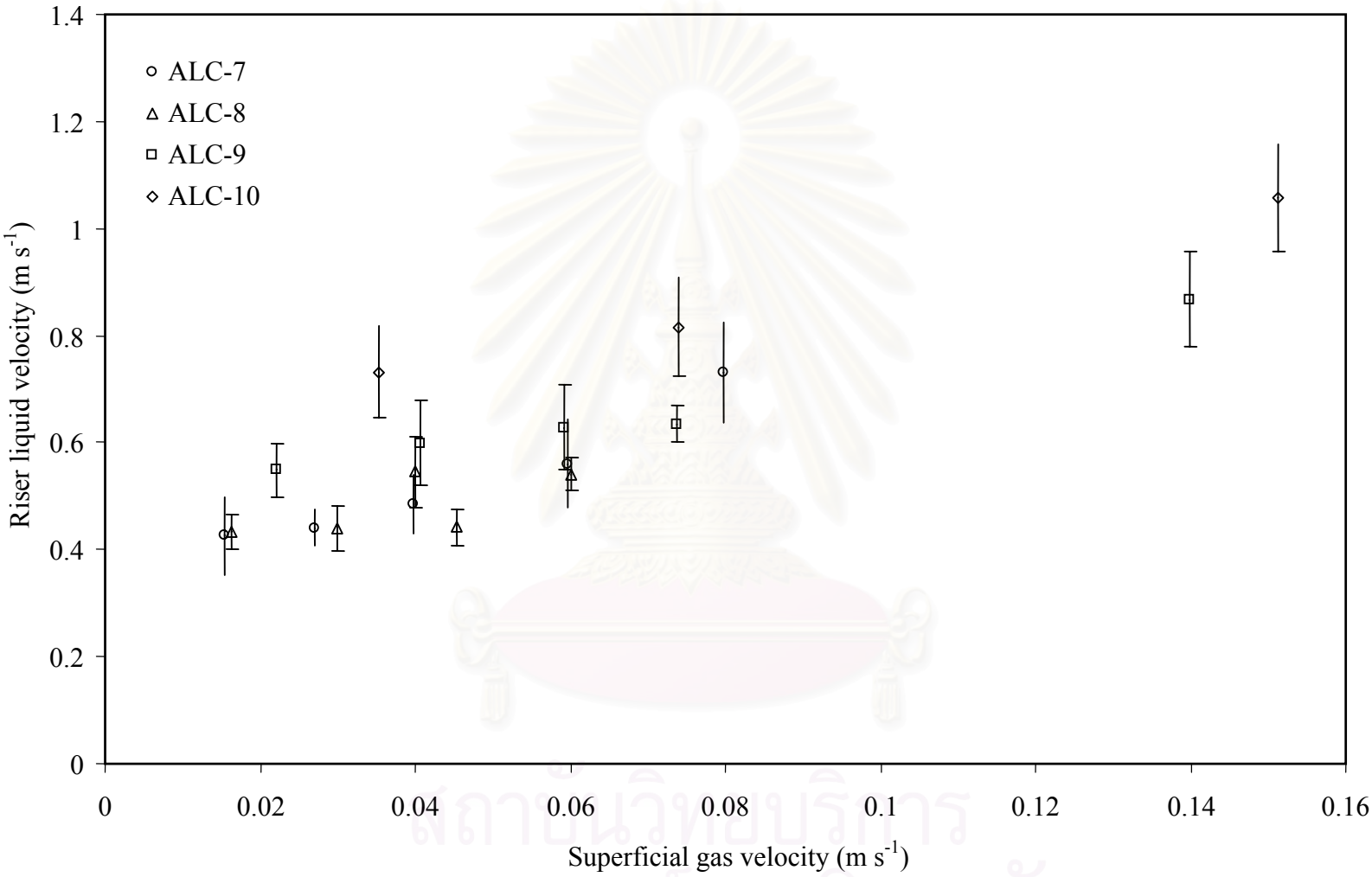

Figure 2.15 Relationship between riser liquid velocity and superficial gas velocity obtained from the draft tube sparged ALC employed in this work

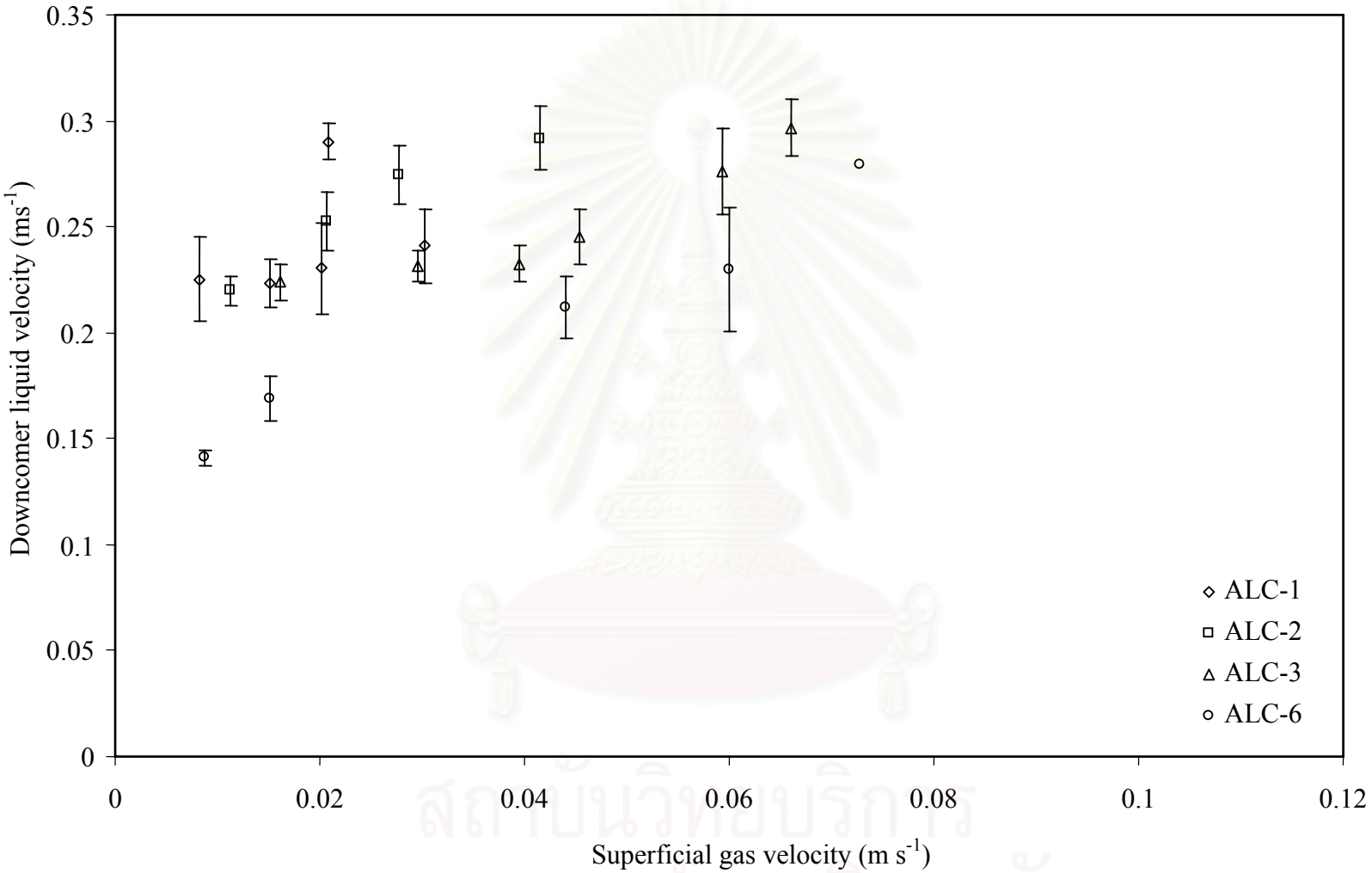

Figure 2.16 Relationship between downcomer liquid velocity and superficial gas velocity obtained from the annulus sparged ALC employed in this work

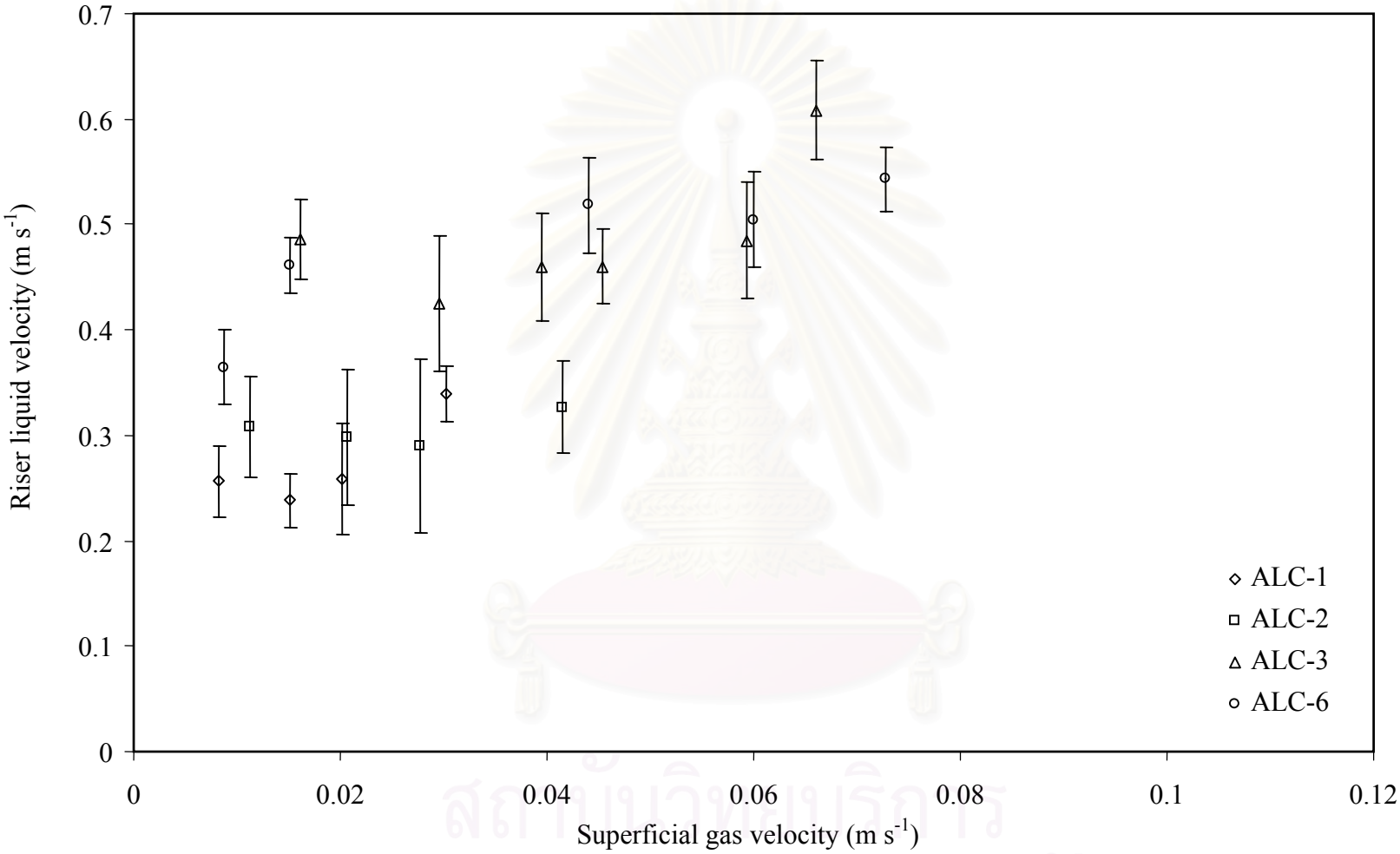

Figure 2.17 Relationship between riser liquid velocity and superficial gas velocity obtained from the annulus sparged ALC employed in this work

Chapter 3

Experiments

3.1 Experimental Apparatus

To achieve the objectives of this study, a series of experiments were arranged. The experiments were designed to allow the adjustment of various parameters as described in detail below.

The schematic diagram of the experimental setup is shown in Figure 3.1 whereas the dimensions of the apparatus are detailed in Figure 3.2. All experiments in this section were performed with a concentric internal loop airlift contactor (ALC) with the main column diameter of 0.137 m and the height of 1.20 m. A draft tube of 1 m in height was inserted centrally inside the outer column. The draft tube stood on four 5 cm-legs which was located equiradially at the bottom end of draft tube. Both the main column and draft tube are made of transparent acrylic plastic to allow visual observation and records of the movement of the color tracer and bubble characteristics, i.e. bubble size and bubble size distribution. The ratio between downcomer and riser cross-sectional areas was altered by changing the draft tube diameter where detailed dimensions of the draft tubes are shown in Table 3.1. Attached to the main column of the ALCs were a series of measuring ports (see Fig. 3.1) for pressure drop measurement (via manometer). These measuring ports were also designed to allow easy injection of dye tracer for the liquid velocity measurement. The dye tracer is blue in color and the specific gravity of this tracer is more or less equal to that of water. At the bottom, a gate valve was installed for draining, and air from compressor was introduced continuously into the contactors through a gas sparger, which could be located at the base of the column either in draft tube or in annular section of the column depending on the mode of gas sparging. Tap water and air were used as liquid and gas phases. Air flowrate was controlled by a calibrated rotameter. The gas velocity in the experiments ranged from 0-0.15 $m \cdot s^{-1}$ used on the cross-sectional area of riser. The sparger is a ring type made of a flexible PVC tube with a diameter of 8 mm. The spargers with three different orifice numbers, i.e. 5, 14 and 30, were employed to investigate the effect of gas sparger on the

behavior of the contactor. All experiments were operated batchwise with respect to the liquid at ambient temperature and atmospheric pressure. The liquid level was always controlled at 3 cm above draft tube to give the total volume of approximately 18 liters. In order to consider the effect of geometrical and operational parameters on bubble properties, bubble properties had been measured by photographic technique using digital video camera (SONY DCR-TRV20E). A lamp was installed normal to the axis of the column to ensure adequate lighting of the images. This was also useful for the observation of the movement of color tracer for the investigation of liquid velocities and the flow pattern of liquid in the contactor.

It can be seen from Table 3.2 that there were different schemes of concentric internal loop ALCs. The design parameters of interest include (i) cross-sectional area ratio between downcomer and riser, (ii) sparger geometry and (iii) mode of gas sparging. Different sets of concentric internal loop ALCs were arranged in order to study the influence of each design parameter (see Table 3.3). In addition, the effects of gas flowrate on system behavior were also investigated in all experiments. Detail of the measurements for each experiment is described later in this chapter.

3.2 Experimental

3.2.1 Bubble characteristic measurement

The measurements of bubble size and its distribution were performed only in the riser of the internal loop ALC with the gas distribution into annulus where the direct observation of bubble size in downcomer was not possible due to the limitation of the photographic technique. The sizes of not less than 200 bubbles were measured for each experiment. The correction to real size was based on the scale attached to the draft tube, which was at the same focal distance as the measured bubbles. In fact, the focus was adjusted on the scale and only the well-focalized bubbles were measured.

A. Experimental procedure

1) Attach scale to the draft tube.
2) Fill tap water into the concentric tube internal loop airlift contactor until liquid level (H_L) reaches the desired level (3 cm above the top of draft tube).
3) Turn on the lamp to illuminate the observation viewpoint.

4) Disperse compressed air from an air compressor continuously into the contactor through a sparger.
5) Adjust superficial gas velocity (u_{sg}) to the desired value by using a calibrated rotameter.
6) Record the images of bubbles at three different heights (x): 0.1m (bottom section), 0.5m (middle section) and 0.9m (top section) from the base of the draft tube using the digital video camera.
7) Repeat Steps 1) to 6) using new geometrical and/or operating parameters.

B. Calculations

For ellipsoidal bubbles, the major and minor axes of bubble images were measured as shown in Figure 3.3. The equivalent size of the bubble (d_B), representing the diameter of a sphere whose volume is equal to that of the bubble, can then be calculated using the conventional expression:

$$d_B = (p^2 q)^{1/3} \tag{3.1}$$

3.2.2 Gas holdup measurement

The overall gas holdup is determined by the volume expansion method. The gas holdup in annular section is determined by the manametric method. The experimental steps are detailed as follows:

A. Experimental procedure

1) Fill tap water into the concentric tube internal loop airlift contactor until liquid level (H_L) reaches the desired level (3 cm above the top of draft tube).
2) Disperse compressed air from an air compressor continuously into the contactor through a sparger.
3) Adjust superficial gas velocity (u_{sg}) to the desired value by using a calibrated rotameter.
4) Read the liquid dispersion height (H_D) to evaluate the overall gas holdup in the contactor (see Section B).
5) Measure pressure difference between two positions (ΔP) in an annular section by water manometer to evaluate gas holdup in the annular section. However, in this case, gas holdup in a draft tube section cannot be measured directly so this value is calculated using Eq. (3.5) (see Section B).

6) Repeat Steps 1) to 5) using new geometrical and/or operating parameters.

B. Calculations

The unaerated and aerated liquid heights are measured and the overall gas holdup is then calculated from following equation:

$$\varepsilon_{Go} = \frac{H_D - H_L}{H_D} \tag{3.2}$$

For the annulus sparged ALC, the riser gas holdup (gas holdup in the annular section) is estimated by measuring the pressure difference (ΔP) between two measuring ports located along the height of the column. Neglecting the acceleration and wall-friction contribution in the momentum balance and with $\rho_L \gg \rho_G$, the gas holdup can be deduced from:

$$\varepsilon_{Gr} = 1 - \frac{\Delta P}{\rho_L g \Delta h} \tag{3.3}$$

It is assumed that the gas holdup in the top section is approximately equal to that in the riser. This allows the estimation of the downcomer gas holdup (gas holdup in the tube) from the overall and riser gas holdups. The relationship between the gas holdups in different parts of an ALC can be written as:

$$\varepsilon_{Go} = \frac{H_{dt} A_r \varepsilon_{Gr} + H_{dt} A_d \varepsilon_{Gd} + (H_D - H_{dt})(A_d + A_r)\varepsilon_{Gt}}{H_D (A_d + A_r)} \tag{3.4}$$

Substituting $\varepsilon_{Gt} = \varepsilon_{Gr}$ into Eq. (3.4) yields:

$$\varepsilon_{Go} = \frac{H_{dt} A_d \varepsilon_{Gd} + (H_D A_d + H_D A_r - H_{dt} A_d)\varepsilon_{Gr}}{H_D (A_d + A_r)} \tag{3.5}$$

or

$$\varepsilon_{Gd} = \frac{\varepsilon_{Go} H_D (A_d + A_r) - (H_D A_d + H_D A_r - H_{dt} A_d)\varepsilon_{Gr}}{H_{dt} A_d} \tag{3.6}$$

3.2.3 Liquid velocity (and internal liquid circulation) measurement

A. Experimental procedure

1) Fill tap water into the concentric tube internal loop airlift contactor until liquid level (H_L) reaches the desired level (3 cm above the top of draft tube).

2) Disperse compressed air from an air compressor continuously into the contactor through a sparger.
3) Adjust superficial gas velocity (u_{sg}) to the desired value by using a calibrated rotameter.
4) Inject dye tracer into the annular section of the ALC to measure liquid velocities in both annular and draft tube sections. The motion of dye tracer is observed visually and a stopwatch is used to measure the time tracer uses to move between 2 positions.

   Notes: - After the liquid velocity measurement by dye tracer, the liquid may not be clear enough to observe on-going phenomena. For this reason, before next experiment is carried out the colored liquid should be drained and new clear water should be re-filled
5) Repeat Steps 1) to 4) using new geometrical and/or operating parameters.

B. Calculation

With the experimental data on the travelling time of tracer between the two points in the contactor, liquid velocities both in riser and downcomer can be evaluated by Eq. (3.7) and (3.8), respectively.

$$v_{Lr} = \frac{L_r}{t_r} \tag{3.7}$$

$$v_{Ld} = \frac{L_d}{t_d} \tag{3.8}$$

3.2.4 Mass transfer measurement

The overall volumetric mass transfer coefficient (k_La) was determined by the dynamic gassing in method[1-3]. A dissolved oxygen meter (Jenway 9300) was used to record the changes in concentration of O_2 in a batch of water that had previously been freed of O_2 by bubbling through with N_2. Experimental methods follow:

A. Experimental procedure

1) Fill tap water into the concentric tube internal loop airlift contactor until liquid level (H_L) reaches the desired level (3 cm above the top of draft tube).
2) Immerge the dissolved oxygen probe into the water in the contactor (see Figure 3.1).

3) Disperse nitrogen gas at the base of the contactor to remove dissolved oxygen from the water.
4) Measure dissolved oxygen concentration in the water by dissolved oxygen meter to ensure that all of the oxygen has been removed.
5) Stop the nitrogen gas flow.
6) Distribute compressed air from an air compressor continuously into the contactor through a sparger.

   Notes: - The value at the rotameter is set to give a desired level of superficial gas velocity.
7) Record the dissolved oxygen concentration with respect to time as soon as air is distributed into the ALC until the water is saturated with oxygen.
8) Repeat Steps 1) to 7) using new geometrical and/or operating parameters.

B. Calculation

The k_La is determined by using the dynamic method. A material balance on dissolved oxygen according to the assumption in Section 1.3.4 gives:

$$\frac{dC}{dt} = k_L a\left(C^* - C\right) = K_L a\left(C^* - C\right) \tag{3.9}$$

Integrate Eq. (3.9) with the limits of $C = C_0$ at $t = 0$ and $C = C$ at $t = t$ results in:

$$\int_{C_0}^{C} \frac{dC}{\left(C^* - C\right)} = k_L a \int_0^t dt \tag{3.10}$$

The result of integration is

$$\ln\left[\frac{C^* - C_0}{C^* - C}\right] = k_L a t \tag{3.11}$$

The value of k_La is obtained from the slope of the linear regression with $\ln\left[\frac{C^* - C_0}{C^* - C}\right]$ with respect to time (t).

3.3 References

1. Koide, K., Sato, H., and Iwamoto, S. 1983. Gas holdup and volumetric liquid-phase mass transfer coefficient in bubble column with draught tube and with gas dispersion into annulus. J. Chem. Eng. Japan 16(5): 407-413.

2. Tung, H.-L., Tu, C.-C., Chang, Y.-Y., and Wu, W.-T. 1998. Bubble characteristics and mass transfer in an airlift reactor with multiple net draft tubes. Bioproc. Eng. 18: 323-328.
3. Bouaifi, M., Hebrard, G., Bastoul, D., and Roustan, M. 2001. A comparative study of gas hold-up, bubble size, interfacial area and mass transfer coefficients in stirred gas-liquid reactors and bubble columns. Chem. Eng. Proc. 97-111.

3.4 Tables and figures

Table 3.1 Dimensions of draft tubes

Draft tube	D_i (m)	D_{io} (m)
Draft tube-1	0.034	0.040
Draft tube-2	0.074	0.070
Draft tube-3	0.093	0.100
Draft tube-4	0.103	0.109

Table 3.2 Specification of ALC used in this work

Key	A_d/A_r	Draft tube	Mode of gas sparging	Number of orifices on sparger
ALC-1	0.067	Draft tube-1	Annulus	14
ALC-2	0.431	Draft tube-2	Annulus	14
ALC-3	0.988	Draft tube-3	Annulus	14
ALC-4	0.988	Draft tube-3	Annulus	30
ALC-5	0.988	Draft tube-3	Annulus	5
ALC-6	1.540	Draft tube-4	Annulus	14
ALC-7	0.649	Draft tube-4	Draft tube	14
ALC-8	1.012	Draft tube-3	Draft tube	14
ALC-9	2.319	Draft tube-2	Draft tube	14
ALC-10	14.852	Draft tube-1	Draft tube	14

Table 3.3 A series of experiments for each hydrodynamic and mass transfer characteristic

	u_{sg}	A_d/A_r	Sparger	mode of gas sparging	distance along axial direction
d_B	•	•	•		•
ε_G	•	•	•	•	
v_L	•	•	•	•	
k_La	•	•	•	•	

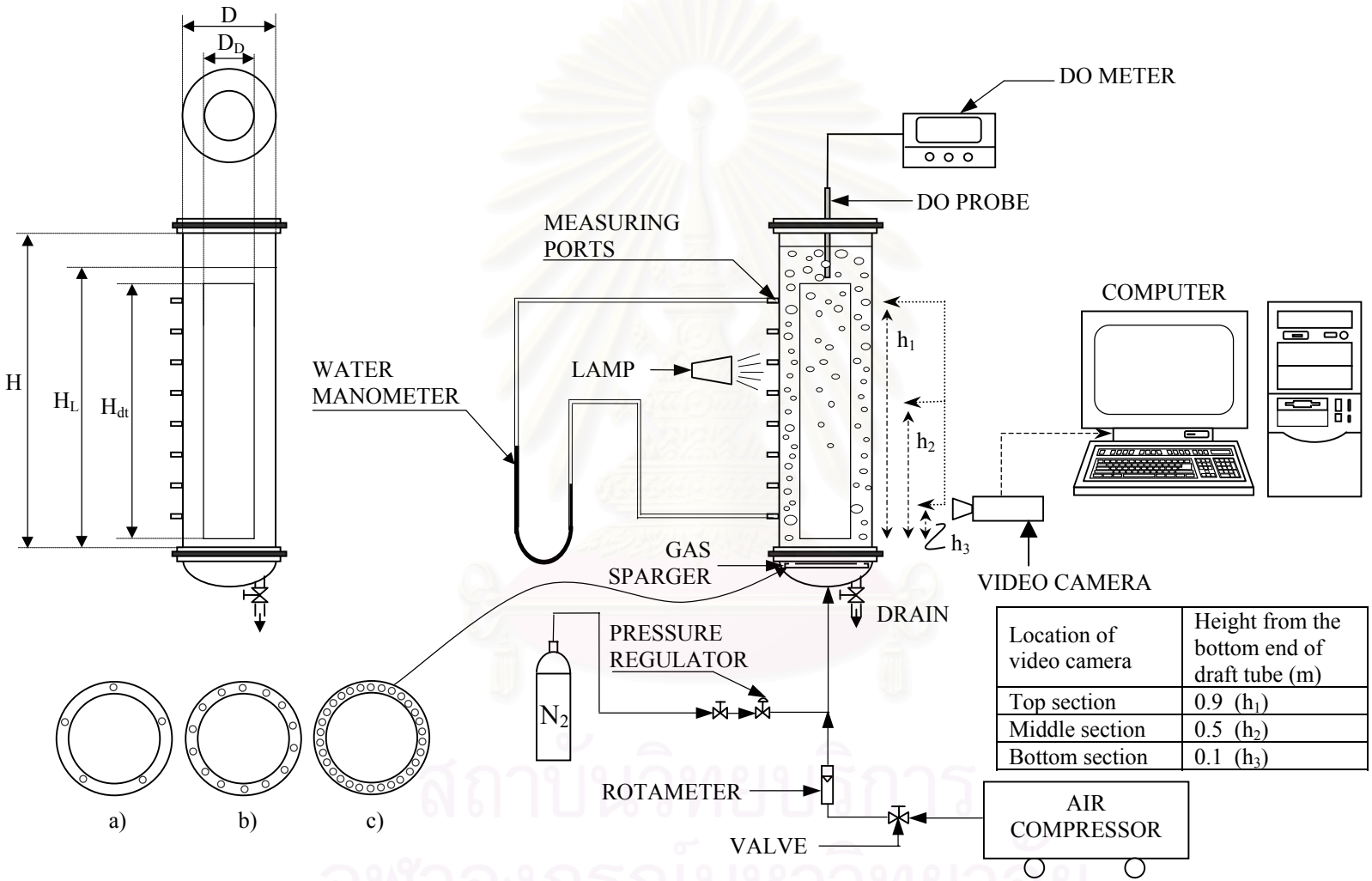

Location of video camera	Height from the bottom end of draft tube (m)
Top section	0.9 (h_1)
Middle section	0.5 (h_2)
Bottom section	0.1 (h_3)

Figure 3.1 Experimental apparatus of the concentric internal loop airlift contactor employed in this work

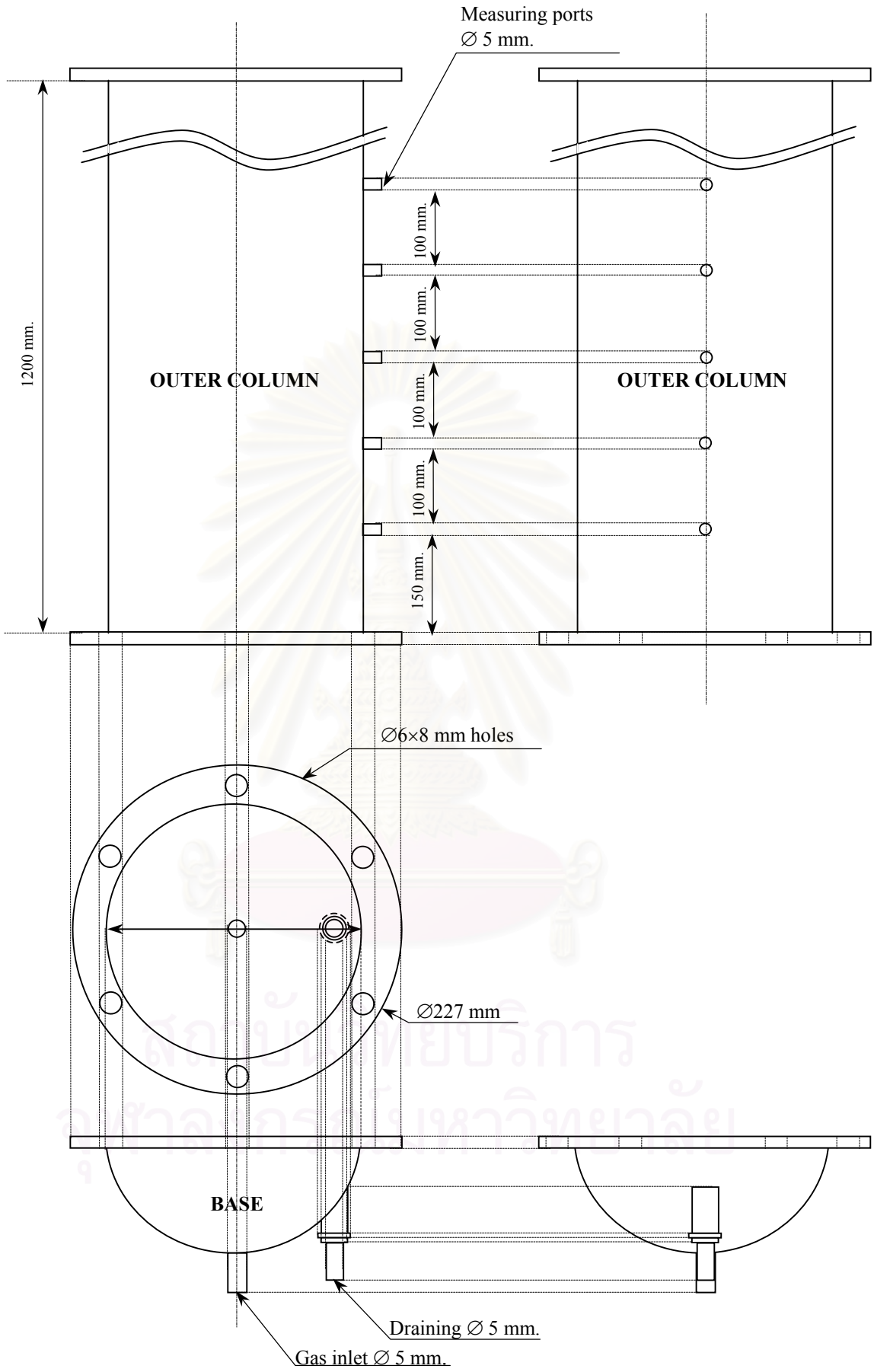

Figure 3.2 Dimensions of the concentric tube airlift contactor employed in this work

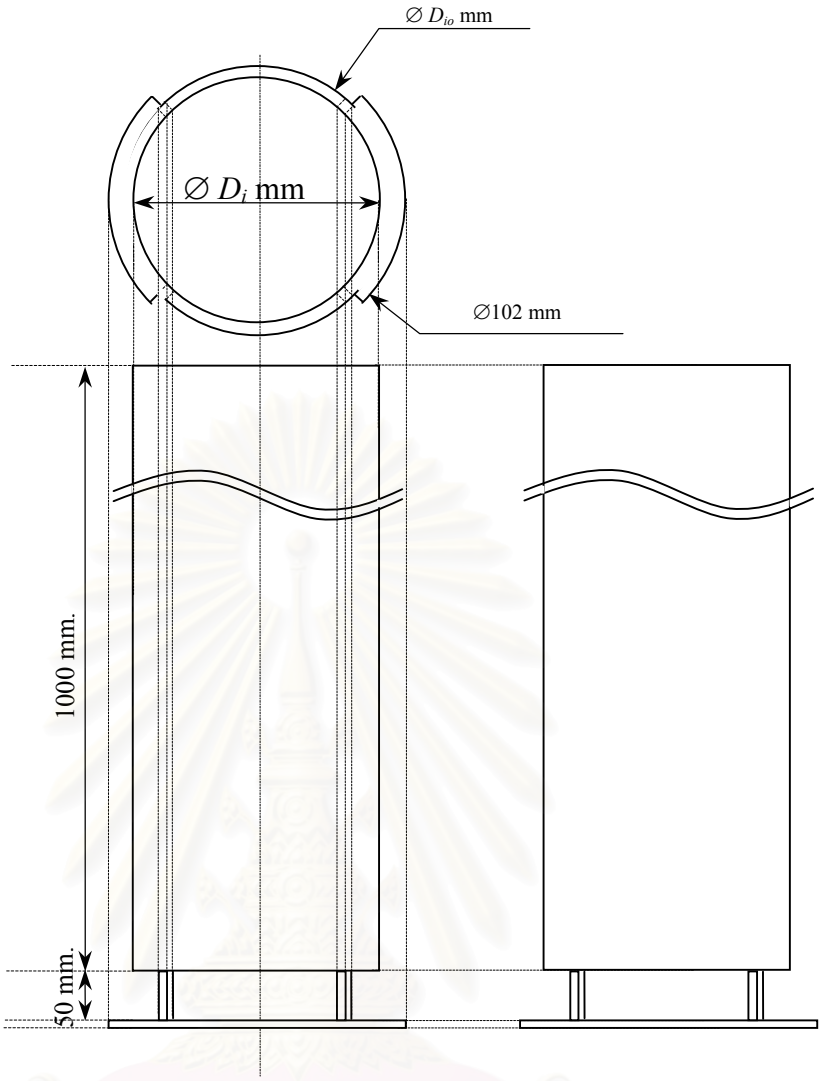

Figure 3.2 (cont.) Dimensions of the concentric tube airlift contactor employed in this work

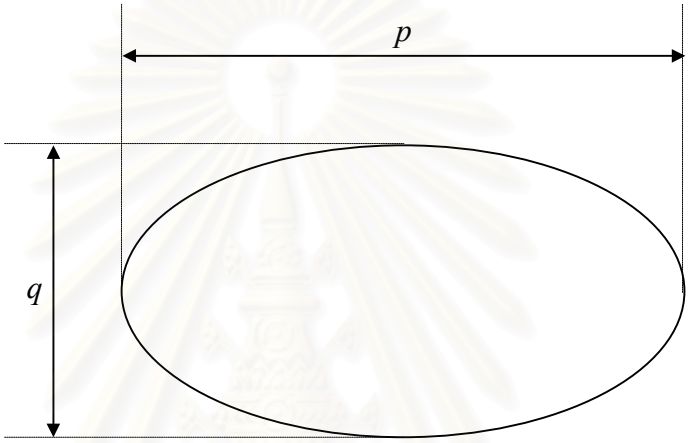

Figure 3.3 Major and minor axes of bubble images

Chapter 4

Bubble Size Distributions

4.1 Backgrounds

Gas-liquid mass transfer is a crucial factor in the design of biological processes particularly aerobic systems where dissolved oxygen in liquid phase can easily become a reaction-limiting factor. Most investigations performed on these systems are limited to the determination of rate of gas-liquid mass transfer via time profile of dissolved oxygen concentration in the system in terms of overall volumetric mass transfer coefficient (K_La) where information about bubble size and its distribution is neglected. Unfortunately, this parameter is global and not sufficient to provide an understanding of the mass transfer mechanisms. The separation of the mass transfer coefficient (K_L) and specific interfacial area (a) should be considered for better comprehension of the gas-liquid mass transfer mechanisms. It also allows us to identify which parameter (K_L or a) controls the mass transfer. Few results concerning individual determinations of K_L and a have yet been obtained. One of the most important factors affecting K_L and a is bubble characteristics in the system. A number of evidences have emphasized the significance of bubble properties in controlling the mass transfer in gas-liquid contacting systems. Fundamentally, systems with smaller bubbles have higher gas-liquid specific interfacial mass transfer area.[1-2] Furthermore small bubbles move at a lower speed than large ones, leading to a higher gas holdup. On the other hand, some literature showed that large bubbles could lead to high turbulent intensity, which enhance the rate of gas-liquid mass transfer.[3]

Most of available research paid little attention to the study of bubble characteristics in airlift contactor (ALC). Thus the understanding of actual phenomena in the system is still unclear. However, a number of investigations concerning bubble characteristics in bubble columns are available. These investigations suggested that bubble characteristics in gas-liquid dispersion depended on various factors such as reactor geometry, operating conditions, gas distribution, physio-chemical properties of the two phases etc.[4-9]

In an earlier study of Koide et al. (1968)[5], the effect of gas flow rate on bubble size and size distribution in various liquid solutions in the bubble column was investigated using a photographic technique. They found that gas flow rate and liquid properties had significant effects on bubble size and its size distribution. The size of bubbles increased with increasing gas flow rate and the bubble size distribution tended to broaden. They stated that when gas flow rate increased, the number of bubbles generated from the distributor per unit time increased, the gas holdup became large, and the chance of coalescence increased. This resulted in large and broad size-distributed bubbles. After that, Bochholz et al. (1978)[10], who investigated relationship among bubble diameter, gas holdup and volumetric mass transfer coefficient reported that bubble coalescence become more significant at higher rate of gas throughput in a pilot scale bubble column. This was in an agreement with a finding of Yu and Kim (1991)[6] who studied the effect of liquid and gas velocities on local gas holdup, bubble chord length, bubble size distribution, bubble velocity and local liquid velocity in two-phase up-flow systems using U-shaped optical fiber and electroconductivity probes. They also concluded that large and broad size-distribution of bubbles was obtained when gas velocity increased. In contrast, Luewisutthichat et al. (1997)[7] studied the bubble characteristics for multiphase flow systems in a two-dimensional column by visual observation together with the image processing of photographs. They reported that no appreciable effect of either gas velocity or liquid velocity on the variation in bubble size was observed. This indicated that a relatively narrow distribution of bubble size existed in the contactors. On the contrary, Colella et al. (1999)[8] who also used photographic and image analysis techniques in their work found that the relative frequency of the occurrence of small bubbles increased upon an increase of the superficial gas velocity (u_{sg}) in bubble columns and airlift reactors. This meant that average mean bubble diameter decreased when u_{sg} increased. It was concluded that bubble-bubble interaction (breakage rate) was enhanced as a result of an increase in u_{sg}. This result was in good agreement with several previous research which also found that bubble size usually decreased with increasing gas input to the system, and therefore high gas-liquid interfacial area was obtained at high gas throughput in bubble column.[1-3,11-12]

There are more contradictions between experimental findings on the effect of superficial liquid velocity on bubble size in bubble columns. Yu and Kim (1991)[6] reported that bubble chord length decreased with increasing superficial liquid velocity

because liquid eddies generated the turbulent in column. In contrast, Luewisutthichat et al. (1997)[7] stated that superficial liquid velocity had no effect on bubble size.

In addition, bubble size was reported to decrease with axial distance along column height.[8,13] Colella et al. (1999)[8] measured local bubble size and its size distribution at several heights from an air sparger and reported that the mean diameter of the bubble decreased and size distribution was relatively flat when height (height form sparger) increased. They explained that the mean bubble size was small at the location far from the sparger because of the dominant breakage mechanism.

Types of gas sparger were also found to have remarkable effect on bubble size distribution in bubble columns. Hebrard et al. (1996)[11] reported that the use of perforated gas spargers led to a larger bubble size and broader bubble size distribution than those obtained from porous or membrane spargers. Colella et al. (1999)[8] stated that sparger design has significant effects on bubble diameter, i.e. the porous sparger produced the smaller bubbles than perforated plate spargers. This result was consistent with that of Camarasa et al. (1999)[9] who also reported that there was a transition between homogeneous and heterogeneous regimes at high gas flow rate when porous plate or multiple-orifice nozzle was used. On the contrary, homogeneous regime was not observed even at low gas flow rate when a single-orifice nozzle was used. This was because porous and multiple-orifice sparger produced smaller bubbles, which did not coalesce at low u_{sg} so it exhibited the homogeneous regime. In contrast, the single-orifice nozzle generated larger bubbles tending to coalesce even at low u_{sg} so the homogeneous regime could not be maintained.

In airlift contactors (ALCs), the volumetric mass transfer rate was often reported as a function of operating and design parameters (as summarized in Table 2.3 in Chapter 2). In gas-liquid contacting systems like ALCs where fluid dynamics of gas and liquid phases are rather complex, only few investigations have looked through their bubble size distribution.

Miyahara et al. (1986)[4] studied bubble properties which included bubble size, bubble size distribution, gas holdup and liquid circulation in a bubble column with a draft tube (or equivalent to an ALC) using a photographic technique. They stated that bubble size distribution in the ALC exhibited the lognormal form, which indicated that there existed a larger portion of small (3-4 mm), rather than large (4-6 mm) gas bubbles in the system. This result agreed well with those of Yu and Kim (1991)[6] and Luewisutthichat et al. (1997).[7] In spite of the presence of liquid circulation in ALC, the

results of Miyahara et al. (1986)[4] suggested that bubble size distribution in ALC follow the same trend as that in the bubble column. However, they revealed that the size of bubbles in the bubble column with draft tube was smaller than that in the bubble column. They also reported that the gas holdup in the bubble column with draft tube was smaller than that in the bubble column. High turbulent intensity in the ALC was considered as a reason for these findings as turbulence tended to break up the large bubble into small ones. It was noted that the turbulence in the ALC was induced from high liquid velocity.

Miyahara and Hayashino (1995)[14] demonstrated further that bubble size distribution in ALC varied with gas throughput such that bubble diameter became larger and size distributions became broader with an increase in u_{sg}. These results were attributed to the predominance of bubble coalescence at low u_{sg} ($0.003<u_{sg}<0.03$ $m \cdot s^{-1}$).

In contrast, Colella et al. (1999)[8] proposed some mechanisms for bubble coalescence and breakage in the annulus sparged ALC and concluded that higher u_{sg} tended to break bubbles into smaller size rather than to coalesce into bigger ones. The relative frequency of small bubble was found to be a function of u_{sg} and axial distance from the sparger.

Literature showed thus far that there existed a number of operational and design parameters affecting the bubble characteristics such as bubble size, and bubble size distribution in gas-liquid contacting system such as ALCs and BCs. The variations of bubble characteristics then leads to the variation of state parameters such as gas holdup and gas-liquid interfacial area. If the bubble characteristics are not well understood, the contactor's behavior such as gas holdup, liquid velocity, and gas-liquid mass transfer with geometrical or operational parameters could not be reasonably explained or predicted. The investigation on the bubble size distribution in the ALC is still limited and, thus far, there has not been sufficient information on effects of design parameters on the size distribution of bubbles.

This work, hence, intends to examine bubble size and its size distribution in the annulus sparged concentric airlift contactor. The dependence of bubble characteristics on the contactor design and operating conditions including superficial gas velocity, axial distance along the column height, ratio between downcomer to riser cross-sectional areas and sparger geometry is comprehensively investigated. This work also scrutinizes the effects of bubble sizes on the overall gas-liquid mass transfer ($K_L a_L$) in ALCs. An empirical model for the prediction of the mass transfer coefficient is proposed.

4.2 Experiments

To achieve the aim of this study, the bubble characteristic was measured according to the procedure explained in Section 3.2.1. Gas holdups, liquid velocities, and overall gas-liquid mass transfer coefficient were estimated using experimental procedures in Sections 3.2.2-3.2.4, respectively.

4.3 Results and discussion

4.3.1 Error compensation in photographic technique

The measurement of bubble diameter in this study was taken along axial direction. The radial distribution of bubble size was not observed as the annulus of the employed ALCs had a rather small cross sectional area where the distance between inner and outer columns was only 0.01-0.05 cm which was approximately in the same order of magnitude with the bubble. This did not allow precise measurement of bubble sizes along radial direction. The measured sizes of bubbles were subject to error due to the curvature of the column surface. To account for this error, an object with a known size was placed along radial direction in the column and its picture was taken for size compensation. The error was then calculated and used as a correction factor for subsequent measurement. Note that the error due to the curvature of the column surface was approximately ±15%. Figure 4.1 is an example of photographs of bubbles obtained from this measurement technique.

4.3.2 Bubble size distribution as a function of superficial gas velocity

Figures 4.2-4.6 show the bubble size distribution in ALC-1 to ALC-5 (see Table 3.2 for description of these various ALCs). The figures present that there was a wide range of bubble sizes in each ALC and the distribution of bubble size varied with superficial gas velocity (u_{sg}). Note that, due to the equipment limitation, the ALC could only be operated with a limited level of u_{sg}. The maximum u_{sg} for each ALC depended markedly on the ratio between downcomer and riser cross sectional areas (A_d/A_r) such that ALC with higher A_d/A_r could be operated with higher level of u_{sg}.

Figures 4.2-4.6 illustrates that, at a low level of u_{sg} (<0.01 m s^{-1}), the bubble size distributions at the bottom section of the ALC in all cases were narrow (standard deviations, *s.d.*, of 1.1-2.3 mm) and followed the normal distribution type. It can be seen

from the figures that a majority of gas bubbles in the system at this condition had diameter of 6.0-8.0 mm. However, the distributions of bubble sizes at the middle and top sections of the ALC at low u_{sg} deviated significantly from the normal type. This variation of bubble distribution along the column height will be explained in the next section. For cases where u_{sg} was between 0.02 and 0.04 $m{\cdot}s^{-1}$, there appeared two or more distinct peaks in the distribution curve which implied that at least two dominant sizes of bubbles were present in the system. For instance, Figure 4.4 demonstrates that, at u_{sg} of 0.0296 $m{\cdot}s^{-1}$, there existed a group of relatively large bubbles with diameters of 7.0-8.0 mm and the other group of smaller bubbles with diameters of 4.0-6.0 mm. Due to the presence of various dominant groups of bubble sizes, the distribution of bubble size became broader (*s.d.*of 1.4-2.7 mm), and the bimodal or multimodal distribution was best to describe the size distribution in this range of u_{sg}. At high u_{sg} (>0.05 $m{\cdot}s^{-1}$), large bubbles disappeared and smaller bubbles with diameter of 3.0-6.0 mm dominated the system. The bubble size distribution in this range of u_{sg} had a standard deviation of 1.2-3.6 mm and was well described by an asymmetric lognormal distribution curve. This finding reveals clearly that an increase in u_{sg} reduced the number of large bubbles and increased the number of smaller size bubbles: the results which were in good agreement with those reported by Mahajan and Narasimhanmurty (1975).[3]

This shift in bubble size from large at low range of u_{sg} to small at high range of u_{sg} indicated that there was bubble breakage taken place in the system.

According to Prince and Blanch[15], bubble breakage was caused by energy from turbulent eddies of appropriate size obtained from interactions between bubbles. Literature has shown that an increase in u_{sg} led to high liquid velocity[16-18] and this might be responsible for the enhancement of turbulent intensity and also more eddies with appropriate size might be created. In other words, higher u_{sg} resulted in greater turbulent intensity which caused more bubble breakage and led to a reduction in average bubble size as illustrated in Figure 4.7. However, further increase in u_{sg} (>0.05 $m{\cdot}s^{-1}$) was no longer observed to have significant effect on bubble size. This may be due to the stability of small bubble against the breakage mechanism at high u_{sg}.[19-20]

4.3.3 Axial variation of bubble size distribution

The bubble size was found to depend significantly on the axial location in the ALC. Figure 4.7 shows that the average bubble size at the base of the contactor was found to be the largest and it continued to decrease as bubbles moved along contactor height. This implied that there existed a breakage mechanism of bubbles. This finding was in good agreement with some reported measurements in bubble columns[8,13] and in the ALC. [14]

In view of bubble size distribution, there was a slight difference in terms of transition of bubble size distributions (unimodal to bimodal or multimodal and to lognormal types) along the column height. In other words, changes in the types of distribution occurred at different levels of u_{sg}. For instance, at the bottom section of ALC-3 in Figure 4.4, the transition from unimodal to bimodal or multimodal distributions occurred at u_{sg} of as high as 0.0296 $m \cdot s^{-1}$, whereas this transition at the top part took place at u_{sg} of as small as 0.0085 $m \cdot s^{-1}$. This result was attributed to the bubble breakage along the column height, which resulted in a high proportion of small bubbles at the higher section where the distribution curve tended to shift faster towards the small size region. This result is consistent with the report of Otake et al. (1977)[13] which stated that bubble coalescence mostly appeared near the sparger outlet. After that, bubble breakage took place constantly along the column height.

4.3.4 Bubble size distribution and the ratio between riser and downcomer cross-sectional areas

To investigate the effect of the ratio between downcomer and riser cross sectional areas (A_d/A_r), the experiment was conducted in the system with three different A_d/A_r, i.e. 0.067 (ALC-1), 0.43 (ALC-2), and 1 (ALC-3). Figure 4.8 summarizes results from these experiments where it was found that, at low gas throughput (u_{sg} < 0.0296 $m \cdot s^{-1}$), A_d/A_r did not significantly affect bubble sizes. However, A_d/A_r tended to have an influence on bubble size and its size distribution at high gas throughput where the ALC with A_d/A_r of 0.43 (ALC-2) was found to give the smallest bubble size. This might be because, at low u_{sg}, the flow behavior in the ALC approached bubbly flow where bubbles moved uniformly and had only slight interaction with each other. Therefore the bubble size was independent of A_d/A_r. However, high u_{sg} raised liquid velocity, which implied that the turbulence intensities were also increased, and the dependency of

bubble size on A_d/A_r in this range of u_{sg} became more apparent. In this case, ALC with larger A_d/A_r (small A_r) caused liquid to move more rapidly than ALC with small A_d/A_r, therefore a greater level of turbulence was obtained and more bubble breakage (smaller bubbles) was observed.

4.3.5 Effect of gas sparger on bubble size distribution

The effect of gas sparger on the distributions of bubble sizes in ALCs is illustrated in Figure 4.9. The average bubble size tended to increase with increasing orifice number of sparger. Bubbles from the sparger with 30 orifices seemed to coalesce quickly once they left the orifices. This was because each orifice was close to each other which facilitated the coalescence between new-born bubbles. In this context, bubbles from the sparger with 5 orifices should be the smallest in size, which was true in most cases but not at the bottom section where average bubble size was found to be much larger than at other sections. It was also found that the distribution of bubble size at this situation (5 orifice sparger) was much wider than other cases. This might be due to the high pressure in the sparger with less number of orifices which caused new-born bubbles to be very large in size and these bubbles broke rapidly after leaving the orifice.

4.3.6 Overall volumetric mass transfer coefficient (K_La_L) in airlift contactors

The relationships between the overall volumetric mass transfer coefficient (K_La_L) in the ALC with various parameters are shown in Figure 4.10. This demonstrates that K_La_L increased with u_{sg} but decreased with increasing A_d/A_r, whilst the influence of number of holes in sparger on K_La_L was negligible in the range of condition employed in this study. The following sub-sections investigate the influence of these parameters on K_La_L in detail.

4.3.6.1 Determination of overall gas-liquid mass transfer coefficient (K_La_L)

With information on bubble size distribution, it was possible to estimate K_La_L in terms of liquid phase mass transfer coefficient (K_L) and specific gas-liquid interfacial area based on liquid volume (a_L) separately. The specific interfacial area (a_L) is defined according to Eq. (4.1) where bubbles are assumed to be spherical with an average diameter of d_B.

$$a_L = \frac{6\varepsilon_G}{(1-\varepsilon_G)d_B} \tag{4.1}$$

Gas holdups (ε_G) were directly measured from the experiments whereas the bubble diameter (d_B) employed in the determination of a_L in Eq. (4.1) is usually reported as "Sauter mean diameter (d_{Bs})" or surface volume mean diameter which can be calculated from:

$$d_{Bs} = \frac{\sum_i n_i d_{B_i}^3}{\sum_i n_i d_{B_i}^2} \tag{4.2}$$

where n_i is the number of bubbles with diameter (d_{Bi}). As reported in previous sections, the bubble size in the riser (d_{Br}) was not uniform along the axial direction. For each experimental condition, specific interfacial area in riser (a_{Lr}) was therefore calculated using information on bubble size distribution along the column height together with riser gas holdup (ε_{Gr}) which was assumed to be uniform in both radial and axial directions as follows:

$$a_{Lr} = \frac{1}{H_{dt}} \int_{x_r=0}^{x_r=H_{dt}} a_{Lr}(x_r)dx_r \tag{4.3}$$

$$a_{Lr} = \frac{1}{H_{dt}} \frac{6\varepsilon_{Gr}}{(1-\varepsilon_{Gr})} \int_{x_r=0}^{x_r=H_{dt}} \frac{1}{d_{Bsr}(x_r)} dx_r \tag{4.4}$$

It is worth noting here that, the integration in Eq. (4.4) was performed by dividing the ALC into 3 sections: bottom, middle, and top, and all bubbles in each section were assumed to have the same size. The relationships between a_{Lr} and u_{sg} for the various ALCs in this work are shown in Figure 4.11.

Due to the limitation of the photographic technique, the direct observation of bubble size in downcomer was not possible. It is necessary to calculate the bubble size in downcomer. It was assumed here that all bubbles were stationary in the downcomer, or in other words, all bubbles in the downcomer had the terminal rise velocity equal to the liquid velocity in the downcomer. Therefore, the average bubble size in downcomer (d_{Bd}) was estimated from experimental data on liquid velocity in downcomer (u_{Ld}) using the Levich equation[21], Eq. (4.5):

$$d_{Bd} = \frac{1.8}{g}\left(\frac{u_{Ld}}{2}\right)^2 \tag{4.5}$$

It was assumed further that there was no variation of bubble size along the radial and axial directions in downcomer. Therefore,

$$d_{Bsd} = d_{Bd} \tag{4.6}$$

a_{Ld} was calculated from the substitution of d_{Bsd} from Eq. (4.6) together with ε_{Gd} (from experiment) into Eq. (4.1). The circulating velocities (in terms of downcomer liquid velocity) in the ALCs were measured and are displayed in Figure 4.12.

The liquid phase mass transfer coefficient (K_L) was commonly reported as a function of properties of liquid and bubble size.[22-25] Several empirical and theoretical correlations for the determination of K_L for various systems are given and summarized in Skelland (1974)[26], Treybal (1980)[27], Welty et al. (1984)[28] and Stanley (1998)[29]. Eq. (4.7) is often employed as an initial point for the establishment of K_L correlation.

$$\mathrm{Sh} = a + b\underbrace{\mathrm{Gr}^{c}\mathrm{Sc}^{d}}_{\text{Free rise bubbles}} + e\overbrace{\mathrm{Re}^{f}\mathrm{Sc}^{h}}^{\text{Forced convection}} \tag{4.7}$$

Generally, Grashof number (Gr) represents mass transfer by natural convection or free rise velocity whilst Reynolds number (Re) is for mass transfer by forced convection. The parameters *a*-*h* in Eq. (4.7) are determined experimentally. In this work, the properties of liquid was not changed and therefore Schmidt number was constant and hence, Eq. (4.7) can be rewritten as:

$$\mathrm{Sh} = a' + b'\mathrm{Gr}^{c'} + d'\mathrm{Re}^{e'} \tag{4.8}$$

Eq. (4.8) requires that slip velocity (v_s) and Sauter bubble diameter (d_{Bs}) are known in a priori. The Sauter mean bubble diameter in riser (d_{Bsr}) was calculated from the information on d_{Bsr} along the column height as follows:

$$d_{Bsr} = \frac{1}{H_{dt}} \int_{x_r=0}^{x_r=H_{dt}} d_{Bs}(x_r)dx_r \tag{4.9}$$

The Sauter bubble diameter in downcomer (d_{Bsd}) was obtained from Eq. (4.6). The slip velocity (v_s) was also calculated separately in each section of the ALC. The slip velocity in the riser (v_{sr}) is a function of the terminal rise velocity of a single bubble (u_∞) which is modified to account for hindering effects from neighboring bubbles in the riser[30-34] such that:

$$v_{sr} = \frac{u_\infty}{(1-\varepsilon_{Gr})} \tag{4.10}$$

The terminal bubble rise velocity (u_∞) can be calculated using the correlation developed by Jamialahmadi et al.[35] for systems with swarm bubbles:

$$u_\infty = \frac{\frac{1}{18}\frac{\rho_L-\rho_G}{\mu_L} g d_{Bs}^2 \left(\frac{3\mu_L+3\mu_G}{2\mu_L+3\mu_G}\right)\sqrt{\frac{2\sigma_L}{d_{Bs}(\rho_L+\rho_G)}+\frac{g d_{Bs}}{2}}}{\sqrt{\left[\frac{1}{18}\frac{\rho_L-\rho_G}{\mu_L} g d_{Bs}^2 \left(\frac{3\mu_L+3\mu_G}{2\mu_L+3\mu_G}\right)\right]^2+\frac{2\sigma_L}{d_{Bs}(\rho_L-\rho_G)}+\frac{g d_{Bs}}{2}}} \tag{4.11}$$

It was assumed here that bubbles in downcomer had terminal rise velocity equal to liquid velocity and bubble size was uniform along the column height. The slip velocity can therefore be estimated from the downcomer liquid velocity:

$$v_{sd} = u_{Ld} \tag{4.12}$$

Substituting d_{Bsr} in Eq. (4.9) and v_{sr} in Eq. (4.10) into Eq. (4.8) leads to the correlation for the determination of K_{Lr} where the same procedure can be applied for d_{Bsd} (Eq. (4.6) and v_{sd} (Eq. (4.12)) to yield the correlation for K_{Ld}.

4.3.6.2 Comparison between $K_L a_L$ from experiment and prediction

The mass transfer rate for the entire contactor was expressed in term of overall volumetric mass transfer coefficient $(K_L a_L)_T$ and this can be calculated from the sum of the mass transfer rates in riser and downcomer as follows:

$$(K_L a_L)_T = \frac{(K_L a_L)_r V_{Lr} + (K_L a_L)_d V_{Ld}}{V_{LT}} \tag{4.13}$$

Where V_{Lr} is the volume of liquid in riser, V_{Ld} the volume of liquid in downcomer and V_{Lt} the total volume of liquid. $(K_L a_L)_r$ and $(K_L a_L)_d$ in this equation are obtained from the product between K_{Lr} and a_{Lr}, and K_{Ld} and a_{Ld}, respectively. Figure 4.13 illustrates the comparison between the predicted $K_L a_L$ from Eq. (4.13) and the experimental value which shows that there was a good agreement between the two when parameters a' - e' in Eq. (4.8) were equal to 0.5, 1.07, 0.469, 0 and 0, respectively (Note that these parameter were obtained from the solver function in the MS Excel 97 where the

objective was a minimal error between experimental and simulation data of K_La). Eq. (4.8) now becomes:

$$\mathrm{Sh} = 0.5 + 1.07\mathrm{Gr}^{0.469} \qquad (4.14)$$

Eq. (4.14) indicates that when the coefficient d' equals zero, Re disappears, which means that forced convection has no effect on the mass transfer. This finding reveals that the mass transfer in the ALC employed in this work depended primarily on the natural convection, and not the force convection.

4.3.6.3 Evaluation of K_La_L in the ALC

Figure 4.14 demonstrates the variations of overall K_L (K_{LT}) and a_L (a_{LT}) with u_{sg} in all of the ALCs employed in this work which reveals that a_L varied almost linearly with u_{sg} whilst K_L only slightly changed with u_{sg}. K_L was found to be constant at 4×10^{-4} $m{\cdot}s^{-1}$ which is equal to that used in literature.[36] Therefore it should be reasonable to conclude that the increase in a_L with u_{sg} in the ALC was the main factor responsible for the increase in K_La_L (see Fig. 4.10). This increase in a_L was attributed to the increase in the overall gas holdup (Fig. 4.15) and the decrease in the bubble size with gas throughput (Fig. 4.7). Figure 4.14 demonstrates that the change in bubble size with u_{sg} did not cause a drastic deviation in the value of K_L and therefore changes in K_L only slightly affect the overall volumetric mass transfer coefficient.

Figure 4.14 also describes effects of A_d/A_r on K_L and a_L (ALC-1, ALC-2 and ALC-3). The ALC with larger A_d/A_r rendered the liquid circulating velocity to be faster (Fig. 4.12) and this reduced gas holdup in the system (Fig. 4.15). Although bubble size in ALC with a large A_d/A_r was found to be smaller than ALC with small A_d/A_r (at high u_{sg}), its effect on the enhancement of specific mass transfer area was overwhelmed by the reduction in gas holdup. This resulted in a smaller a_L in ALCs with high A_d/A_r. In contrast, the increase in A_d/A_r did not seem to have significant influence on the mass transfer coefficient (K_L). Hence, the decrease in K_La_L with A_d/A_r in Figure 4.7 was mainly due to the decrease in a_L.

Figure 4.10 indicates that the influence of number of orifices in the sparger on K_La_L was negligible in the range of conditions used in this study. This was verified by the analysis in this section and the results in Figure 4.14 (ALC-3, ALC-4, and ALC-5) revealed that both K_L and a_L were found not to be influenced by the number of orifices

in the sparger. As a_L varies inversely with bubble size, and since a larger number of orifices resulted in a larger bubble size, the ALC with this type of sparger should have led to a system with a smaller a_L. However, the results clearly illustrate that this was not the case and a_L in ALC-4 (30 orifice sparger) was found to be similar to a_L in ALC-5 (5 orifice sparger). This was because the effect of the larger bubble size on the specific area was compensated by the effect of larger overall gas holdup in the system.

4.4 Concluding remarks

This work illustrated the effect of various design and operating parameters on bubble size distribution in the airlift contactor. The results suggested that, with a proper design of the airlift contactor, one might, to some extent, be able to control the bubble behavior in the system. A technique for the estimation of specific interfacial area based on the information on bubble size distribution was then proposed along with the development of an empirical correlation for the prediction of mass transfer coefficient in terms of dimensionless variables (Sherwood and Grashof number). It was shown that a thorough investigation on the effect of various parameters on the rate of gas-liquid mass transfer could be performed with additional data on bubble size distribution. This is particularly useful for further development and control of the ALC for applications where gas-liquid mass transfer is important.

4.5 References

1. Hinze, J.O. 1955. Fundamentals of the hydrodynamic mechanism of splitting in dispersion processes. AIChE J. 33: 289-295.
2. Akita, K., and Yoshida, F. 1974. Bubble size, interfacial area and liquid phase mass transfer coefficient in bubble columns. Ind. Eng. Chem. Proc. Des. Dev. 13: 84-91.
3. Mahajan, S.P., and Narasimhamurty, G.S.R. 1975. Size, Size Distribution & Interfacial Area for Gas-Liquid Dispersions Formed on Perforated Plates. Ind. J. Tech. 13: 541-547.
4. Miyahara, T., Hamaguchi, M., Sukeda, Y., and Takahashi, T. 1986. Size of Bubbles and liquid circulation in a bubble column with a draught tube and sieve plate Can. J. Chem. Eng. 64: 718-725.

5. Koide, K., S. Kato, Tanaka, Y., and Kubota, H. 1968. Bubbles generated from porous plate. J. Chem. Eng. Japan. 1: 51-56.
6. Yu, Y.H., Kim, S.D. 1991. Bubble properties and local liquid velocity in the radial direction of cocurrent gas-liquid flow. Chem. Eng. Sci. 46: 313-320.
7. Luewisutthichat, W., Tsutsumi, A. and Yoshida, K. 1997. Bubble characteristics in multiphase flow systems: bubble sizes and size distributions. J. Chem. Eng. Japan 30: 461-466.
8. Colella, D., Vinci, D., Bagatin, R., Masi M, Bakr, E.A. 1999. A study on coalescence and breakage mechanisms in three different bubble columns. Chem. Eng. Sci. 54: 4767-4777.
9. Camarasa, E., Vial, C., Poncin, S., Wild, G., Midoux, N. and Bouillard, J. 1999. Influence of coalescence behavior of the liquid and of gas sparging on hydrodynamics and bubble characteristics in a bubble column. Chem. Eng. Proc. 38: 329-344.
10. Bochholz, H., Buchholz, R., Lucke, J., and Schugerl, K. 1978. Bubble swarm behavior and gas absorption in non-Newtonian fluids in sparged columns. Chem. Eng. Sci. 33: 1061-1070.
11. Hebrard, G., Bastoul, D., and Roustan, M. 1996. Influence of the gas sparger on the hydrodynamic behavior of bubble columns. Trans. Inst. Chem. Eng. 74: 406-414.
12. Couvert, A., Roustan, M., and Chatellier, P. 1999. Two-phase hydrodynamic study of a rectangular airlift loop reactor with an internal baffle. Chem. Eng. Sci. 54: 5245-5252.
13. Otake, T., Tone, S., Nakao, K., and Mitsuhashi, Y. 1977. Coalescence and breakup of bubbles in liquids. Chem. Eng. Sci. 32: 377-383.
14. Miyahara, T., and Hayashino, T. 1995. Size of bubbles generated from perforated plates in a non-Newtonian liquids. J. Chem. Eng. Japan 28: 596-601.
15. Prince, M.J., and Blanch, H.W. 1990. Bubble coalescence and break-up in air-sparged bubble columns. AIChE J. 36: 1485-1499.
16. Bello, R.A., Robinson, C.W., and Moo-Young, M. 1985. Gas hold-up and overall volumetric oxygen transfer coefficient in airlift contactors. Biotechnol. Bioeng. 27: 369-381.
17. Chisti, M.Y. 1989. Airlift Bioreactors. London and New York: Elsevier Applied Science.

18. Choi, K.H. and Lee, W.K. 1993. Circulation liquid velocity, gas holdup and volumetric oxygetransfer coefficient in external-loop airlift reactors, J. Chem. Tech. Biotech. 56: 51-58.
19. Kawase, Y. and Moo-Young, M. 1990. Mathematical Models for design of bioreactors: Applications of Kolmogoroff's theory of isotropic turbulence. Chem. Eng. J. 43: B19-B41.
20. Hesketh, R.P., Etchells, E.W., and Russell, T.W.F. 1991. Bubble breakage in pipeline flow. Chem. Eng. Sci. 46 (1): 1-9.
21. Levich, V.G. 1962. Physicochemical Hydrodynamics. New Jersey: Prentice-Hall.
22. Higbie, R. 1935. Rate of absorption of a pure gas into a still liquid during short period of exposure. Trans. Am. Inst. Chem. Eng. 31: 365-389.
23. Calderbank, P.H., and Moo-Young, M. 1961. The continuous phase heat and mass transfer properties of dispersions. Chem. Eng. Sci. 16: 39.
24. Calderbank, P. H. 1967. Mass transfer in fermentation equipment in Biochemical and Biological Engineering Science. Vol.2, N. Blakebrough, Academic, New York, pp. 102-180.
25. Bailey, J.E., and Ollis, D.F. 1977. Biochemical Engineering Fundamentals. New York: McGraw-Hill.
26. Skelland, A.H.P. 1974. Diffusional Mass Transfer. New York: Wiley.
27. Treybal, R.E. 1980. Mass Transfer Operations. New York: McGraw-Hill.
28. Welty, J.R., Wicks C.E., and Wilson, R.E. 1984. Fundamentals of Momentum, Heat, and Mass Transfer. New York: Wiley.
29. Stanley, M. 1998. An introduction to mass and heat transfer. Wiley, New York.
30. Richardson, J.F., and Zaki, W.N. 1954. Sedimentation and fluidization: Part I, Trans. Inst. Chem. Eng. 32: 35.
31. Marrucci, G. 1965. Rising velocity of a swarm of spherical bubbles. Ind. Eng. Chem. Fundam. 4: 224-225.
32. Davidson J.F., and Harrison, D. 1966. The behavior of a continuity bubbling fluidized bed. Chem. Eng. Sci. 21: 731.
33. Turner, J.C.R. 1966. On bubble flow in liquids and fluidized beds. Chem. Eng. Sci. 21: 971.
34. Wallis, G.B. 1969. One Dimensional Two-Phase Flow. New York: McGraw-Hill.
35. Jamialahmadi, M., Branch, C., and Müller-Steinhagen. 1994. Terminal bubble rise velocity in liquids. Trans. Inst. Chem. Eng. 72: Part A, 119-122.

36. Cockx, A., Do-Quang, Z., Audic, J.M., Liné, A., Roustan, M. 2001. Global and local mass transfer coefficients in waste water treatment process by computational fluid dynamics. Chem. Eng. Proc. 40:187-194.

4.6 Figures

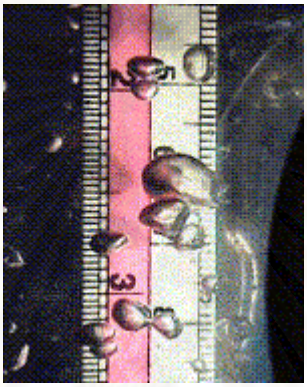

Figure 4.1 An example of photographs of bubbles obtained from this measurement technique

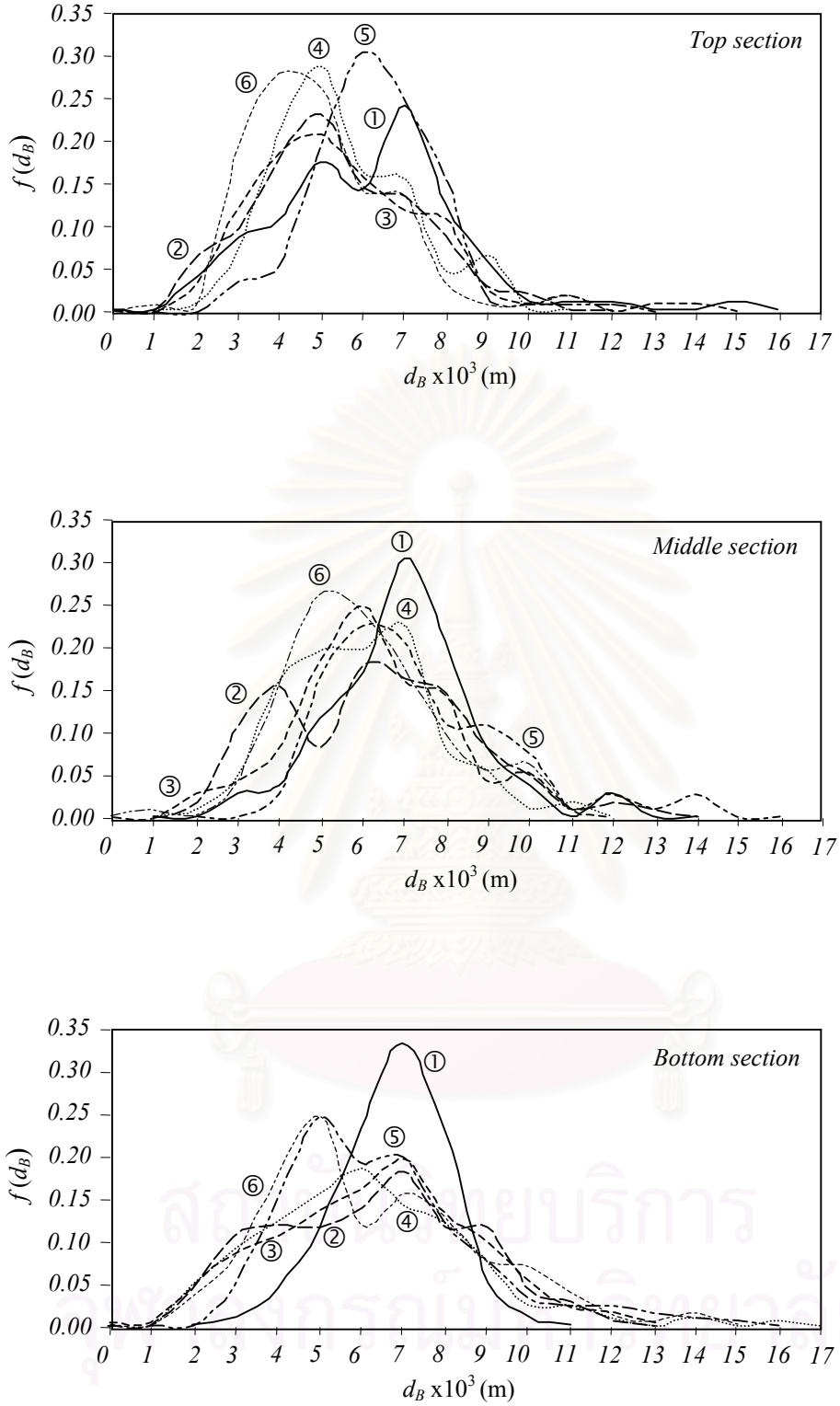

Figure 4.2 Frequency distribution of bubble sizes in ALC-1 at various u_{sg}: (1) u_{sg} = 0.0085 m s^{-1} (2) u_{sg} = 0.016 m s^{-1} (3) u_{sg} = 0.0225 m s^{-1} (4) u_{sg} = 0.0296 m s^{-1} (5) u_{sg} = 0.0395 m s^{-1} (6) u_{sg} = 0.0415 m s^{-1}

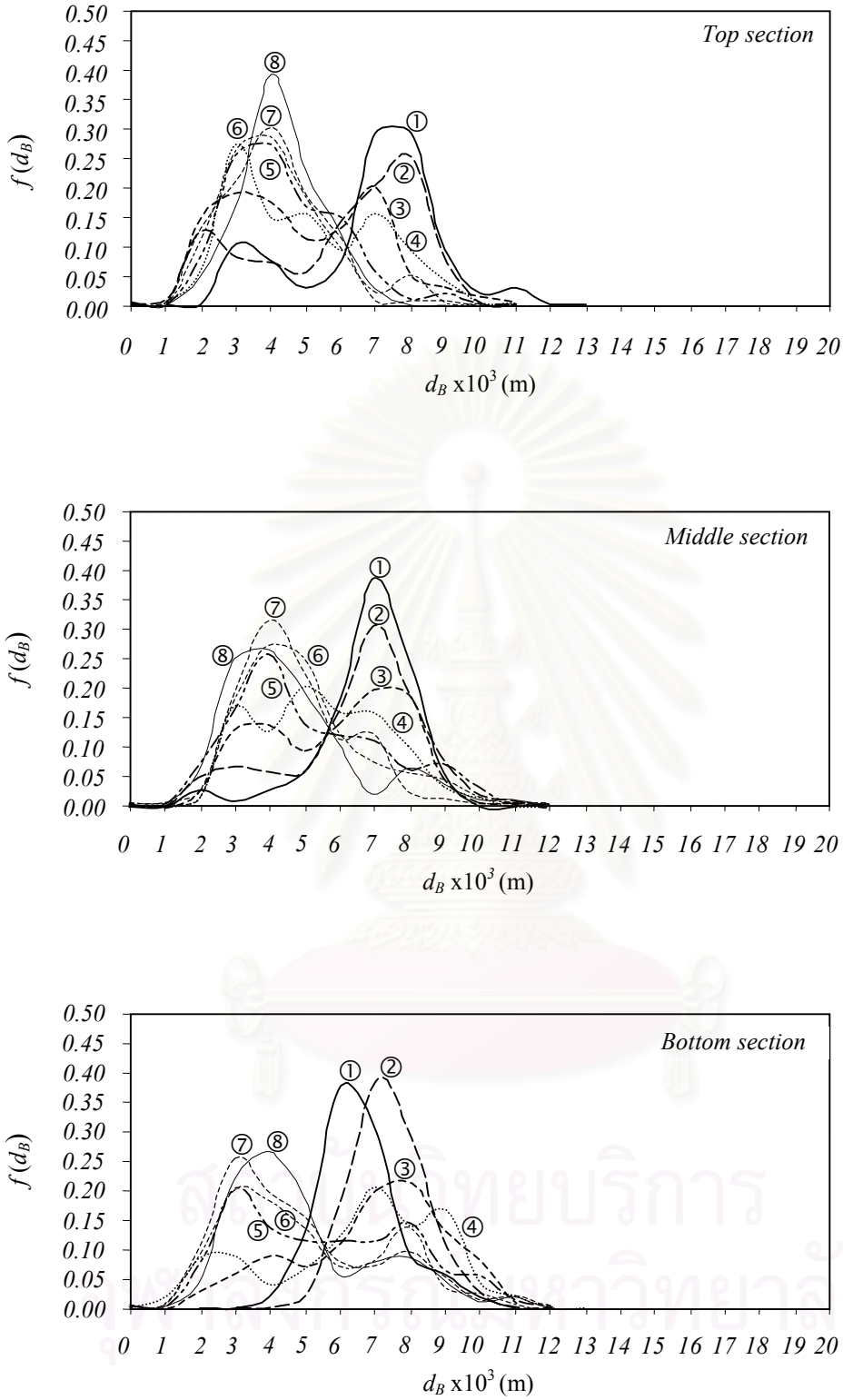

Figure 4.3 Frequency distribution of bubble sizes in ALC-2 at various u_{sg}: (1) u_{sg} = 0.0059 m s^{-1} (2) u_{sg} = 0.0113 m s^{-1} (3) u_{sg} = 0.0165 m s^{-1} (4) u_{sg} = 0.0207 m s^{-1} (5) u_{sg} = 0.0276 m s^{-1} (6) u_{sg} = 0.0339 m s^{-1} (7) u_{sg} = 0.0415 m s^{-1}(8) u_{sg} = 0.0516 m s^{-1}

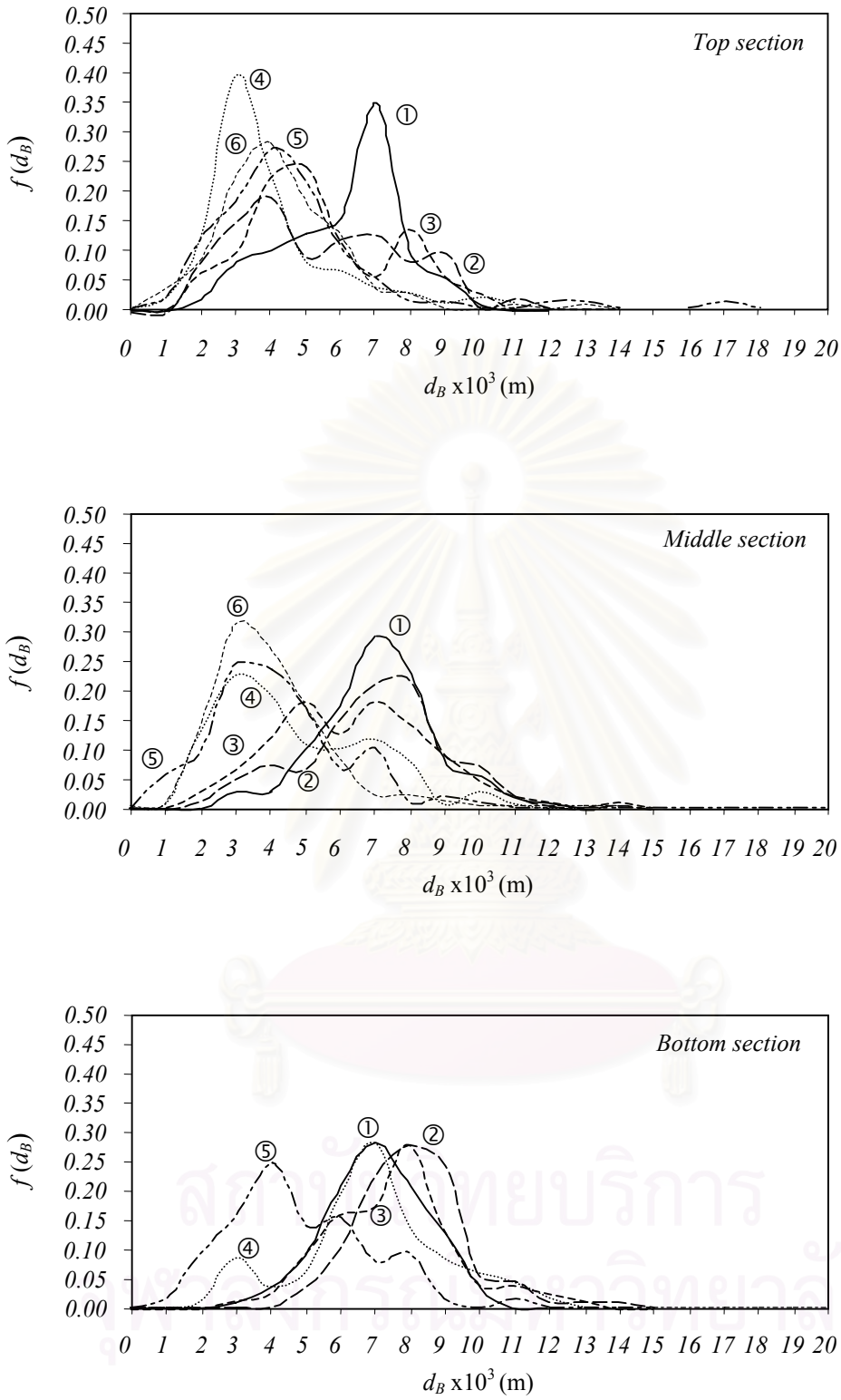

Figure 4.4 Frequency distribution of bubble sizes in ALC-3 at various u_{sg}: (1) u_{sg} = 0.0059 m s^{-1} (2) u_{sg} = 0.0225 m s^{-1} (3) u_{sg} = 0.0296 m s^{-1} (4) u_{sg} = 0.0395 m s^{-1} (5) u_{sg} = 0.0593 m s^{-1} (6) u_{sg} = 0.0737 m s^{-1}

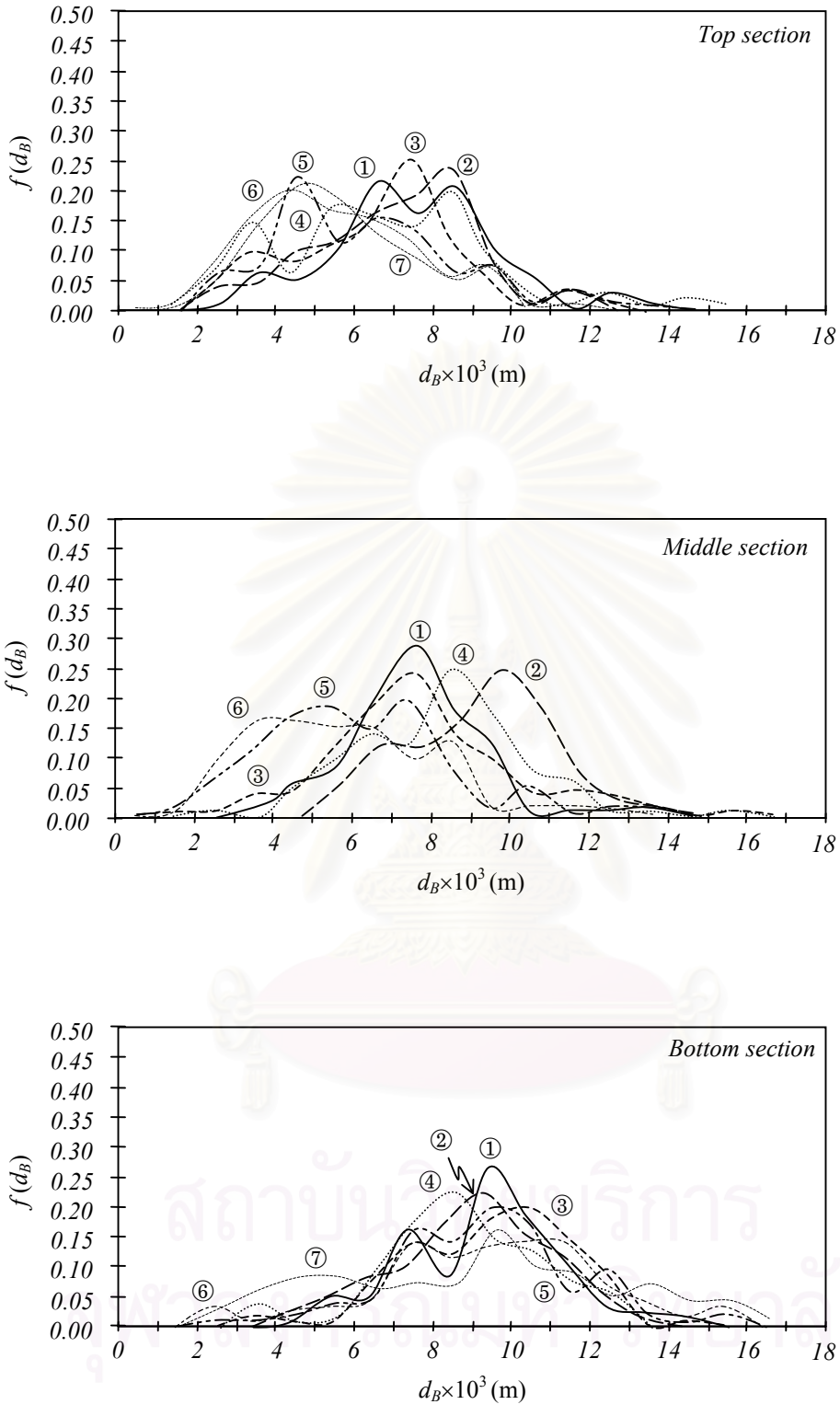

Figure 4.5 Frequency distribution of bubble sizes in ALC-4 at various u_{sg}: (1) u_{sg} = 0.0085 m s^{-1} (2) u_{sg} = 0.0116 m s^{-1} (3) u_{sg} = 0.0225 m s^{-1} (4) u_{sg} = 0.0296 m s^{-1} (5) u_{sg} = 0.0395 m s^{-1} (6) u_{sg} = 0.0593 m s^{-1}

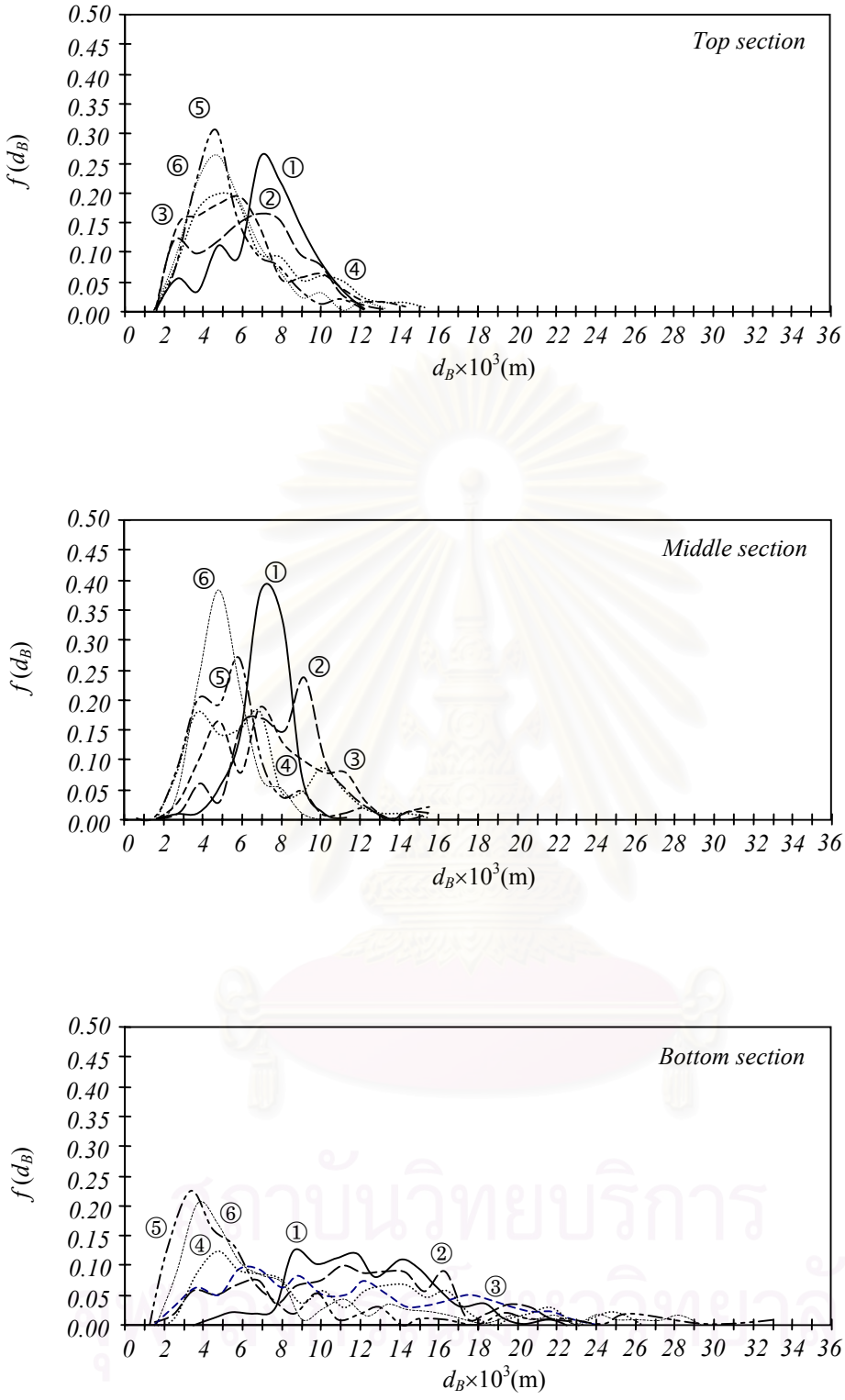

Figure 4.6 Frequency distribution of bubble sizes in ALC-5 at various u_{sg}: (1) u_{sg} = 0.0085 m s^{-1} (2) u_{sg} = 0.016 m s^{-1} (3) u_{sg} = 0.0225 m s^{-1} (4) u_{sg} = 0.0296 m s^{-1} (5) u_{sg} = 0.0395 m s^{-1} (6) u_{sg} = 0.0415 m s^{-1}

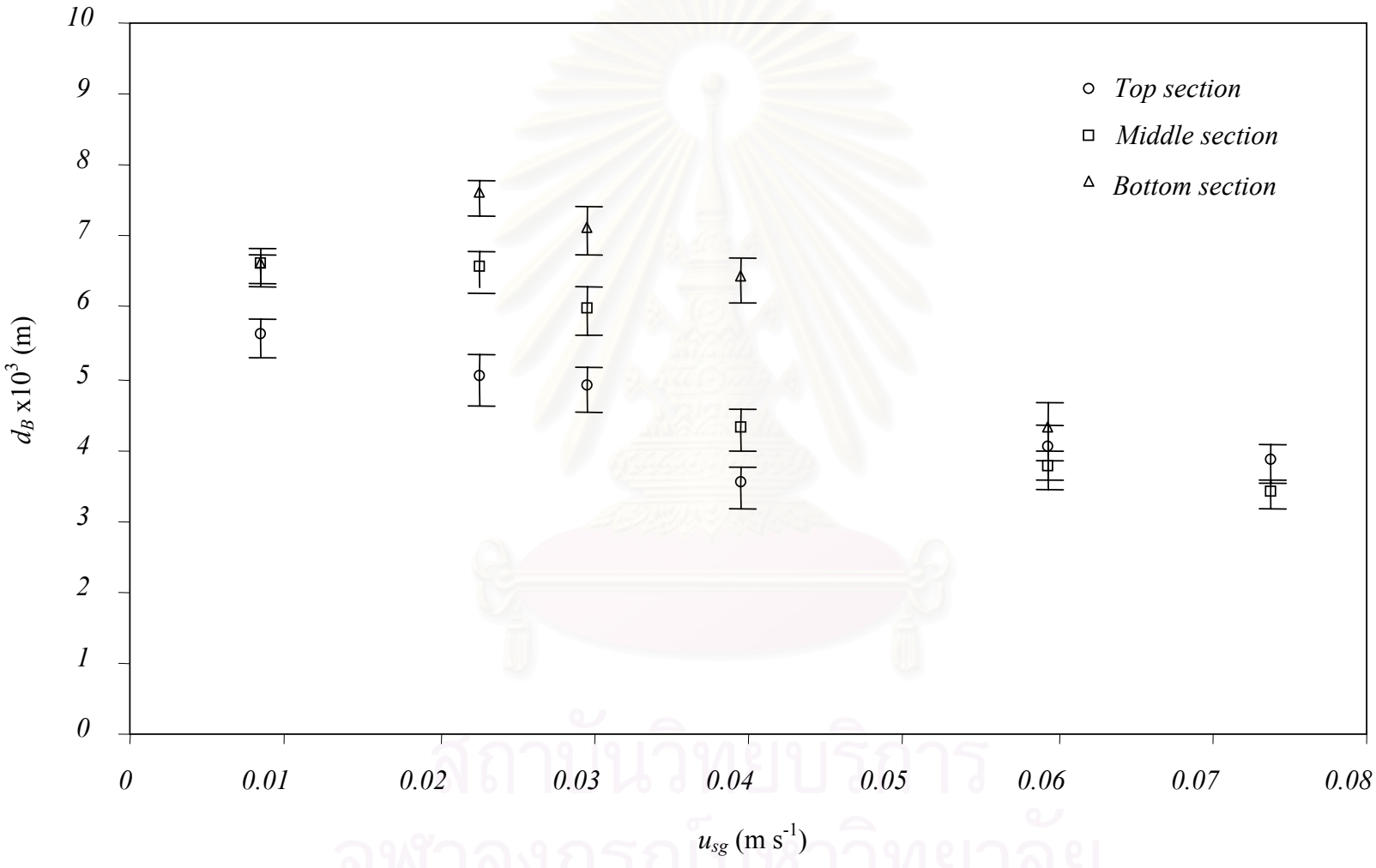

Figure 4.7 Relationship between average bubble diameter (d_B) and superficial gas velocity (u_{sg}) along axial location in ALC-3

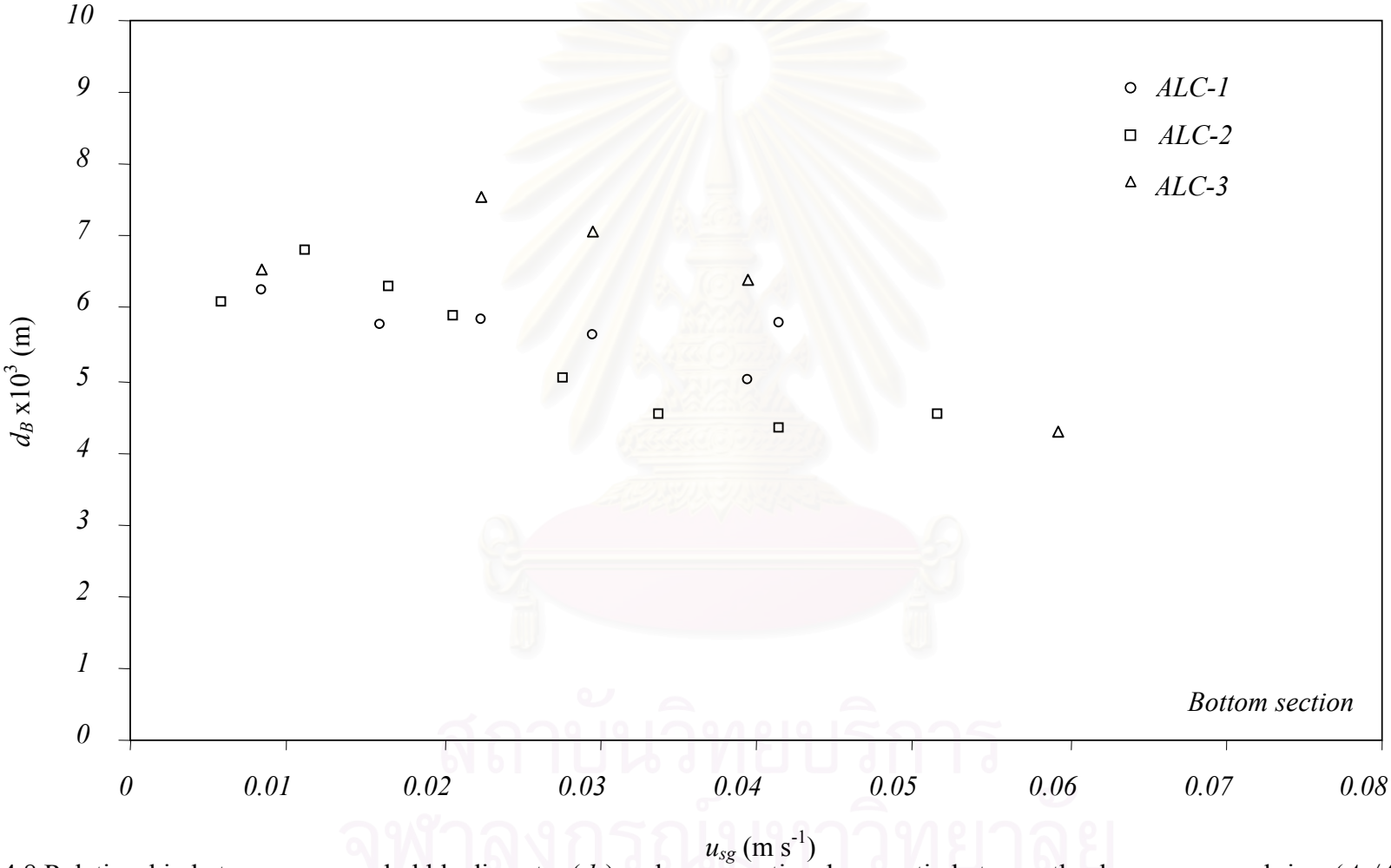

Figure 4.8 Relationship between average bubble diameter (d_B) and cross-sectional area ratio between the downcomer and riser (A_d/A_r)

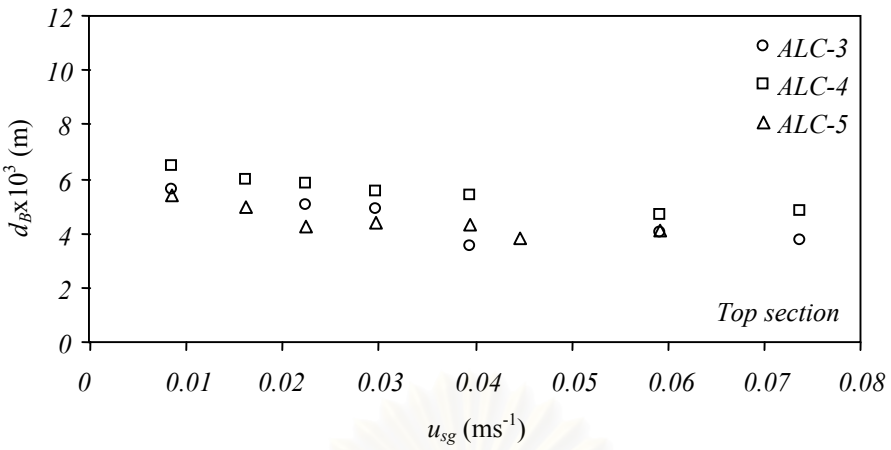

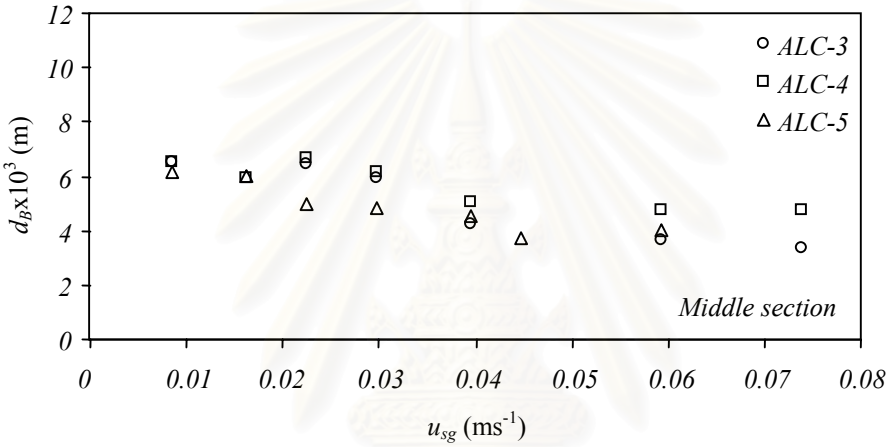

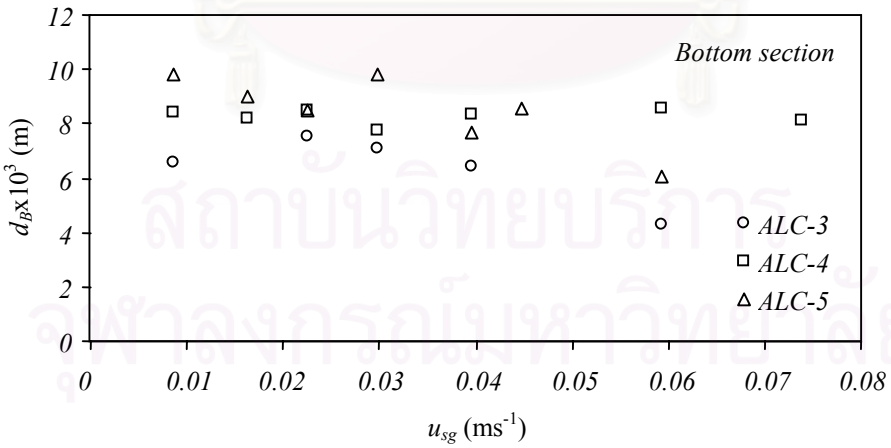

Figure 4.9 Relationship between average bubble diameter, d_B and orifice number, n along axial location

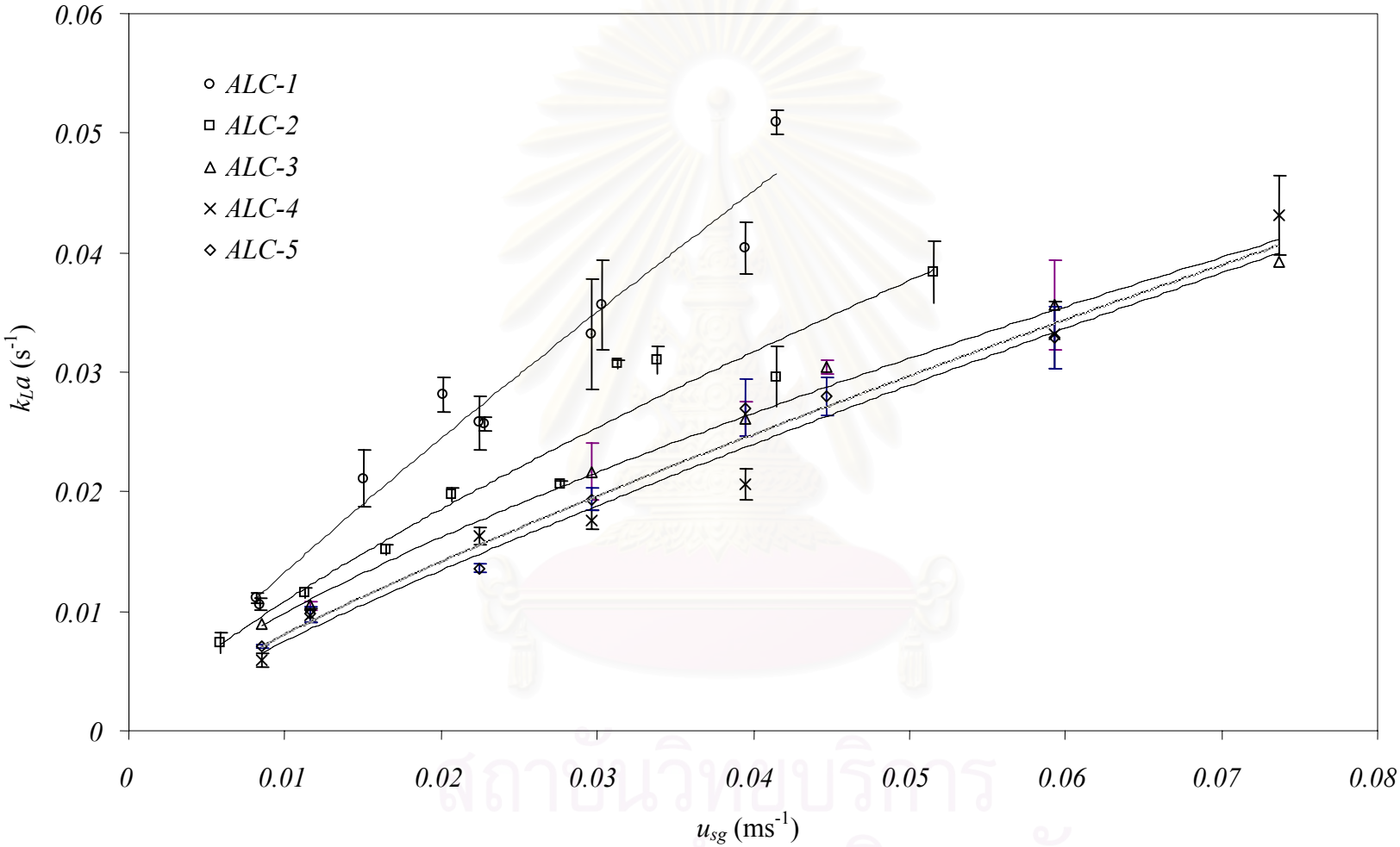

Figure 4.10 Relationship between experimental data of overall volumetric mass transfer coefficient, $(k_La_L)_T$ and superficial gas velocity, u_{sg}

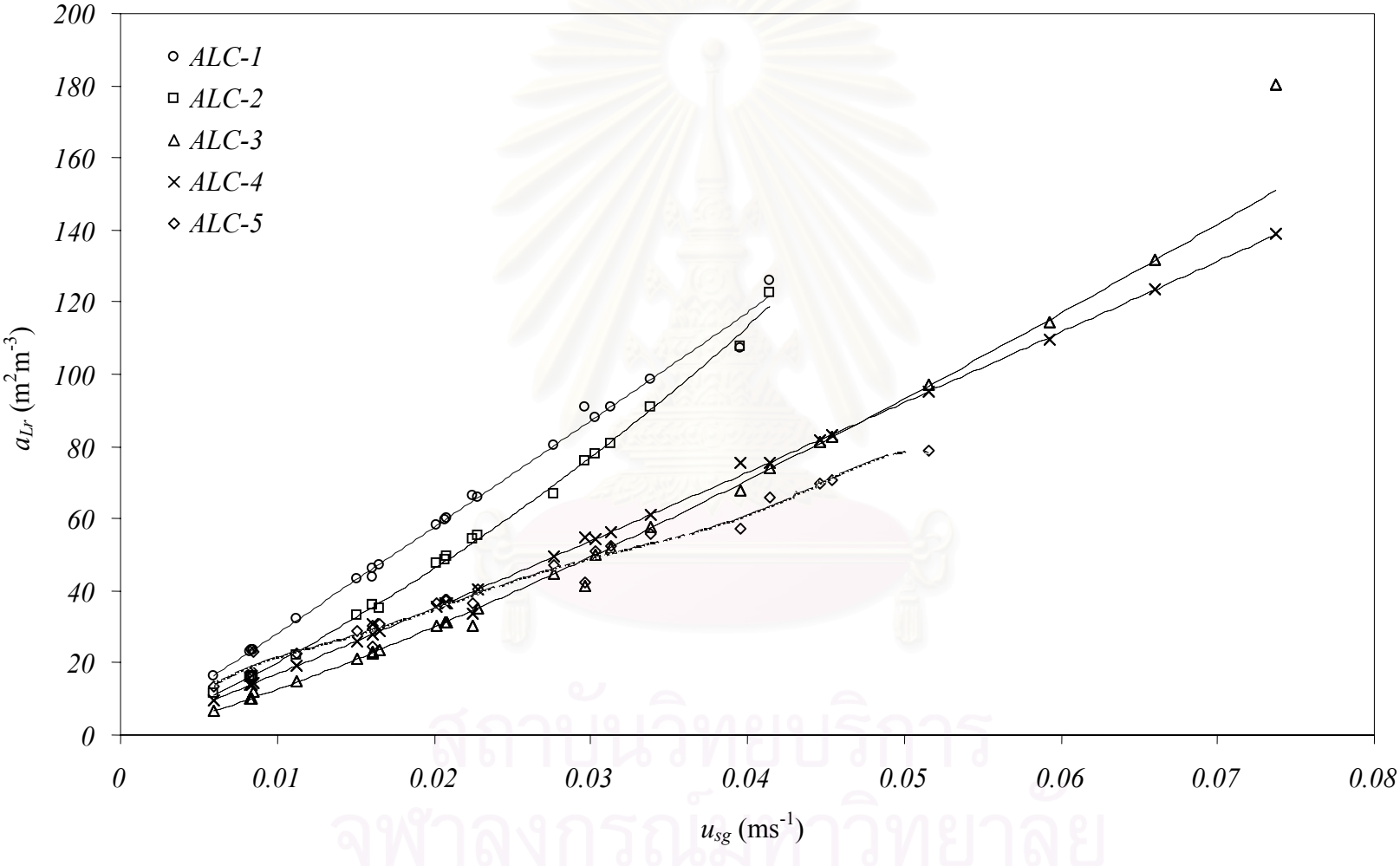

Figure 4.11 Relationship between specific interfacial area in riser, a_{Lr}, and superficial gas velocity, u_{sg}

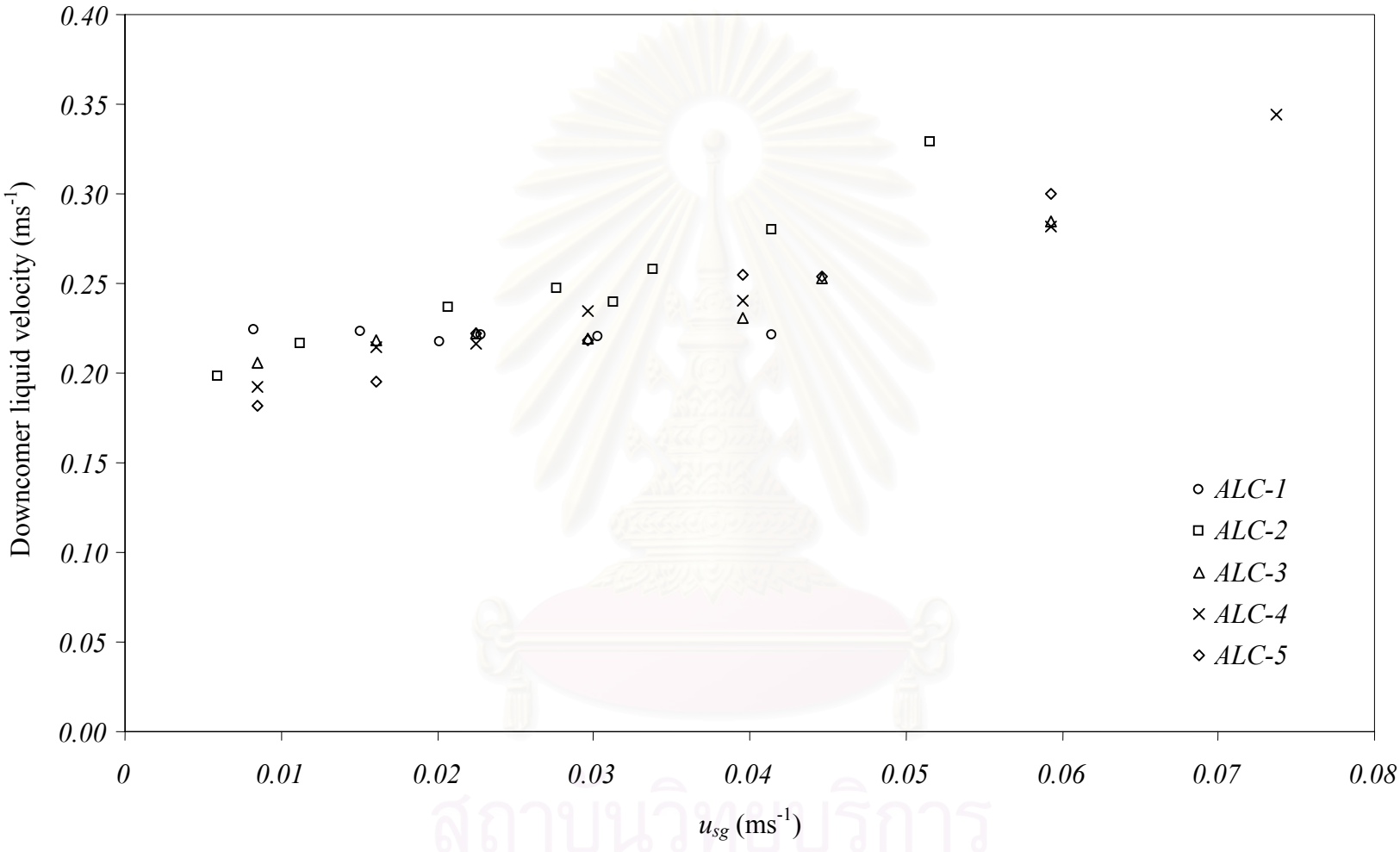

Figure 4.12 Relationship between superficial liquid velocity in downcomer (u_{Ld}) and superficial gas velocity (u_{sg})

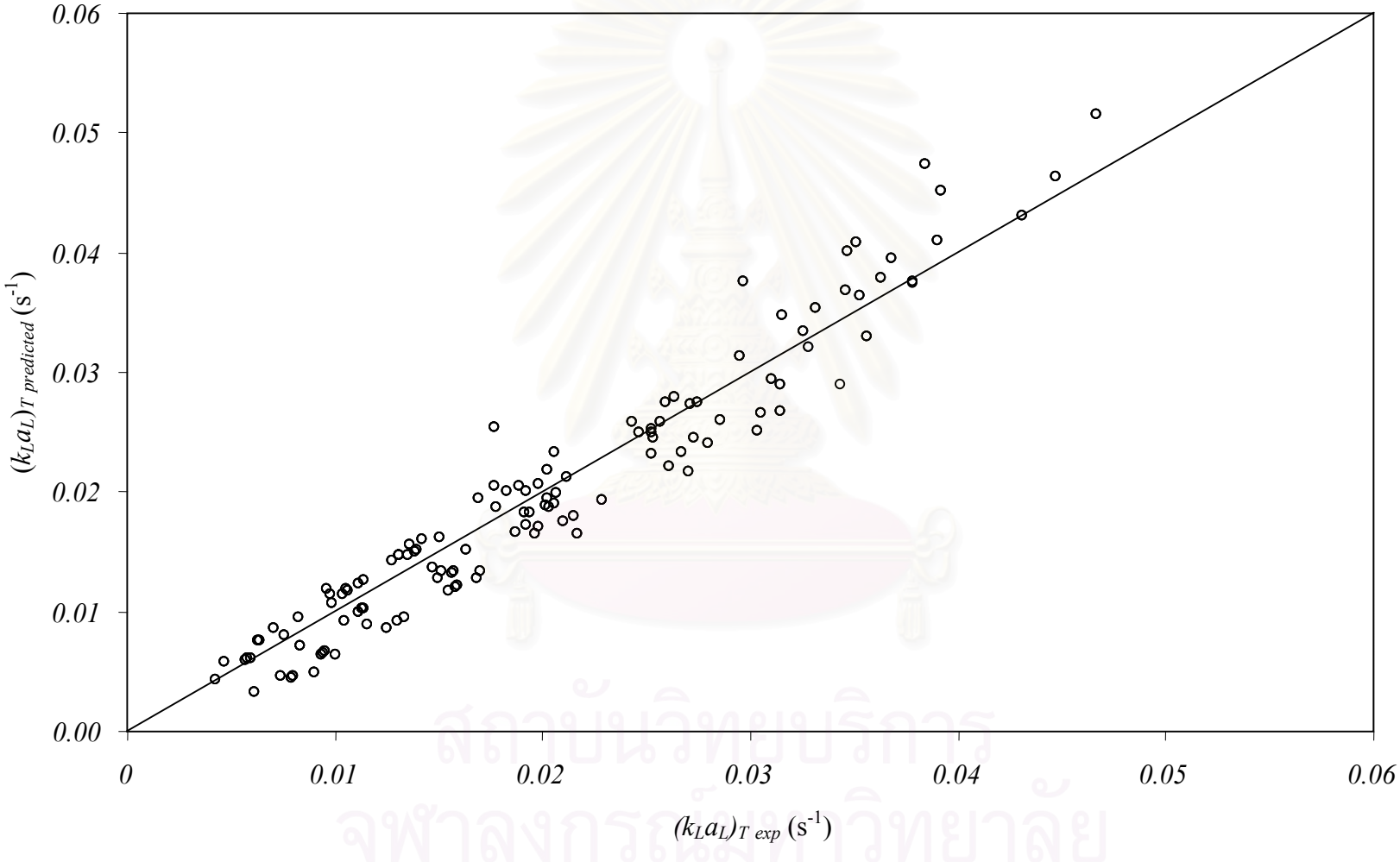

Figure 4.13 Comparison of $(k_La_L)_T$ estimated by Eq. (4.12) with values observed in this work

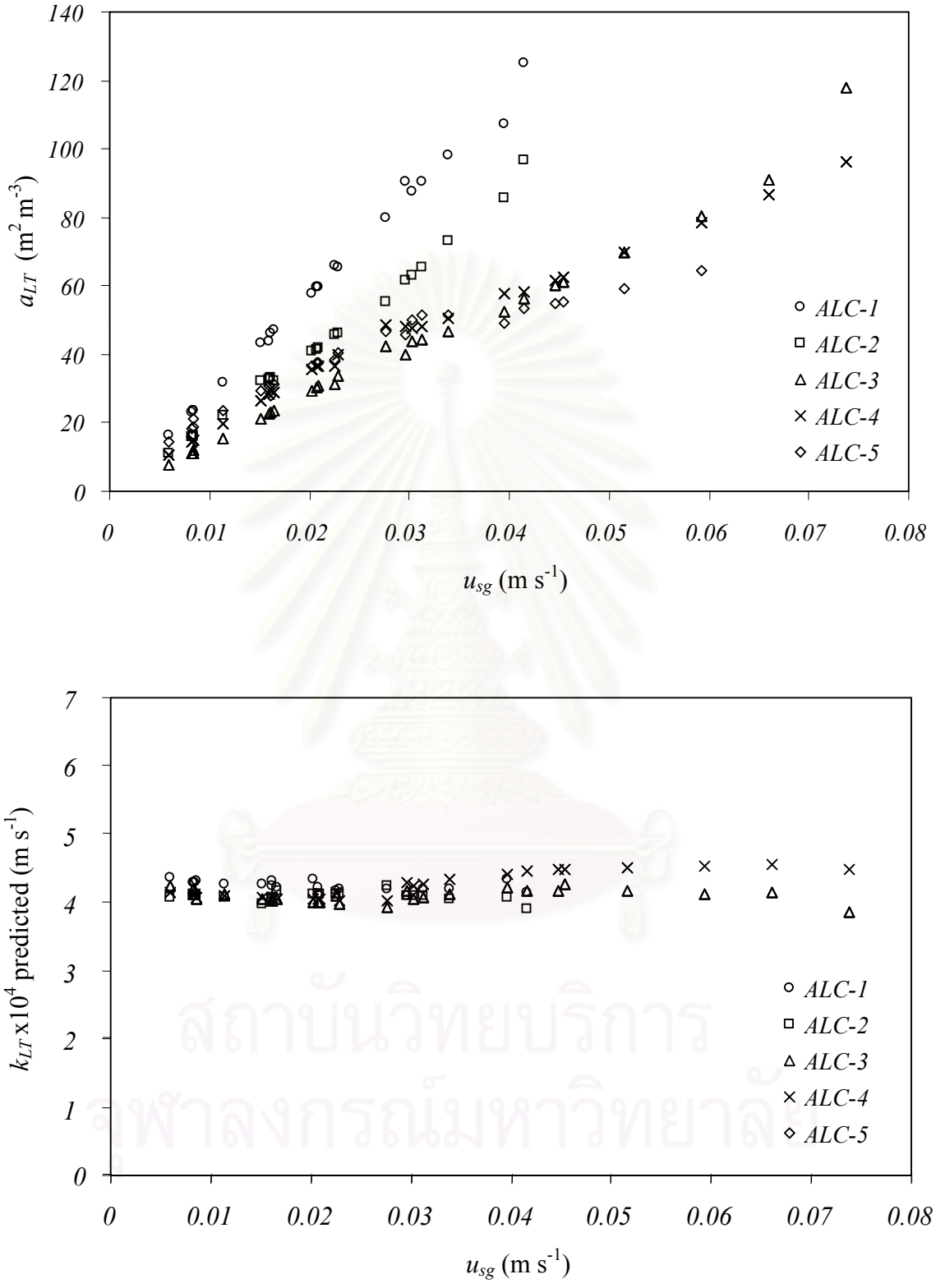

Figure 4.14 Effects of superficial gas velocity (u_{sg}) on (a) overall specific interfacial area (a_{LT}) and b) overall gas-liquid mass transfer coefficient (k_{LT})

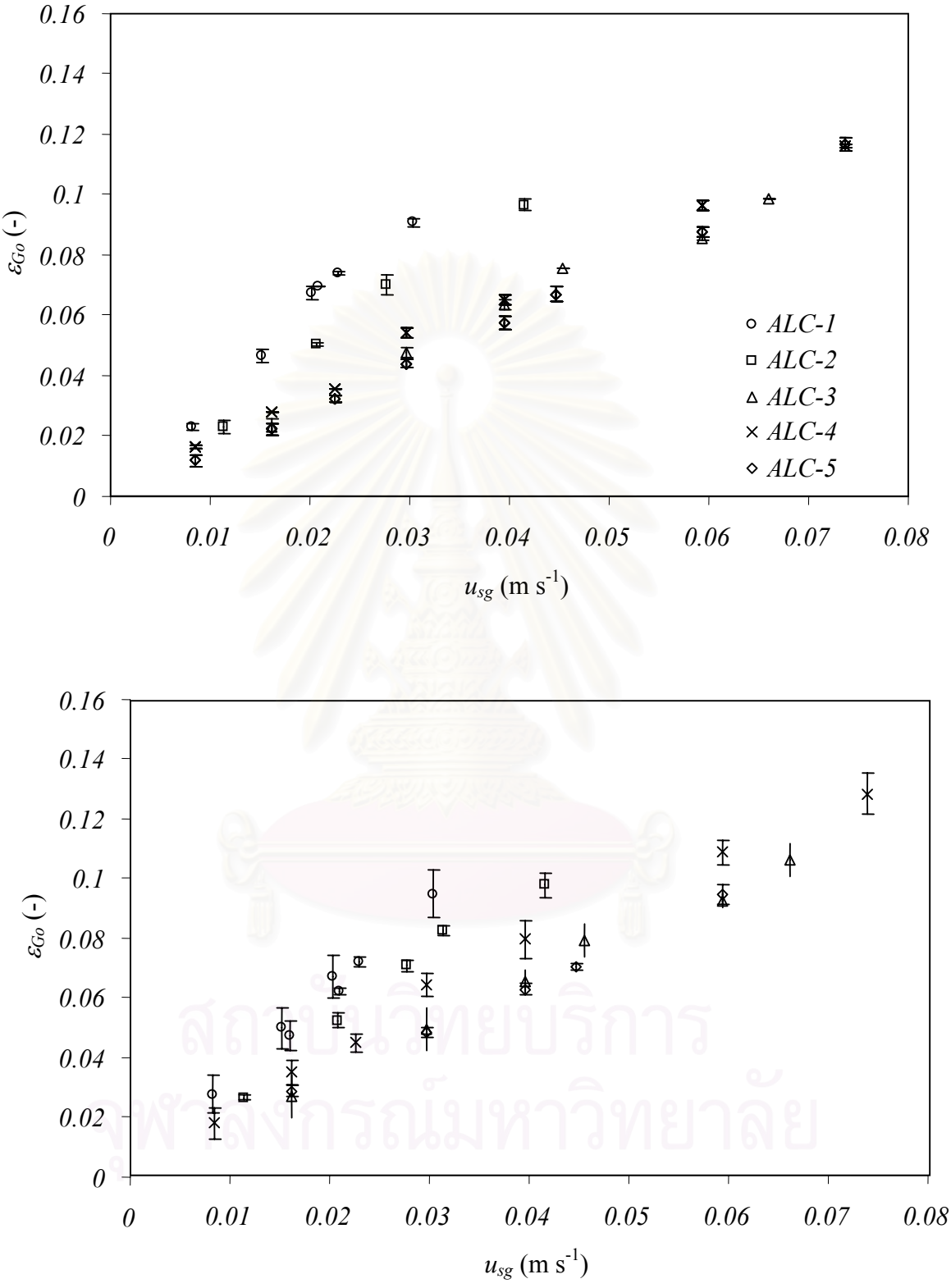

Figure 4.15 Effects of superficial gas velocity (u_{sg}) on (a) Overall gas holdup (ε_{Go}) and (b) Riser gas holdup (ε_{Gr})

Chapter 5

Internal Liquid Circulation

5.1 Backgrounds

Primary liquid circulation between riser and downcomer in the airlift contactors is one characteristic which distinguishes them from other types of gas-liquid contacting devices. This type of liquid circulation is induced mainly from the transfer of momentum from inlet gas to liquid and also from the difference in the densities of the fluids in riser and downcomer. Along with this primary liquid circulation, there also exists a secondary liquid circulation which takes place locally either in riser or downcomer sections. This type of liquid flow is usually known as "internal liquid circulation". This fluid flow pattern is similar to that which dominates the behavior of bubble columns.[1-6] However, its role in characterizing the behavior of airlift contactors is still unclear. Few investigators have addressed the existence of this type of flow. In the verification of energy balance model by Jones (1985)[7], it was found that the measurement of liquid velocity did not correspond well with the model prediction. This was concluded to be attributed to the existence of internal liquid circulation in riser. Shortly after that, Merchuk and Siegel (1988)[8] observed that the up-flow pattern in riser was occasionally suppressed and became more turbulent, especially at high gas flowrate. They concluded that there must be internal liquid circulation taking place in riser of the airlift contactor.

Further development of mathematical models for airlift contactors often emphasized that internal liquid circulation must have taken place within the system. For instance, Calvo and León (1991)[9] incorporated the turbulent energy dissipation due to the internal liquid circulation in the riser into their energy conservation based model and found that their simulation results agreed well with a wide range of reported experimental data. Some did represent this liquid circulation by other means such as the work by Wachi et al. (1991)[10] which stated that there were fluid flow contraction at the entrances of riser and downcomer. This flow contraction was dependent markedly on the draft tube diameter, or rather, the ratio between the cross sectional area of

downcomer and riser, where the increase in draft tube diameter for a draft tube sparged airlift contactor resulted in a relatively larger flow contraction at the riser entrance. In downcomer, the flow contraction tended to have the maximum value for the case of intermediate size draft tube. This was because the increase in draft tube diameters reduced the flow convergence in downcomer, probably due to the lower overflow velocity at the top of the larger draft tube. The correspondingly high liquid velocity in the narrow annulus induced a more uniform flow pattern in the downcomer, but further increases in draft tube diameter may finally induce liquid recirculation in the riser itself.[7]

It is therefore the aim of this work to investigate the local fluid flow behavior within the annulus sparged airlift contactor. The effects of geometrical and operational parameters are included in the study. The model for predicting proportion of internal liquid circulation based on material and mechanical energy conservation is proposed.

5.2 Mathematical model with internal liquid circulation

To evaluate the existing of internal liquid recirculation within riser, the mathematical model based on mass and energy conservations is developed into which the internal liquid circulation is incorporated. This model is established based on the following assumptions:

1. Uniform gas holdup in riser and downcomer along the radial and axial directions
2. Negligible interaction between the gas phase and the wall, i.e. the influence of the gas phase on the friction are negligible[11]
3. Negligible gravitational force on the gas phase
4. One-directional isothermal flow
5. Steady state conditions
6. No gas recirculation in riser section ($\varepsilon_{Gr,up}$=0)[12]

5.2.1 Steady state macroscopic mass balance (Continuity equation):

The steady state mass balance equation has the form:[13]

$$0 = \Delta \dot{w} \tag{5.1}$$

where $\dot{w}$ is the mass flowrate.

For the liquid phase, the mass flow in downcomer is equal to that in riser:

$$\dot{w}_{Ld} = \dot{w}_{Lr} \tag{5.2}$$

Liquid mass flowrate could be defined by

$$\dot{w}_L = \rho_L v_L A_L = \rho_L v_L A\left(1-\varepsilon_G\right) \tag{5.3}$$

Substituting Eq. (5.3) into Eq. (5.2) yields

$$\rho_L v_{Ld} A_d (1-\varepsilon_{Gd}) = \rho_L v_{Lr} A_r (1-\varepsilon_{Gr}) \tag{5.4}$$

or

$$v_{Ld} A_d (1-\varepsilon_{Gd}) = v_{Lr} A_r (1-\varepsilon_{Gr}) \tag{5.5}$$

This is a simple form of continuity equation for the case where internal liquid circulation was assumed not to exist. To account for the existing of internal liquid circulation in riser, the schematic diagram of liquid flow in riser are proposed as displayed in Figure 5.1. The system considered here is the flow of liquid entering the downcomer at plane "1", flowing through the bottom section and exiting the riser at plane "2". The liquid flow in riser was divided into two distinct regions: the uniformly distributed bubble region in the inner annular region and the bubble-free in outer annular region ($\varepsilon_{Gr,down} = 0$). It was assumed that the uniform bubble region was also uniform in gas holdup. For this case, the RHS of the mass balance of liquid phase, Eq. (5.5), should include the liquid recirculation term which can be expressed as:

$$v_{Ld} A_d (1-\varepsilon_{Gd}) = v_{Lr,up} A_{r,up} (1-\varepsilon_{Gr,up}) - v_{Lr,down} A_{r,down} (1-\varepsilon_{Gr,down}) \tag{5.6}$$

where the $v_{Lr,up}$ is the riser liquid velocity in upflow region which occupies the area of $A_{r,up}$, the $v_{Lr,down}$ the riser liquid velocity in downflow region which occupies the area of $A_{r,down}$. The minus in front of the 2nd term on the RHS of Eq. (5.6) is subject to mass flowrate of internal liquid recirculation which flows downwards in the riser. The relationship between $A_{r,up}$ and $A_{r,down}$ for internal liquid recirculation in riser can be written as:

$$A_{r,up} + A_{r,down} = A_r \tag{5.7}$$

where $A_{r,up}$ is the upflow area in the riser, $A_{r,down}$ the downflow area in the riser. Substituting $A_{r,up}$ from Eq. (5.7) into Eq. (5.6) gives:

$$v_{Ld} A_d (1-\varepsilon_{Gd}) = v_{Lr,up} \left(A_r - A_{r,down}\right)(1-\varepsilon_{Gr,up}) - v_{Lr,down} A_{r,down} (1-\varepsilon_{Gr,down}) \tag{5.8}$$

5.2.2 Steady state macroscopic energy balance (Bernoulli equation):

The energy balance can be expressed using the Bernoulli equation:[13]

$$0 = \Delta \frac{1}{2} \frac{\langle \overline{v}^3 \rangle}{\langle \overline{v} \rangle} + \Delta\Phi + \int_{P_1}^{P_2} \frac{1}{\rho} dP + \hat{W} + \hat{E}_v \tag{5.9}$$

where Φ is the potential energy per unit mass, $\hat{W}$ the rate at which the system performs mechanical work on its surroundings and $\hat{E}_v$ the friction loss or the rate at which mechanical energy is irreversibly converted to thermal energy.

Eq. (5.9) can be written in a simple form as:

$$0 = \Delta \frac{1}{2} \langle \overline{v} \rangle^2 + g\Delta h + \int_{P_1}^{P_2} \frac{1}{\rho} dP + \hat{W} + \hat{E}_v \tag{5.10}$$

The integral appearing in Eq. (5.10) can be evaluated for incompressible fluid as follows:

$$\int_{P_1}^{P_2} \frac{1}{\rho} dP = \frac{1}{\rho} \left(P_2 - P_1 \right) \tag{5.11}$$

where subscript '*1*' is at plane '1' and '*2*' for plane '2'. It can be seen in Figure 5.1 that plane '1' and plane '2' locates at the same horizontal level. Therefore this term becomes negligible in Eq. (5.10).

The energy input to any ALCs is derived from the two main sources: (i) potential energy due to isothermal gas expansion and (ii) kinetic energy as described in Section 2.2.2 in Chapter 2, Eq. (2.17).

$$P_G = Q_{Gm} RT \ln \left(1 + \frac{\rho_L g H_L}{P_t} \right) + \frac{1}{2} \eta M_w Q_{Gm} u_{Go}^2 \tag{2.17}$$

Usually, the kinetic energy term is found negligible when compared to the isothermal expansion and therefore:

$$\hat{W} = P_G = Q_{Gm} RT \ln \left(1 + \frac{\rho_L g H_L}{P_t} \right) \tag{5.12}$$

or

$$\hat{W} = P_G = P_b Q_G \ln \left(1 + \frac{\rho_L g H_L}{P_t} \right) \tag{5.13}$$

The friction losses ($\hat{E}_v$) are composed of frictions from all sections of straight conduits and all fittings which could be calculated according to Eq. (5.14).

$$\hat{E}_v = \sum_i \hat{E}_{vi} \tag{5.14}$$

Substituting Eqs. (5.13) and (5.14) into Eq. (5.10) yields

$$0 = \Delta\frac{1}{2}\langle\overline{v}\rangle^2 + g\Delta h + P_b Q_G \ln\left(1+\frac{\rho_L g H_L}{P_t}\right) + \sum_i \hat{E}_{vi} \tag{5.15}$$

Usually the energy term due to the gas flow is found negligible when compared to the energy term due to liquid flow, and this energy term is not considered in this work (Assumption 2 in Section 5.2). Thus, with the consideration of internal liquid circulation in riser as displayed in Figure 5.1, the energy balance of liquid phase, Eq. (5.15), can be rewritten as:

$$\begin{aligned} 0 = {} & \frac{1}{2}\dot{w}_{Ld}v_{Ld}^2 - \frac{1}{2}\dot{w}_{Lr,up}v_{Lr,up}^2 + \frac{1}{2}\dot{w}_{Lr,down}v_{Lr,down}^2 \\ & - \dot{w}_{Ld}gh_d + \dot{w}_{Lr,up}gh_r - \dot{w}_{Lr,down}gh_r \\ & + P_b Q_G \ln\left(1+\frac{\rho_L g H_L}{P_t}\right) + \sum_i \hat{E}_{vi} \end{aligned} \tag{5.16}$$

Substituting $\dot{w}$ from Eq. (5.4) into Eq. (5.16) yields

$$\begin{aligned} 0 = {} & \frac{1}{2}\rho_L A_d\left(1-\varepsilon_{Gd}\right)v_{Ld}^3 - \frac{1}{2}\rho_L A_{r,up}\left(1-\varepsilon_{Gr,up}\right)v_{Lr,up}^3 + \frac{1}{2}\rho_L A_{r,down}\left(1-\varepsilon_{Gr,down}\right)v_{Lr,down}^3 \\ & - \rho_L A_d\left(1-\varepsilon_{Gd}\right)v_{Ld}gh_d + \rho_L A_{r,up}\left(1-\varepsilon_{Gr,up}\right)v_{Lr,up}gh_r - \rho_L A_{r,down}\left(1-\varepsilon_{Gr,down}\right)v_{Lr,down}gh_r \\ & + P_b Q_G \ln\left(1+\frac{\rho_L g H_L}{P_t}\right) + \sum_i \hat{E}_{vi} \end{aligned} \tag{5.17}$$

Energy dissipations ($\hat{E}_v$) taken into consideration in this work are those due to the frictions in the conduits, i.e., riser, downcomer and bottom section, $\hat{E}_{vr}$, $\hat{E}_{vd}$, and $\hat{E}_{vb}$, respectively. These energy dissipations can be calculated according to Eq. (5.18).

$$\hat{E}_{vi} = \sum_i\left(\frac{1}{2}\rho_L A\left(1-\varepsilon_G\right)v_L^3\frac{L}{R_h}f\right)_i + \sum_i\left(\frac{1}{2}\rho_L A\left(1-\varepsilon_G\right)v_L^3 e_v\right)_i \tag{5.18}$$

where $\sum_i \left(\frac{1}{2} \rho_L A (1-\varepsilon_G) v_L^3 \frac{L}{R_h} f \right)_i$ is the sum on all friction losses in sections of straight conduits such as riser and downcomer, and $\sum_i \left(\frac{1}{2} \rho_L A (1-\varepsilon_G) v_L^3 e_v \right)_i$ friction losses at top and bottom sections. However, at the top section, it is noted that for the open liquid surface the pressure drop can usually be neglected.[14-15]

Eq. (5.18) can be written in a simple form as follows:

$$\hat{E}_{vi} = \sum_i \left(\frac{1}{2} \rho_L A (1-\varepsilon_G) v_L^3 \left(\frac{L}{R_h} f + e_v \right) \right)_i \tag{5.19}$$

where f is the friction factor, R_h mean hydraulic radius and e_v friction loss factor.
In annular conduit, f is a function of Reynolds number according to:[13]

$$\left.\begin{aligned} f &= \frac{16}{\mathrm{Re}} \qquad \text{for Re<2100} \\ f &= \frac{0.0791}{\mathrm{Re}^{1/4}} \qquad \text{for 2100<Re<}10^5 \end{aligned}\right\} \tag{5.20}$$

where Re is Reynolds number which is defined as

$$\mathrm{Re} = \frac{4 R_h \langle v_L \rangle \rho_L}{\mu_L} \tag{5.21}$$

Mean hydraulic radius (R_h) is defined as

$$R_h = \frac{S}{Z} \tag{5.22}$$

where S is the cross section of the stream and Z the wetted perimeter

In the determination of these energy dissipations, the friction loss factor (e_v) for the bottom section of the contactor which is assumed to be two 90^o elbow (rounded) has to be known and the value of 0.4-0.9 for each elbow provided in Bird et al (1960)[13] was employed in this work. The energy dissipation due to the friction in the riser (annulus section) is calculated in the same fashion as that in downcomer. However, there exist two distinct flow behaviors in the riser: upflow and downflow due to internal liquid recirculation. Hence, the total energy dissipation becomes

$$\hat{E}_v = \frac{1}{2}\dot{w}_{Ld} v_{Ld}^2 \left(\frac{L_d}{R_h} f_d\right) + \frac{1}{2}\dot{w}_{Ld} v_{Ld}^2 e_v + \frac{1}{2}\dot{w}_{Lr,up} v_{Lr,up}^2 \left(\frac{L_{r,up}}{R_{hr,up}} f_{r,up}\right) + \frac{1}{2}\dot{w}_{Lr,down} v_{Lr,down}^2 \left(\frac{L_{r,down}}{R_{hr,down}} f_{r,down}\right) \tag{5.23}$$

$$\hat{E}_v = \frac{1}{2}\rho_L A_d (1-\varepsilon_{Gd}) v_{Ld}^3 \left(\frac{L_d}{R_{hd}} f_d + e_v\right) + \frac{1}{2}\rho_L A_{r,up} (1-\varepsilon_{Gr,up}) v_{Lr,up}^3 \left(\frac{L_{r,up}}{R_{hr,up}} f_{r,up}\right) + \frac{1}{2}\rho_L A_{r,down} (1-\varepsilon_{Gr,down}) v_{Lr,down}^3 \left(\frac{L_{r,down}}{R_{hr,down}} f_{r,down}\right) \tag{5.24}$$

Substituting Eq. (5.24) into Eq. (5.17) yields

$$\begin{aligned} 0 = {} & \frac{1}{2}\rho_L A_d \left(1-\varepsilon_{Gd}\right) v_{Ld}^3 - \frac{1}{2}\rho_L A_{r,up} \left(1-\varepsilon_{Gr,up}\right) v_{Lr,up}^3 + \frac{1}{2}\rho_L A_{r,down} \left(1-\varepsilon_{Gr,down}\right) v_{Lr,down}^3 \\ & - \rho_L A_d \left(1-\varepsilon_{Gd}\right) v_{Ld} g h_d + \rho_L A_{r,up} \left(1-\varepsilon_{Gr,up}\right) v_{Lr,up} g h_r - \rho_L A_{r,down} \left(1-\varepsilon_{Gr,down}\right) v_{Lr,down} g h_r \\ & + P_b Q_G \ln\left(1 + \frac{\rho_L g H_L}{P_t}\right) - \frac{1}{2}\rho_L A_d (1-\varepsilon_{Gd}) v_{Ld}^3 \left(\frac{L_d}{R_{hd}} f_d + e_v\right) \\ & - \frac{1}{2}\rho_L A_{r,up} (1-\varepsilon_{Gr,up}) v_{Lr,up}^3 \left(\frac{L_{r,up}}{R_{hr,up}} f_{r,up}\right) \\ & - \frac{1}{2}\rho_L A_{r,down} (1-\varepsilon_{Gr,down}) v_{Lr,down}^3 \left(\frac{L_{r,down}}{R_{hr,down}} f_{r,down}\right) \end{aligned} \tag{5.25}$$

5.3 Experiments

To achieve the aim of this section, experimental data on gas holdups and liquid velocities were carried out as described in Sections 3.2.2 and 3.2.3. The ALCs employed in this Chapter are those operated in annulus sparged mode: ALC-1, ALC-2, ALC-3 and ALC-6, whose specifications are shown in Table 3.2.

5.4 Results and discussion

5.4.1 Existence of internal liquid circulation: Experimental evidence

Experiments carried out in internal loop ALCs (annulus sparged) showed that, within the range of u_{sg} and A_d/A_r employed in this work, the color tracer in the

downcomer moved in a uniform pattern with slight dispersion. It was therefore assumed that there was no internal liquid circulation in the downcomer and that the fluid in the downcomer moved uniformly across the cross sectional area. This implied that the velocity measurement in the downcomer with a color tracer (Experiment in Section 3.2.3) provided reliable results.

Experiments, on the other hand, illustrated that there was turbulence in the color tracer as it moved along the riser of the ALC. In addition, liquid velocities measured in the riser and downcomer did not follow the continuity equation (Eq. (5.5)) where the net liquid flow in riser has to be equal to that in downcomer. Figures 5.2-5.5 displays the riser liquid velocity measured from the experiment compared with the riser liquid velocity computed from Eq. (5.5) using v_{Ld} from experiment in ALC with different ratios of downcomer to riser cross-sectional areas (A_d/A_r). It can be seen that the measured riser liquid velocity was always higher than that predicted from Eq. (5.5). This means that there must exist a downflow of liquid in the riser to counterbalance the excess liquid flow due to a high upflow velocity. In other words, an internal liquid circulation must have taken place in the riser of the annulus sparged internal loop ALCs.

5.4.2 Determination of internal liquid circulation

The simple calculation model based on principals of conservation of mass and energy described above (Eqs. (5.8) and (5.25)) was employed to estimate the proportion of the internal circulation of liquid in the riser. These equations have to be solved simultaneously to yield the liquid velocity in downflow region of riser ($v_{Lr,down}$) and the area occupied by this type of flow in the riser ($A_{r,down}$).

To solve these equations, some parameters including downcomer liquid velocity (v_{Ld}), downcomer gas holdup (ε_{Gd}), liquid velocity in upflow region of riser ($v_{Lr,up}$), gas holdup in upflow region of riser ($\varepsilon_{Gr,up}$), and gas holdup in downflow region of riser ($\varepsilon_{Gr,down}$) were necessary. In this work, v_{Ld} was considered uniform along the radial and axial directions, and hence, could be obtained directly from experiments as indicated in the previous section. It was assumed further that the measurement of riser liquid velocity by the color tracer technique gave the upflow velocity ($v_{Lr,up}$). The overall gas holdup (ε_{Go}) and gas holdup in riser (ε_{Gr}) were obtained directly from experiments whereas the ε_{Gd}, which could not be measured simply by manometer measurement, was

calculated from the experimental data of ε_{Go} and ε_{Gr} using Eq. (3.6). $\varepsilon_{Gr,up}$ can subsequently be calculated from

$$\varepsilon_{Gr,up} A_{r,up} = \varepsilon_{Gr} A_r \tag{5.26}$$

Gas holdup in the downflow region of riser $\varepsilon_{Gr,down}$ was assumed to be zero according to Assumption 7 in Section 5.2. A proper arrangement of Eqs (5.8) and (5.25) leads to two equations with two variables, i.e. liquid velocity in downflow region of riser ($v_{Lr,down}$) and area occupied by downflow region of riser ($A_{r,down}$). It is therefore possible to solve these equations by a standard nonlinear iterative procedure. The results of the calculations are given in the next sections of this Chapter.

5.4.3 Effect of superficial gas velocity (u_{sg}) on internal liquid circulation

As stated earlier, the internal liquid circulation was considered in terms of downflow and upflow liquid fractions in the riser. The volumetric flowrate of liquid in upflow ($Q_{Lr,up}$) and downflow ($Q_{Lr,down}$) sections were calculated by

$$Q_{Lr,i} = v_{Lr,i} A_{r,i} (1-\varepsilon_{Gr,i}) \tag{5.27}$$

where i = '*up*' for upflow in riser and '*down*' for downflow in riser.

Figure 5.6 displays the experimental results on $v_{Lr,up}$ and the simulation results in $v_{Lr,down}$ in the ALCs (ALC-1, ALC-2, ALC-3 and ALC-6) at various u_{sg}. It is apparent in the figure that both $v_{Lr,up}$ and $v_{Lr,down}$ varied with u_{sg} where increasing u_{sg} always resulted in a higher level of these liquid velocities. This was not unexpected as an increase in gas velocity effectively implied a larger energy input to the system and high liquid velocity was induced. However, the effect of u_{sg} on $v_{Lr,up}$ was less pronounced than that on $v_{Lr,down}$. It is also interesting to observe that the downflow velocity was in many cases higher than the upflow velocity particularly in the ALC with large A_r (small A_d/A_r). This might present some misleading results that the downflow was more important than the upflow of liquid but further investigation showed that the upflow was actually the dominant flow regime.

The determination of the upflow and downflow area fractions resulted in a plot in Figure 5.7. The upflow area ($A_{r,up}$) was found to increase steadily with the increase in u_{sg} whilst the opposite was found for the downflow area ($A_{r,down}$). These results indicated that at low u_{sg} (<0.02 $m \cdot s^{-1}$), the internal liquid circulation occupied

approximately 20-25% of riser cross-sectional area. The downflow occupied less area where only about 12-15% of riser cross-sectional area was observed at u_{sg} above 0.06 m· s^{-1}. The upflow area fraction increased slightly with u_{sg} from 75-80% at low u_{sg} (0.008-0.02 m· s^{-1}) to about 80-85% at above 0.02 m· s^{-1}.

Results in Figures 5.6-5.7 along with the data on riser gas holdup (in Chapter 2) made it possible to calculate the liquid flow fraction in the riser of the ALC, and these results are illustrated in Figure 5.8. Despite its high downflow velocity, most of the liquid was found to flow upwards as the area for the upflow was much larger than that of downflow. Both liquid flows were not significantly influenced by u_{sg} as the increase in the liquid velocity was compensated by the increase in the gas holdup at high u_{sg}.

5.4.4 Effect of cross-sectional area ratio between downcomer and riser (A_d/A_r) on internal liquid circulation

The effect of A_d/A_r on internal liquid circulation can also be extracted from Figures 5.6-5.7. Figure 5.6 illustrates that upflow velocity ($v_{Lr,up}$) increased as A_d/A_r increased. In contrast, the downflow velocity ($v_{Lr,down}$) decreased with an increase in A_d/A_r. An increase in A_d/A_r effectively meant a system with a smaller cross sectional area for riser and this created a favorable condition for the liquid to flow upwards (to take account for the large quantity of liquid flow in downcomer). At this condition, less liquid flowed downwards in the riser as downcomer presented an easier pathway for the downflow liquid. On the other hand, the system with small downcomer (small A_d/A_r) led to a more difficult liquid flow in downcomer and more liquid found its way down in the riser instead. This will be subsequently explained in more detail when the effect of A_d/A_r on the liquid flowrate is mentioned. The effect of A_d/A_r on the fraction of area for upflow and downflow in the riser was not detected in this work as elucidated in Figure 5.7. This meant that the downflow would always exist in the annulus sparged ALC with a predictable fraction of the total cross sectional area. This fraction of downflow in the riser was only dependent on u_{sg}.

Figure 5.9 illustrates that $Q_{Lr,up}$ and $Q_{Lr,down}$ were affected significantly by A_d/A_r. At a specified u_{sg}, $Q_{Lr,up}$ and $Q_{Lr,down}$ decreased as A_d/A_r increased. However, $Q_{Lr,down}$ was influenced by A_d/A_r in a much greater extent than $Q_{Lr,up}$. As A_d/A_r increased from 0.067 to 1.54, a small reduction in $Q_{Lr,up}$ (from 0.0025 to 0.002 $m^3 \cdot s^{-1}$) was noticed, where $Q_{Lr,down}$ markedly decreased from 0.0023 to 0.0002 $m^3 \cdot s^{-1}$. Meantime, Q_{Ld}

increased rather significantly from 0.0002 to 0.0016 $m^3 \cdot s^{-1}$ in the same u_{sg} range. The explanation follows.

The ALC employed in this study was the concentric tube type where the gas was sparged into the annulus section (as illustrated in Fig. 2.2b). The size of the outer column used was fixed and the draft tube was changed to alter the A_d/A_r. The smallest size draft tube used (d=0.034 m) gave the smallest A_d and the largest A_r resulting in the smallest A_d/A_r (ALC-1). The small downcomer area in this system obstructed the flow of liquid into the downcomer. As a result, the liquid tended to recirculate into riser itself rather than flow downward into downcomer section (high $Q_{Lr,down}$). On the other hand, the largest size draft tube (d=0.103 m) gave the largest A_d and the smallest A_r where the largest A_d/A_r was reached (ALC-6). This type of ALC promoted an easy flow-path to the downcomer and therefore allowed more liquid to circulate through the downcomer. Hence, less liquid circulation in the riser was observed.

5.5 Concluding remarks

A mathematical calculation based on mass and energy conservations in an annulus sparged airlift contactor in which internal liquid circulation occurred was presented. It was shown that, in an internal loop annulus sparged ALC, Q_L and v_L were dependent on the u_{sg} and A_d/A_r. The internal circulation was slightly affected by u_{sg}, but was significantly affected by the configuration of the system, A_d/A_r.

The existing of internal liquid circulation in riser presents a significant role on the prediction of liquid velocity in ALC. The results from this work show that the conventional methods for the liquid velocity measurement might have to be modified with a consideration for the internal liquid circulation.

5.6 References

1. Beek, W.J. 1965. Oscillations and vortices in a batch of liquid sustained by a gas flow. Symp. on two-phase flow, 2: T405.
2. De Never, N. 1968. Bubble driven fluid circulations. AIChE J. 14: 222.
3. Freedman, W., and Davidson, J.F. 1969. Hold-up and liquid circulation in bubble columns. Trans. Instn. Chem. Engrs. 47: T251.
4. Hills, J.H. 1974. Radial non-uniformity of velocity and voidage in a bubble columns. Trans. Instn. Chem. Engrs. 52: 1.

5. Rietema, K. 1982. Science and technology of dispersed two-phase systems-I and II: I. General Aspects. Chem. Eng. Sci. 37: 1125-1150.
6. Tzeng, J.-W., Chen, R.C., and Fan, L.-S. 1993. Visualization of flow characteristics in a 2-D bubble column and three-phase fluidized bed. AIChE J. 39: 733-744.
7. Jones, A.G. 1985. Liquid circulation in a draft-tube bubble column. Chem. Eng. Sci. 40(3): 449-462.
8. Merchuk, J., and Siegel, M.H. 1988. Air-lift reactors in chemical and biological technology. J. Chem. Tech. Biotech. 41: 105-120.
9. Calvo, E.G., and Letón, P. 1991. A fluid dynamic model for bubble columns and airlift reactors. Chem. Eng. Sci. 46(11): 2947-2951.
10. Wachi, W., Jones, A.G., and Elson, T.P. 1991. Flow dynamics in a draft-tube bubble column using various liquids. Chem. Eng. Sci. 46(2): 657-663.
11. Wallis, G.B. 1969. One-dimensional two-phase flow, McGraw-Hill, New York.
12. Lockett M.J., and Kirkpatrick, R.D. 1975. Ideal bubbly flow and actual flow in bubble columns. Trans. Instn. Chem. Engrs. 53: 267-273.
13. Bird, R.B., Stewart, W.E., and Lightfoot, E.N. 1960. “Transport Phenomena”. New York: John Wiley & Sons.
14. Kubota, H., Hosono, Y., and Fujie, K. 1978. Characteristic evaluations of ICI airlift type deep shaft aerator. J. Chem. Eng. Japan 11(4): 319-325.
15. Chisti M.Y. 1989. “Airlift Bioreactors” Elsevier Applied Science. London and New York.

5.7 Figures

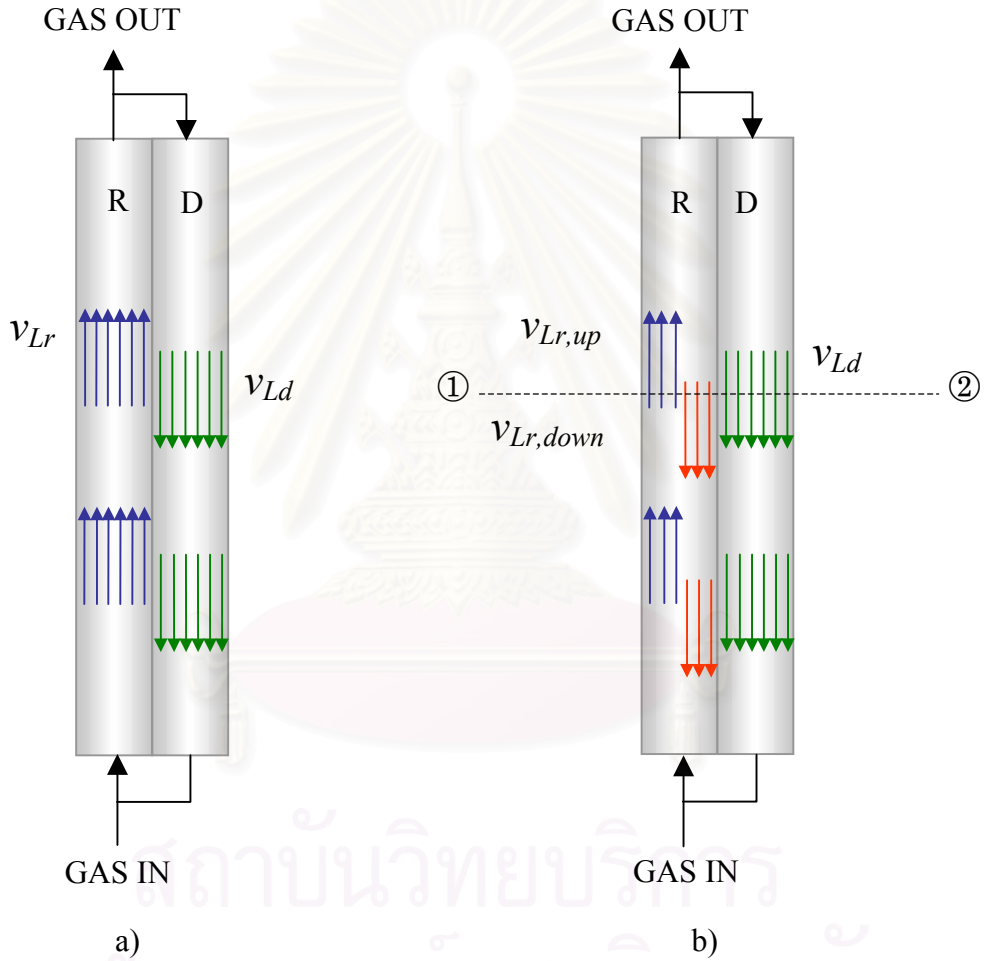

Figure 5.1 Schematic diagram of liquid flow in ALC: a) a conventional model for liquid flow; b) an ALC with internal liquid circulation

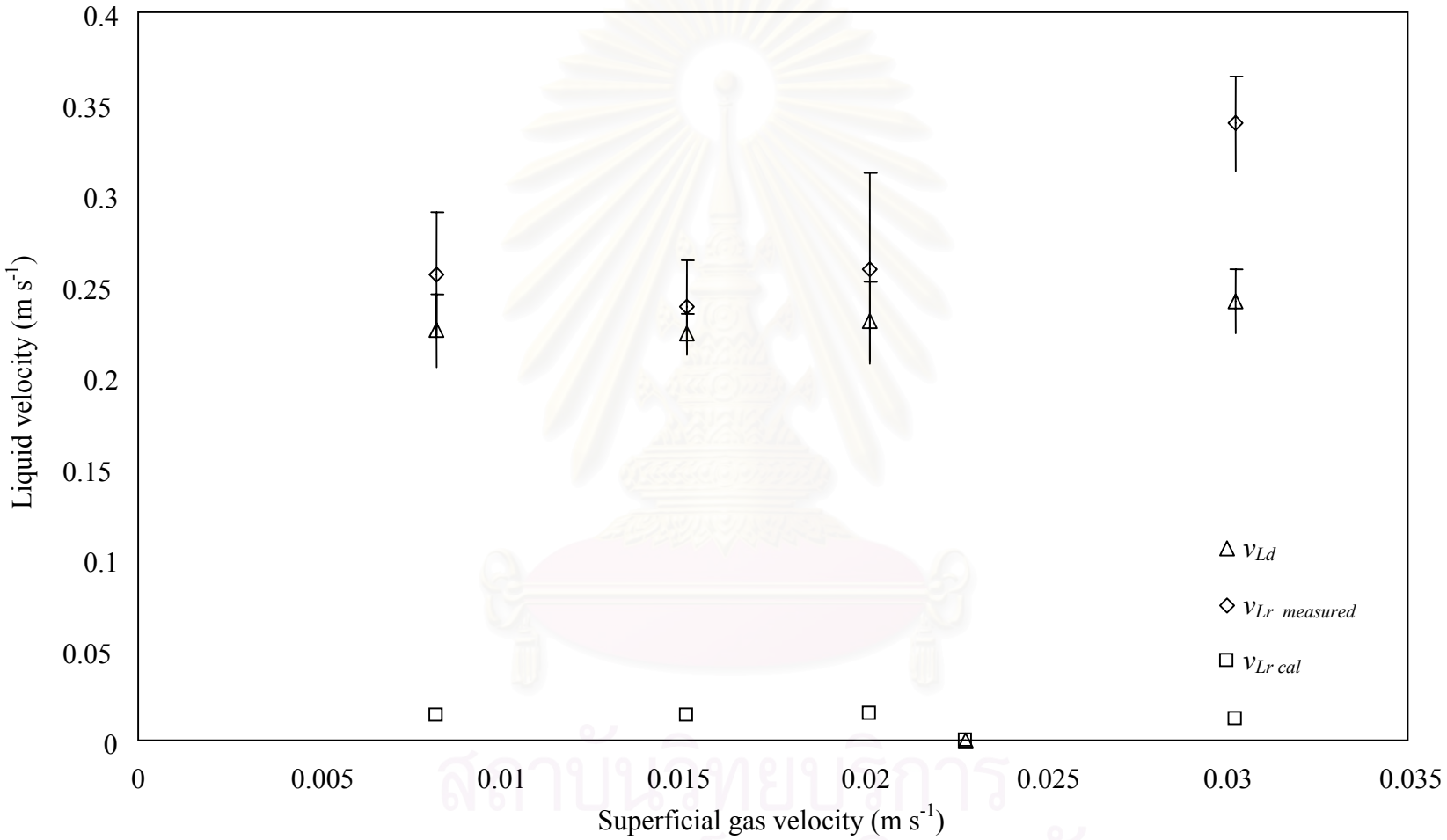

Figure 5.2 Comparison between riser liquid velocity calculated according to Eq. (5.5) and those measured from experiments in ALC-1

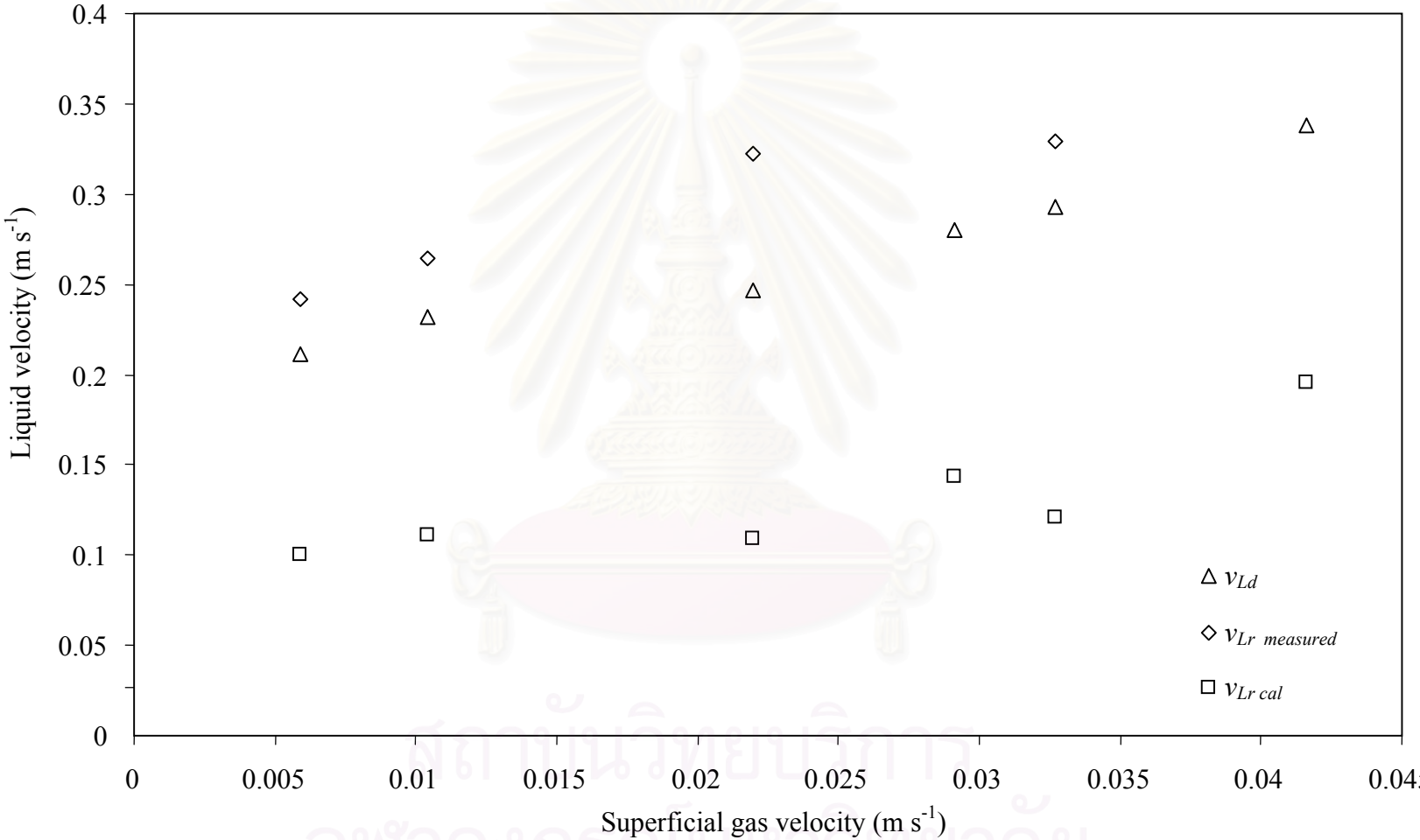

Figure 5.3 Comparison between riser liquid velocity calculated according to Eq. (5.5) and those measured from experiments in ALC-2

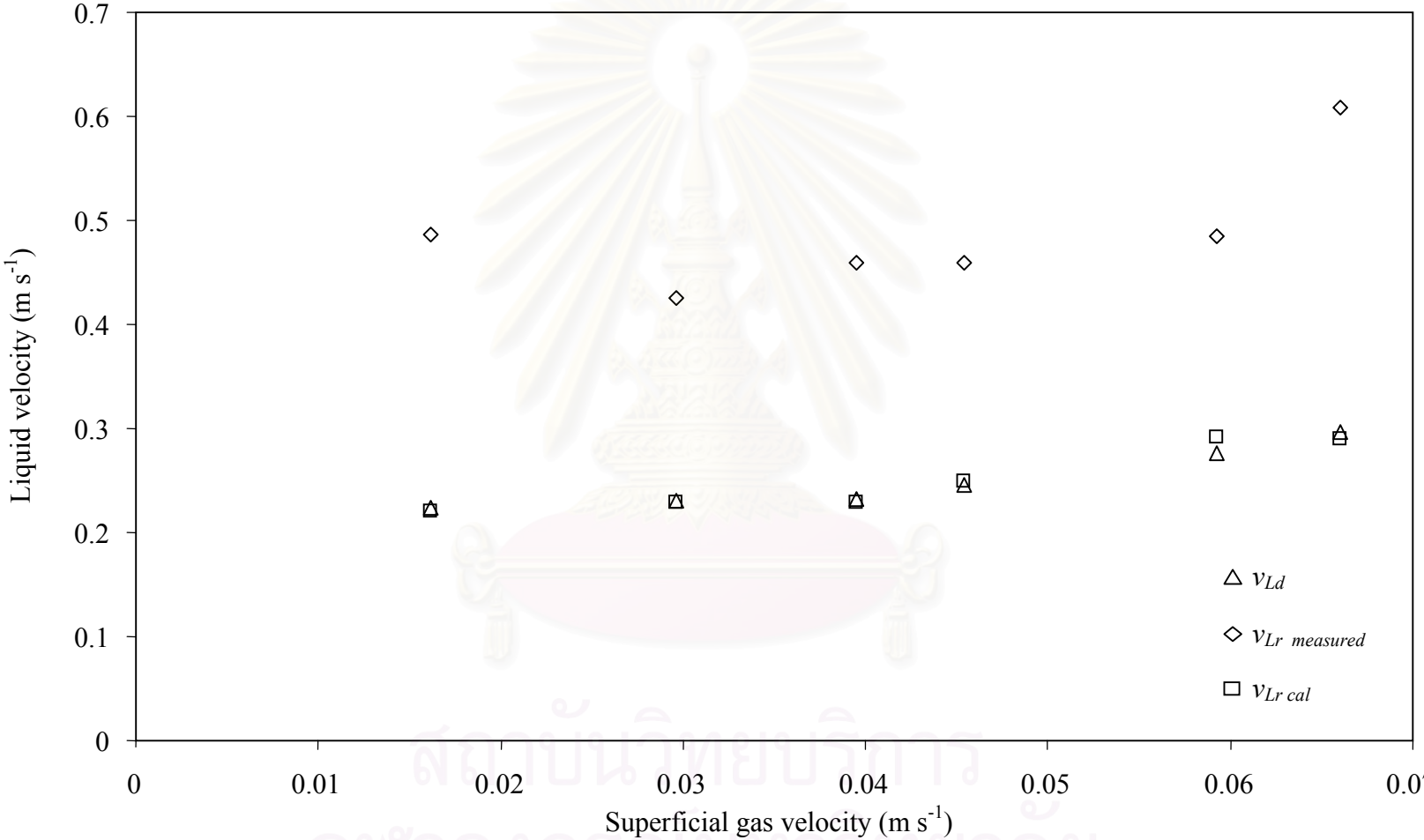

Figure 5.4 Comparison between riser liquid velocity calculated according to Eq. (5.5) and those measured from experiments in ALC-3

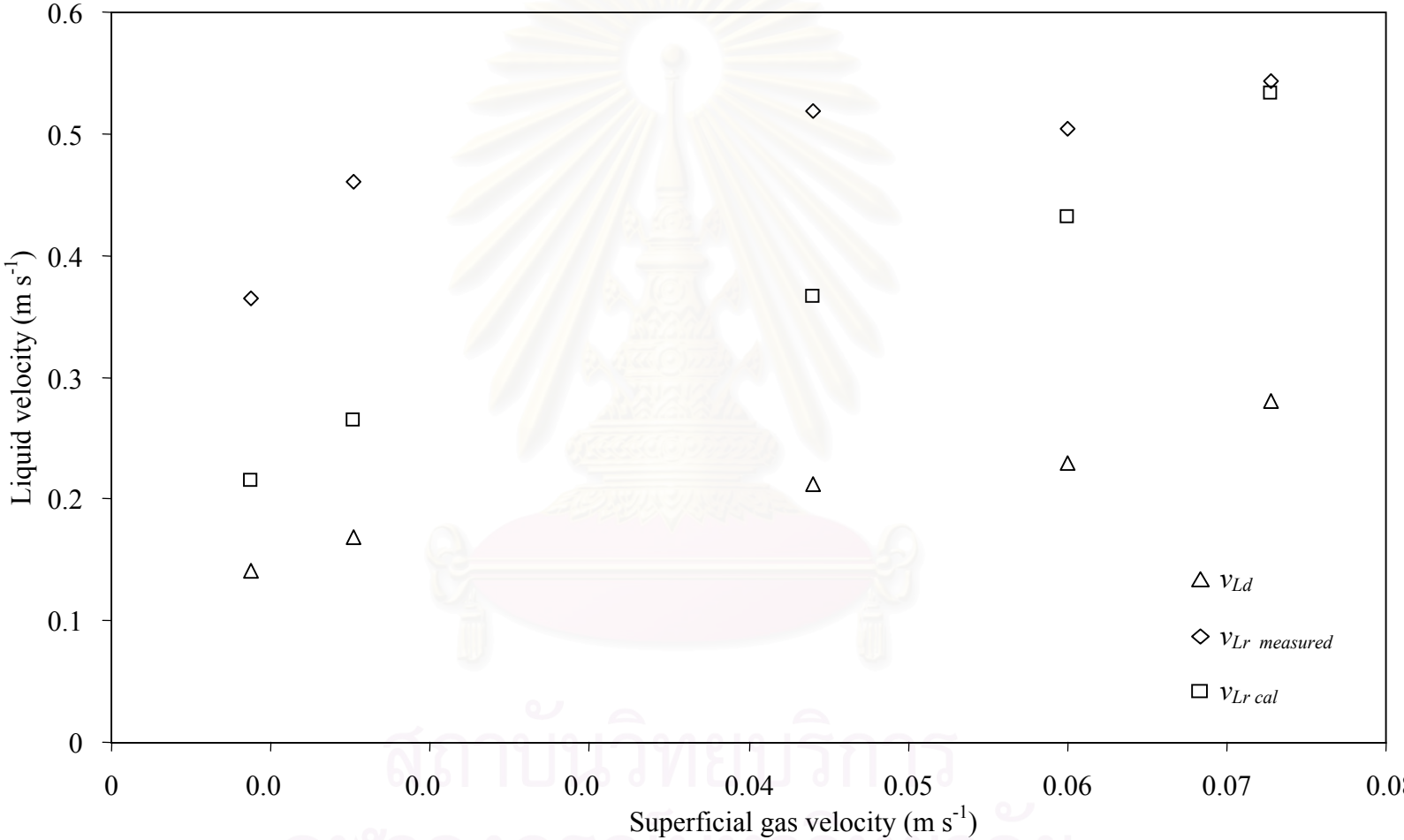

Figure 5.5 Comparison between riser liquid velocity calculated according to Eq. (5.5) and those measured from experiments in ALC-6

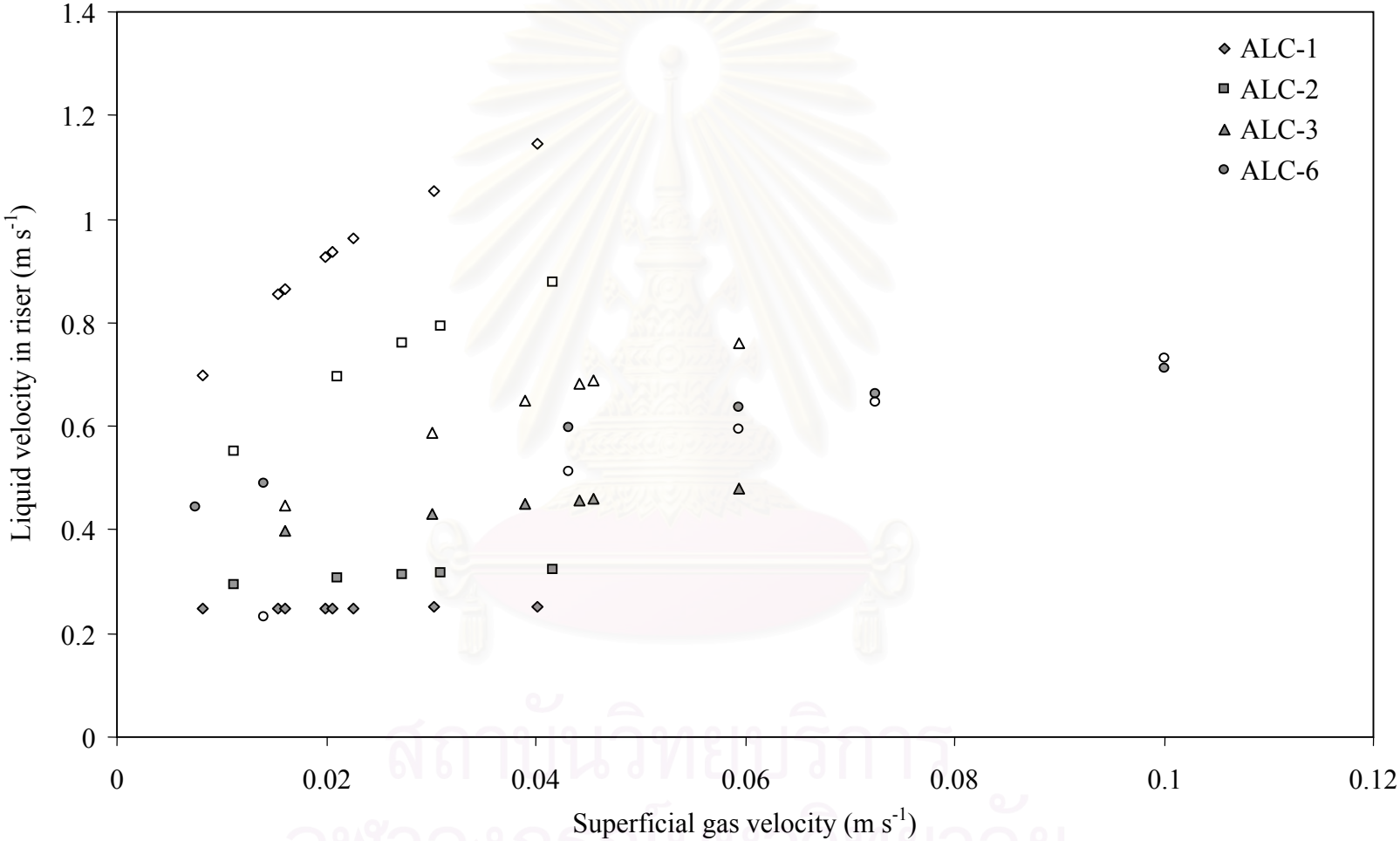

Figure 5.6 Upflow (filled symbols) and downflow (unfilled symbols) liquid velocities in riser of each ALC at various superficial gas velocities

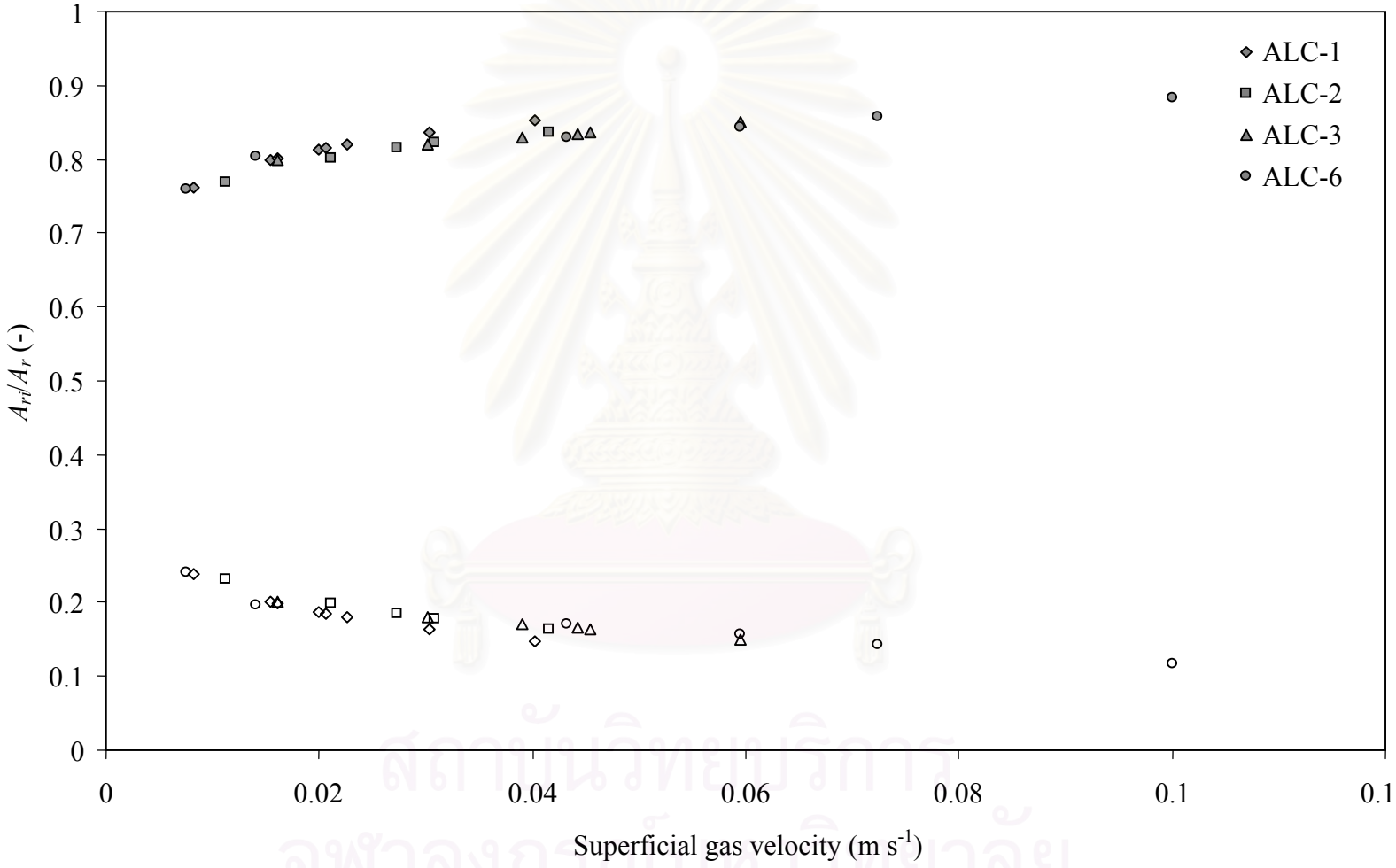

Figure 5.7 Fraction of upflow (filled symbols) and downflow (unfilled symbols) areas in riser of each ALC at various superficial gas velocities

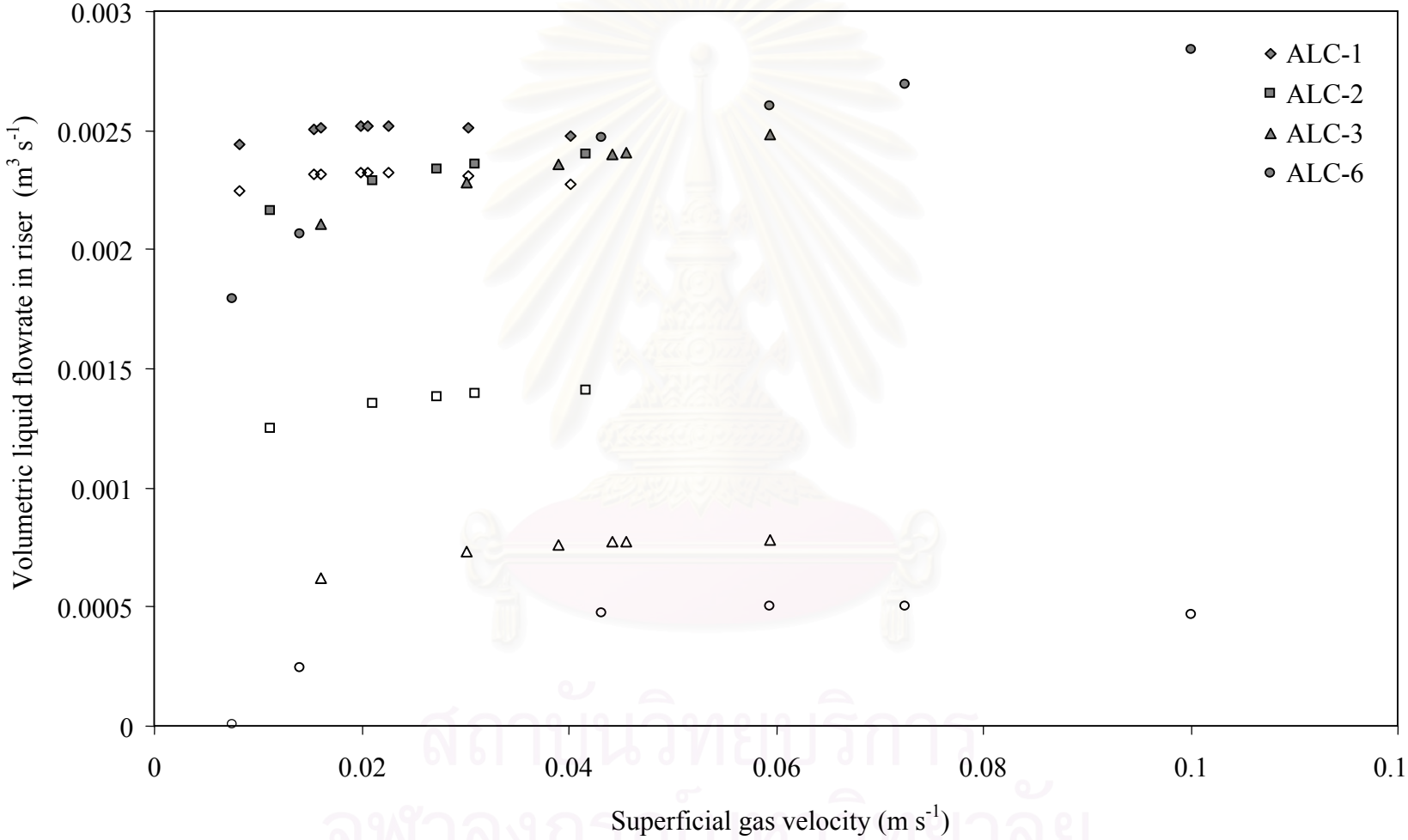

Figure 5.8 Upflow (filled symbols) and downflow (unfilled symbols) liquid flowrate in riser of each ALC at various superficial gas velocities

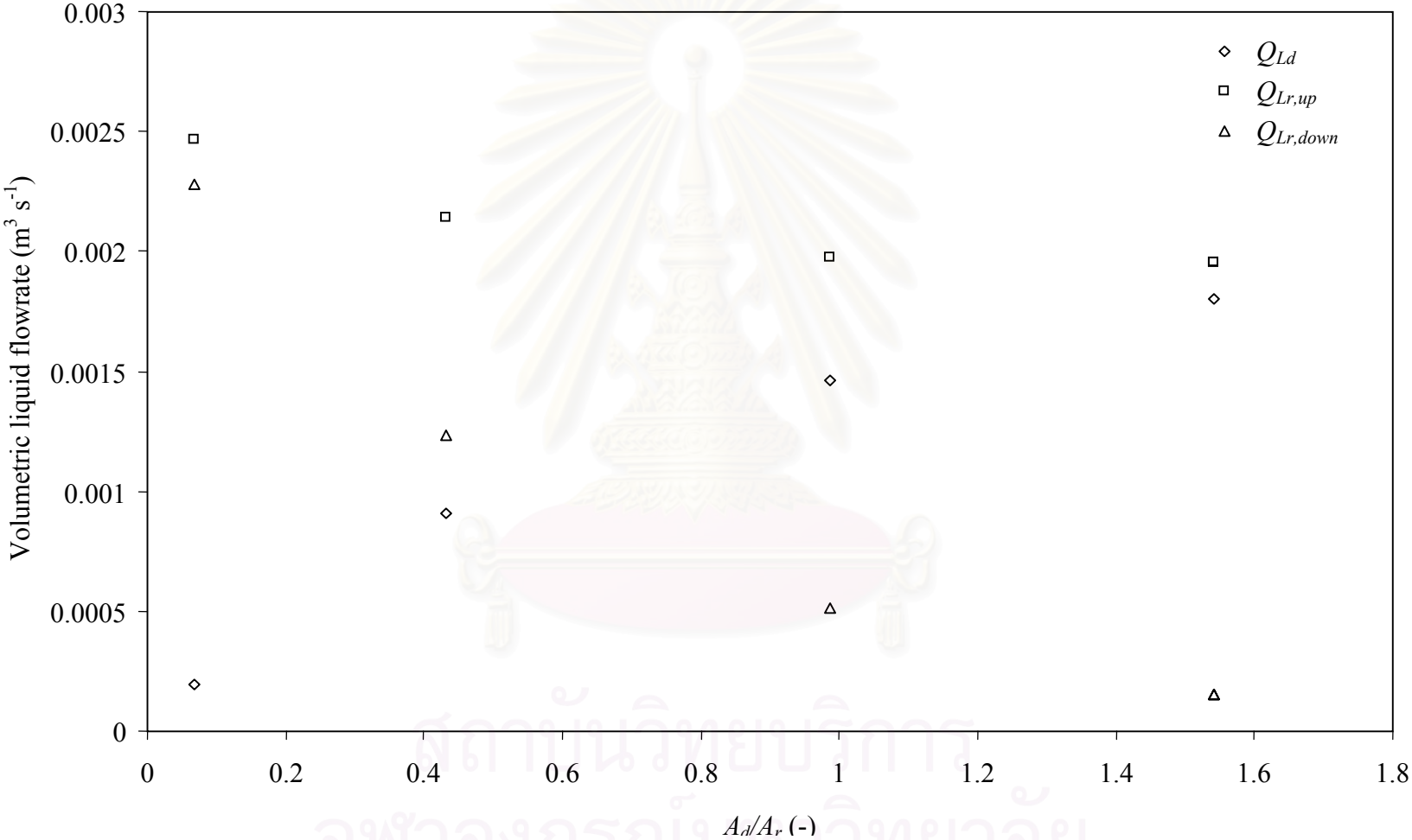

Figure 5.9 Liquid volumetric flow rate in each section at various A_d/A_r

Chapter 6

Mathematical Model for the Prediction of Gas-Liquid Mass Transfer in ALCs

6.1 Backgrounds

One of the most important factors in the operation of airlift contactors (ALCs) is the rate of gas-liquid mass transfer which controls the uptake and removal of low soluble components such as oxygen and carbon dioxide. Extensive effort has been paid to investigate the mass transfer characteristics of ALCs and these were reviewed by Chisti (1998)[1], and Merchuk and Gluz (1999).[2] A number of empirical correlations for estimating mass transfer in terms of the overall mass transfer coefficient (K_La) were available according to various geometrical and operational conditions of the contactor (as summarized in Table 2.1 in Chapter 2). This parameter is important for the construction of mathematical mass transfer model for the ALC as it provides information on the rate at which mass transfer takes place through the gas-liquid interface.

Several mathematical models for mass transfer based on material conservation principals in the ALC have been proposed.[3-9] These models considered the ALC to be composed of several regions for which mixing characteristics were different. For example, Fields and Slater (1983)[10] showed that, in a concentric tube ALC, gas-liquid separator behaved almost like a perfectly mixed model, whereas the riser and downcomer could be represented by axial dispersion models. Similarly, Merchuk and Siegel[11] reported in 1988 that fluid flow in the riser and downcomer in the ALC could be represented with a plug flow model, and a perfectly mixed section for the gas separator. Verlaan (1989)[12] and Merchuk and Yunger (1990)[13] also used a similar model in their work for investigating mixing behavior in ALCs. These mixing characteristic models were then applied to evaluate mass transfer characteristics in ALC. André et al. (1983)[3] used a tank-in-series model for both riser and downcomer to incorporate back-mixing, and the gas separator was considered as a well-mixed region in describing mass transfer in external loop ALC. However, their system was assumed to work with very

low gas throughput so that the circulation of the gas phase in the downcomer did not have to be considered. In the work of Lindert et al. (1992)[4], various different models such as continuous stirred tank reactor (CSTR), plug flow reactor (PFR), axial dispersion models were taken into consideration in the estimate of oxygen transfer coefficient in both annulus sparged internal loop and external loop ALCs. Merchuk et al. (1992)[5] proposed that ALC consists of riser and downcomer in which mixing was represented by axial dispersion model in both liquid and gas phases. The gas separator was represented by a perfectly mixed model. Their model assumed further that each of the hydrodynamic regions of the reactor had a different mass transfer coefficient. Dhaouadi et al. (1997)[6] formulated the model for ALC by considering the reactor to consist of four sections: riser, downcomer, gas-liquid separator, and bottom junction. The liquid flows in riser and downcomer were described by plug flow with axial dispersion models, whereas the remaining two sections as CSTRs. The gas flow in riser was represented as plug flow. A tanks-in-series model was also employed to describe the mass transfer behavior in the ALC.[8] Dhaouadi et al. (2001)[9] proposed the model where gas and liquid flow in riser and downcomer were considered as plug flow but the mixed zones at the separator and the bottom junction were neglected.

These literatures showed that oxygen concentration profiles in ALC could be predicted by mathematical models based on material conservation equations. However, many of these models were simplified by neglecting the mass transfer kinetics between gas and liquid in the various sections of the system especially in downcomer. For this reason, most of these models were valid to the data in systems with low gas fraction in downcomer such as external loop ALCs.

In general, the plug flow with dispersion is best to describe the behavior of liquid and gas flow in riser, whereas the CSTR model is best to describe the behavior of liquid and gas flow in gas-liquid separator. In the downcomer, there are differences between external loop and internal loop ALC. In external loop ALCs, the interaction between gas and liquid in the downcomer may be neglected without interrupting the predicting capability of the model because there exists very little, if not none, amount of gas in this section. However, this situation is unlikely for internal loop ALCs where a large fraction of gas holdup is usually present in the various sections of the system. Mathematical models for the internal loop ALC were usually more complicated and subject to parameter fittings with experimental data.[14] This, by and large, limits the use of the models to some specific experimental ranges.

This work intends to investigate the accuracy of the mass transfer model developed for the internal loop ALC by assuming the ALC to comprise three interconnecting sections where the interactions between gas and liquid in each section is taken into consideration. To ensure the general use of the model, parameter estimations are performed using independent experiments, and in many cases, they are obtained from other independent sources.

6.2 Experiments

To achieve the aim of this section, experimental data on gas holdups, liquid velocities and overall gas-liquid mass transfer coefficient were carried out as detailed in Sections 3.2.2 - 3.2.4, respectively. The ALCs employed for the work in this chapter are ALC-1 and ALC-8 where Table 6.1 shows the operating conditions of these systems.

6.3 Mathematical Model Development

The ALC is assumed to consist of three main sections as shown in a schematic diagram in Figure 6.1. The first section is the 'riser' to which the gas is supplied. A mixture of gas and liquid moves from the riser to 'gas separator' which is located at the top of the contactor. A large fraction of gas bubbles disengages from the system here whilst liquid and the remaining portion of gas move further to the 'downcomer'. In this last section, no gas supply is provided and the fluid content moves downwards and re-enters the riser at the bottom of the column together with the inlet gas. To construct a mathematical model for this system, each part of the ALC is considered separately as illustrated in the right side of Figure 6.1. The riser and downcomer are represented by the dispersion model with the exchange of oxygen between gas and liquid phases in each volume element. No liquid is added or removed from the system, whereas gas enters the system only at the bottom section of the riser and leaves the contactor at the gas separator. The behavior of the gas separator is assumed to be well mixed. Hence, the overall model is represented by a series of various types of reactors, i.e. dispersion-stirred tank-dispersion.

For simplicity, the model is developed by considering the following assumptions:
1. The effect of hydrostatic head on solubility of oxygen is negligible. This is reasonable for small-scale systems.

2. The overall volumetric mass transfer coefficient is uniform for all sections in the contactor.

3. The gas holdup is uniform within each individual region.

4. The system is isothermal.

5. There is no radial effect in the ALC.

6. Oxygen is sparingly soluble in water and Henry's law can be applied to explain the solubility of oxygen in the contactor.

7. The behavior of the gas in the system is ideal.

8. The operating parameters, e.g. gas holdups, liquid circulation flowrate, are not a function of time and space.

Following the continuity equation principal, the following set of equations is obtained.

For gas phase oxygen concentration in the riser and downcomer:

At $0 < z_i < L_i$:

$$\frac{\partial O_{Gi}(z_i,t)}{\partial t} = -v_{Gi}\frac{\partial O_{Gi}(z_i,t)}{\partial z_i} + D_{Gi}\frac{\partial^2 O_{Gi}(z_i,t)}{\partial z_i^2} - \frac{(1-\varepsilon_{Gi})}{\varepsilon_{Gi}}K_L a\left(\frac{O_{Gi}(z_i,t)}{H} - O_{Li}(z_i,t)\right) \tag{6.1}$$

For liquid phase oxygen concentration in the riser and downcomer:

At $0 < z_i < L_i$:

$$\frac{\partial O_{Li}(z_i,t)}{\partial t} = -v_{Li}\frac{\partial O_{Li}(z_i,t)}{\partial z_i} + D_{Li}\frac{\partial^2 O_{Li}(z_i,t)}{\partial z_i^2} + K_L a\left(\frac{O_{Gi}(z_i,t)}{H} - O_{Li}(z_i,t)\right) \tag{6.2}$$

where $i = r$ for *riser* and $i = d$ for *downcomer*, H is the Henry's law constant.

For gas phase oxygen concentration in the gas separator:

$$\frac{dO_{Gt}}{dt} = \frac{\varepsilon_{Gr}A_r v_{Gr}O_{Gr}(z_r = L_r) - \varepsilon_{Gd}A_d v_{Gd}O_{Gd}(z_d = 0) - Q_{G,out}O_{Gt}}{\varepsilon_{Gt}V_t} - \left(\frac{1-\varepsilon_{Gt}}{\varepsilon_{Gt}}\right)K_L a\left(O_{Gt} - HO_{Lt}\right) \tag{6.3}$$

For liquid phase oxygen concentration in the gas separator:

$$\frac{dO_{Lt}}{dt} = \frac{(1-\varepsilon_{Gr})A_r v_{Lr}O_{Lr}(z_r = L_r) - (1-\varepsilon_{Gd})A_d v_{Ld}O_{Ld}(z_d = 0)}{(1-\varepsilon_{Gt})V_t} + K_L a\left(\frac{O_{Gt}}{H} - O_{Lt}\right) \tag{6.4}$$

Boundary and initial conditions for this set of equations are given in Table 6.2, Eqs. (6.5) - (6.16). This set of equations is made dimensionless by introducing the following dimensionless variables:

$$\left.\begin{aligned} \tau &= \frac{t}{\overline{t}} = \frac{tv_{Ld}A_d}{V_r} \\ Z &= \frac{z}{L} \\ \overline{O}_L &= \frac{O_L}{O_L^*} \\ \overline{O}_G &= \frac{O_G}{O_{G,in}} \end{aligned}\right\} \tag{6.17}$$

Substitute Eq. (6.17) into Eqs (6.1) – (6.4) to yield the set of equations of dimensionless variables in Eqs. (6.18) – (6.23).

For gas phase oxygen concentration in the riser:

$$\frac{\partial \overline{O}_{Gr}}{\partial \tau_r} = -\frac{v_{Gr}\overline{t}}{L_r}\frac{\partial \overline{O}_{Gr}}{\partial z_r} + \frac{D_{Gr}\overline{t}}{L_r^2}\frac{\partial^2 \overline{O}_{Gr}}{\partial z_r^2} - \frac{(1-\varepsilon_{Gr})K_L a\overline{t}}{\varepsilon_{Gr}}\left[\overline{O}_{Gr}(Z_r) - \overline{O}_{Lr}(Z_r)\right] \tag{6.18}$$

For liquid phase oxygen concentration in the riser:

$$\frac{\partial \overline{O}_{Lr}}{\partial \tau_r} = -\frac{v_{Lr}\overline{t}}{L_r}\frac{\partial \overline{O}_{Lr}}{\partial z_r} + \frac{D_{Lr}\overline{t}}{L_r^2}\frac{\partial^2 \overline{O}_{Lr}}{\partial z_r^2} - K_L a\overline{t}\left[\overline{O}_{Gr}(Z_r) - \overline{O}_{Lr}(Z_r)\right] \tag{6.19}$$

For gas phase oxygen concentration in the downcomer:

$$\frac{\partial \overline{O}_{Gd}}{\partial \tau_d} = -\frac{v_{Gd}\overline{t}}{L_d}\frac{\partial \overline{O}_{Gd}}{\partial z_d} + \frac{D_{Gd}\overline{t}}{L_d^2}\frac{\partial^2 \overline{O}_{Gd}}{\partial z_d^2} - \frac{(1-\varepsilon_{Gd})K_L a\overline{t}}{\varepsilon_{Gd}}\left[\overline{O}_{Gd}(Z_d) - \overline{O}_{Ld}(Z_d)\right] \tag{6.20}$$

For liquid phase oxygen concentration in the downcomer:

$$\frac{\partial \overline{O}_{Ld}}{\partial \tau_d} = -\frac{v_{Ld}\overline{t}}{L_d}\frac{\partial \overline{O}_{Ld}}{\partial z_d} + \frac{D_{Ld}\overline{t}}{L_d^2}\frac{\partial^2 \overline{O}_{Ld}}{\partial z_d^2} - K_L a\overline{t}\left[\overline{O}_{Gd}(Z_d) - \overline{O}_{Ld}(Z_d)\right] \tag{6.21}$$

For gas phase oxygen concentration in the gas-liquid separator:

$$\frac{d\overline{O}_{Gt}}{d\tau_t} = \frac{\overline{t}Q_{Gr}}{V_t\varepsilon_{Gt}}\overline{O}_{Gr}(Z_r = L_r) - \frac{\overline{t}Q_{G,out}}{V_t\varepsilon_{Gt}}\overline{O}_{Gt} - \frac{\overline{t}Q_{Gd}}{V_t\varepsilon_{Gt}}\overline{O}_{Gt} - \frac{K_L a(1-\varepsilon_{Gt})\overline{t}}{\varepsilon_{Gt}}\left[\overline{O}_{Gt} - \overline{O}_{Lt}\right] \tag{6.22}$$

For liquid phase oxygen concentration in the gas-liquid separator:

$$\frac{d\overline{O}_{Lt}}{d\tau_t} = \frac{\overline{t}Q_{Lr}}{V_t(1-\varepsilon_{Gt})}\overline{O}_{Lr}(Z_r = L_r) - \frac{\overline{t}Q_{L,out}}{V_t(1-\varepsilon_{Gt})}\overline{O}_{Lt} - \frac{\overline{t}Q_{Ld}}{V_t(1-\varepsilon_{Gt})}\overline{O}_{Lt} - K_L a\overline{t}\left[\overline{O}_{Gt} - \overline{O}_{Lt}\right] \tag{6.23}$$

Similarly, Eq. (6.17) were also substituted into initial and boundary condition, Eqs. (6.5) – (6.16), to yield the initial and boundary condition of dimensionless variables, Eqs. (6.24) – (6.35) in Table 6.2.

The resulting dimensionless Eqs. (6.18) and (6.23) are partial differential equations and therefore are discretized using finite difference method. This leads to a set of ordinary

difference equations that can be integrated via the 4th order Runge-Kutta integration method.[18] The number of discretization points is selected as the smallest where no further changes in the simulation results are no longer observed with the increase in the discretization points. The simulation results are verified with experimental findings as explained later on in this chapter.

6.4 Parameter Estimations

The oxygen concentration in liquid phase in internal loop airlift contactor (ALC) was predicted by dispersion model as shown in the previous section. To predict oxygen concentation in liquid phase according to the proposed model, hydrodynamic and mass transfer parameters including gas holdups (ε_G), liquid velocities (v_L), gas velocities (v_G), dispersion coefficients (D) and overall volumetric gas-liquid mass transfer coefficient (K_La) had to be known in a priori. In this work, these parameters were obtained from the reported experiments with similar conditions.

For draft tube sparged ALCs, the reported correlations of Koide et al. (1983a)[17] were used for predicting ε_{Go} and K_La, whereas the correlations of Korpijarvi et al. (1999)[14] were used for predicting ε_{Gr} and ε_{Gd}. Riser superficial liquid velocity (u_{Lr}) was predicted by the correlation of Chisti et al. (1988).[19] These employed correlations for the draft tube sparged ALCs are summarized in Table 6.3, Eqs. (6.36) - (6.40).

The parameters for annulus sparged ALCs could not be obtained from the literature for the range of operating conditions in this work. Hence, experiments had to be conducted to establish necessary empirical correlations for the estimates of gas holdup, liquid velocity, and overall gas-liquid mass transfer coefficient. Details of these experiments are provided in Sections 3.2.2 - 3.2.4, respectively. The resulting correlations are Eqs. (6.41) - (6.45) as reported in Table 6.4.

Other parameters could subsequently be calculated by using the following equations. Firstly, the downcomer liquid velocity (v_{Ld}) was calculated using the continuity equation:

$$v_{Lr} A_r \left(1-\varepsilon_{Gr}\right) = v_{Ld} A_d \left(1-\varepsilon_{Gd}\right) \qquad (6.46)$$

where the riser liquid velocities (v_{Lr}) in draft tube sparged and annulus sparged ALCs were estimated from Eqs. (6.40) and (6.45), respectively. Riser gas velocity (v_{Gr}) was calculated from v_{Lr} and slip velocity in the riser (v_{Sr}) as follows:

$$v_{Gr} = v_{Lr} + v_{Sr} \tag{6.47}$$

In general, v_{Sr} is a function of the terminal rise velocity of a single bubble (u_∞) where the hindering effects from neighboring bubbles in the riser is taken into account. Literature showed that v_{Sr} did not vary much with conditions in the ALC, and it was assumed here to be constant at 0.25 ms^{-1}.[20]

Downcomer gas velocity (v_{Gd}) was, in a similar fashion, calculated using the continuity equation.

$$v_{Gd} = \frac{v_{Gr} A_r \varepsilon_{Gr} - Q_{G,in}}{A_d \varepsilon_{Gd}} \tag{6.48}$$

At this point, axial dispersion coefficients in gas and liquid phases both in riser and downcomer (D_{Gr}, D_{Gd}, D_{Lr}, D_{Ld}) remained still unknown. Liquid phase dispersion coefficients (D_{Lr} and D_{Ld}) were reported by several investigators as shown in Table 6.5. The reported values were assimilated into the model directly without manipulation. Gas phase dispersion coefficients (D_{Gr} and D_{Gd}) were reported[27-28] to be 2 - 5 m^2s^{-1} for the ALC at u_{sg} between 0.01-0.1 ms^{-1}.

Preliminary simulations were conducted to test the sensitivity of the simulation results on the variation in the dispersion coefficients both in liquid and gas phases. The time profiles of the oxygen concentrations from the various simulations with different values of dispersion coefficients in the range reported in the previous paragraph were not significantly different from each other. This indicated that, within the range of dispersion coefficients reported in literature, there was no meaningful difference in the responding time to reach equilibrium concentration. Hence, the values of D_{Lr}, D_{Ld}, D_{Gr}, D_{Gd} used in all simulations were selected arbitrarily as 0.01, 0.01, 3 and 1 m^2s^{-1}, respectively.

6.5 Model Verification

To verify the ability of the model in predicting oxygen mass transfer behavior between gas and liquid phases in the internal loop ALC, the simulation results were compared with experimental data both from this work and elsewhere. Details of all design and operating conditions of the employed experimental works are provided in Table 6.1. Suksoir (2000)[29] performed several numerical analysis, i.e. Crank-Nicholson,

Forward Finite Difference, and the 4th order Runge-Kutta integration method.in solving the mathematical models for ALCs where riser and downcomer were represented by the dispersion model and the gas separator by the stirred tank model. He reported that these several numerical techniques provided similar sets of results indicating that the model predictions were accurate and consistent. The results presented hereafter in this work were limited to those obtained from the 4th order Runge-Kutta integration method.

For annulus sparged ALCs, Eqs. (6.41)-(6.45) were used in estimating the hydrodynamic and mass transfer parameters in the model. Figure 6.2 illustrates the comparisons between the simulation results and experimental data on liquid phase oxygen concentration in the riser (O_{Lr}) in the system at different superficial gas velocities (u_{sg}). In general, both simulation results and experimental data demonstrated that the oxygen concentration profile reached equilibrium concentration more rapidly with increasing u_{sg}. It can be seen that the model produced results with a reasonable accuracy when compared with experimental data for all range of u_{sg} (0.01-0.12 ms^{-1}). The model was further verified by comparing the results at various ratios between downcomer and riser cross sectional areas (A_d/A_r) Both experimental results from the present work and from literature were used in this comparison as demonstrated in Figure 6.3. The oxygen concentration profile was found to reach equilibrium more quickly when A_d/A_r decreased. These results were consistent with the data reported by other researchers.[14,16-17,30] It was found that the model was able to accurately predict the behavior of liquid phase oxygen concentration.

Figure 6.4 depicts the comparison between the simulation results and experimental data on O_{Lr} at different draft tube heights (H_{dt}). The simulation was found to agree well with the reported experiment indicating that H_{dt} had negligible effect on transient oxygen concentration in liquid phase.[16]

To further verify the validity of the model, experimental data in the draft tube sparged ALC presented in this work and those reported by Koide et al. (1983a)[17] were also compared with the simulation results. In this case, Eqs. (6.41)–(6.45) were no longer appropriate due to differences in hydrodynamic and mass transfer behavior in the annulus sparged and draft tube sparged ALCs. These equations were therefore substituted by the reported empirical correlations for the draft tube sparged ALC, Eqs. (6.36)–(6.40). Figures 6.5-6.7 show a comparison between experimental data and simulation results on O_{Lr} in the draft tube sparged ALC at different u_{sg}, A_d/A_r and H_{dt} respectively. The results indicate a good agreement between simulation and experiment.

6.6 Concluding remarks

In brief, the developed model was found to be reasonably accurate in predicting the mass transfer behavior in the internal loop ALC both annulus sparged and draft tube sparged type without the need of parameter fittings. This shows that the ALC can well be represented by a series of mathematical model where the riser and downcomer are represented by the dispersion model and the gas separator by the stirred tank. Experiment verifications of the model with a larger range of design/operating conditions of the ALC are still necessary to ensure the general application of this model.

6.7 References

1. Chisti, M.Y. 1998. Pneumatically agitated bioreactors in industrial and environmental bioprocessing: hydrodynamics. Appl. Mech. Rev. 51: 33-112.
2. Merchuk, J.C., and Gluz, M. 1999. In Bioreactors, airlift reactors; Flickinger, M.C., Drew, S.W., Eds.; Encycolpedia of Bioprocess Technology: Fermentation, Biocatalysis and Bioseparation Vol. 1, Wiley, New York, pp 320-353.
3. André, G., Robinson, C.W., and Young, M.M. 1983. New criteria for application of the well-mixed model to gas-liquid mass transfer studies. Chem. Eng. Sci. 38: 1845-1984.
4. Lindert, M., Kochbeck, B., Prüss, J., Warnecke, H.-J., and Hempel, D.C. 1992. Scale-up of airlift-loop bioreactors based on modeling the oxygen mass transfer. Chem. Eng. Sci. 47: 2281-2286.
5. Merchuk, J.C., Osemberg, G., Siegel, M., and Shacham, M. 1992. A method for evaluation of mass transfer coefficients in the different regions of air lift reactors. Chem. Eng. Sci. 47: 2221-2226.
6. Dhaouadi, H., Poncin, S., Hornut, J.M., Wild, G., Oinas, P., and Korpijarvi, J. 1997. Mass transfer in an external-loop airlift reactor: experiments and modeling. Chem. Eng. Sci. 52: 3909-3917.
7. Choi, K.H. 1999. A mathematical model for unsteady-state oxygen transfer in an external-loop airlift reactor. Korean. Chem. Eng. 16: 441-448.
8. Camarasa, E., Meleiro, L.A.C., Carvalho, E., Domingues, A., Filho, R.M., Wild, G., Poncin, S., Midoux, N., and Bouillard. J. 2001. A complete model for oxidation air-lift reactors. Comp. Chem. Eng. 25: 577-584.

9. Dhaouadi, H., Poncin, S., Midoux, N., and Wild, G. 2001. Gas-liquid mass transfer in an airlift reactor—analytical solution and experimental confirmation. Chem. Eng. Proc. 40: 129-133.
10. Fields, P.R., and Slater, N.K.H. 1983. Tracer disperdion in a laboratory air-lift reactor. Chem. Eng. Sci. 38: 647-653.
11. Merchuk, J.C. and Siegel, M.H. 1988. Air-lift reactors in chemical and biological technology. J. Chem. Tech. Biotechnol. 41: 105-120.
12. Verlaan, P., van Eija, A.M.M., Tramper, J., and van't Riet, K., and Luyben, K.Ch.A.M. 1989. Estimation of axial dispersion in individual sections of an airlift-loop reactor. Chem. Eng. Sci. 44: 1139-1146.
13. Merchuk, J.C., and Yunger, R. 1990. The role of the gas-liquid separator of airlift reactors in the mixing process. Chem. Eng. Sci. 45: 2973-2975.
14. Korpijarvi, J., Oinas, P., and Reunanen, J. 1999. Hydrodynamics and mass transfer in an airlift reactor. Chem. Eng. Sci. 54: 2255-2262.
15. Bello, R. A., Robinson, C. W., and Young, M.M. 1985b. Gas holdup and overall volumetric oxygen transfer coefficient in airlift contactors. Biotech. Bioeng. 27: 369-381.
16. Koide K., Sato, H., and Iwamoto, S.. 1983b. Gas holdup and volumetric liquid-phase mass transfer coefficient in bubble column with draught tube and with gas dispersion into annulus. J. Chem. Eng. Japan 16(5): 407-413.
17. Koide, K., Kurematsu, K., Iwamoto, S., Iwata, Y., and Horibe, K. 1983a. Gas holdup and volumetric liquid-phase mass transfer coefficient in bubble column with draught tube and with gas dispersion into tube. J. Chem. Eng. Japan 16: 413-419.
18. Chapra, S.C., and Canale, R.P. 1998. Numerical methods for engineers with programming and software applications. McGraw-Hill, New York, 3rd Edn.
19. Chisti, M.Y., Halard, B., and Young, M.M. 1988. Liquid circulation in airlift reactors. Chem. Eng. Sci. 43: 451 – 457.
20. Merchuk, J.C. and Stein, Y. 1981. Local holdup and liquid velocity in airlift reactors. AIChE J. 27:377-388.
21. Kochbeck, B., Lindert, M., and Hempel, D.C. 1992. Hydrodynamics and local parameters three-phase-flow in airlift-loop reactors of different scale. Chem. Eng. Sci. 47: 3443-3450.

22. Lu, W.-J., Hwang, S.-J. and Chang, C.-M. 1994. Liquid mixing in two-and three-phase airlift reactors. Chem. Eng. Sci. 49: 1465-1468.
23. Koch beck, B., and Hempel, D.C. 1994. Liquid velocity and dispersion coefficient in an airlift reactor with inverse internal loop. Chem. Eng. Technol. 17: 401-405.
24. Wu, W.-T., and Jong, J.-Z. 1994. Liquid-phase dispersion in an airlift reactor with a net draft tube. Bioproc. Eng. 11: 43-47.
25. Gavrilescu, M., and Tudose, R.Z. 1997. Mixing studies in external-loop airlift reactors. Chem. Eng. J. 66:97-104.
26. Merchuk, J.C., Contreras, A., Garcia, F., and Molina, E. 1998. Studies of mixing in a concentric tube airlift bioreactor with different spargers. Chem. Eng. Sci. 53: 709-719.
27. Mangartz, K.-H., and Pilhofer, T.H. 1981. Interpretation of mass transfer measurements in bubble columns considering dispersion of both phases. Chem. Eng. Sci. 36: 1069-1077.
28. Rüffer, H.M., Wan, L., Lübbert, A., and Schügerl, K. 1994. Interpretation of gas residence time distributions in large airlift tower loop reactors. Bioproc. Eng. 11: 153-159.
29. Suksoir, V. “Transient models for oxygen mass transfer in airlift contactor”. Master Thesis. Graduate School. Chulalongkorn University. 2000.
30. Chisti, M.Y., and Young, M.M. 1987. Airlift reactors: characteristics, applications and design considerations. Chem. Eng. Commun. 60: 195-242.

6.8 Tables and figures

Table 6.1 Design and operating parameters for the experiment reported in literature

Ref. No.	Source	H_{dt} (m)	A_d/A_r (-)	u_{sg} (ms^{-1})	Sparger location
W11	This work	1	0.067	0.01	Annular
W12		1	0.067	0.07	
W13		1	0.067	0.12	
B11	Bello *et al*. (1985)	1.45	0.56	0.01	
K11	Koide *et al*. (1983a)[10]	0.7	0.54	0.01	
K21		1.4	0.54	0.01	
K31		2.1	0.54	0.01	
K41		1.4	1.327	0.01	
W21	This work	1	1	0.023	Draft tube
W22		1	1	0.04	
W23		1	1	0.06	
W24		1	1	0.08	
K51	Koide *et al*. (1983b)	1.4	0.69	0.03	
K61		1.4	1.39	0.03	
K71		1.4	3.31	0.03	
K81		0.7	1.76	0.03	
K91		1.4	1.76	0.03	
K82		0.7	1.76	0.08	
K92		1.4	1.76	0.08	

Table 6.2 Initial and boundary conditions in each section of the ALC

Riser	*I.C.*	Gas	$O_{Gr}\left(0 \le z_r \le L_r, t=0\right)=0$	(6.5)	$\bar{O}_{Gr}\left(0 \le z_r \le 1, \tau=0\right)=0$	(6.24)
	B.C.1		$O_{Gr}\left(z_r=0, t>0\right)$ $=\left(\frac{v_{Gd}A_d O_{Gd}\left(z_r=0,t>0\right)+Q_{G,in}O_{G,in}}{v_{Gr}A_r}\right)$	(6.6)	$\bar{O}_{Gr}\left(Z_r=0,\tau>0\right)$ $=\left(\frac{v_{Gd}A_d \bar{O}_{Gd}\left(Z_r=0,\tau>0\right)Q_{G,in}\bar{O}_{G,in}}{v_{Gr}A_r}\right)$	(6.25)
			$Q_{G,in}$ = inlet gas flowrate (m^3s^{-1})		$Q_{G,in}$ = inlet gas flowrate (m^3s^{-1})	
	B.C.2		$O_{Gr}\left(z_r=L_r, t>0\right)=O_{Gt}\left(t>0\right)$	(6.7)	$\bar{O}_{Gr}\left(Z_r=1,\tau=0\right)=\bar{O}_{Gt}\left(\tau>0\right)$	(6.26)
	I.C.	Liquid	$O_{Lr}\left(0 \le z_r \le L_r, t=0\right)=0$	(6.8)	$\bar{O}_{Lr}\left(0 \le Z_r \le 1,\tau=0\right)=0$	(6.27)
	B.C.1		$O_{Lr}\left(z_r=0, t>0\right)=O_{Ld}\left(z_d=L_d, t>0\right)$	(6.9)	$\bar{O}_{Lr}\left(Z_r=0,\tau>0\right)=\bar{O}_{Ld}\left(Z_d=1,\tau>0\right)$	(6.28)
	B.C.2		$O_{Lr}\left(z_r=L_r, t>0\right)=O_{Lt}\left(t>0\right)$	(6.10)	$\bar{O}_{Lr}\left(Z_r=1,\tau>0\right)=\bar{O}_{Lr}\left(\tau>0\right)$	(6.29)
Downcomer	*I.C.*	Gas	$O_{Gd}\left(0 \le z_d \le L_d, t=0\right)=0$	(6.11)	$\bar{O}_{Gd}\left(0 \le Z_d \le 1,\tau=0\right)=0$	(6.30)
	B.C.		$O_{Gd}\left(z_d=0, t>0\right)=O_{Gt}\left(t>0\right)$	(6.12)	$\bar{O}_{Gd}\left(Z_d=0,\tau>0\right)=\bar{O}_{Gt}\left(\tau>0\right)$	(6.31)
	I.C.	Liquid	$O_{Ld}\left(0 \le z_d \le L_d, t=0\right)=0$	(6.13)	$\bar{O}_{Ld}\left(0 \le Z_d \le 1,\tau=0\right)=0$	(6.32)
	B.C.		$O_{Ld}\left(z_d=0, t>0\right)=O_{Lt}\left(t>0\right)$	(6.14)	$\bar{O}_{Ld}\left(Z_d=0,\tau>0\right)=\bar{O}_{Lt}\left(\tau>0\right)$	(6.33)
Gas-liquid separator	*I.C.*	Gas	$O_{Lt}\left(t=0\right)=0$	(6.15)	$\bar{O}_{Lt}\left(\tau=0\right)=0$	(6.34)
		Liquid	$O_{Gt}\left(t=0\right)=0$	(6.16)	$\bar{O}_{Gt}\left(\tau=0\right)=0$	(6.35)

**I.C.*—Initial Condition, *B.C.*—Boundary Condition

Table 6.3 Empirical correlations used for predicting hydrodynamic and mass transfer behaviors in draft tube sparged ALCs

Correlation		References
$\frac{\varepsilon_{Go}}{(1-\varepsilon_{Go})^4} = 0.124\left(\frac{u_{sg}\mu_L}{\sigma_L}\right)^{0.966}\left(\frac{\rho_L\sigma_L^3}{g\mu_L^4}\right)^{0.294}\left(\frac{D_i}{D_o}\right)^{0.114}$ for water-air system	(6.36)	Koide *et al*. (1983a)[10]
$\frac{k_L a D_o^2}{D_{O_2}} = 0.477\left(\frac{\mu_L}{\rho_L D_{O_2}}\right)^{0.5}\left(\frac{gD_o^2\rho_L}{\sigma_L}\right)^{0.873}\left(\frac{gD_o^3\rho_L^2}{\mu_L^2}\right)^{0.257}\left(\frac{D_i}{D_o}\right)^{-0.542}\varepsilon_{Go}^{1.36}$	(6.37)	
$\left.\begin{aligned}\varepsilon_{Gr} &= 0.67u_{sg}^{0.57} \quad \text{for } A_d/A_r = 0.59\\ \varepsilon_{Gr} &= 0.85u_{sg}^{0.66} \quad \text{for } A_d/A_r = 1.22\\ \varepsilon_{Gr} &= 0.77u_{sg}^{0.66} \quad \text{for } A_d/A_r = 2.70\\ \varepsilon_{Gr} &= 0.65u_{sg}^{0.78} \quad \text{for } A_d/A_r = 7.14\end{aligned}\right\}$	(6.38)	Korpijarvi *et al*. (1999)[8]
$\varepsilon_{Gd} = 0.84\varepsilon_{Gr}$	(6.39)	
$v_{Lr}(1-\varepsilon_{Gr}) = \left(\frac{2gH_D(\varepsilon_{Gr}-\varepsilon_{Gd})(1-\varepsilon_{Gd})^2}{11.402(A_d/A_b)^{0.789}(A_r/A_d)^2}\right)^{0.5}$	(6.40)	Chisti *et al*. (1988)[11]

Table 6.4 Empirical correlations used for predicting hydrodynamic and mass transfer behaviors in annulus sparged ALCs

Correlation	
$K_L a = 0.288\left(A_d / A_r\right)^{-0.17} u_{sg}^{0.74}$	(6.41)
$\varepsilon_{Go} = 1.267\left(A_d / A_r\right)^{-0.25} u_{sg}^{0.93}$	(6.42)
$\varepsilon_{Gr} = 1.306\left(A_d / A_r\right)^{-0.21} u_{sg}^{0.92}$	(6.43)
$\varepsilon_{Gd} = 0.865\varepsilon_{Gr} - 0.0038$	(6.44)
$v_{Lr} = 0.241 + 0.604\left(A_d / A_r\right)^{1.142} u_{sg}^{0.324}$	(6.45)

Table 6.5 Dispersion coefficients reported in literatures for ALC

Authors	D_L (m^2/s)	Range of u_{sg} (ms^{-1})	Reactor
Verlaan (1989)[12]	0.01-0.12	0.01-0.14	External loop ALC
Kochbek et al. (1992)[21]	0.01-0.08	0.01-0.08	
Lu and Hwang (1994)[22]	0.006-0.033	0.007-0.15	Internal loop ALC
Kochbeck and Hempel (1994)[23]	0.004-0.016	0.01-0.07	Internal loop ALC
Wu and Jong (1994)[24]	0.005-0.08	0-0.07	Internal loop ALC
Gavrilescu and Tudose (1997) [25]	0.001-0.08	0.01-0.2 (lab scale)	External loop ALC
	0.001-0.25	0.01-0.12 (pilot scale)	
Merchuk et al. (1998)[26]	0.01-0.1	< 0.2	Internal loop ALC

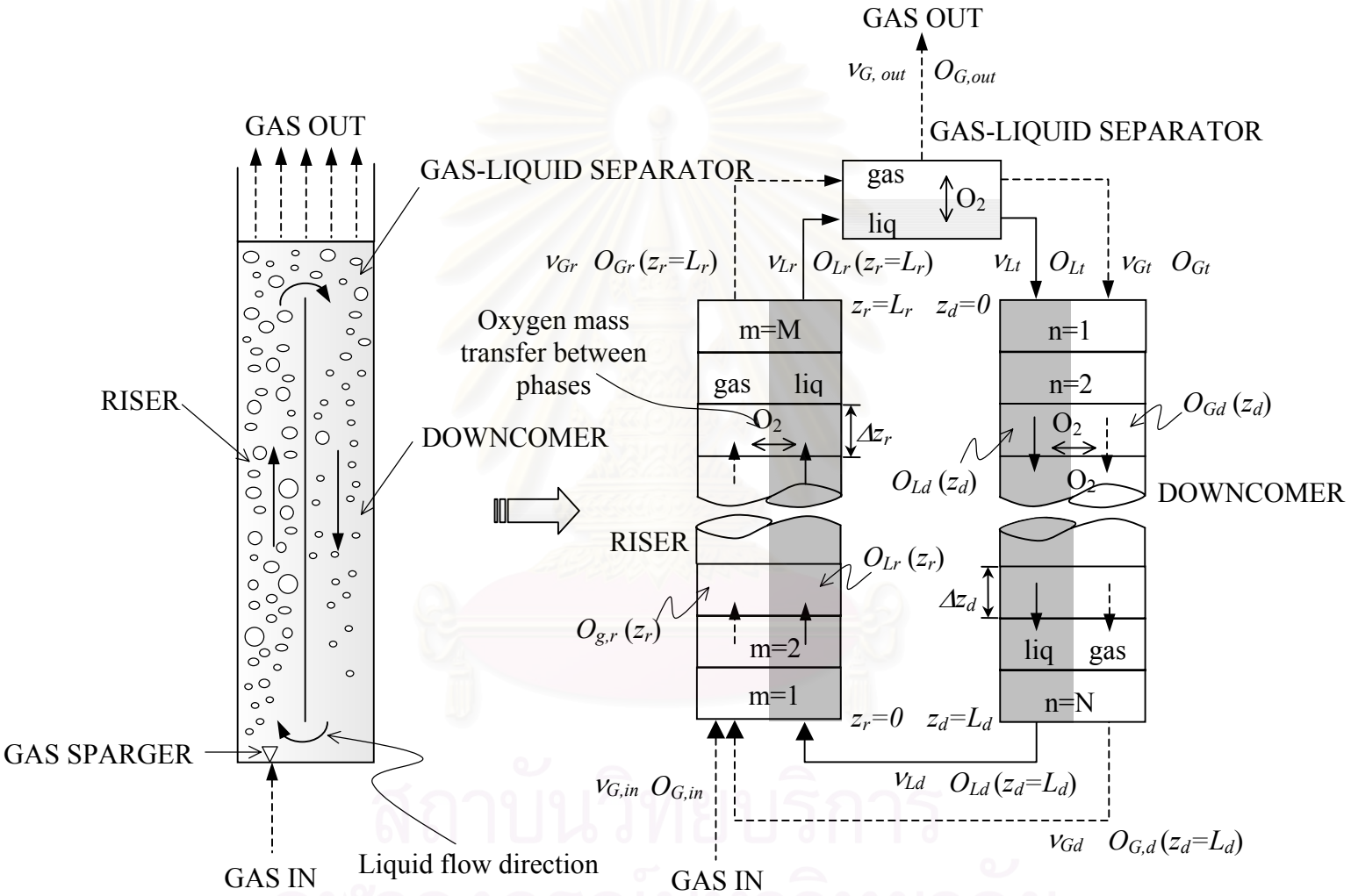

Figure 6.1 Block flow representation of the internal loop ALC.

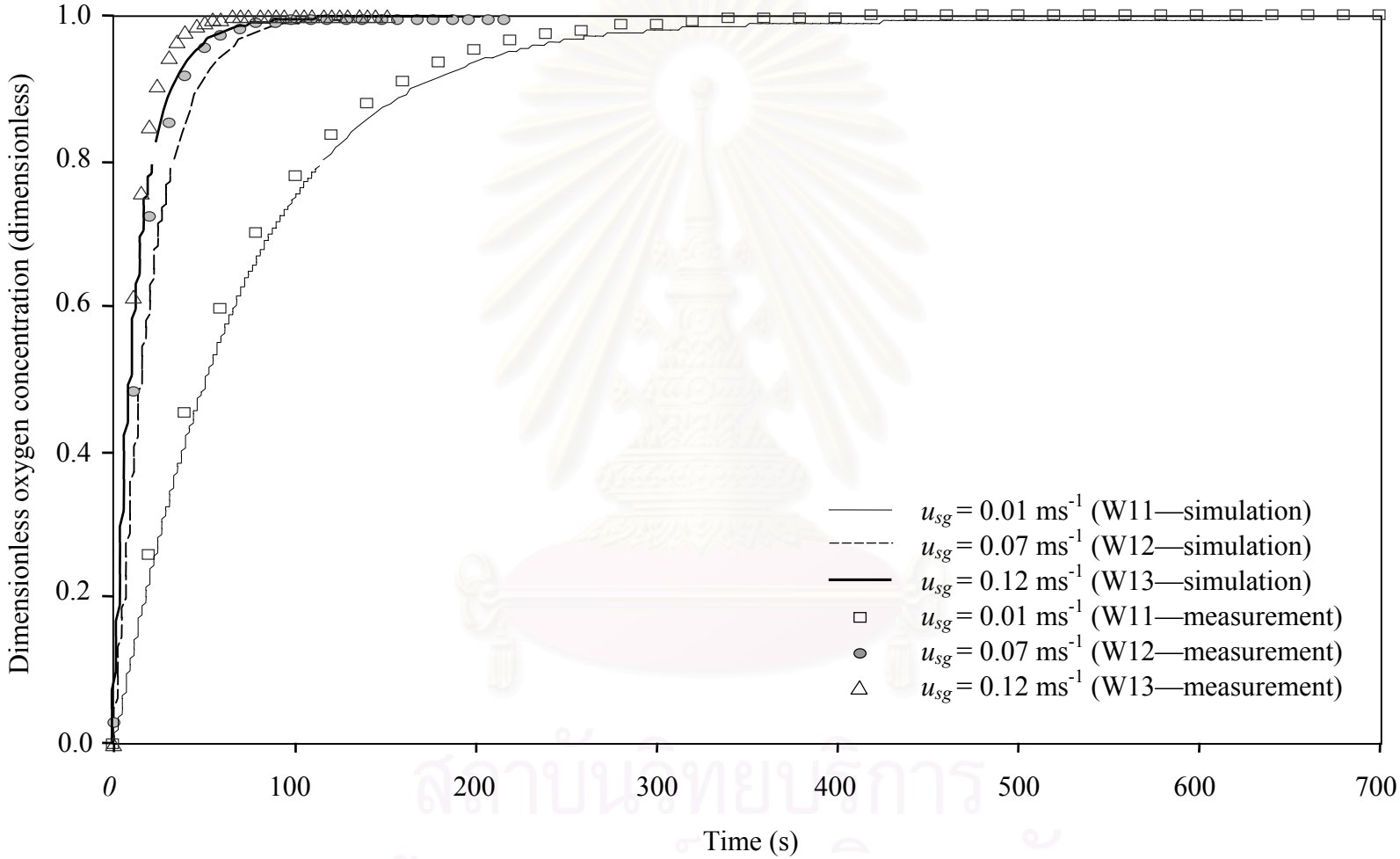

Figure 6.2 Comparison between simulation results and measurement of time profiles of O_{Lr} in annulus sparged ALCs: Effect of u_{sg}

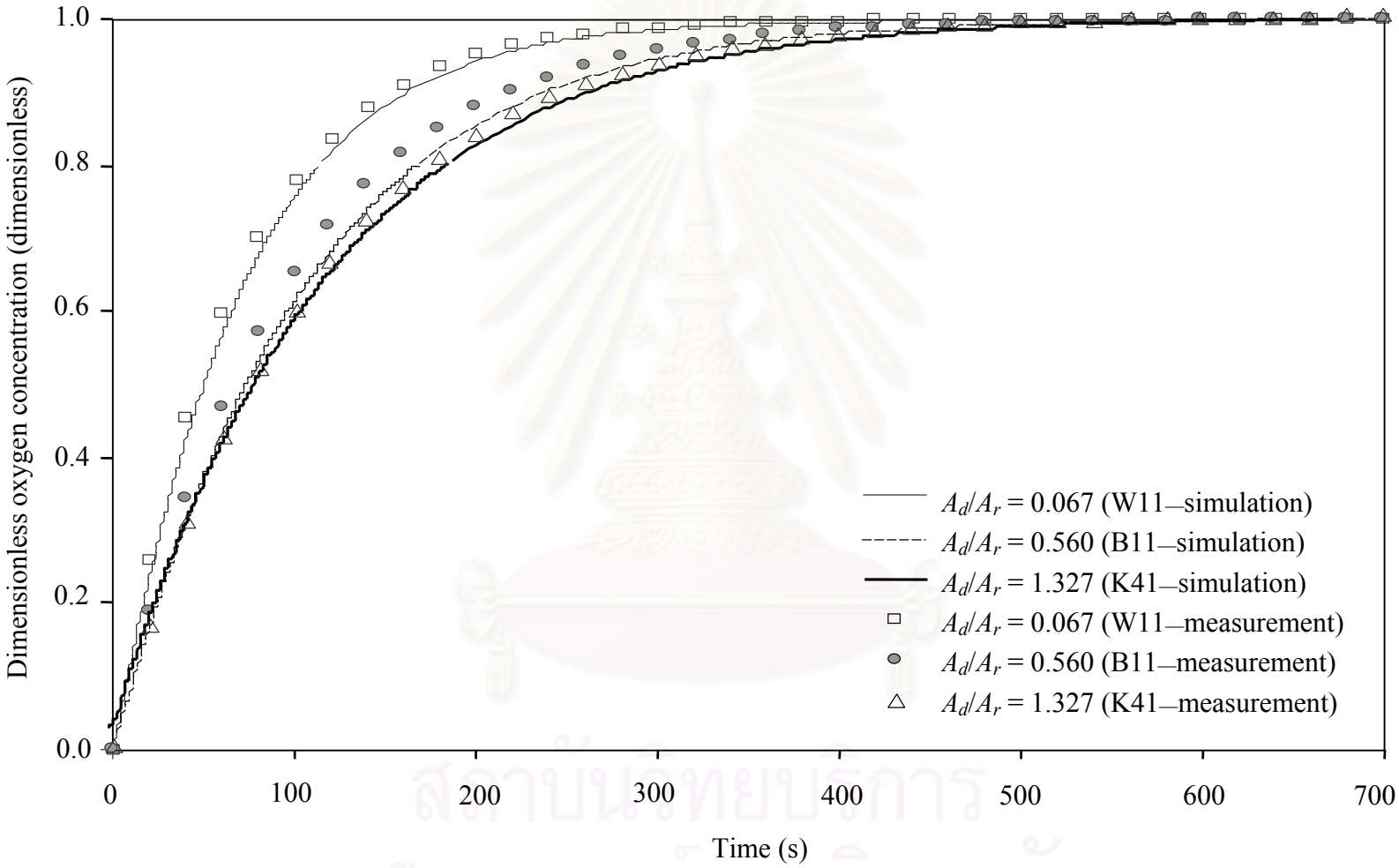

Figure 6.3 Comparison between simulation results and measurement of time profiles of O_{Lr} in annulus sparged ALCs: Effect of A_d/A_r

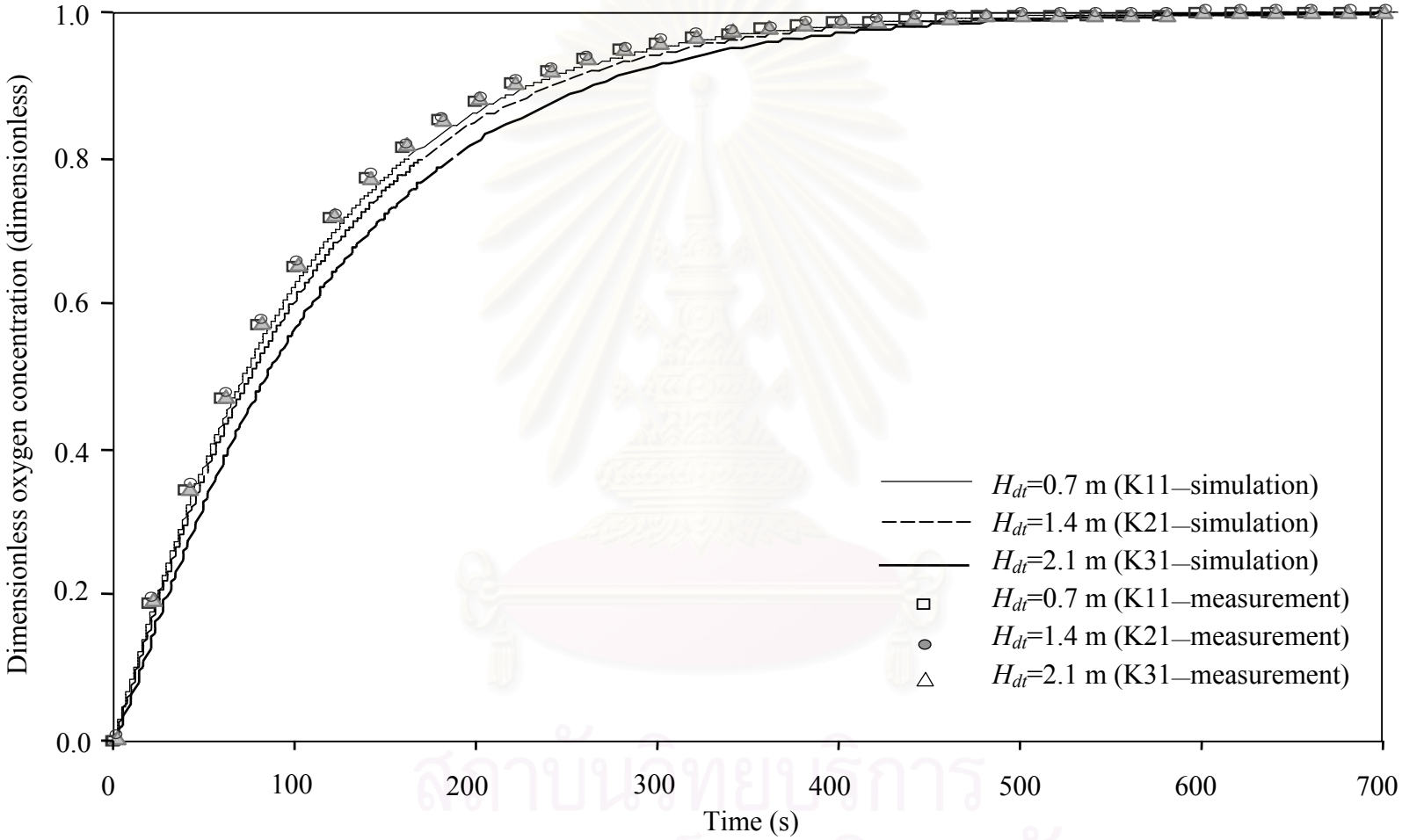

Figure 6.4 Comparison between simulation results and measurement of time profiles of O_{Lr} in annulus sparged ALCs: Effect of H_{dt}

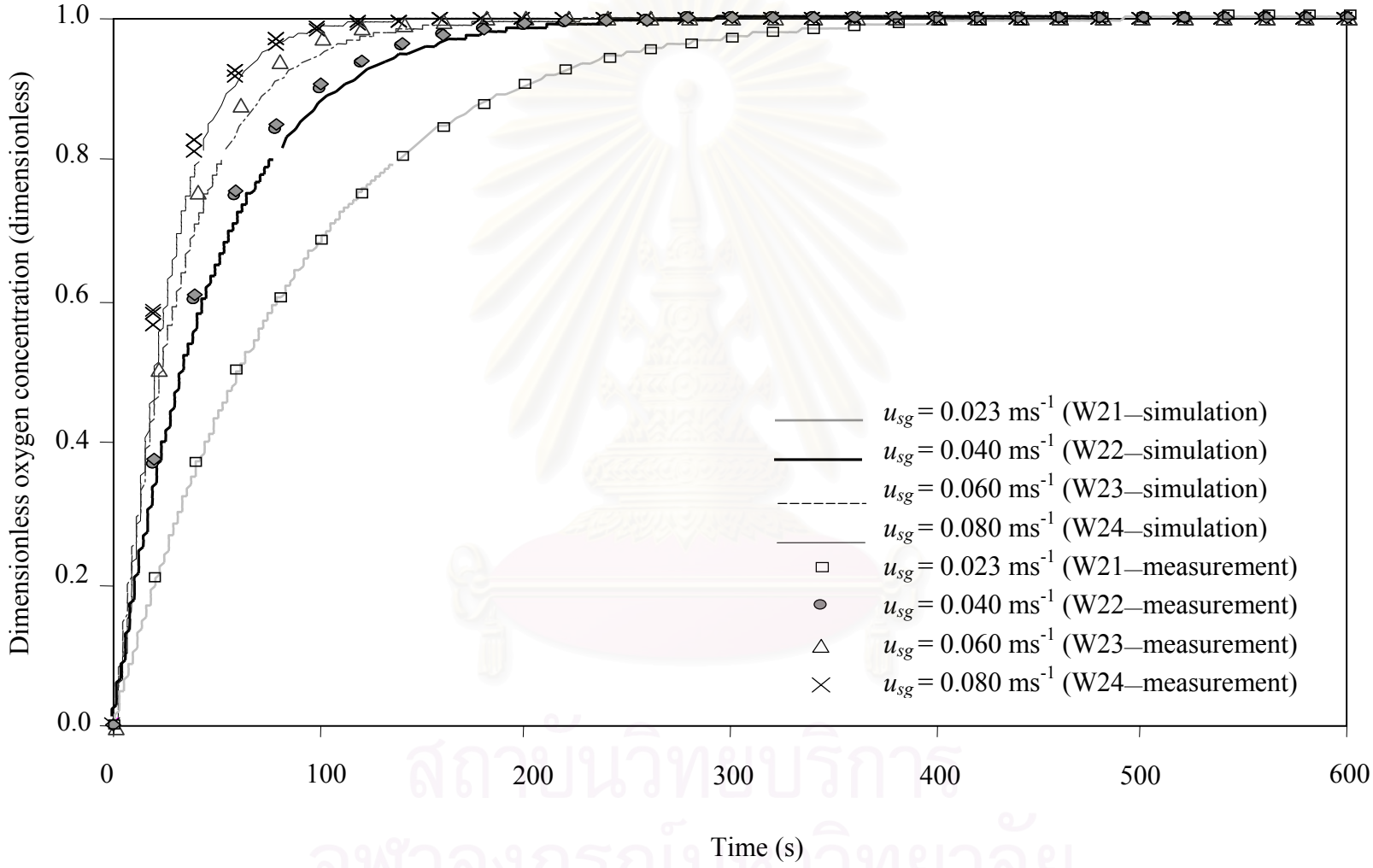

Figure 6.5 Comparison between simulation results and measurement of time profiles of O_{Lr} in draft tube sparged ALCs: Effect of u_{sg}

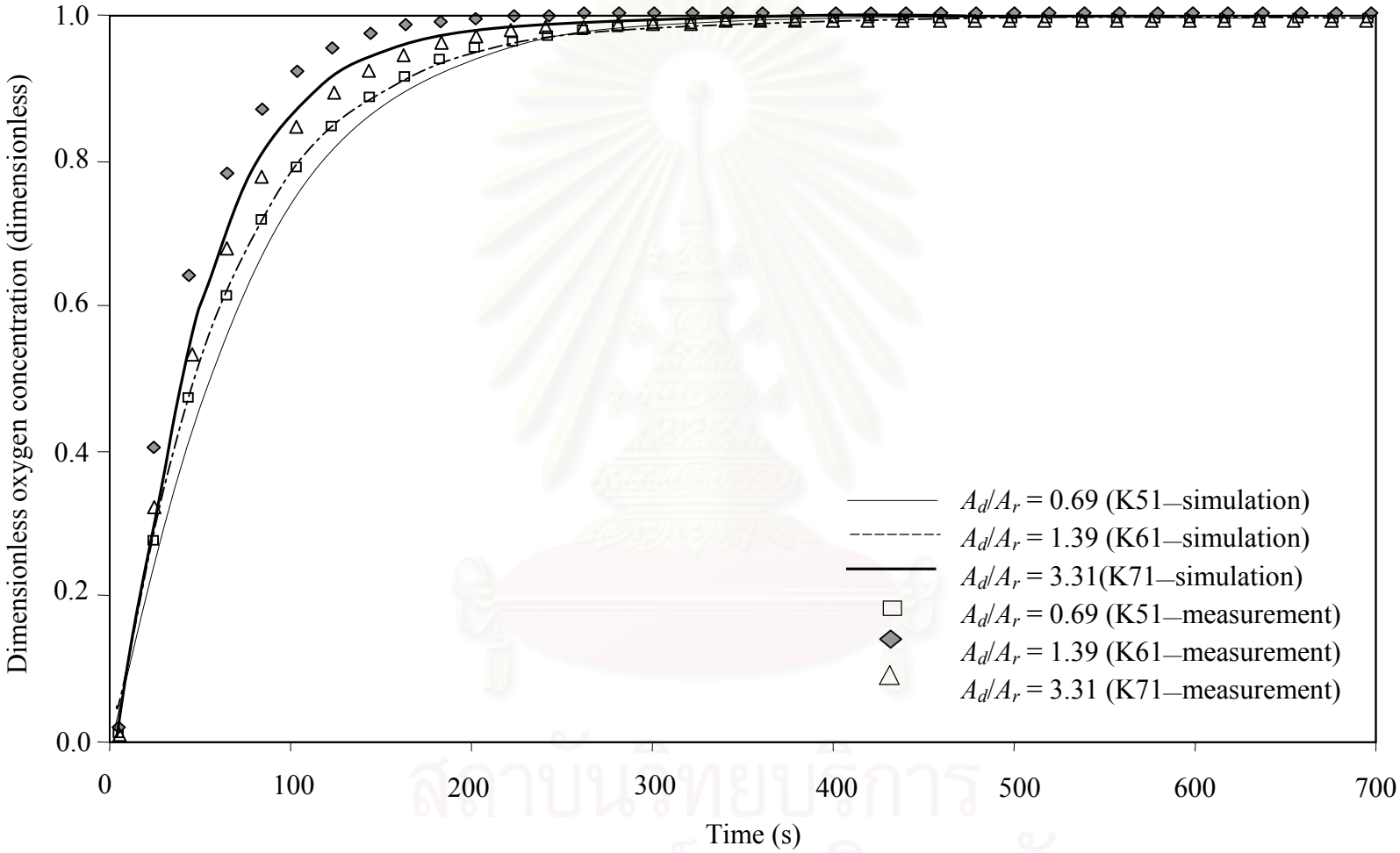

Figure 6.6 Comparison between simulation results and measurement of time profiles of O_{Lr} in draft tube sparged ALCs: Effect of A_d/A_r

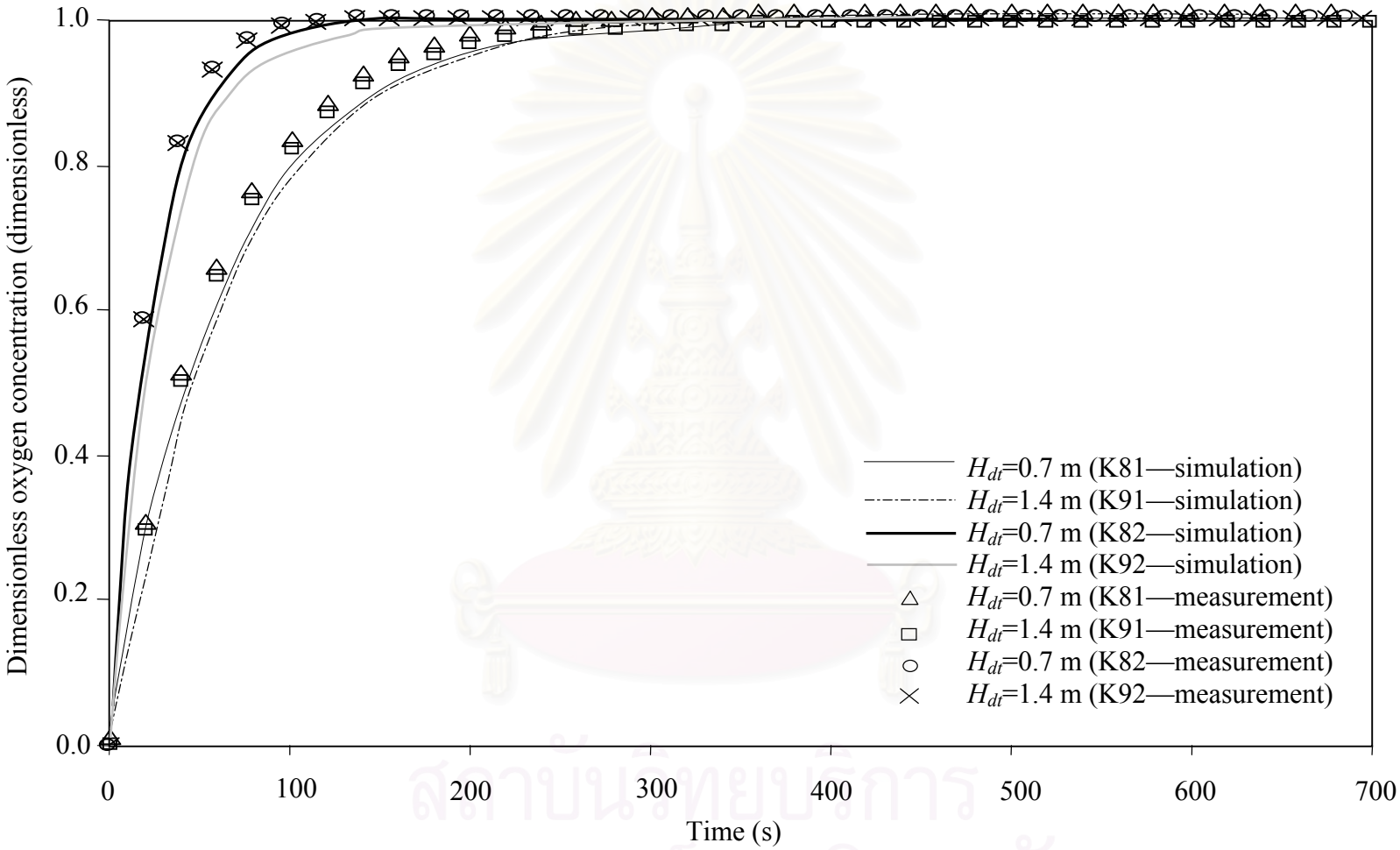

Figure 6.7 Comparison between simulation results and measurement of time profiles of O_{Lr} in draft tube sparged ALCs: Effect of H_{dt}

Chapter 7

Conclusions

7.1 Achievements

The major achievements obtained from this work include:

(i) Operational and geometrical parameters including superficial gas velocity, ratio between cross-sectional areas of downcomer and riser, and sparger design had a significant role on bubble size distribution in the ALC. These parameters in turn affected the gas-liquid mass transfer rate in the system.

Increasing gas velocity in the airlift contactor considerably reduced the size of bubble and shifted the distribution of bubble size from the normal to log-normal types. Bubble size was found to decrease along the axial distance in the riser of the ALC. An increase in the ratio between cross-sectional areas of downcomer and riser resulted in a decrease in bubble size at high superficial gas velocity. Spargers with a large number of orifices led to a larger bubble size in the system whereas a comparatively broad bubble size distribution was caused by employing a gas sparger with small number of orifices.

The analysis on the gas-liquid mass transfer rate revealed that the mass transfer coefficient did not vary considerably with conditions employed in this work but rather remained constant at approximate 0.0004 ms^{-1}. The specific interfacial area played a more significant role in controlling the overall rate of mass transfer in the system. Hence, the conditions with a small bubble size became more favorable in terms of high gas-liquid mass transfer rate as they provided a higher mass transfer area per unit volume of gas input.

(ii) At certain operating conditions, there existed an inequality of liquid flowrate in riser and downcomer. This was caused by the existing of internal liquid circulation in riser of ALC. The proportion of this type of liquid circulation in riser could be determined using the mathematical model constructed based on principals of material and energy conservations. The model required knowledge

of the gas holdups and the liquid velocities. The magnitude of this internal liquid circulation was affected principally by the operating parameter (u_{sg}) and geometrical parameter (A_d/A_r) in the system.

(iii) Gas-liquid oxygen mass transfer could be successfully described by a mathematical model based on principals of material conservation. It has been shown that the ALC could well be described by a set of simple continuity equations where each part of the ALC could be represented by a fundamental reactor. The riser and downcomer were described by dispersion model. The gas-liquid separator was represented by perfectly mixed model. The model was fulfilled with empirical equation for the prediction of hydrodynamic parameters. The simulation results agreed well with experimental data over a wide range of design and operating conditions.

7.2 Contributions

This work contributes significantly to the basic knowledge on the behavior of ALC. Firstly, apart from the liquid velocity and gas holdup, the work shows that there are still other important parameters that could be controlled to adjust the behavior of the system. One of the most obvious parameters is the bubble size distribution where it was illustrated that this could be manipulated within a certain range. For example, adjusting the sparger design or the size of riser might result in a smaller bubble size. The ability to adjust this parameter will be useful particularly in the situation where the mass transfer rate between gas and liquid phases is important. Internal liquid circulation was also found in this work to exist and it is possible that this parameter be adjustable variable. This finding might be the key to explain various findings in the literature especially the inconsistency between theory and experimental. In addition, the knowledge is highly significant as it indicates that the conventional measurement for liquid velocity should be modified to include the effect of internal liquid circulation.

Apart from the experimental part, this work also contributes greatly to the development of a mathematical model for the ALC. Although this model contains no fitting parameters, the model performance is highly satisfactory as the simulation results were found to agree well with experimental data over a wide range of operating conditions. Within the scope of this work, the model shows its capability in describing the behavior of both annulus sparged and draft tube sparged ALCs.

Overall, this work is considered a successful initial step in the attempt to explain various phenomena that take place in the ALC. In terms of research work, it provides starting points and directions for which future research should be conducted, and in application aspect, it gives basic fundamentals essential for the manipulation of the system performance.

7.3 Recommendations for future research

There are still several points in this research that need further refinement. One of the obvious aspects that should be seriously investigated is the modification of the mathematical model. Although the mathematical model developed in Chapter 6 could satisfactorily predict the behavior of the ALC, it still has not incorporated several mass transfer/transport phenomena taken place in the system. For instance, the internal liquid circulation in the riser as reported in Chapter 5 have not yet been taken into consideration. In addition, the effect of bubble size distribution on the performance of the system as indicated in Chapter 4 should also be considered in the development of the mathematical model. Due to the time limitation, this rectification has not yet been achieved successfully but the author strongly believes that this will significantly improve the quality of the prediction.

The other aspect that needs a prompt attention is on the scale up of this system. Dimensional analysis should be evaluated for this system which would be beneficial for the future development of a large scale ALC. This knowledge will contribute greatly to the fundamental understanding of the system which is important in the implementation of the ALC to the desired applications.

APPENDICES

Appendix A

Program source codes

This appendix presents all of the main programs used in this work. The program was written in MATLAB (VERSION 6.1)

```
#-----------------------------------------------------
%File Name:DISPERSION MODEL
%Programe PFR with or without Dispersion term in RISER
and DOWNCOMER
%ALC-1
#-----------------------------------------------------
clear

%Geometrical parameters
%Column and draft tube dimensions
D1=input('Enter inside diameter of draft tube (m) = ');
D2=input('Enter outside diameter of draft tube (m) =
');
D3=input('Enter inside diameter of outer column (m) =
');
D4=input('Enter inside diameter of gas-liquid separator
(m) = ');

%Cross-sectional area of riser (A1)
A1=(pi/4)*(D3^2-D2^2);
%Cross-sectional area of gas-liquid separator (A2)
A2=(pi/4)*(D4^2);
%Cross-sectional area of downcomer (A3)
A3=(pi/4)*(D1^2);
%Ad/Ar
ratio=A3/A1;

%Draft tube height (H1)
H1=input('Enter height of draft tube (m) = ');

%Operational parameters
%Superficial gas velocity (m/s)
usg=input('Enter inlet superficial gas velocity
(m/s)=');
Qg_in=usg*A1;

H3=input('Enter unaerated liquid height (m) = ');

%e0=input('enter overall gas holdup (-) = ');
e0=1.267*ratio^-0.25*usg^0.93;
Hd=H3/(1-e0);
H2=Hd-H1;

%Volume of riser (V1), gas-liquid separator (V2) and
downcomer (V3)
V1=A1*H1;
V2=A2*H2;
V3=A3*H1;

e1=1.306*ratio^-0.21*usg^0.92;
%e1=input('enter gas holdup in the riser (-) = ');
e2=e1;
%e3=input('enter gas holdup in downcomer (-)= ');
e3=0.865*e1-0.0038;

kla_riser=0.288*ratio^-0.17*usg^0.74;
%kla_riser=input('enter kla in riser (1/s) = ');
%kla_downcomer=input('enter kla in downcomer (1/s) =
');
%kla_top=input('enter kla in gas-liquid separator (1/s)
= ');
kla_downcomer=kla_riser;
kla_top=kla_riser;

d_bubble=0.05;
%x=2.14*s_tension/(denst*d_bubble)+(0.505*10*d_bubble);
%ub_terminal=sqrt(x);
%v_slip=ub_terminal*(1-e1)^0.702
%v_slip=input('enter slip velocity, m/s = ');
v_slip=0.25;

vl_riser=0.241+0.604*ratio^1.142*usg^0.324;
```

```
%vl_riser=input('enter riser liquid velocity (ms/) =
');
vl_downcomer=vl_riser*A1*(1-e1)/A3/(1-e3);
vg_riser=vl_riser+v_slip;
vg_downcomer=(vg_riser*A1*e1-Qg_in)/(A3*e3);

t_factor=V1/(A3*vl_downcomer);
z_factor=H1;

m=input('enter number of interval(Dispersion model) in
riser, m = ');
n=input('enter number of interval(Dispersion model) in
downcomer, n = ');
%m=4;
%n=4;
del_z1=H1/m;
del_z2=H1/n;

%disp1=3;
%disp2=0.01;
%disp3=1;
%disp4=0.01;

%disp2=0.007563*ul_riser^0.19*ratio^-(0.93+0.23*log
(ul_riser))
disp1=input('gas phase dispersion coefficient in riser
of the contactor, Dgr = ');
disp2=input('liquid phase dispersion coefficient in
riser of the contactor, Dlr = ');
disp3=input('gas phase dispersion coefficient in
downcomer of the contactor, Dgd = ');
disp4=input('liquid phase dispersion coefficient in
downcomer of the contactor, Dld = ');

Henry=35.4;

%COEFICIENT OF RISER(Dispersion)
%GAS PHASE COEFICIENT
beta1=-vg_riser*t_factor/z_factor;
BETA1=beta1/del_z1;
BETA_1=beta1/2/del_z1;
alpha1=disp1*t_factor/z_factor^2;
ALPHA1=alpha1/del_z1^2;
gamma1=-(1-e1)*kla_riser*t_factor/e1/Henry;

%LIQUID PHASE COEFICIENT
coef1=-vl_riser*t_factor/z_factor;
COEF1=coef1/del_z1;
COEF_1=coef1/2/del_z1;
coef2=disp2*t_factor/z_factor^2;
COEF2=coef2/del_z1^2;
coef3=kla_riser*t_factor;

%COEFICIENT OF DOWNCOMER(Dispersion)
%GAS PHASE COEFICIENT
beta3=-vg_downcomer*t_factor/z_factor;
BETA3=beta3/del_z2;
BETA_3=beta3/2/del_z2;
alpha3=disp3*t_factor/z_factor^2;
ALPHA3=alpha3/del_z2^2;
gamma3=-(1-e3)*kla_downcomer*t_factor/e3/Henry;

%LIQUID PHASE COEFICIENT
coef7=-vl_downcomer*t_factor/z_factor;
COEF7=coef7/del_z2;
COEF_7=coef7/2/del_z2;
coef8=disp4*t_factor/z_factor^2;
COEF8=coef8/del_z2^2;
coef9=kla_downcomer*t_factor;

%COEFICIENT OF GAS SEPARATOR(CSTR)
%GAS PHASE COEFICIENT
```

```
%Input from riser
alpha2=e1*A1*vg_riser*t_factor/(e2*V2);
%Output to downcomer
beta2=-vg_downcomer*A3*e3*t_factor/(e2*V2);
%Output by mass transfer
gamma2=-(1-e2)*kla_top*t_factor/e2/Henry;
%Output to atm
ceta2=-Qg_in*t_factor/(e2*V2);

%LIQUID PHASE COEFICIENT
coef4=(1-e1)*A1*vl_riser*t_factor/(1-e2)/V2;
coef5=-vl_downcomer*A3*(1-e3)*t_factor/(1-e2)/V2;
coef6=kla_top*t_factor;

%SET UP INITIAL AND BOUNDARY CONDITIONS
for j=1:1:m
Og_riser(1,j)=0;
Ol_riser(1,j)=0;
end

Og_top(1)=0;
Ol_top(1)=0;

for j=1:1:n
Og_downcomer(1,j)=0;
Ol_downcomer(1,j)=0;
end

%SOLVE FOR OXYGEN RESPONSE
%Programe Beginning

%FIND OXYGEN CONCENTRATION WITH TIME

%del_t1=0.001;
%del_t2=0.002;

del_t1=input('enter step size at the 1st period of time
= ');
del_t2=input('enter step size at the 2nd period of time
= ');

z=1;
k=1;
c1=1;
c2=1;

while Ol_riser(1,m)<0.9999;

   if Ol_riser(1,m)<0.8;
      h=del_t1;
      c1=z;
   else
      h=del_t2;
      c2=z;
      end

%Runge Kutta
%SET UP k l m n o p

      k11(1)=BETA1*(Og_riser(1,2)-Og_riser(1,1));
      k12(1)=ALPHA1*(Og_riser(1,3)-2*Og_riser
(1,2)+Og_riser(1,1));
      k13(1)=gamma1*(Og_riser(1,1)-Ol_riser(1,1));
      k1(1)=h*(k11(1)+k12(1)+k13(1));

      k11(2)=BETA_1*(Og_riser(1,3)-Og_riser(1,1));
      k12(2)=ALPHA1*(Og_riser(1,3)-2*Og_riser
(1,2)+Og_riser(1,1));
      k13(2)=gamma1*(Og_riser(1,2)-Ol_riser(1,2));
      k1(2)=h*(k11(2)+k12(2)+k13(2));

   for j=3:1:m-2
```

```
      k11(j)=BETA1*(-Og_riser(1,j+2)+8*Og_riser(1,j+1)-
8*Og_riser(1,j-1)+Og_riser(1,j-2))/12;
      k12(j)=ALPHA1*(-Og_riser(1,j+2)+16*Og_riser
(1,j+1)-30*Og_riser(1,j)+16*Og_riser(1,j-1)-Og_riser
(1,j-2))/12;
      k13(j)=gamma1*(Og_riser(1,j)-Ol_riser(1,j));
      k1(j)=h*(k11(j)+k12(j)+k13(j));
   end

      k11(m-1)=BETA_1*(Og_riser(1,m)-Og_riser(1,m-2));
      k12(m-1)=ALPHA1*(Og_riser(1,m)-2*Og_riser(1,m-
1)+Og_riser(1,m-2));
      k13(m-1)=gamma1*(Og_riser(1,m-1)-Ol_riser(1,m-
1));
      k1(m-1)=h*(k11(m-1)+k12(m-1)+k13(m-1));

      k11(m)=BETA1*(Og_riser(1,m)-Og_riser(1,m-1));
      k12(m)=ALPHA1*(Og_riser(1,m)-2*Og_riser(1,m-
1)+Og_riser(1,m-2));
      k13(m)=gamma1*(Og_riser(1,m)-Ol_riser(1,m));
      k1(m)=h*(k11(m)+k12(m)+k13(m));

      l11(1)=COEF1*(Ol_riser(1,2)-Ol_riser(1,1));
      l12(1)=COEF2*(Ol_riser(1,3)-2*Ol_riser
(1,2)+Ol_riser(1,1));
      l13(1)=coef3*(Og_riser(1,1)-Ol_riser(1,1));
      l1(1)=h*(l11(1)+l12(1)+l13(1));

      l11(2)=COEF_1*(Ol_riser(1,3)-Ol_riser(1,1));
      l12(2)=COEF2*(Ol_riser(1,3)-2*Ol_riser
(1,2)+Ol_riser(1,1));
      l13(2)=coef3*(Og_riser(1,2)-Ol_riser(1,2));
      l1(2)=h*(l11(2)+l12(2)+l13(2));

   for j=3:1:m-2
```

```
      l11(j)=COEF1*(-Ol_riser(1,j+2)+8*Ol_riser(1,j+1)-
8*Ol_riser(1,j-1)+Ol_riser(1,j-2))/12;
      l12(j)=COEF2*(-Ol_riser(1,j+2)+16*Ol_riser
(1,j+1)-30*Ol_riser(1,j)+16*Ol_riser(1,j-1)-Ol_riser
(1,j-2))/12;
      l13(j)=coef3*(Og_riser(1,j)-Ol_riser(1,j));
      l1(j)=h*(l11(j)+l12(j)+l13(j));
   end

      l11(m-1)=COEF_1*(Ol_riser(1,m)-Ol_riser(1,m-2));
      l12(m-1)=COEF2*(Ol_riser(1,m)-2*Ol_riser(1,m-
1)+Ol_riser(1,m-2));
      l13(m-1)=coef3*(Og_riser(1,m-1)-Ol_riser(1,m-1));
      l1(m-1)=h*(l11(m-1)+l12(m-1)+l13(m-1));

      l11(m)=COEF1*(Ol_riser(1,m)-Ol_riser(1,m-1));
      l12(m)=COEF2*(Ol_riser(1,m)-2*Ol_riser(1,m-
1)+Ol_riser(1,m-2));
      l13(m)=coef3*(Og_riser(1,m)-Ol_riser(1,m));
      l1(m)=h*(l11(m)+l12(m)+l13(m));

      m1=h*(alpha2*Og_riser(1,m)+beta2*Og_top
(1)+gamma2*(Og_top(1)-Ol_top(1))+ceta2*Og_top(1));
      n1=h*(coef4*Ol_riser(1,m)+coef5*Ol_top(1)+coef6*
(Og_top(1)-Ol_top(1)));

      o11(1)=BETA3*(Og_downcomer(1,2)-Og_downcomer
(1,1));
      o12(1)=ALPHA3*(Og_downcomer(1,3)-2*Og_downcomer
(1,2)+Og_downcomer(1,1));
        o13(1)=gamma3*(Og_downcomer(1,1)-Ol_downcomer
(1,1));
      o1(1)=h*(o11(1)+o12(1)+o13(1));

      o11(2)=BETA_3*(Og_downcomer(1,3)-Og_downcomer
(1,1));
```

```
      o12(2)=ALPHA3*(Og_downcomer(1,3)-2*Og_downcomer
(1,2)+Og_downcomer(1,1));
      o13(2)=gamma3*(Og_downcomer(1,2)-Ol_downcomer
(1,2));
      o1(2)=h*(o11(2)+o12(2)+o13(2));

      for j=3:1:n-2
      o11(j)=BETA3*(-Og_downcomer(1,j+2)+8*Og_downcomer
(1,j+1)-8*Og_downcomer(1,j-1)+Og_downcomer(1,j-2))/12;
      o12(j)=ALPHA3*(-
Og_downcomer(1,j+2)+16*Og_downcomer(1,j+1)-
30*Og_downcomer(1,j)+16*Og_downcomer(1,j-1)-
Og_downcomer(1,j-2))/12;
      o13(j)=gamma3*(Og_downcomer(1,j)-Ol_downcomer
(1,j));
      o1(j)=h*(o11(j)+o12(j)+o13(j));
      end

      o11(n-1)=BETA_3*(Og_downcomer(1,n)-Og_downcomer
(1,n-2));
      o12(n-1)=ALPHA3*(Og_downcomer(1,n)-2*Og_downcomer
(1,n-1)+Og_downcomer(1,n-2));
      o13(n-1)=gamma3*(Og_downcomer(1,n-1)-Ol_downcomer
(1,n-1));
      o1(n-1)=h*(o11(n-1)+o12(n-1)+o13(n-1));

      o11(n)=BETA3*(Og_downcomer(1,n)-Og_downcomer(1,n-
1));
      o12(n)=ALPHA3*(Og_downcomer(1,n)-2*Og_downcomer
(1,n-1)+Og_downcomer(1,n-2));
      o13(n)=gamma3*(Og_downcomer(1,n)-Ol_downcomer
(1,n));
      o1(n)=h*(o11(n)+o12(n)+o13(n));

      p11(1)=COEF7*(Ol_downcomer(1,2)-Ol_downcomer
(1,1));
      p12(1)=COEF8*(Ol_downcomer(1,3)-2*Ol_downcomer
(1,2)+Ol_downcomer(1,1));
      p13(1)=coef9*(Og_downcomer(1,1)-Ol_downcomer
(1,1));
      p1(1)=h*(p11(1)+p12(1)+p13(1));

      p11(2)=COEF_7*(Ol_downcomer(1,3)-Ol_downcomer
(1,1));
      p12(2)=COEF8*(Ol_downcomer(1,3)-2*Ol_downcomer
(1,2)+Ol_downcomer(1,1));
      p13(2)=coef9*(Og_downcomer(1,2)-Ol_downcomer
(1,2));
      p1(2)=h*(p11(2)+p12(2)+p13(2));

      for j=3:1:n-2
      p11(j)=COEF7*(-Ol_downcomer(1,j+2)+8*Ol_downcomer
(1,j+1)-8*Ol_downcomer(1,j-1)+Ol_downcomer(1,j-2))/12;
      p12(j)=COEF8*(-
Ol_downcomer(1,j+2)+16*Ol_downcomer(1,j+1)-
30*Ol_downcomer(1,j)+16*Ol_downcomer(1,j-1)-
Ol_downcomer(1,j-2))/12;
      p13(j)=coef9*(Og_downcomer(1,j)-Ol_downcomer
(1,j));
      p1(j)=h*(p11(j)+p12(j)+p13(j));
   end

      p11(n-1)=COEF_7*(Ol_downcomer(1,n)-Ol_downcomer
(1,n-2));
      p12(n-1)=COEF8*(Ol_downcomer(1,n)-2*Ol_downcomer
(1,n-1)+Ol_downcomer(1,n-2));
      p13(n-1)=coef9*(Og_downcomer(1,n-1)-Ol_downcomer
(1,n-1));
      p1(n-1)=h*(p11(n-1)+p12(n-1)+p13(n-1));

      p11(n)=COEF7*(Ol_downcomer(1,n)-Ol_downcomer(1,n-
1));
```

```
      p12(n)=COEF8*(Ol_downcomer(1,n)-2*Ol_downcomer
(1,n-1)+Ol_downcomer(1,n-2));
      p13(n)=coef9*(Og_downcomer(1,m)-Ol_downcomer
(1,n));
      p1(n)=h*(p11(n)+p12(n)+p13(n));

      k21(1)=BETA1*(Og_riser(1,2)+k1(2)/2-Og_riser
(1,1)-k1(1)/2);
      k22(1)=ALPHA1*(Og_riser(1,3)+k1(3)/2-2*(Og_riser
(1,2)+k1(2)/2)+Og_riser(1,1)+k1(1)/2);
      k23(1)=gamma1*(Og_riser(1,1)+k1(1)/2-Ol_riser
(1,1)-l1(1)/2);
      k2(1)=h*(k21(1)+k22(1)+k23(1));

      k21(2)=BETA_1*(Og_riser(1,3)+k1(3)/2-Og_riser
(1,1)-k1(1)/2);
      k22(2)=ALPHA1*(Og_riser(1,3)+k1(3)/2-2*(Og_riser
(1,2)+k1(2)/2)+Og_riser(1,1)+k1(1)/2);
      k23(2)=gamma1*(Og_riser(1,2)+k1(2)/2-Ol_riser
(1,2)-l1(2)/2);
      k2(2)=h*(k21(2)+k22(2)+k23(2));

   for j=3:1:m-2
      k21(j)=BETA1*(-Og_riser(1,j+2)-k1(j+2)/2+8*
(Og_riser(1,j+1)+k1(j+1)/2)-8*(Og_riser(1,j-1)+k1(j-
1)/2)+Og_riser(1,j-2)+k1(j-2)/2)/12;
      k22(j)=ALPHA1*(-Og_riser(1,j+2)-k1(j+2)/2+16*
(Og_riser(1,j+1)+k1(j+1)/2)-30*(Og_riser(1,j)+k1
(j)/2)+16*(Og_riser(1,j-1)+k1(j-1)/2)-Og_riser(1,j-2)-
k1(j-2)/2)/12;
      k23(j)=gamma1*(Og_riser(1,j)+k1(j)/2-Ol_riser
(1,j)-l1(j)/2);
      k2(j)=h*(k21(j)+k22(j)+k23(j));
   end
```

```
      k21(m-1)=BETA_1*(Og_riser(1,m)+k1(m)/2-Og_riser
(1,m-2)-k1(m-2)/2);
      k22(m-1)=ALPHA1*(Og_riser(1,m)+k1(m)/2-2*
(Og_riser(1,m-1)+k1(m-1)/2)+Og_riser(1,m-2)+k1(m-2)/2);
      k23(m-1)=gamma1*(Og_riser(1,m-1)+k1(m-1)/2-
Ol_riser(1,m-1)-l1(m-1)/2);
      k2(m-1)=h*(k21(m-1)+k22(m-1)+k23(m-1));

      k21(m)=BETA1*(Og_riser(1,m)+k1(m)/2-Og_riser(1,m-
1)-k1(m-1)/2);
      k22(m)=ALPHA1*(Og_riser(1,m)+k1(m)/2-2*(Og_riser
(1,m-1)+k1(m-1)/2)+Og_riser(1,m-2)+k1(m-2)/2);
      k23(m)=gamma1*(Og_riser(1,m)+k1(m)/2-Ol_riser
(1,m)-l1(m)/2);
      k2(m)=h*(k21(m)+k22(m)+k23(m));

      l21(1)=COEF1*(Ol_riser(1,2)+l1(2)/2-Ol_riser
(1,1)-l1(1)/2);
      l22(1)=COEF2*(Ol_riser(1,3)+l1(3)/2-2*(Ol_riser
(1,2)+l1(2)/2)+Ol_riser(1,1)+l1(1)/2);
      l23(1)=coef3*(Og_riser(1,1)+k1(1)/2-Ol_riser
(1,1)-l1(1)/2);
      l2(1)=h*(l21(1)+l22(1)+l23(1));

      l21(2)=COEF_1*(Ol_riser(1,3)+l1(3)/2-Ol_riser
(1,1)-l1(1)/2);
      l22(2)=COEF2*(Ol_riser(1,3)+l1(3)/2-2*(Ol_riser
(1,2)+l1(2)/2)+Ol_riser(1,1)+l1(1)/2);
      l23(2)=coef3*(Og_riser(1,2)+k1(2)/2-Ol_riser
(1,2)-l1(2)/2);
      l2(2)=h*(l21(2)+l22(2)+l23(2));

for j=3:1:m-2
      l21(j)=COEF1*(-Ol_riser(1,j+2)-l1(j+2)/2+8*
(Ol_riser(1,j+1)+l1(j+1)/2)-8*(Ol_riser(1,j-1)+l1(j-
1)/2)+Ol_riser(1,j-2)+l1(j-2)/2)/12;
```

```
      l22(j)=COEF2*(-Ol_riser(1,j+2)-l1(j+2)/2+16*
(Ol_riser(1,j+1)+l1(j+1)/2)-30*(Ol_riser(1,j)+l1
(j)/2)+16*(Ol_riser(1,j-1)+l1(j-1)/2)-Ol_riser(1,j-2)-
l1(j-2)/2)/12;
      l23(j)=coef3*(Og_riser(1,j)+k1(j)/2-Ol_riser
(1,j)-l1(j)/2);
      l2(j)=h*(l21(j)+l22(j)+l23(j));
end
      l21(m-1)=COEF_1*(Ol_riser(1,m)+l1(m)/2-Ol_riser
(1,m-2)-l1(m-2)/2);
      l22(m-1)=COEF2*(Ol_riser(1,m)+l1(m)/2-2*(Ol_riser
(1,m-1)+l1(m-1)/2)+Ol_riser(1,m-2)+l1(m-2)/2);
      l23(m-1)=coef3*(Og_riser(1,m-1)+k1(m-1)/2-
Ol_riser(1,m-1)-l1(m-1)/2);
      l2(m-1)=h*(l21(m-1)+l22(m-1)+l23(m-1));

      l21(m)=COEF1*(Ol_riser(1,m)+l1(m)/2-Ol_riser(1,m-
1)-l1(m-1)/2);
      l22(m)=COEF2*(Ol_riser(1,m)+l1(m)/2-2*(Ol_riser
(1,m-1)+l1(m-1)/2)+Ol_riser(1,m-2)+l1(m-2)/2);
      l23(m)=coef3*(Og_riser(1,m)+k1(m)/2-Ol_riser
(1,m)-l1(m)/2);
      l2(m)=h*(l21(m)+l22(m)+l23(m));

      m2=h*(alpha2*(Og_riser(1,m)+k1(m)/2)+beta2*
(Og_top(1)+m1/2)+gamma2*((Og_top(1)+m1/2)-(Ol_top
(1)+n1/2))+ceta2*(Og_top(1)+m1/2));
      n2=h*(coef4*(Ol_riser(1,m)+l1(m)/2)+coef5*(Ol_top
(1)+n1/2)+coef6*((Og_top(1)+m1/2)-(Ol_top(1)+n1/2)));

      o21(1)=BETA3*(Og_downcomer(1,2)+o1(2)/2-
Og_downcomer(1,1)-o1(1)/2);
      o22(1)=ALPHA3*(Og_downcomer(1,3)+o1(3)/2-2*
(Og_downcomer(1,2)+o1(2)/2)+Og_downcomer(1,1)+o1(1)/2);
        o23(1)=gamma3*(Og_downcomer(1,1)+o1(1)/2-
Ol_downcomer(1,1)-p1(1)/2);
      o2(1)=h*(o21(1)+o22(1)+o23(1));

      o21(2)=BETA_3*(Og_downcomer(1,3)+o1(3)/2-
Og_downcomer(1,1)-o1(1)/2);
      o22(2)=ALPHA3*(Og_downcomer(1,3)+o1(3)/2-2*
(Og_downcomer(1,2)+o1(2)/2)+Og_downcomer(1,1)+o1(1)/2);
      o23(2)=gamma3*(Og_downcomer(1,2)+o1(2)/2-
Ol_downcomer(1,2)-p1(2)/2);
      o2(2)=h*(o21(2)+o22(2)+o23(2));

   for j=3:1:n-2
      o21(j)=BETA3*(-Og_downcomer(1,j+2)-o1(j+2)/2+8*
(Og_downcomer(1,j+1)+o1(j+1)/2)-8*(Og_downcomer(1,j-
1)+o1(j-1)/2)+Og_downcomer(1,j-2)+o1(j-2)/2)/12;
      o22(j)=ALPHA3*(-Og_downcomer(1,j+2)-o1(j+2)/2+16*
(Og_downcomer(1,j+1)+o1(j+1)/2)-30*(Og_downcomer
(1,j)+o1(j)/2)+16*(Og_downcomer(1,j-1)+o1(j-1)/2)-
Og_downcomer(1,j-2)-o1(j-2)/2)/12;
      o23(j)=gamma3*(Og_downcomer(1,j)+o1(j)/2-
Ol_downcomer(1,j)-p1(j)/2);
      o2(j)=h*(o21(j)+o22(j)+o23(j));
   end

      o21(n-1)=BETA_3*(Og_downcomer(1,n)+o1(n)/2-
Og_downcomer(1,n-2)-o1(n-2)/2);
      o22(n-1)=ALPHA3*(Og_downcomer(1,n)+o1(n)/2-2*
(Og_downcomer(1,n-1)+o1(n-1)/2)+Og_downcomer(1,n-2)+o1
(n-2)/2);
      o23(n-1)=gamma3*(Og_downcomer(1,n-1)+o1(n-1)/2-
Ol_downcomer(1,n-1)-p1(n-1)/2);
      o2(n-1)=h*(o21(n-1)+o22(n-1)+o23(n-1));

      o21(n)=BETA3*(Og_downcomer(1,n)+o1(n)/2-
Og_downcomer(1,n-1)-o1(n-1)/2);
```

```
      o22(n)=ALPHA3*(Og_downcomer(1,n)+o1(n)/2-2*
(Og_downcomer(1,n-1)+o1(n-1)/2)+Og_downcomer(1,n-2)+o1
(n-2)/2);
      o23(n)=gamma3*(Og_downcomer(1,n)+o1(n)/2-
Ol_downcomer(1,n)-p1(n)/2);
      o2(n)=h*(o21(n)+o22(n)+o23(n));

      p21(1)=COEF7*(Ol_downcomer(1,2)+p1(2)/2-
Ol_downcomer(1,1)-p1(1)/2);
      p22(1)=COEF8*(Ol_downcomer(1,3)+p1(3)/2-2*
(Ol_downcomer(1,2)+p1(2)/2)+Ol_downcomer(1,1)+p1(1)/2);
      p23(1)=coef9*(Og_downcomer(1,1)+o1(1)/2-
Ol_downcomer(1,1)-p1(1)/2);
      p2(1)=h*(p21(1)+p22(1)+p23(1));

      p21(2)=COEF_7*(Ol_downcomer(1,3)+p1(3)/2-
Ol_downcomer(1,1)-p1(1)/2);
      p22(2)=COEF8*(Ol_downcomer(1,3)+p1(3)/2-2*
(Ol_downcomer(1,2)+p1(2)/2)+Ol_downcomer(1,1)+p1(1)/2);
      p23(2)=coef9*(Og_downcomer(1,2)+o1(2)/2-
Ol_downcomer(1,2)-p1(2)/2);
      p2(2)=h*(p21(2)+p22(2)+p23(2));

   for j=3:1:n-2
      p21(j)=COEF7*(-Ol_downcomer(1,j+2)-p1(j+2)/2+8*
(Ol_downcomer(1,j+1)+p1(j+1)/2)-8*(Ol_downcomer(1,j-
1)+p1(j-1)/2)+Ol_downcomer(1,j-2)+p1(j-2)/2)/12;
      p22(j)=COEF8*(-Ol_downcomer(1,j+2)-p1(j+2)/2+16*
(Ol_downcomer(1,j+1)+p1(j+1)/2)-30*(Ol_downcomer
(1,j)+p1(j)/2)+16*(Ol_downcomer(1,j-1)+p1(j-1)/2)-
Ol_downcomer(1,j-2)-p1(j-2)/2)/12;
      p23(j)=coef9*(Og_downcomer(1,j)+h/2*o1(j)-
Ol_downcomer(1,j)-h/2*p1(j));
      p2(j)=h*(p21(j)+p22(j)+p23(j));

   end
      p21(n-1)=COEF_7*(Ol_downcomer(1,n)+p1(n)/2-
Ol_downcomer(1,n-2)-p1(n-2)/2);
      p22(n-1)=COEF8*(Ol_downcomer(1,n)+p1(n)/2-2*
(Ol_downcomer(1,n-1)+p1(n-1)/2)+Ol_downcomer(1,n-2)+p1
(n-2)/2);
      p23(n-1)=coef9*(Og_downcomer(1,n-1)+o1(n-1)/2-
Ol_downcomer(1,n-1)-p1(n-1)/2);
      p2(n-1)=h*(p21(n-1)+p22(n-1)+p23(n-1));

      p21(n)=COEF7*(Ol_downcomer(1,n)+p1(n)/2-
Ol_downcomer(1,n-1)-p1(n-1)/2);
      p22(n)=COEF8*(Ol_downcomer(1,n)+p1(n)/2-2*
(Ol_downcomer(1,n-1)+p1(n-1)/2)+Ol_downcomer(1,n-2)+p1
(n-2)/2);
      p23(n)=coef9*(Og_downcomer(1,n)+o1(n)/2-
Ol_downcomer(1,n)-p1(n)/2);
      p2(n)=h*(p21(n)+p22(n)+p23(n));

      k31(1)=BETA1*(Og_riser(1,2)+k2(2)/2-Og_riser
(1,1)-k2(1)/2);
      k32(1)=ALPHA1*(Og_riser(1,3)+k2(3)/2-2*(Og_riser
(1,2)+k2(2)/2)+Og_riser(1,1)+k2(1)/2);
      k33(1)=gamma1*(Og_riser(1,1)+k2(1)/2-Ol_riser
(1,1)-l2(1)/2);
      k3(1)=h*(k31(1)+k32(1)+k33(1));

      k31(2)=BETA_1*(Og_riser(1,3)+k2(3)/2-Og_riser
(1,1)-k2(1)/2);
      k32(2)=ALPHA1*(Og_riser(1,3)+k2(3)/2-2*(Og_riser
(1,2)+k2(2)/2)+Og_riser(1,1)+k2(1)/2);
      k33(2)=gamma1*(Og_riser(1,2)+k2(2)/2-Ol_riser
(1,2)-l2(2)/2);
      k3(2)=h*(k31(2)+k32(2)+k33(2));
      for j=3:1:m-2
```

```
      k31(j)=BETA1*(-Og_riser(1,j+2)-k2(j+2)/2+8*
(Og_riser(1,j+1)+k2(j+1)/2)-8*(Og_riser(1,j-1)+k2(j-
1)/2)+Og_riser(1,j-2)+k2(j-2)/2)/12;
      k32(j)=ALPHA1*(-Og_riser(1,j+2)-k2(j+2)/2+16*
(Og_riser(1,j+1)+k2(j+1)/2)-30*(Og_riser(1,j)+k2
(j)/2)+16*(Og_riser(1,j-1)+k2(j-1)/2)-Og_riser(1,j-2)-
k2(j-2)/2)/12;
      k33(j)=gamma1*(Og_riser(1,j)+k2(j)/2-Ol_riser
(1,j)-l2(j)/2);
      k3(j)=h*(k31(j)+k32(j)+k33(j));
   end

      k31(m-1)=BETA_1*(Og_riser(1,m)+k2(m)/2-Og_riser
(1,m-2)-k2(m-2)/2);
      k32(m-1)=ALPHA1*(Og_riser(1,m)+k2(m)/2-2*
(Og_riser(1,m-1)+k2(m-1)/2)+Og_riser(1,m-2)+k2(m-2)/2);
      k33(m-1)=gamma1*(Og_riser(1,m-1)+k2(m-1)/2-
Ol_riser(1,m-1)-l2(m-1)/2);
      k3(m-1)=h*(k31(m-1)+k32(m-1)+k33(m-1));

      k31(m)=BETA1*(Og_riser(1,m)+k2(m)/2-Og_riser(1,m-
1)-k2(m-1)/2);
      k32(m)=ALPHA1*(Og_riser(1,m)+k2(m)/2-2*(Og_riser
(1,m-1)+k2(m-1)/2)+Og_riser(1,m-2)+k2(m-2)/2);
      k33(m)=gamma1*(Og_riser(1,m)+k2(m)/2-Ol_riser
(1,m)-l2(m)/2);
      k3(m)=h*(k31(m)+k32(m)+k33(m));

      l31(1)=COEF1*(Ol_riser(1,2)+l2(2)/2-Ol_riser
(1,1)-l2(1)/2);
      l32(1)=COEF2*(Ol_riser(1,3)+l2(3)/2-2*(Ol_riser
(1,2)+l2(2)/2)+Ol_riser(1,1)+l2(1)/2);
      l33(1)=coef3*(Og_riser(1,1)+k2(1)/2-Ol_riser
(1,1)-l2(1)/2);
      l3(1)=h*(l31(1)+l32(1)+l33(1));

      l31(2)=COEF_1*(Ol_riser(1,3)+l2(3)/2-Ol_riser
(1,1)-l2(1)/2);
      l32(2)=COEF2*(Ol_riser(1,3)+l2(3)/2-2*(Ol_riser
(1,2)+l2(2)/2)+Ol_riser(1,1)+l2(1)/2);
      l33(2)=coef3*(Og_riser(1,2)+k2(2)/2-Ol_riser
(1,2)-l2(2)/2);
      l3(2)=h*(l31(2)+l32(2)+l33(2));

      for j=3:1:m-2
      l31(j)=COEF1*(-Ol_riser(1,j+2)-1/2*l2(j+2)+8*
(Ol_riser(1,j+1)+1/2*l2(j+1))-8*(Ol_riser(1,j-1)+1/2*l2
(j-1))+Ol_riser(1,j-2)+1/2*l2(j-2))/12;
      l32(j)=COEF2*(-Ol_riser(1,j+2)-1/2*l2(j+2)+16*
(Ol_riser(1,j+1)+1/2*l2(j+1))-30*(Ol_riser(1,j)+1/2*l2
(j))+16*(Ol_riser(1,j-1)+1/2*l2(j-1))-Ol_riser(1,j-2)-
1/2*l2(j-2))/12;
      l33(j)=coef3*(Og_riser(1,j)+1/2*k2(j)-Ol_riser
(1,j)-1/2*l2(j));
      l3(j)=h*(l31(j)+l32(j)+l33(j));
   end
      l31(m-1)=COEF_1*(Ol_riser(1,m)+l2(m)/2-Ol_riser
(1,m-2)-l2(m-2)/2);
      l32(m-1)=COEF2*(Ol_riser(1,m)+l2(m)/2-2*(Ol_riser
(1,m-1)+l2(m-1)/2)+Ol_riser(1,m-2)+l2(m-2)/2);
      l33(m-1)=coef3*(Og_riser(1,m-1)+k2(m-1)/2-
Ol_riser(1,m-1)-l2(m-1)/2);
      l3(m-1)=h*(l31(m-1)+l32(m-1)+l33(m-1));

      l31(m)=COEF1*(Ol_riser(1,m)+l2(m)/2-Ol_riser(1,m-
1)-l2(m-1)/2);
      l32(m)=COEF2*(Ol_riser(1,m)+l2(m)/2-2*(Ol_riser
(1,m-1)+l2(m-1)/2)+Ol_riser(1,m-2)+l2(m-2)/2);
      l33(m)=coef3*(Og_riser(1,m)+k2(m)/2-Ol_riser
(1,m)-l2(m)/2);
      l3(m)=h*(l31(m)+l32(m)+l33(m));
```

```
      m3=h*(alpha2*(Og_riser(1,m)+k2(m)/2)+beta2*
(Og_top(1)+m2/2)+gamma2*((Og_top(1)+m2/2)-(Ol_top
(1)+n2/2))+ceta2*(Og_top(1)+m2/2));
      n3=h*(coef4*(Ol_riser(1,m)+l2(m)/2)+coef5*(Ol_top
(1)+n2/2)+coef6*((Og_top(1)+m2/2)-(Ol_top(1)+n2/2)));

      o31(1)=BETA3*(Og_downcomer(1,2)+o2(2)/2-
Og_downcomer(1,1)-o2(1)/2);
      o32(1)=ALPHA3*(Og_downcomer(1,3)+o2(3)/2-2*
(Og_downcomer(1,2)+o2(2)/2)+Og_downcomer(1,1)+o2(1)/2);
      o33(1)=gamma3*(Og_downcomer(1,1)+o2(1)/2-
Ol_downcomer(1,1)-p2(1)/2);
      o3(1)=h*(o31(1)+o32(1)+o33(1));

      o31(2)=BETA_3*(Og_downcomer(1,3)+o2(3)/2-
Og_downcomer(1,1)-o2(1)/2);
      o32(2)=ALPHA3*(Og_downcomer(1,3)+o2(3)/2-2*
(Og_downcomer(1,2)+o2(2)/2)+Og_downcomer(1,1)+o2(1)/2);
      o33(2)=gamma3*(Og_downcomer(1,2)+o2(2)/2-
Ol_downcomer(1,2)-p2(2)/2);
      o3(2)=h*(o31(2)+o32(2)+o33(2));

   for j=3:1:n-2
      o31(j)=BETA3*(-Og_downcomer(1,j+2)-1/2*o2(j+2)+8*
(Og_downcomer(1,j+1)+1/2*o2(j+1))-8*(Og_downcomer(1,j-
1)+1/2*o2(j-1))+Og_downcomer(1,j-2)+1/2*o2(j-2))/12;
      o32(j)=ALPHA3*(-Og_downcomer(1,j+2)-1/2*o2
(j+2)+16*(Og_downcomer(1,j+1)+1/2*o2(j+1))-30*
(Og_downcomer(1,j)+1/2*o2(j))+16*(Og_downcomer(1,j-
1)+1/2*o2(j-1))-Og_downcomer(1,j-2)-1/2*o2(j-2))/12;
      o33(j)=gamma3*(Og_downcomer(1,j)+1/2*o2(j)-
Ol_downcomer(1,j)-1/2*p2(j));
      o3(j)=h*(o31(j)+o32(j)+o33(j));
   end

      o31(n-1)=BETA_3*(Og_downcomer(1,n)+o2(n)/2-
Og_downcomer(1,n-2)-o2(n-2)/2);
      o32(n-1)=ALPHA3*(Og_downcomer(1,n)+o2(n)/2-2*
(Og_downcomer(1,n-1)+o2(n-1)/2)+Og_downcomer(1,n-2)+o2
(n-2)/2);
      o33(n-1)=gamma3*(Og_downcomer(1,n-1)+o2(n-1)/2-
Ol_downcomer(1,n-1)-p2(n-1)/2);
      o3(n-1)=h*(o31(n-1)+o32(n-1)+o33(n-1));

      o31(n)=BETA3*(Og_downcomer(1,n)+o2(n)/2-
Og_downcomer(1,n-1)-o2(n-1)/2);
      o32(n)=ALPHA3*(Og_downcomer(1,n)+o2(n)/2-2*
(Og_downcomer(1,n-1)+o2(n-1)/2)+Og_downcomer(1,n-2)+o2
(n-2)/2);
      o33(n)=gamma3*(Og_downcomer(1,n)+o2(n)/2-
Ol_downcomer(1,n)-p2(n)/2);
      o3(n)=h*(o31(n)+o32(n)+o33(n));

      p31(1)=COEF7*(Ol_downcomer(1,2)+p2(2)/2-
Ol_downcomer(1,1)-p2(1)/2);
      p32(1)=COEF8*(Ol_downcomer(1,3)+p2(3)/2-2*
(Ol_downcomer(1,2)+p2(2)/2)+Ol_downcomer(1,1)+p2(1)/2);
      p33(1)=coef9*(Og_downcomer(1,1)+o2(1)/2-
Ol_downcomer(1,1)-p2(1)/2);
      p3(1)=h*(p31(1)+p32(1)+p33(1));

      p31(2)=COEF_7*(Ol_downcomer(1,3)+p2(3)/2-
Ol_downcomer(1,1)-p2(1)/2);
      p32(2)=COEF8*(Ol_downcomer(1,3)+p2(3)/2-2*
(Ol_downcomer(1,2)+p2(2)/2)+Ol_downcomer(1,1)+p2(1)/2);
      p33(2)=coef9*(Og_downcomer(1,2)+o2(2)/2-
Ol_downcomer(1,2)-p2(2)/2);
      p3(2)=h*(p31(2)+p32(2)+p33(2));

   for  j=3:1:n-2
```

```
      p31(j)=COEF7*(-Ol_downcomer(1,j+2)-1/2*p2(j+2)+8*
(Ol_downcomer(1,j+1)+1/2*p2(j+1))-8*(Ol_downcomer(1,j-
1)+1/2*p2(j-1))+Ol_downcomer(1,j-2)+1/2*p2(j-2))/12;
      p32(j)=COEF8*(-Ol_downcomer(1,j+2)-1/2*p2
(j+2)+16*(Ol_downcomer(1,j+1)+1/2*p2(j+1))-30*
(Ol_downcomer(1,j)+1/2*p2(j))+16*(Ol_downcomer(1,j-
1)+1/2*p2(j-1))-Ol_downcomer(1,j-2)-1/2*p2(j-2))/12;
      p33(j)=coef9*(Og_downcomer(1,j)+1/2*o2(j)-
Ol_downcomer(1,j)-1/2*p2(j));
      p3(j)=h*(p31(j)+p32(j)+p33(j));
   end

        p31(n-1)=COEF_7*(Ol_downcomer(1,n)+p2(n)/2-
Ol_downcomer(1,n-2)-p2(n-2)/2);
      p32(n-1)=COEF8*(Ol_downcomer(1,n)+p2(n)/2-2*
(Ol_downcomer(1,n-1)+p2(n-1)/2)+Ol_downcomer(1,n-2)+p2
(n-2)/2);
        p33(n-1)=coef9*(Og_downcomer(1,n-1)+o2(n-1)/2-
Ol_downcomer(1,n-1)-p2(n-1)/2);
      p3(n-1)=h*(p31(n-1)+p32(n-1)+p33(n-1));

      p31(n)=COEF7*(Ol_downcomer(1,n)+p2(n)/2-
Ol_downcomer(1,n-1)-p2(n-1)/2);
      p32(n)=COEF8*(Ol_downcomer(1,n)+p2(n)/2-2*
(Ol_downcomer(1,n-1)+p2(n-1)/2)+Ol_downcomer(1,n-2)+p2
(n-2)/2);
        p33(n)=coef9*(Og_downcomer(1,n)+o2(n)/2-
Ol_downcomer(1,n)-p2(n)/2);
      p3(n)=h*(p31(n)+p32(n)+p33(n));

      k41(1)=BETA1*(Og_riser(1,2)+k3(2)-Og_riser(1,1)-
k3(1));
      k42(1)=ALPHA1*(Og_riser(1,3)+k3(3)-2*(Og_riser
(1,2)+k3(2))+Og_riser(1,1)+k3(1));
        k43(1)=gamma1*(Og_riser(1,1)+k3(1)-Ol_riser
(1,1)-l3(1));
      k4(1)=h*(k41(1)+k42(1)+k43(1));

      k41(2)=BETA_1*(Og_riser(1,3)+k3(3)-Og_riser(1,1)-
k3(1));
      k42(2)=ALPHA1*(Og_riser(1,3)+k3(3)-2*(Og_riser
(1,2)+k3(2))+Og_riser(1,1)+k3(1));
      k43(2)=gamma1*(Og_riser(1,2)+k3(2)-Ol_riser(1,2)-
l3(2));
      k4(2)=h*(k41(2)+k42(2)+k43(2));

   for  j=3:1:m-2
      k41(j)=BETA1*(-Og_riser(1,j+2)-k3(j+2)+8*
(Og_riser(1,j+1)+k3(j+1))-8*(Og_riser(1,j-1)+k3(j-
1))+Og_riser(1,j-2)+k3(j-2))/12;
      k42(j)=ALPHA1*(-Og_riser(1,j+2)-1*k3(j+2)+16*
(Og_riser(1,j+1)+k3(j+1))-30*(Og_riser(1,j)+k3(j))+16*
(Og_riser(1,j-1)+k3(j-1))-Og_riser(1,j-2)-k3(j-2))/12;
      k43(j)=gamma1*(Og_riser(1,j)+k3(j)-Ol_riser(1,j)-
l3(j));
      k4(j)=h*(k41(j)+k42(j)+k43(j));
   end

      k41(m-1)=BETA_1*(Og_riser(1,m)+k3(m)-Og_riser
(1,m-2)-k3(m-2));
      k42(m-1)=ALPHA1*(Og_riser(1,m)+k3(m)-2*(Og_riser
(1,m-1)+k3(m-1))+Og_riser(1,m-2)+k3(m-2));
      k43(m-1)=gamma1*(Og_riser(1,m-1)+k3(m-1)-Ol_riser
(1,m-1)-l3(m-1));
      k4(m-1)=h*(k41(m-1)+k42(m-1)+k43(m-1));

      k41(m)=BETA1*(Og_riser(1,m)+k3(m)-Og_riser(1,m-
1)-k3(m-1));
      k42(m)=ALPHA1*(Og_riser(1,m)+k3(m)-2*(Og_riser
(1,m-1)+k3(m-1))+Og_riser(1,m-2)+k3(m-2)/2);
      k43(m)=gamma1*(Og_riser(1,m)+k3(m)-Ol_riser(1,m)-
l3(m));
```

```
        k4(m)=h*(k41(m)+k42(m)+k43(m));

      l41(1)=COEF1*(Ol_riser(1,2)+l3(2)-Ol_riser(1,1)-
l3(1));
      l42(1)=COEF2*(Ol_riser(1,3)+l3(3)-2*(Ol_riser
(1,2)+l3(2))+Ol_riser(1,1)+l3(1));
        l43(1)=coef3*(Og_riser(1,1)+k3(1)-Ol_riser
(1,1)-l3(1));
      l4(1)=h*(l41(1)+l42(1)+l43(1));

      l41(2)=COEF_1*(Ol_riser(1,3)+l3(3)-Ol_riser(1,1)-
l3(1));
      l42(2)=COEF2*(Ol_riser(1,3)+l3(3)-2*(Ol_riser
(1,2)+l3(2))+Ol_riser(1,1)+l3(1));
        l43(2)=coef3*(Og_riser(1,2)+k3(2)-Ol_riser
(1,2)-l3(2));
      l4(2)=h*(l41(2)+l42(2)+l43(2));

   for j=3:1:m-2
      l41(j)=COEF1*(-Ol_riser(1,j+2)-1*l3(j+2)+8*
(Ol_riser(1,j+1)+1*l3(j+1))-8*(Ol_riser(1,j-1)+1*l3(j-
1))+Ol_riser(1,j-2)+1*l3(j-2))/12;
      l42(j)=COEF2*(-Ol_riser(1,j+2)-1*l3(j+2)+16*
(Ol_riser(1,j+1)+1*l3(j+1))-30*(Ol_riser(1,j)+1*l3
(j))+16*(Ol_riser(1,j-1)+1*l3(j-1))-Ol_riser(1,j-2)-
1*l3(j-2))/12;
      l43(j)=coef3*(Og_riser(1,j)+1*k3(j)-Ol_riser
(1,j)-1*l3(j));
      l4(j)=h*(l41(j)+l42(j)+l43(j));
   end

      l41(m-1)=COEF_1*(Ol_riser(1,m)+l3(m)-Ol_riser
(1,m-2)-l3(m-2));
      l42(m-1)=COEF2*(Ol_riser(1,m)+l3(m)-2*(Ol_riser
(1,m-1)+l3(m-1))+Ol_riser(1,m-2)+l3(m-2));
      l43(m-1)=coef3*(Og_riser(1,m-1)+k3(m-1)-Ol_riser
(1,m-1)-l3(m-1));
      l4(m-1)=h*(l41(m-1)+l42(m-1)+l43(m-1));

      l41(m)=COEF1*(Ol_riser(1,m)+l3(m)-Ol_riser(1,m-
1)-l3(m-1));
      l42(m)=COEF2*(Ol_riser(1,m)+l3(m)-2*(Ol_riser
(1,m-1)+l3(m-1))+Ol_riser(1,m-2)+l3(m-2)/2);
      l43(m)=coef3*(Og_riser(1,m)+k3(m)-Ol_riser(1,m)-
l3(m));
      l4(m)=h*(l41(m)+l42(m)+l43(m));

      m4=h*(alpha2*(Og_riser(1,m)+k3(m))+beta2*(Og_top
(1)+m3)+gamma2*((Og_top(1)+m3)-(Ol_top(1)+n3))+ceta2*
(Og_top(1)+m3));
        n4=h*(coef4*(Ol_riser(1,m)+l3(m))+coef5*(Ol_top
(1)+n3)+coef6*((Og_top(1)+m3)-(Ol_top(1)+n3)));

      o41(1)=BETA3*(Og_downcomer(1,2)+o3(2)-
Og_downcomer(1,1)-o3(1));
      o42(1)=ALPHA3*(Og_downcomer(1,3)+o3(3)-2*
(Og_downcomer(1,2)+o3(2))+Og_downcomer(1,1)+o3(1));
      o43(1)=gamma3*(Og_downcomer(1,1)+o3(1)-
Ol_downcomer(1,1)-p3(1));
      o4(1)=h*(o41(1)+o42(1)+o43(1));

      o41(2)=BETA_3*(Og_downcomer(1,3)+o3(3)-
Og_downcomer(1,1)-o3(1));
      o42(2)=ALPHA3*(Og_downcomer(1,3)+o3(3)-2*
(Og_downcomer(1,2)+o3(2))+Og_downcomer(1,1)+o3(1));
      o43(2)=gamma3*(Og_downcomer(1,2)+o3(2)-
Ol_downcomer(1,2)-p3(2));
      o4(2)=h*(o41(2)+o42(2)+o43(2));
    for j=3:1:n-2
```

```
      o41(j)=BETA1*(-Og_downcomer(1,j+2)-1*o3(j+2)+8*
(Og_downcomer(1,j+1)+1*o3(j+1))-8*(Og_downcomer(1,j-
1)+1*o3(j-1))+Og_downcomer(1,j-2)+1*o3(j-2))/12;
      o42(j)=ALPHA1*(-Og_downcomer(1,j+2)-1*o3(j+2)+16*
(Og_downcomer(1,j+1)+1*o3(j+1))-30*(Og_downcomer
(1,j)+1*o3(j))+16*(Og_downcomer(1,j-1)+1*o3(j-1))-
Og_downcomer(1,j-2)-1*o3(j-2))/12;
        o43(j)=gamma1*(Og_downcomer(1,j)+1*o3(j)-
Ol_downcomer(1,j)-1*p3(j));
      o4(j)=h*(o41(j)+o42(j)+o43(j));
      end

        o41(n-1)=BETA_3*(Og_downcomer(1,n)+o3(n)-
Og_downcomer(1,n-2)-o3(n-2));
      o42(n-1)=ALPHA3*(Og_downcomer(1,n)+o3(n)-2*
(Og_downcomer(1,n-1)+o3(n-1))+Og_downcomer(1,n-2)+o3(n-
2));
      o43(n-1)=gamma3*(Og_downcomer(1,n-1)+o3(n-1)-
Ol_downcomer(1,n-1)-p3(n-1));
      o4(n-1)=h*(o41(n-1)+o42(n-1)+o43(n-1));

      o41(n)=BETA3*(Og_downcomer(1,n)+o3(n)-
Og_downcomer(1,n-1)-o3(n-1));
      o42(n)=ALPHA3*(Og_downcomer(1,n)+o3(n)-2*
(Og_downcomer(1,n-1)+o3(n-1))+Og_downcomer(1,n-2)+o3(n-
2)/2);
      o43(n)=gamma3*(Og_downcomer(1,n)+o3(n)-
Ol_downcomer(1,n)-p3(n));
      o4(n)=h*(o41(n)+o42(n)+o43(n));

      p41(1)=COEF7*(Ol_downcomer(1,2)+p3(2)-
Ol_downcomer(1,1)-p3(1));
      p42(1)=COEF8*(Ol_downcomer(1,3)+p3(3)-2*
(Ol_downcomer(1,2)+p3(2))+Ol_downcomer(1,1)+p3(1));
      p43(1)=coef9*(Og_downcomer(1,1)+o3(1)-
Ol_downcomer(1,1)-p3(1));
      p4(1)=h*(p41(1)+p42(1)+p43(1));

      p41(2)=COEF_7*(Ol_downcomer(1,3)+p3(3)-
Ol_downcomer(1,1)-p3(1));
      p42(2)=COEF8*(Ol_downcomer(1,3)+p3(3)-2*
(Ol_downcomer(1,2)+p3(2))+Ol_downcomer(1,1)+p3(1));
        p43(2)=coef9*(Og_downcomer(1,2)+o3(2)-
Ol_downcomer(1,2)-p3(2));
      p4(2)=h*(p41(2)+p42(2)+p43(2));

    for j=3:1:n-2
      p41(j)=COEF7*(-Ol_downcomer(1,j+2)-1*p3(j+2)+8*
(Ol_downcomer(1,j+1)+1*p3(j+1))-8*(Ol_downcomer(1,j-
1)+1*p3(j-1))+Ol_downcomer(1,j-2)+1*p3(j-2))/12;
      p42(j)=COEF8*(-Ol_downcomer(1,j+2)-1*p3(j+2)+16*
(Ol_downcomer(1,j+1)+1*p3(j+1))-30*(Ol_downcomer
(1,j)+1*p3(j))+16*(Ol_downcomer(1,j-1)+1*p3(j-1))-
Ol_downcomer(1,j-2)-1*p3(j-2))/12;
        p43(j)=coef9*(Og_downcomer(1,j)+1*o3(j)-
Ol_downcomer(1,j)-1*p3(j));
      p4(j)=h*(p41(j)+p42(j)+p43(j));
      end

      p41(n-1)=COEF_7*(Ol_downcomer(1,n)+p3(n)-
Ol_downcomer(1,n-2)-p3(n-2));
      p42(n-1)=COEF8*(Ol_downcomer(1,n)+p3(n)-2*
(Ol_downcomer(1,n-1)+p3(n-1))+Ol_downcomer(1,n-2)+p3(n-
2));
        p43(n-1)=coef9*(Og_downcomer(1,n-1)+o3(n-1)-
Ol_downcomer(1,n-1)-p3(n-1));
      p4(n-1)=h*(p41(n-1)+p42(n-1)+p43(n-1));

      p41(n)=COEF7*(Ol_downcomer(1,n)+p3(n)-
Ol_downcomer(1,n-1)-p3(n-1));
```

```
      p42(n)=COEF8*(Ol_downcomer(1,n)+p3(n)-2*
(Ol_downcomer(1,n-1)+p3(n-1))+Ol_downcomer(1,n-2)+p3(n-
2)/2);
      p43(n)=coef9*(Og_downcomer(1,n)+o3(n)-
Ol_downcomer(1,n)-p3(n));
      p4(n)=h*(p41(n)+p42(n)+p43(n));

for j=2:1:m
Og_riser(1,j)=Og_riser(1,j)+1/6*(k1(j)+2*k2(j)+2*k3
(j)+k4(j));
Ol_riser(1,j)=Ol_riser(1,j)+1/6*(l1(j)+2*l2(j)+2*l3
(j)+l4(j));
end

Og_top(1)=Og_top(1)+1/6*(m1+2*m2+2*m3+m4);
Ol_top(1)=Ol_top(1)+1/6*(n1+2*n2+2*n3+n4);

for j=2:1:n
Og_downcomer(1,j)=Og_downcomer(1,j)+1/6*(o1(j)+2*o2
(j)+2*o3(j)+o4(j));
Ol_downcomer(1,j)=Ol_downcomer(1,j)+1/6*(p1(j)+2*p2
(j)+2*p3(j)+p4(j));
end

Og_riser(1,1)=(e3*A3*vg_downcomer*Og_downcomer
(1,n)+Qg_in)/(e1*A1*vg_riser);
Ol_riser(1,1)=((1-e3)*A3*vl_downcomer*Ol_downcomer
(1,n))/((1-e1)*A1*vl_riser);

Og_downcomer(1,1)=Og_top(1);
Ol_downcomer(1,1)=Ol_top(1);

z=z+1;

if floor((z-1)/100)==ceil((z-1)/100);
   fprintf('z=%f \n',z);
   fprintf('Olr=%f \n',Ol_riser(1,m));
end

   if Ol_riser(1,m)<0.8;
      if floor((z-1)/200)==ceil((z-1)/200)
            Olrm(k,1)=Ol_riser(1,m);
            Oldn(k,1)=Ol_downcomer(1,n);
            Olt(k,1)=Ol_top(1);
            Ogrm(k,1)=Og_riser(1,m);
            Ogdn(k,1)=Og_downcomer(1,n);
         Ogt(k,1)=Og_top(1);
         k=k+1;
      end
   else
      if floor((z-1)/500)==ceil((z-1)/500)
            Olrm(k,1)=Ol_riser(1,m);
            Oldn(k,1)=Ol_downcomer(1,n);
            Olt(k,1)=Ol_top(1);
            Ogrm(k,1)=Og_riser(1,m);
            Ogdn(k,1)=Og_downcomer(1,n);
            Ogt(k,1)=Og_top(1);
         k=k+1;
      end
   end
end

t1f=floor((c1-1)/200)*200;
t2i=ceil((c1-1)/500)*500;
t2f=floor((c2-1)/500)*500;

t=[0:200:t1f,t2i:500:t2f-500];

save OlrmW11 Olrm -ascii;
save OgrmW11 Ogrm -ascii;
save OldnW11 Oldn -ascii;
save OgdnW11 Ogdn -ascii;
```

```
save OltW11 Olt -ascii;
save OgtW11 Ogt -ascii;
save parameterW11 c1 c2 -ascii;

%figure(1)
%plot(t,Olrm,'c');
%title('Ol_riser');
%xlabel('time(-)');
%ylabel('dimensionless concentration of oxygen(-)');
%grid on

%figure(2)
%plot(t,Oldn,'m');
%title('Ol_downcomer');
%xlabel('time(-)');
%ylabel('dimensionless concentration of oxygen(-)');
%grid on

%figure(3)
%plot(t,Olt,'g');
%title('Ol_top');
%xlabel('time(-)');
%ylabel('dimensionless concentration of oxygen(-)');
%grid on

%figure(4)
%plot(t,Ogrm,'c');
%title('Og_riser');
%xlabel('time(-)');
%ylabel('dimensionless concentration of oxygen(-)');
%grid on

%figure(5)
%plot(t,Ogdn,'m');
%title('Og_downcomer');
%xlabel('time(-)');
%ylabel('dimensionless concentration of oxygen(-)');
%grid on

%figure(6)
%plot(t,Ogt,'g');
%title('Og_top');
%xlabel('time(-)');
%ylabel('dimensionless concentration of oxygen(-)');
%grid on

fprintf('Ad/Ar = %0.5f\n',ratio);
fprintf('Qg_in = %0.5f\n',Qg_in);
fprintf('usg = %0.5f\n',usg);
fprintf('eo = %0.5f\n',e0);
fprintf('er = %0.5f\n',e1);
fprintf('egs = %0.5f\n',e2);
fprintf('ed = %0.5f\n',e3);
fprintf('kLa_riser = %0.5f\n',kla_riser);
fprintf('kLa_downcomer = %0.5f\n',kla_downcomer);
fprintf('kLa_top = %0.5f\n',kla_top);
%fprintf('dB = %0.5f\n',d_bubble);
fprintf('vg_riser = %0.5f\n',vg_riser);
fprintf('vg_downcomer = %0.5f\n',vg_downcomer);
fprintf('vl_riser = %0.5f\n',vl_riser);
fprintf('vl_downcomer = %0.5f\n',vl_downcomer);
fprintf('v_slip= %0.5f\n',v_slip);
fprintf('t_factor = %0.5f\n',t_factor);
fprintf('z_factor = %0.5f\n',z_factor);
fprintf('c1 = %0.5f\n',c1);
fprintf('c2 = %0.5f\n',c2);
fprintf('del_t1 = %0.5f\n',del_t1);
fprintf('del_t2 = %0.5f\n',del_t2);
```

Appendix B

Published papers

B1. Effect of unaerated liquid height on gas holdup and liquid velocity in internal-loop airlift contactors

B2. Bubble size distribution and gas-liquid mass transfer in airlift contactors.

B3. Mathematical models for the prediction of gas-liquid mass transfer in airlift contactor

B4. Bubble size distribution and mass transfer in annulus sparged airlift contactor

Biography

Miss Porntip Wongsuchoto was born on 14th July, 1977 in Bangkok. She finished her higher secondary course from Bodin Decha (Sing Singhasenee) School in March, 1994. After that, she studied in the major of Chemical Engineering in Faculty of Engineering at Chulalongkorn University. She continued her further study for Doctoral's degree in Chemical Engineering at Chulalongkorn University. She participated in the Biochemical Engineering research group and achieved her Doctoral's degree in April, 2003.